CHARACTERIZATION AND SOURCE APPORTIONMENT OF AMBIENT PM2.5 IN ATLANTA, GEORGIA: ON-ROAD EMISSION, BIOMASS BURNING AND SOA IMPACT

A Dissertation
Presented to
The Academic Faculty

by

Bo Yan

In Partial Fulfillment
of the Requirements for the Degree
Doctor of Philosophy in the
School of Earth and Atmospheric Sciences

Georgia Institute of Technology
December 2009

CHARACTERIZATION AND SOURCE APPORTIONMENT OF AMBIENT PM2.5 IN ATLANTA, GEORGIA: ON-ROAD EMISSION, BIOMASS BURNING AND SOA IMPACT

Approved by:

Dr. Armistead G. Russell, Advisor
School of Civil and Environmental Engineering
Georgia Institute of Technology

Dr. Mei Zheng, Co-Advisor
School of Earth and Atmospheric Sciences
Georgia Institute of Technology

Dr. Michael H. Bergin
School of Civil and Environmental Engineering
Georgia Institute of Technology

Dr. Rodney J. Weber
School of Earth and Atmospheric Sciences
Georgia Institute of Technology

Dr. Yuhang Wang
School of Earth and Atmospheric Sciences
Georgia Institute of Technology

Date Approved: August 19, 2009

To my wife and family

ACKNOWLEDGEMENTS

I wish to express my heartfelt gratitude to many people for providing me indispensable guidance, great support, kind help and continuous encouragement in the past six years. First and foremost, I would like to thank my advisor, Dr. Ted Russell, who helped me get into this research field, gave me opportunities to study and investigate in lab and field, guided me with his insightful expertise and knowledge, and encouraged me to go beyond what I could do alone. His mentorship widened my scientific view and enabled me to develop various knowledge, skills, and experience that are invaluable for my future career as a research scientist. I am greatly thankful to Dr. Mei Zheng, who, as a co-advisor, provided me with much academic guidance in atmospheric chemistry and technical support in lab experiments with her deep insight, broad outlook and hands-on expertise in organic compound analysis. Thanks also to Dr. Rodney Weber for his helpful suggestion and kind support on field sampling and lab measurement. I also appreciate Dr. Michael Bergin and Dr. Yuhang Wang for serving on my thesis committee.

I would like to thank a number of group members, colleagues, and friends at Georgia Tech for their help, support, and friendship which always accompanied me during the years of graduate study. I thank Dr. Yongtao Hu for his long term help with air pollution modeling and paper review. I appreciate Drs. Lin Ke, Yingjun Chen, Liping Yu, Xiang Ding as well as Meiyu Dong and Bo Wang for their assistance in organic tracer analysis. I am thankful to Dr. Amy Sullivan and Xiaolu Zhang for field sampling and WSOC analysis, and to Dr. Sangil Lee, Charles Evan Cobb, Santosh Chandru, Hyeon Kook Kim, and Sivaraman Balachandran for assistance with field sampling and lab

experiments of TOT and IC. Thanks also go to Dr. Di Tian, Dr. Amit Marmur, Jaemeen Baek, Farhan Akhtar, Burcak Kaynak, Dr. K.J. Liao, Dr. Efthimios Tagaris, Dr. Talat Odman, Wenxian Zhang, Jorge Pachon, Gretchen Goldman, Soonchul Kwon, and Shannon Capps.

Finally, and above all, I would like to especially thank my wife, Tong, for her countless love, support and patience, and my family for their encouragement from the beginning through the end. Without these, I cannot be here ever.

TABLE OF CONTENTS

LIST OF TABLES

LIST OF FIGURES

SUMMARY

Airborne fine particulate matter ($PM_{2.5}$) has been linked to adverse human health effects, reduced visibility, climate change, and other air quality concerns. Typically, the major contributors of $PM_{2.5}$ include mobile source emissions, biomass burning, and secondary sources with anthropogenic and biogenic nature in origin. The metropolitan Atlanta, GA area, located in the southeastern U.S and populated by over 5.4 million residents, is of particular interest for air quality study and air pollutant control due to high emissions of mobile sources, biomass burning, coal-fired power plants and biogenic volatile organic compounds (VOC), with vigorous photochemical processes occurring as well.

Effective control strategies for air pollutants require a detailed investigation of chemical composition of airborne $PM_{2.5}$ in this area as well as quantitative identification of specific source impacts on ambient air quality. In this research, various airborne $PM_{2.5}$ samples were collected and analyzed, which are directly impacted or dominated by on-road mobile and other typical urban emissions, regional transport sources, prescribed burning plumes, wildfire plumes, as well as secondary sources with anthropogenic and biogenic nature in origin. Day-night, seasonal and spatial variations of $PM_{2.5}$ characterization were also studied. The impacts or contributions of major sources were identified quantitatively through the receptor source apportionment models. These modeling results, especially on-road mobile source contributions and secondary organic carbon (SOC) were assessed by multiple approaches to provide additional information for $PM_{2.5}$ control strategies. Furthermore, season- and location-specific source profiles were

developed in this research to reflect real-world and representative local emission characterizations of on-road mobile sources, aged prescribed burning plumes, and wildfire plumes. Secondary organic aerosol (SOA), a major component of $PM_{2.5}$ in the summer, was also explored for contribution and individual sources.

To investigate on-road emissions, regional transport and SOA effects, 12-hr and 24-hr $PM_{2.5}$ filter samples were collected in summer 2005 and winter 2006 from three sites: two from urban Atlanta (one site adjacent to a freeway and another 400 m away), and one at a rural site. Detailed $PM_{2.5}$ chemical speciation was conducted, including organic carbon (OC), elemental carbon (EC), water-soluble OC (WSOC), ionic species, tens of trace metals, and over one hundred of solvent-extractable organic compounds. In particular, this research focused on primary and secondary organic molecular markers in airborne $PM_{2.5}$, which were identified and quantified by the gas chromatography/mass spectrometry (GC/MS) method, as well as source apportionment for fine OC and $PM_{2.5}$.

Our results show that organic matter, sulfate and ammonium are major components of $PM_{2.5}$ in both seasons, with significantly higher levels found in the summer; whereas nitrate is important only in the winter. Sulfate dominates $PM_{2.5}$ in the summer, particularly on haze days. Homogeneous distributions of WSOC reflect impacts from SOA in the summer and from biomass burning emissions in the winter. Primary organic compounds usually exhibit different attributes of day vs. night, whereas secondary organic tracers vary little. Much higher concentrations of automotive-related primary species, especially EC and some primary organic compounds are observed at the roadside site. Season-specific on-road mobile source profiles were developed by using differences in chemical species concentrations between the roadside site and the nearby

campus site. Calculated on-road source profiles differ from mobile source profiles measured in laboratory elsewhere. Significant seasonal differences are observed for 2-methyltetrols, *cis*-pinonic acid and pinic acid, organic tracers of biogenic SOA. Little correlation is found between 2-methyltetrols with *cis*-pinonic or pinic acid, whereas *cis*-pinonic and pinic acids are strongly correlated with each other. In addition, particulate organic matter (OM) was estimated through mass balance analysis of gravimetric $PM_{2.5}$, and the OM/OC ratio was found to depend on season and location.

Source apportionment of $PM_{2.5}$ and organic carbon were performed using the molecular marker-based chemical mass balance (CMB-MM) model. Contributions of major primary sources were calculated, including diesel vehicle exhaust, gasoline vehicle exhaust, wood combustion, meat cooking, road dust, and vegetative detritus. CMB-MM modeled roadway-related source contributions (i.e., diesel vehicle exhaust, gasoline vehicle exhaust and road dust) were evaluated at the roadside site by comparing to differences of total OC measurements between the roadside site and the nearby campus site. As a particular focus of this active research, SOC contribution was estimated by four different approaches: (1) the CMB-MM model; (2) the EC tracer method; (3) the WSOC method; (4) the secondary organic tracer method. Finally, fraction boundaries of SOC in total OC were estimated at the roadside, the campus and the rural sites for the summer and the winter. Results suggest that SOC fractions in total OC usually distributed in a range with WSOC-estimated SOC as the lower bound and with CMB-MM-estimated SOC as the upper bound.

To better understand the processes impacting the aging of prescribed fire and wildfire plumes, a detailed chemical speciation of $PM_{2.5}$ and carbonaceous aerosols was

conducted by GC/MS analysis. Ambient concentrations of many organic species (levoglucosan, resin acids, retene, *n*-alkanes, and *n*-alkanoic acids) associated with wood burning emission were significantly elevated on the event days, whereas steranes, cholesterol and major polycyclic aromatic hydrocarbons (PAHs) did not show obvious increases. It is interesting to note that ambient hopanes increased significantly during wildfire smoke events, implying that hopanes, which are thought as unique tracers of mobile sources, can also be produced by thermal alteration of biogenic hopanoid precursors in the atmosphere. Strong odd over even carbon-number predominance was found for *n*-alkanes versus even over odd predominance for *n*-alkanoic acids. Observations suggest that resin acids altered during transport from burning sites to monitors. Our study also indicates that large quantities of biogenic VOCs and semivolatile organic compounds (SVOCs) were released both as products of combustion and unburned vegetation heated by the fire. Higher leaf temperature can stimulate biogenic VOC and SVOC emissions, which enhance formation of SOA in the atmosphere. This is supported by elevated ambient concentrations of secondary organic tracers (dicarboxylic acids, 2-methyltetrols, *cis*-pinonic acid, and pinic acid). An approximate source profile was built for the aged fire plume to help better understand the evolution of wood smoke emissions and for use in source impact assessment.

CMB-Regular and CMB-MM approaches were used and compared in this study to obtain source apportionment of $PM_{2.5}$ data from the Southeastern Aerosol Research and Characterization Study (SEARCH) project. Temporal (winter and summer) and spatial impacts (urban and rural) on source contributions were analyzed. Results indicate a few similarities in source contributions between the two approaches. Secondary sources

including secondary sulfate, ammonium, and nitrate contribute the majority of $PM_{2.5}$ mass in the Southeast in both summer (>50%) and winter (>40%). Motor vehicle exhaust and wood burning are the major primary sources of $PM_{2.5}$ in this area. Motor vehicle exhaust, paved road dust and wood burning impacts were calculated using both CMB-Regular and CMB-MM. However, the differences in source apportionments between the two approaches are sometimes rather great. This disagreement can be traced to differences in: (1) fitting species selected; (2) source category identified; (3) source profile applied; and (4) model uncertainty generated.

CHAPTER 1

INTRODUCTION

1.1 Research Motivation

Airborne particulate matter (PM), especially fine particulate matter ($PM_{2.5}$, particles with an aerodynamic diameter equal to or less than 2.5 μm), has been linked to adverse human health effects, reduced visibility, climate change, and other air quality concerns. Over the past decades, numerous epidemiological studies have proposed that long-term and even short-term PM exposure could lead to acute or chronic adverse impacts on human health such as increased rates of cardiopulmonary morbidity and mortality, elevated hospitalization for respiratory disease, declines in lung function, and aggravated asthma [*Dockery et al.*, 1993; *Pope et al.*, 1995; *Pope*, 2007]. New statistical evidence further indicates that a reduction in exposure to ambient $PM_{2.5}$ would significantly improve life expectancies in the United States [*Pope et al.*, 2009]. As a direct consequence of such health studies, the U.S. Environmental Protection Agency (USEPA) established the National Ambient Air Quality Standard (NAAQS) for ambient $PM_{2.5}$ in 1997. This standard was further enhanced in 2006 with the effective criteria of 35 and 15 μg m^{-3} for 24-hr and annual average ambient $PM_{2.5}$ concentrations, respectively.

With the properties of light scattering and light absorbing in the atmosphere, particulate matter goes beyond the human health effects and can play an important role in visibility reduction and global climate change [*Charlson et al.*, 1992; *IPCC*, 2007; *Malm et al.*, 1994; *Sloane et al.*, 1991]. $PM_{2.5}$, for example, is considered to be a major factor to

reduce visibilities and cause hazes in the United States, including many national parks and wilderness areas (http://www.epa.gov/visibility). Atmospheric aerosols also influence the radiative budget of the Earth-atmosphere system directly and indirectly, thereby impacting global climate conditions [*Haywood and Boucher*, 2000]. In addition, deposition of PM can affect surface soil, water, vegetation, and even the diversity of ecosystems (http://www.epa.gov/acidrain/effects).

Typically, the major contributors of $PM_{2.5}$ include mobile source emissions, biomass burning, and secondary sources with anthropogenic and biogenic nature in origin. The metropolitan Atlanta, GA area, located in the southeastern U.S and populated by over 5.4 million residents, is of particular interest for air quality study and air pollutant control due to high emissions of mobile sources, biomass burning, coal-fired power plants and biogenic volatile organic compounds (VOCs), with vigorous photochemical processes occurring as well. The Atlanta metropolitan area is growing as the eighth largest urban region in the United States and the most populous in the southeastern United States (http://www.census.gov/Press-Release/www/releases/archives/population). With a large population and low residence density, Atlanta has the highest number of total daily vehicle miles traveled (DVMT) in the U.S., ranked fifth among the American urbanized areas according to the Federal Highway Administration (FHWA) annual report [*U.S DOT*, 2001]. As a result, large amounts of air pollutants ($PM_{2.5}$, ozone, etc.) or their precursors are emitted by the on-road motor vehicles in this area.

Biomass burning, including wildland fire and industrial and residential wood burning, is another major contributor of $PM_{2.5}$ in the southeastern U.S. Wildland fire (wildfire and prescribed burning) is estimated to contribute about 20% of total $PM_{2.5}$

emissions in the United States [*U.S. EPA*, 2000]. In 2007, a total of 85,705 wildland fires were reported nationally to burn 37,749 square kilometers, 170% above the 10-year average [*NIFC*, 2008]. Among these burned forests, over 60% were treated with wildfires. The frequency and intensity of wildfire are expected to increase in the future as a result of climate change, which is elevating spring and summer temperatures [*Flannigan et al.*, 1998; *Westerling et al.*, 2006]. During the same period, 12,744 square kilometers of wildlands were treated with prescribed fires, which is 1,732 square kilometers above the previous year's total and is the highest since 1998 [*NIFC*, 2008]. The Southern Geographic Area where Georgia is located usually has the most prescribed fire projects and acres treated. Such large and increasing emission contributions are of concern to air quality managers and policy makers, particularly in the areas with active prescribed fires and wildfires, large urban populations, and local air qualities near or above the applicable air quality standards such as the southeastern U.S. The prescribed fires, for example, on February 28, 2007 in Georgia and later the Georgia–Florida massive wildfires lasting from April through June severely impacted the metropolitan Atlanta and nearby areas with thick wood smoke (haze) for hours and even days at a time [*Hu et al.*, 2008; *Lee et al.*, 2008].

Secondary aerosols originating either from anthropogenic or biogenic sources are also thought to be a significant contributor to airborne $PM_{2.5}$, especially in summer time. In Atlanta, for example, over half of the $PM_{2.5}$ mass has been estimated to be secondary [*Kim et al.*, 2003; *Zheng et al.*, 2002] due to strong atmospheric photochemical process and abundant emissions of $PM_{2.5}$ gas precursors such as sulfur dioxide (SO_2), nitrogen oxides (NO_x), gaseous ammonia, as well as anthropogenic and biogenic VOCs. The main

secondary $PM_{2.5}$ components include particulate sulfate (SO_4^{2-}), nitrate (NO_3^-), ammonium (NH_4^+), and secondary organic aerosol (SOA). Their gas precursors are emitted by combustion of fossil fuels (coal, diesel and gasoline, etc.), agricultural and industrial activities, and natural processes. In particular, biogenic secondary sources are increasingly considered to be important in the areas with intensive emissions of biogenic VOCs, such as in the forest-rich southeastern U.S. (67% of the state land in Georgia is forest [*U.S. Forest Service*, 2004]).

Impacted by these primary emissions and secondary sources, Atlanta and its surrounding areas are still struggling to attain the NAAQS, and are ranked among the most polluted cities in the country, e.g., sixth for highest levels of year-round soot, and 12th for ground-level ozone (www.lungusa.org). Wholly or in part, 27 counties in Georgia, which are mostly located in the metro Atlanta and nearby areas, are designated as non-attainment areas for ambient $PM_{2.5}$ concentrations by the U.S EPA (http://www.epa.gov/air/oaqps/greenbk/qnay). In 2007, the 24-hr $PM_{2.5}$ and 8-hr O_3 levels in Atlanta exceeded the NAAQS on 24 and 29 days, respectively [*Georgia EPD*, 2007]. As a complex mixture of many components, $PM_{2.5}$ can be either emitted directly by primary sources or formed from precursors through photochemical processes in the atmosphere. Effective strategies to control airborne $PM_{2.5}$ first require a detailed investigation and understanding of the $PM_{2.5}$ chemical composition in the Atlanta area, including organic matter (OM), water-soluble OC (WSOC), elemental carbon (EC), ionic species (sulfate, nitrate, ammonium, etc.), and trace metals.

1.2 $PM_{2.5}$ Composition and Speciation

Although previous studies have reported chemical composition of airborne $PM_{2.5}$ and particulate OM in the Atlanta area and the southeastern U.S. [*Baumann et al.*, 2003; *Edgerton et al.*, 2005; 2006; *Hansen et al.*, 2003; *Zheng et al.*, 2002; *Zheng et al.*, 2006b], few research has explored detailed composition of $PM_{2.5}$ and OM, which is immediately impacted and dominated by on-road vehicular emissions. Moreover, local source composition profiles of mobile emissions, a major source of primary $PM_{2.5}$ and OM, have not yet been investigated in the southeastern U.S. As a result, source profiles developed in laboratory and elsewhere (e.g., in California [*Cooper et al.*, 1987; *Lough et al.*, 2007; *Schauer et al.*, 1999b; 2002b] and Colorado [*Watson et al.*, 1998]) were used in the previous source apportionment studies in this area [*Lee et al.*, 2007; *Marmur et al.*, 2005; *Zheng et al.*, 2002; *Zheng et al.*, 2007]. This could result in significant errors in source contributions estimated by receptor models owing to seasonal and regional inconsistencies of the emission profiles. Previous studies have proposed that the dilution and cooling processes applied to the present laboratory emission test samplers cannot accurately represent the real-world atmospheric mixing, and would result in significant bias in source profiles tested in laboratory [*Donahue et al.*, 2006; *Lipsky and Robinson*, 2006; *Shrivastava et al.*, 2006]. Seasonal variations of mobile source compositions due to cold start of vehicles and gas-particle partitioning were also mentioned elsewhere [*Lough et al.*, 2005a; *Robinson et al.*, 2007]. To better examine the $PM_{2.5}$ composition directly impacted by on-road emissions and to assess in-use mobile source profiles for different seasons in the southeast U.S., 12-hr and 24-hr field experiments were performed in urban Atlanta, adjacent to a freeway (roadside) and 400 m away (near-road), as well as at a

rural site, with particular focus on on-road emissions, regional transport, secondary source effects and seasonal variations of $PM_{2.5}$ composition.

As a complex mixture of many organic compounds, OM is typically a major component in ambient $PM_{2.5}$ in most areas, accounting for up to 80% of the $PM_{2.5}$ mass [*Hansen et al.*, 2003; *Turpin et al.*, 2000]. Previous studies also have shown that the major component of $PM_{2.5}$ from forest burning events is OM, making up 30–70% of $PM_{2.5}$ mass [*Nopmongcol et al.*, 2007; *Robinson et al.*, 2004; *Ward et al.*, 2006]. However, detailed data speciating OM in $PM_{2.5}$ impacted by wildland fires is sparse, and even less data is available for aged plumes. During the February 28, 2007 prescribed burning event, hourly ambient OC reached 72 $\mu g\ m^{-3}$ and contributed approximately 51% of the ambient $PM_{2.5}$ in Atlanta [*Lee et al.*, 2008]. From April through June 2007, massive wildfires led to dozens of hazy days over vast areas and a few metropolitan cities including Atlanta, Miami, FL and Birmingham, AL. The maximum 24-hr OC of up to 80 $\mu g\ m^{-3}$ was found in the plumes and the average 24-hr ambient OC made up 40–55% of $PM_{2.5}$ mass, or 60–85% of $PM_{2.5}$ mass when converted to OM by a factor of 1.5 [*Lee et al.*, 2008]. These smoke events provide special opportunities to characterize OM in such carbonaceous aerosols, to further understand atmospheric processes that impact the aging of fire plumes, to assess formation of biogenic SOA enhanced by wildland fires, and to approximate the source composition profiles of prescribed burning and wildfire emissions, which can be used for future source apportionment studies.

One method to develop a more detailed understanding of the composition of particulate organic matter is gas chromatography/mass spectrometry (GC/MS), allowing hundreds of organic compounds to be identified and quantified such as *n*-alkanes,

hopanes, steranes, *n*-alkanoic acids, alkanedioic acids, polycyclic aromatic hydrocarbons (PAHs), resin acids, and others (syringols, levoglucosan, cholesterol, 2-methyltetrols, etc.). Many of these compounds are relatively unique tracers for certain sources and widely used to track specific sources of carbonaceous aerosols [*Cass*, 1998; *Claeys et al.*, 2004a; *Kavouras et al.*, 1998; *Simoneit*, 2002; *Yu et al.*, 1999b].

In brief, hopanes and steranes are emitted from both gasoline- and diesel-powered vehicles [*Simoneit*, 1985; *Zielinska et al.*, 2004] and have been widely used as molecular markers of vehicular emissions in source apportionment of $PM_{2.5}$ and OC [*Fraser et al.*, 2003b; *Schauer et al.*, 1996; *Zheng et al.*, 2002; *Zheng et al.*, 2006b; *Zheng et al.*, 2007]. Cholesterol, found in animal fats and oils, is thought to be an excellent molecular marker of meat cooking emissions [*Rogge et al.*, 1991]. Vegetative detritus emissions are characterized by high-molecular weight *n*-alkanes with pronounced odd over even carbon number predominance [*Rogge et al.*, 1993a]. Source impacts from biomass burning are usually traced through levoglucosan, resin acids, syringols, and retene. As a pyrolysis product of cellulose in wood biopolymers, levoglucosan has been considered a particularly useful molecular marker of biomass burning [*Simoneit et al.*, 1999]. Resin acids are thermal alteration products of coniferous wood resins and emitted exclusively from softwood burning (various pines, firs, etc.) [*Rogge et al.*, 1998; *Simoneit et al.*, 1993; *Standley and Simoneit*, 1994]. In contrast, hardwood combustion produces much higher quantities of syringols [*Hawthorne et al.*, 1988; *Hawthorne et al.*, 1989]. Although PAHs are emitted from multiple combustion processes of fuels (biomass, natural gas, diesel, and gasoline) and ubiquitous in the atmosphere, retene, a thermal alteration of

abietane compounds (resin diterpenoids), is considered as an organic tracer specific for coniferous wood burning [*Ramdahl*, 1983].

In addition to primary components of $PM_{2.5}$, SOA formation can result from gaseous emissions of isoprenoids (isoprene and monoterpene) [*Claeys et al.*, 2004a; *Kavouras et al.*, 1998]. Isoprene and monoterpene are the top two prevalent precursors of biogenic SOA. Liao et al. estimated that 58.2% and 37.3% of biogenic SOA come from isoprene and monoterpene emissions, respectively [*Liao et al.*, 2007]. A few biogenic SOA species linked to isoprene and monoterpene-derived $PM_{2.5}$ have been identified and quantified including 2-methyltetrols (oxidation products of isoprene), *cis*-pinonic acid and pinic acid (oxidation products of monoterpene) [*Claeys et al.*, 2004a; *Claeys et al.*, 2004b; *Yu et al.*, 1999a; *Yu et al.*, 1999b]. Although dicarboxylic acids (alkanedioic acids and dicarboxylic aromatic acids) can be emitted from various primary sources (mobile emission, meat cooking, etc.), previous studies suggest that atmospheric photochemical formation is probably the main source [*Fine et al.*, 2004b; *Fraser et al.*, 2003a; *Yan et al.*, 2008a]. Thus, field measurements of these compounds provide information on biogenic SOA source contributions to ambient $PM_{2.5}$.

1.3 Source Apportionment of $PM_{2.5}$ and OC

Effective control strategies for air pollutants require quantitative identification of specific source impacts on ambient air quality. Unfortunately, only a small fraction of OM in aerosols can be characterized quantitatively on the molecular level by current speciation methodologies, e.g., GC/MS, and the majority of $PM_{2.5}$ organic matter is unextractable and nonelutable [*Zheng et al.*, 2002]. However, this small fraction of

elutable compounds contains species which can be used as tracers for major sources of primary OC, and then major source contributions to $PM_{2.5}$ and organic aerosols can be calculated by source apportionment modeling with organic tracers measured in extractable and elutable fraction.

One of most popular approaches to calculate source contributions for $PM_{2.5}$ is the chemical mass balance (CMB) air quality model. As a receptor model, the CMB model has been widely applied for source apportionment of ambient pollutants, especially PM [*Friedlander*, 1973; *Hopke*, 2003; *Kowalczyk et al.*, 1978; *Miller et al.*, 1972; *Watson*, 1979; *Watson et al.*, 1984; *Watson et al.*, 1990; *Watson et al.*, 1994; *Watson et al.*, 2002]. The CMB model is based on a variety of assumptions: 1) compositions of source emissions are constant over the period of ambient and source sampling; 2) chemical species are relatively stable and conservative during transport from emissions to the receptor; 3) major sources contributing to the receptor are included in the model; 4) the number of source categories is less than the number of chemical species; 5) source profiles are linearly independent of each other (without collinear problems); and 6) measurement uncertainties are random, uncorrelated, and normally distributed [*U.S. EPA*, 2004]. Mathematically, the fundamental principle of CMB can be expressed as:

$$C_{ik} = \sum_{j=1}^{m} a_{ij} S_{jk} + e_{ik} \qquad i = 1,2,.....,n$$

where C_{ik} is the ambient concentration of chemical species i at a specific receptor site k; a_{ij} is the fraction of chemical species i in the OC (or $PM_{2.5}$) emission from source j, also called source profile abundances; S_{jk} is the contribution of source j to the OC (or $PM_{2.5}$) concentration at the receptor site k; and e_{ik} is error term.

Historically, elemental and ionic species were first applied in the inorganic species-based CMB (CMB-Regular) model to apportion source contributions [*Cass and Mcrae*, 1983; *Chan et al.*, 1999; *Chen et al.*, 2001; *Chow et al.*, 1992; *Chow et al.*, 1995; *Cooper and Watson*, 1980; *Gordon*, 1980; *Hidy and Venkataraman*, 1996; *Ward and Smith*, 2005]. However, the CMB-Regular approach is limited in its ability to distinguish contributions of some important or potentially important sources of OC and $PM_{2.5}$, such as diesel vehicle exhaust, gasoline vehicle exhaust, wood combustion, meat cooking, vegetative detritus, and natural gas combustion. Through introducing organic molecular markers, some of which are reasonably unique tracers for specific sources, to the CMB-Regular model, the molecular marker-based CMB (CMB-MM) model was first developed by Schauer et al. (1996) and have been widely applied in source apportionment studies [*Fraser et al.*, 2003b; *Schauer et al.*, 1996; *Schauer*, 1998; *Schauer and Cass*, 2000; *Sheesley et al.*, 2004; *Zheng et al.*, 2002; *Zheng et al.*, 2006b; *Zheng et al.*, 2007].

Typically, CMB-MM is used to apportion source contributions to primary OC (POC) in $PM_{2.5}$, which is emitted directly from primary sources, e.g., mobile sources, biomass burning, and meat cooking. Source contribution to secondary OC (SOC) cannot be obtained directly through CMB-MM modeling, but is usually estimated by the difference between measured total OC and POC identified by CMB-MM [*Schauer et al.*, 1996; *Zheng et al.*, 2002]. This would lead to large uncertainties when the estimated POC is greatly biased owing to a lack of local and representative emission source profiles in the methodology. Recent studies indicate that CMB-MM source apportionment results are sensitive to the emission source profiles applied in the model [*Lough and Schauer*,

2007; *Robinson et al.*, 2006c; *Subramanian et al.*, 2006; 2007]. It is very hard to effectively assess those modeled contributions from primary and secondary sources without knowledge of real-world emissions and formation of ambient $PM_{2.5}$.

On the other hand, SOC is a major component of total OC, especially in summer when vigorous photochemical processing, together with enhanced VOC emissions, promotes formation of SOA in the atmosphere. In the southeastern U.S and California areas, 30–80% of the total OC in summer is estimated as SOC with different approaches [*Hildemann et al.*, 1993; *Turpin and Huntzicker*, 1995; *Zheng et al.*, 2007]. However, very few studies have assessed uncertainties or errors associated with SOC estimates. The current knowledge about atmospheric formation, condensation/partition, and composition of SOA is still very poor, and no direct measurement of SOA is available. Thus, SOC estimates are primarily performed indirectly. Other than the CMB-MM approach, the EC tracer method is widely applied to separate SOC from POC based on a large set of ambient OC/EC observations in the same location [*Chu*, 2005; *Turpin and Huntzicker*, 1995]. Recent studies also propose using WSOC as an indicator of SOC since it usually correlated to SOA formation, especially in summer [*Kondo et al.*, 2007; *Miyazaki et al.*, 2006; *Weber et al.*, 2007]. Furthermore, new developments on smog chamber irradiation experiments provided a different approach, called the secondary organic tracer method, which was used to estimate major source contributions to fine SOC originating from some prevalent gaseous precursors, such as isoprene and monoterpene [*Edney et al.*, 2005; *Kleindienst et al.*, 2007a; *Offenberg et al.*, 2007].

In order to identify and quantify the impacts of specific emission sources on air quality in the metropolitan Atlanta and surrounding areas, the CMB-MM approach was

used for source apportionment of fine organic carbon and $PM_{2.5}$ at the roadside, urban and rural sites in the summer and the winter. As a focus of active research, mobile source contributions identified by CMB-MM were compared to the measured OC from the roadside and nearby sites. Intercomparisons of SOC estimates from the four approaches described above provide helpful information for evaluating CMB-MM performance and better understanding SOA composition in $PM_{2.5}$. In addition, both the CMB-MM and CMB-Regular approaches were employed for source apportionment of $PM_{2.5}$ to identify and quantify the impacts of specific emission sources on air quality in the southeastern U.S. The CMB results calculated from the two approaches can help provide more comprehensive information of major sources in this region. Furthermore, intercomparison between the two approaches can also be used to evaluate and improve CMB source apportionment applications and to better understand their limitations.

1.4 Structure and Scope of the Thesis

The principal objectives of this study are (1) to characterize airborne $PM_{2.5}$ and fine organic matter impacted by on-road mobile emissions, biomass burning, and secondary sources; (2) to develop locally or seasonally representative source profiles for on-road emissions and aged wildland fire emissions; and (3) to apportion and assess the contributions from these major $PM_{2.5}$ sources. This section provides an overview of the research presented in the following chapters.

Chapter 2: Roadside, urban and rural comparison of primary and secondary organic molecular markers in ambient $PM_{2.5}$. Detailed speciation of $PM_{2.5}$ carbonaceous aerosols was conducted by GC/MS analysis at the roadside, urban and rural

sites with particular focus on automotive-related primary organic compounds and biogenic secondary organic tracers. Day–night, seasonal and spatial variations of $PM_{2.5}$ organic composition were investigated. Season-specific on-road mobile source primary OC profiles were developed by using differences in organic species concentrations between the roadside site and the nearby campus site. Seasonal differences and inter-correlation were studied for organic tracers of biogenic SOA, including 2-methyltetrols, *cis*-pinonic acid and pinic acid.

Chapter 3: Characterization of airborne $PM_{2.5}$ at roadside, urban and rural sites in the summer and the winter. $PM_{2.5}$ filter samples (12- and 24-hr) were collected in the summer and the winter from three sites: two from urban Atlanta (one site adjacent to a freeway and another 400 m away), and one at a rural site. Detailed $PM_{2.5}$ composition was investigated including OC, EC, WSOC, ionic species and trace metals, as well as their day–night, seasonal and spatial variations. Season-specific on-road mobile source primary $PM_{2.5}$ profiles were developed for this region by using differences in individual species concentrations between the roadside site and the nearby urban site. Particulate organic matter (OM) was estimated through mass balance analysis of gravimetric $PM_{2.5}$, and WSOC was also investigated spatially and seasonally.

Chapter 4: Source apportionment of $PM_{2.5}$ organic carbon and SOA impact: spatial and temporal variations. Major source contributions to ambient $PM_{2.5}$ and OC in the metropolitan Atlanta and surrounding areas were apportioned using the molecular marker-based chemical mass balance (CMB-MM) model. The calculated source contributions, especially secondary OC contributions, were assessed by the masured OC differences and the results from other source apportionment approaches, including the EC

tracer method (i.e., OC/EC ratio), WSOC measurements (i.e. correlation between WSOC and SOA or biomass burning), and the secondary organic tracer method (i.e., biogenic SOA yields estimated by the chamber irradiation experiments). Fraction boundary of SOC estimate in total measured OC was approximated for the urban and rural areas in the summer and the winter.

Chapter 5: Organic composition of carbonaceous aerosols in an aged prescribed fire plume. Detailed speciation of carbonaceous aerosols was conducted for aged smoke from a prescribed fire (dominated by conifers) by GC/MS analysis. Before, on, and after the smoke event, ambient wood burning-derived organic species were investigated including levoglucosan, resin acids, retene, *n*-alkanes, and *n*-alkanoic acids. An approximate source profile was built for the aged fire plume to help better understand the evolution of wood smoke emissions and for use in source impact assessment. In addition, ambient concentrations of secondary organic tracers (dicarboxylic acids, 2-methyltetrols, *cis*-pinonic acid and pinic acid) were measured to explore emissions of biogenic volatile organic compounds (VOCs) and semivolatile organic compounds (SVOCs), which are significantly enhanced by higher leaf temperatures in the fire.

Chapter 6: Detailed chemical characterization and aging of wildfire aerosols in the southeastern U.S. The intensive Georgia–Florida wildfire smoke events occurred in a warm and photochemically reactive season (from April through June, 2007) in the southeastern U.S. The plumes were sampled by several downwind monitors at different distances away from the fires. Detailed composition of wildfire-derived $PM_{2.5}$ was explored with particular focus on development of aged wildfire emission source profiles and evolution processes of particulate organic compounds associated with biomass

burning during transport from the wildfire location to the monitors. Impact of wildfire-enhanced biogenic SOA was studied by measured secondary organic tracers, including dicarboxylic acids, 2-methyltetrols, *cis*-pinonic acid and pinic acid. Furthermore, thermal alteration of biological hopanes to geological hopanes was studied.

Chapter 7: Analysis of source apportionment applications for $PM_{2.5}$ in the Southeast: intercomparison between two approaches. Both CMB-Regular and CMB-MM approaches were used and compared for conducting source apportionment of ambient $PM_{2.5}$ data from the Southeastern Aerosol Research and Characterization Study (SEARCH) project. Temporal (winter and summer) and spatial impacts (urban and rural) on source contributions were analyzed. The possible reasons, which cause disagreements between the two approaches, were discussed including fitting species, source category, source profile, and model uncertainty. Intercomparison between the two approaches provides more comprehensive information of major sources in this region. Such analysis can be used to evaluate and to improve CMB source apportionment applications and to better understand their limitations.

Chapter 8: Conclusions and future research. The major conclusions and findings of this research are summarized. Future work are described or suggested to extend this research.

CHAPTER 2

ROADSIDE, URBAN AND RURAL COMPARISON OF PRIMARY AND SECONDARY ORGANIC MOLECULAR MARKERS IN AMBIENT PM2.5

(Bo Yan, Mei Zheng, Yongtao Hu, Xiang Ding, Amy P. Sullivan, Rodney J. Weber, Jaemeen Baek, Eric S. Edgerton, and Armistead G. Russell. *Environmental Science & Technology*, 43 (12), 4287-4293, 2009)

Abstract

$PM_{2.5}$ filter samples (12- and 24-hr) were collected in urban Atlanta, GA, next to a freeway and 400 m away, as well as at a rural site, with particular focus on exploring on-road emissions, regional transport and biogenic effects. Detailed speciation of $PM_{2.5}$ carbonaceous aerosols was conducted by GC/MS. Diurnal, seasonal and spatial variations of $PM_{2.5}$ organic composition were investigated. Primary organic compounds usually exhibit different attributes of day vs. night while secondary organic tracers varied little. Much higher concentrations of automotive-related primary organic compounds are observed at the roadside site, including *n*-alkanes, hopanes, steranes, and polycyclic aromatic hydrocarbons (PAHs). Season-specific on-road mobile source primary OC profiles were developed by using differences in organic species concentrations between the roadside site and the nearby site. Calculated on-road source profiles differ from mobile source profiles measured in the lab. Significant seasonal differences are observed for 2-methyltetrols, *cis*-pinonic acid and pinic acid, organic tracers of biogenic secondary

organic aerosols (SOA). Little correlation is found between 2-methyltetrols with *cis*-pinonic or pinic acid, though *cis*-pinonic and pinic acids are strongly correlated.

2.1 Introduction

Epidemiological studies suggest that exposure to fine particulate matter ($PM_{2.5}$) is associated with adverse health effects [*Dockery et al.*, 1993; *Pope et al.*, 2002], and sources of organic compounds appear to be of particular interest [*Sarnat et al.*, 2008]. Organic matter is one of major components in ambient $PM_{2.5}$ in most areas, accounting for up to 80% of the $PM_{2.5}$ mass [*Hansen et al.*, 2003; *Turpin et al.*, 2000]. As a complex mixture of many organic compounds, particulate organic matter can be either emitted directly by primary sources or created from chemical reactions in the atmosphere. One method to develop a more detailed understanding of the composition of particulate organic matter is gas chromatography/mass spectrometry (GC/MS), allowing hundreds of organic compounds to be identified and quantified. Many of these compounds are relatively unique tracers for certain sources and widely used to track specific sources of carbonaceous aerosols [*Cass*, 1998; *Claeys et al.*, 2004a; *Kavouras et al.*, 1998; *Simoneit*, 2002; *Yu et al.*, 1999b].

Although previous studies of $PM_{2.5}$ composition in the southeastern U.S have been reported [*Zheng et al.*, 2002; *Zheng et al.*, 2006b], few studies have investigated detailed chemical composition of carbonaceous aerosols that are immediately impacted and dominated by on-road vehicular emissions. Moreover, local source profiles of mobile emissions, a major source of primary organic matter and $PM_{2.5}$, have not been developed for the Southeast. Consequently, source profiles developed elsewhere have been used in

previous research on source apportionment [*Zheng et al.*, 2002; *Zheng et al.*, 2007]. Due to seasonal and regional inconsistency of source composition profiles, this could result in errors in source contributions estimated by receptor models. This study uses roadside, near-road and rural speciated organic $PM_{2.5}$ measurements to assess in-use mobile source profiles for the summer and winter.

Secondary organic aerosols (SOA) are also thought to be a significant contributor to particulate organic matter, especially in the summer when over half of organic matter in the $PM_{2.5}$ mass has been estimated to be SOA [*Bhave et al.*, 2007; *Lim and Turpin*, 2002; *Zheng et al.*, 2007]. SOA is produced in the atmosphere through photochemical oxidation of anthropogenic and biogenic volatile organic compounds (VOCs). Biogenic secondary sources are increasingly considered an important contributor to SOA in the areas with intensive emissions of biogenic VOCs, such as in the forest-rich southeastern U.S (e.g., 67% of the state land in Georgia is forest [*U.S. Forest Service*, 2004]). Isoprene and monoterpene are the top two prevalent precursors of biogenic SOA. Liao et al. estimated that 58.2% and 37.3% of biogenic SOA come from isoprene and monoterpene emissions, respectively [*Liao et al.*, 2007].

A few distinct SOA tracers linked to isoprene and monoterpene-derived $PM_{2.5}$ have been identified and quantified from ambient samples, including 2-methyltetrols (oxidation products of isoprene), *cis*-pinonic acid and pinic acid (oxidation products of monoterpenes) [*Claeys et al.*, 2004a; *Kavouras et al.*, 1998; *Yu et al.*, 1999b]. Although dicarboxylic acids (alkanedioic acids and dicarboxylic aromatic acids) can be emitted from various primary sources (mobile emission, meat cooking, etc.), previous studies suggested that atmospheric photochemical formation is probably the main source [*Fine et*

al., 2004b; *Fraser et al.*, 2003a; *Yan et al.*, 2008a]. Thus, field measurements of these compounds provide information on biogenic SOA source contributions to ambient $PM_{2.5}$.

To better understand the composition and sources of organic $PM_{2.5}$, field experiments were conducted in urban Atlanta, GA, next to a freeway and 400 m away, as well as at a rural site, with particular focus on off- and on-road emissions, regional transport and effects of biogenic emissions.

2.2 Experimental Section

2.2.1 Field Sampling

High-volume (Hi-Vol) particulate samplers (Thermo Anderson) and three-channel particulate composition monitors (PCM) were used to collect ambient $PM_{2.5}$ filter samples. Hi-Vol samplers (flow rate of 1.13 m^3 min^{-1}) used pre-baked quartz microfibre filters (8 x 10 in, Whatman), and PCM samplers (flow rate of 16.7 L min^{-1}) had diffusion denuders followed by pre-baked quartz microfibre filters in one channel and pre-weighed Teflon filters (47 mm, Pall Life Sciences) in the other two channels. Although it is recognized that there exist potential impacts from positive or negative artifacts on organic compound measurement without or with denuders in the Hi-Vol or PCM samplers, respectively, the reported results of organic compounds are not artifact corrected because the major organic tracers studied in this research are dominantly in a condensed phase [*Schauer et al.*, 1996].

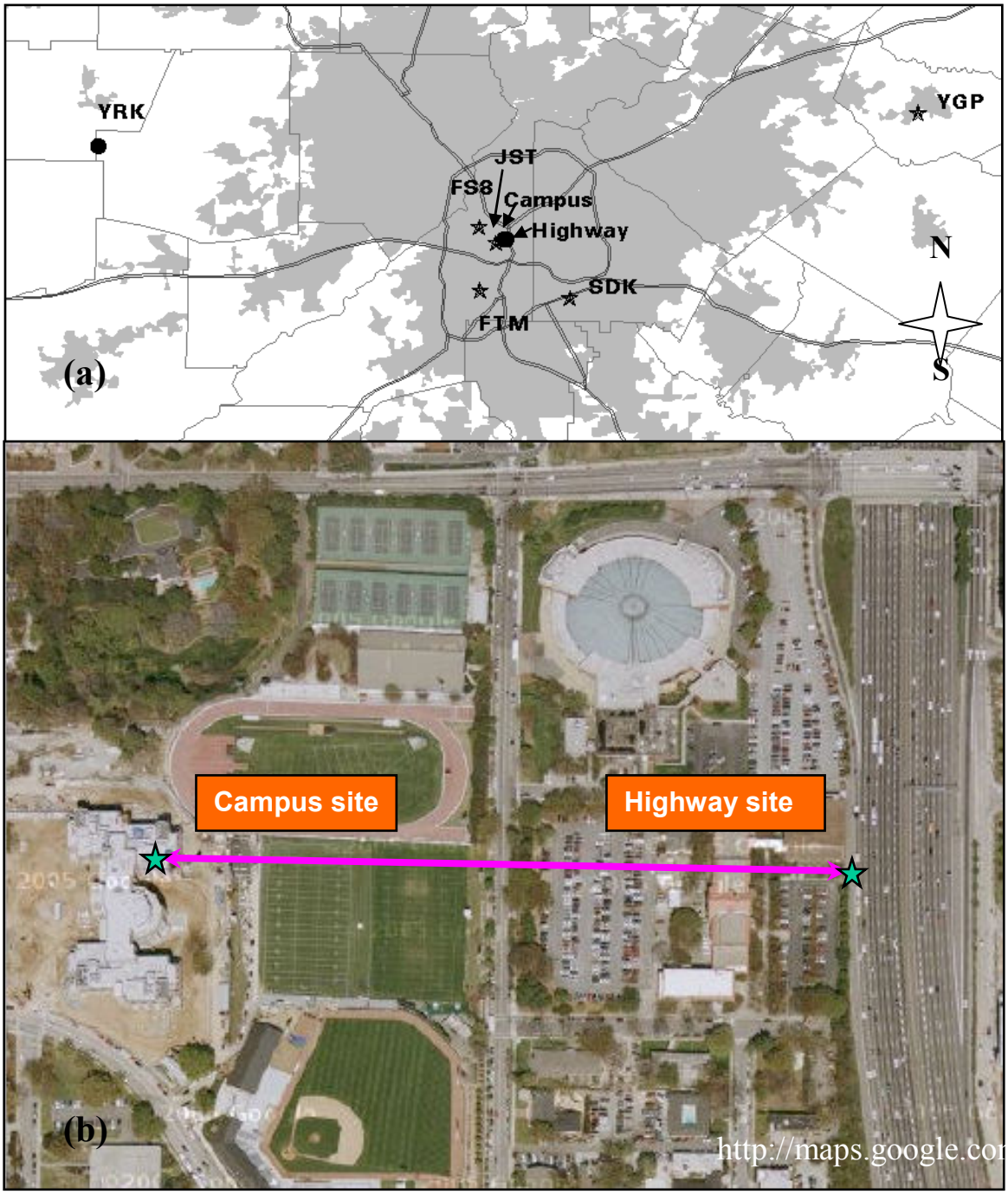

Figure 2.1. (a) Map of all sampling sites including the Highway, Campus, Jefferson Street (JST), Yorkville (YRK) and ASACA sites (FTM, FS8, SDK and YGP); (b) Highway site, 3 m away from the I-75/85 highway, and Campus site on the roof of Ford ES&T Building on the Georgia Tech campus. The prevailing winds in the metro Atlanta and Yorkville are northerly and westerly (northwesterly or southwesterly) in the summer, and northwesterly and easterly (northeasterly or southeasterly) in the winter, with variations due to local terrain and building effects in this complex urban area.

Three sampling sites were utilized (Figure 2.1): (1) an interstate highway roadside; (2) the Georgia Institute of Technology campus (400 m away from the roadside site); (3) a rural site at Yorkville, GA (impacted primarily by biogenic emissions and regional transport). The roadside site is 3 m away from the I–75/85 freeway in Midtown Atlanta that carries about 280,000 vehicles per day [*Georgia Department of Transportation.*, 2006], 97% of which are light duty, gasoline-powered vehicles [*Kall and Guensler*, 2007]. The Yorkville site, 55 km northwest of the metro Atlanta, is one of the sampling sites in the Southeastern Aerosol Research and Characterization Experiment (SEARCH) air quality monitoring network [*Hansen et al.*, 2003]. At both the roadside site and the Yorkville site, $PM_{2.5}$ samplers were operating on the ground while at Georgia Tech campus site, samplers were operating on a roof approximately 16 m above ground. These sites were complemented by a SEARCH site (the Jefferson Street (JST), 2 km southwest of Georgia Tech), four sites from the Assessment of Spatial Aerosol Composition in Atlanta (ASACA) [*Butler et al.*, 2003], and routine monitors around Atlanta (Figure 2.1).

Field sampling was carried out during two seasons: summer (June–July, 2005) and winter (January 2006). In the summer study, 12-hr (10am–10pm–10am) back-to-back sampling was conducted simultaneously at both the roadside site and the campus site on Jun 15–18, 2005 (a total of 14 samples), and 24-hr (10am–10am) measurements were taken simultaneously at both the campus site and the Yorkville site on non-rainy days on July 8–26, 2005 (16 samples). Three consecutive heavy haze days (July 24–26, 2005) were captured by the samplers at both the campus and the Yorkville sites. The 10am–10pm period is aimed at capturing photochemically formed and altered organic carbon

constituents while the 10pm–10am period is directed toward sampling when photochemistry is playing less of a role in altering organic $PM_{2.5}$ composition. Diurnal variations of some primary emissions can be explored separately by daytime and nighttime samples. For example, primary emissions from on-road rush hours (evening vs. morning), urban factories, and meat cooking are characterized by different attributes of day vs. night. Similarly in the winter study, 12-hr samples were taken simultaneously on Jan 19–26, 2006 both at the roadside site and the campus site (32 samples) and 24-hr sampling was conducted at Yorkville (7 samples).

Hi-Vol samples were analyzed for organic carbon/elemental carbon (OC/EC), water-soluble OC (WSOC), and particulate organic compounds with thermal optical transmittance (TOT), total organic carbon (TOC) analyzer, and GC/MS, respectively. PCM samples were analyzed for OC/EC, $PM_{2.5}$ mass, water-soluble ionic species, and trace metals by using TOT, gravimetry, ion chromatography (IC), and X-ray fluorescence (XRF), respectively. Details of $PM_{2.5}$ sampling (Hi-Vol and PCM) and chemical composition measurements (OC, EC, WSOC, ions and tracer metals) are described elsewhere [*Lee et al.*, 2005a; *Sullivan and Weber*, 2006].

2.2.2 Organic Speciation

Hi-Vol samples along with field blanks were analyzed for solvent-extractable organic compounds using a standardized GC/MS method and both methylation and silylation [*Nolte et al.*, 2002; *Zheng et al.*, 2002; *Zheng et al.*, 2006b]. Briefly, each filter (one half or quarter section of an entire Hi-Vol filter) is spiked with a deuterated internal standard (IS) mixture previously and then successively extracted using hexane and benzene/isopropanol (2:1, v/v) with 15-min mild sonication. There are 16 deuterated

compounds in the IS mixture solution including: benzaldehyde-*d*6, dodecane-*d*26, decanoic acid-*d*19, phthalic acid 3,4,5,6-*d*4, acenaphthene-*d*10, levoglucosan-U-^{13}C6, hexadecane-*d*34, eicosane-*d*42, heptadecanoic acid-*d*33, 4,4'-dimethoxybenzophenone-*d*8, chysene-*d*12, octacosane-*d*58, ααα-20R-cholestane-*d*4, cholesterol-2,2,3,4,4,6-*d*6, dibenz[ah]anthracene-*d*14, and hexatriacontane-*d*74. The volume of IS solution spiked into one sample depends on the measured mass of OC on the filter section extracted, i.e., 250 μL IS solution per mg OC. For each sample, two hexane sonication extractions are followed by three consecutive benzene/isopropanol extractions. After filtering, the extracts are gradually concentrated to about 250 μL with rotary evaporation followed by blowdown with ultra pure nitrogen gas. Finally, half of each concentrated extract are derivatized with fresh diazomethane to convert organic acids to their methyl esters. Diazomethane (CH_2N_2) is generated by a set of standard generator and method descried by previous study [*Zheng et al.*, 2002]. These methylated extracts are analyzed by GC/MS along with authentic standards, which contain the same IS mixture and target compounds. To quantify a few polar organic compounds (levoglucosan, cholesterol, 2-methyltetrols), underivatized remains of concentrated extracts are silylated with BSTFA (N, O-bis(trimethylsilyl)acetamide) to convert polar compounds to trimethylsilyl (TMS) derivatives. After one hour reaction at 70 ºC, these silylated extracts are immediately analyzed using GC/MS along with authentic standards that are also silylated. These derivatized $PM_{2.5}$ samples are analyzed by an Agilent GC/MSD (6890 GC / 5973N MSD) equipped with a 30 m HP-5 MS capillary column (0.25 mm i.d. and 0.25 μm film thickness). The operation parameters of GC/MSD applied in this study are same as previous experiments [*Zheng et al.*, 2002] include: 1 μL splitless injection, 4 minutes

solvent delay, 50-500 amu scan range, electron ionization (EI) mode with 70 eV. The temperature ramp of GC is set up as follow: holding at 65 ^{o}C for 2 min, increasing up to 300 ^{o}C at a rate of 10 ^{o}C/min and holding for 20 min. Identification and quantification of target organic compounds in $PM_{2.5}$ can be determined with the standardized method developed by previous studies [*Rogge et al.*, 1993a; b; *Schauer et al.*, 1996; *Schauer and Cass*, 2000; *Simoneit and Mazurek*, 1982; *Zheng et al.*, 2002]. In brief, each target organic compound in the present study was identified with its chemical characteristics and retention time, and then quantified by referring to a deuterated IS whose has similar chemical structure and retention time with the target compounds. To quantify target compounds more precisely, relative response factor (RRF) is calculated for each target compound from authentic standards.

The reported results are field blank corrected, but not adjusted for recoveries. Detailed Quality Assurance/Quality Control (QA/QC) procedures were described previously, including recoveries, detection limits (shown in Table A.1) and analysis precision for organic compounds [*Ding et al.*, 2008; *Yan et al.*, 2008a; *Zheng et al.*, 2006a; *Zheng et al.*, 2006b; *Zheng et al.*, 2007]. Briefly, an autotune and sensitivity test is always carried out before sample analysis to check performance of GC/MS instrument. If these tests met the criteria requested, a few solvent blanks are then run in GC/MS to ensure a good performance of GC column. During each sequence, the same set of authentic standards was run once separately at the beginning, middle and end of an operation sequence. Thus, three RRFs were obtained for each target compound after a sequence run and an optima factor can be calculated from the calibration curve and used to correct quantification of target compounds.

2.2.3 Trace Gas and Meteorological Data

Trace gases (O_3, SO_2, NO_2 and NO) and meteorological data (temperature, solar radiation and relative humidity) were measured at the Yorkville site and JST [*Edgerton et al.*, 2006; *Hansen et al.*, 2003].

2.3 Results and Discussion

2.3.1 Organic Matter in $PM_{2.5}$

Our measurements indicate that organic matter (OM, using an OM/OC factor of 2 [*El-Zanan et al.*, 2009]) is a major component of ambient $PM_{2.5}$ in both the summer and the winter, and accounts for 51 to 72% of the $PM_{2.5}$ mass at the urban sites, and 40 to 54% at the rural location, depending upon season (Table 2.1).

2.3.2 Day–Night Variation of Primary Organic Tracers

Diurnal trends of primary organic tracers were studied by comparing 12-hr daytime concentrations with the surrounding 12-hr nighttime data. To better exhibit variations of primary source emissions, the ambient data of organic compounds were normalized to the observed OC (Figure 2.2). Day–night differences exist for many primary organic compounds in $PM_{2.5}$, suggesting a different mix of primary sources in the day and night. *n*-Alkanes and *n*-alkanoic acids, two dominant organic compound homologues in urban $PM_{2.5}$, display higher fractions in fine organic matter in the daytime. Their average normalized data are 11±12 and 13±18 ng/μg OC in the daytime versus 7.6±10 and 7.7±9.4 ng/μg OC in the nighttime, respectively. PAHs and cholesterol also show similar trends with ratios of 2.0±2.4 and 0.12±0.20 ng/μg OC in the daytime

while 1.4±2.0 and 0.08±0.10 ng/μg OC at night. Hopanes and steranes, tracers of vehicular emissions, demonstrate very small daytime and nighttime variations (Figure 2.2). In contrast, reverse day–night variations exist for levoglucosan and resin acids, tracers of wood combustion and abundant in the winter, implying local wood combustion for residential heating at night in cold weather.

2.3.3 Spatial and Seasonal Variations of Primary Organic Tracers

Distinct spatial variations are found during both seasons (Figure 2.3). The highest concentrations of automotive-related primary organic compounds are measured at the roadside site, including *n*-alkanes, hopanes, steranes, and PAHs. Their concentrations are significantly lower at the nearby on-campus site and much lower at Yorkville. On average, the roadside concentrations are about 2.3 times higher than the campus in both seasons while the campus is 3.3 and 1.4 times higher than Yorkville in the summer and the winter, respectively (Table 2.2).

On-road vehicle emissions are a major source of *n*-alkanes, which are highest at the roadside site (40–61 ng m^{-3} in the summer and the winter, respectively), significantly lower at the campus site (19–38 ng m^{-3}), and lowest at Yorkville (2.9–19 ng m^{-3}). Vegetative detritus is another major contributor of *n*-alkanes. Vegetatively-derived *n*-alkanes homologues are characterized by an odd carbon-number predominance (carbon-number maximum C_{max}=29 or 31), especially in the warm season [*Rogge et al.*, 1993a]. Hopanes and steranes also display spatial variation, dropping by over 60% from the roadside site to the campus site in both seasons and about 30% lower than on-campus at Yorkville (Table 2.2; Figure 2.3). It is interesting that no significant seasonal difference in hopanes and steranes is observed at all sites. This observation differs from a previous

study that reported source contributions of mobile sources to organic matter and $PM_{2.5}$ are higher in winter, especially for gasoline-powered vehicle exhaust [*Zheng et al.*, 2006b]. PAHs and *n*-alkanoic acids are emitted from motor vehicles, and their concentrations tend to be 50–70% less at the campus site than by the roadway. Significantly higher PAH and *n*-alkanoic acid concentrations are observed in the winter, particularly at Yorkville, probably as a result of more biomass burning emissions. These organic compounds are largely emitted from wood combustion [*Yan et al.*, 2008a] while vehicular emissions remain relatively consistent. This is further supported by higher levels of organic tracers of biomass burning. Levoglucosan and resin acids show little spatial variation, especially in the winter when biomass burning is a major source of fine primary OC over this region. However, large seasonal variations are found for these organic tracers. Levoglucosan and resin acids are 50 and 3.4 ng m^{-3} on average in the summer compared to 239 and 22 ng m^{-3} in the winter, respectively, suggesting intensive wood burning activities (including residential, commercial and prescribed burning), and, possibly, reduced atmospheric decomposition. Seasonal differences may also be caused by reduced atmospheric dispersion and increased condensation of organic compounds at colder temperatures.

Cholesterol levels are similar at the two urban locations, and low at Yorkville. Higher concentrations are found in the winter, implying greater chemical stability and reduced atmospheric dispersion recognizing that cholesterol exists in a condensed phase in the atmosphere.

Table 2.1. Average Concentrations and Standard Divisions of Organic Compounds in $PM_{2.5}$ at the Three Sampling Sites (unit: ng m^{-3})

Organic Compound	Highway Roadside		Georgia Tech. Campus			Yorkville (YRK)	
	Summer–12	Winter–12	Summer–12	Summer–24	Winter–12	Summer–24	Winter–24
n-Alkanes	40.1 ± 22.1	60.9 ± 42.0	25.1 ± 8.11	12.8 ± 7.96	38.0 ± 46.7	2.89 ± 1.43	18.8 ± 10.6
Hopanes	6.08 ± 1.80	5.74 ± 1.89	2.42 ± 1.23	2.13 ± 0.81	1.96 ± 1.55	0.44 ± 0.18	0.55 ± 0.27
Steranes	1.89 ± 0.58	1.48 ± 0.49	0.73 ± 0.35	0.37 ± 0.28	0.53 ± 0.45	0.03 ± 0.06	0.07 ± 0.07
PAHs	11.0 ± 7.81	14.8 ± 11.5	3.19 ± 2.43	3.17 ± 2.56	4.19 ± 5.76	0.12 ± 0.06	2.19 ± 1.16
n-Alkanoic acids	67.7 ± 41.0	75.6 ± 97.0	32.0 ± 14.4	29.1 ± 20.9	39.5 ± 40.0	19.3 ± 15.4	31.0 ± 21.8
Resin acids	6.30 ± 6.78	24.1 ± 27.6	2.77 ± 2.43	3.16 ± 1.66	20.7 ± 33.3	1.38 ± 0.65	21.2 ± 25.3
Levoglucosan	58.8 ± 42.0	285 ± 241	52.1 ± 31.8	61.1 ± 31.0	215 ± 184	26.8 ± 15.0	218 ± 189
Cholesterol	0.31 ± 0.31	0.62 ± 0.64	0.30 ± 0.22	0.31 ± 0.26	0.45 ± 0.39	0.11 ± 0.11	0.27 ± 0.30
Aromatic acids	11.3 ± 6.26	11.6 ± 14.0	9.25 ± 6.37	13.6 ± 11.8	4.64 ± 4.34	3.54 ± 1.61	5.58 ± 3.89
Dicarboxylic acids	25.5 ± 15.6	46.0 ± 68.1	22.1 ± 12.7	49.1 ± 39.7	20.3 ± 20.1	39.0 ± 18.2	35.4 ± 31.5
2-Methyltetrols	6.05 ± 8.84	0.001 ± 0.004	1.32 ± 1.38	209 ± 302	0.09 ± 0.25	168 ± 123	0.77 ± 0.58
cis-Pinonic acid	22.9 ± 13.7	24.3 ± 32.2	27.9 ± 16.3	1.30 ± 1.10	28.0 ± 30.0	5.84 ± 13.2	105 ± 115
Pinic acid	2.28 ± 1.12	2.32 ± 3.37	3.11 ± 2.43	1.84 ± 1.34	1.91 ± 2.28	2.52 ± 1.40	6.25 ± 8.07
OC (μg m^{-3})	8.16 ± 1.15	5.08 ± 2.52	5.53 ± 0.98	7.34 ± 3.15	3.60 ± 2.78	4.96 ± 1.82	2.04 ± 1.54
EC (μg m^{-3})	4.06 ± 1.05	2.74 ± 1.34	0.96 ± 0.51	0.80 ± 0.35	0.89 ± 0.74	0.25 ± 0.09	0.27 ± 0.15
$PM_{2.5}$ (μg m^{-3})	22.7 ± 3.26	14.8 ± 5.24	16.4 ± 1.55	28.8 ± 14.6	11.3 ± 5.34	24.6 ± 12.0	7.60 ± 3.23
$OM/PM_{2.5}$	72%	69%	67%	51%	64%	40%	54%

Note: 'Summer–12', 'Summer–24', 'Winter–12', and 'Winter–24' denote 12-hr summer (June), 24-hr summer (July), 12-hr winter (January), and 24-hr winter (January) filer-based field samples, respectively. 'OM' indicates organic matter converted from OC by an OM/OC factor of 2 [*El-Zanan et al.*, 2009].

Table 2.2. Average Concentrations of Organic Compounds Normalized to the Georgia Tech Campus Values (Campus-12 or -24)

Organic Compounds	Highway-S12 [a]	Campus-S12 [a]	Campus-S24 [a]	YRK-S24 [b]	Highway-W12 [c]	Campus-W12 [c]	YRK-W24 [c]
Tricosane	1.57	1.00	0.32	0.22	1.68	1.00	0.69
Tetracosane	2.00	1.00	0.50	0.27	1.77	1.00	0.66
Pentacosane	1.73	1.00	0.65	0.21	1.92	1.00	0.70
Hexacosane	2.13	1.00	1.54	0.21	1.72	1.00	0.75
Heptacosane	1.16	1.00	0.68	0.25	1.41	1.00	0.73
Octacosane	1.38	1.00	1.25	0.30	1.40	1.00	0.73
Nonacosane	1.27	1.00	0.37	0.31	1.38	1.00	0.70
Triacontane	1.84	1.00	1.35	0.21	1.75	1.00	0.64
Hentriacontane	1.41	1.00	0.54	0.23	1.67	1.00	0.61
Dotriacontane	2.27	1.00	1.46	0.21	1.78	1.00	0.54
Tritriacontane	2.11	1.00	0.88	0.18	1.59	1.00	0.58
17a(H)-21b(H)-29-Norhopane	2.37	1.00	0.70	0.22	3.12	1.00	0.30
17a(H)-21b(H)-Hopane	2.55	1.00	1.01	0.21	2.83	1.00	0.28
22,29,30-Trisnorneohopane	2.36	1.00	0.80	0.49	3.19	1.00	0.41
20S,R-5a(H),14a(H),17a(H)-Cholestanes	2.30	1.00	0.63	0.31	2.57	1.00	0.24
20R-5a(H),14b(H),17b(H)-Cholestane	2.67	1.00	0.64	0.37	2.83	1.00	0.20
20S,R-5a(H),14b(H),17b(H)-Ergostanes	2.37	1.00	0.92	nd	2.86	1.00	0.19
20S,R-5a(H),14b(H),17b(H)-Sitostanes	2.70	1.00	0.98	0.23	2.56	1.00	0.22
Benzo(b)fluoranthene	3.59	1.00	1.58	0.08	3.07	1.00	0.76
Benzo(k)fluoranthene	3.62	1.00	2.16	0.07	3.11	1.00	0.81
Benzo(e)pyrene	3.78	1.00	1.52	0.07	3.45	1.00	0.69
Indeno(1,2,3-cd)fluoranthene	2.21	1.00	0.98	0.06	3.76	1.00	0.89
Indeno(1,2,3-cd)pyrene	2.41	1.00	0.93	0.08	3.49	1.00	0.75

Picene	3.19	1.00	3.96	nd	2.10	1.00	0.97
Benzo(ghi)perylene	2.41	1.00	0.81	0.05	4.40	1.00	0.56
Pimaric acid	nd	nd	nd	1.03	1.19	1.00	1.07
Sandaracopimaric acid	nd	nd	nd	0.48	1.08	1.00	1.40
Isopimaric acid	nd	nd	nd	nd	0.81	1.00	1.30
Dehydroabietic acid	3.02	1.00	1.01	0.35	1.05	1.00	1.01
Abietic acid	8.01	1.00	nd	nd	0.65	1.00	0.85
7-Oxodehydroabietic acid	0.89	1.00	1.20	0.56	1.66	1.00	1.02
Aromatic acids	1.22	1.00	1.48	0.26	2.50	1.00	1.20
n-Alkanoic acids	2.12	1.00	0.91	0.66	1.91	1.00	0.78
9-Hexadecenoic acid	nd	1.00	0.96	nd	5.09	1.00	nd
9,12-Octadecanedienoic acid	0.55	1.00	1.23	0.30	2.75	1.00	0.35
9-Octadecenoic acid	1.07	1.00	0.79	0.40	2.15	1.00	0.32
cis-Pinonic acid	0.82	1.00	0.05	4.50	0.87	1.00	3.75
Pinic acid	0.73	1.00	0.59	1.37	1.22	1.00	3.28
Dicarboxylic diacids	1.15	1.00	2.22	0.79	2.21	1.00	1.68
Nonanal	1.29	1.00	1.71	0.28	1.16	1.00	0.81
Benz(de)anthracen-7-one	4.54	1.00	1.79	0.11	3.26	1.00	0.49
Levoglucosan	1.13	1.00	1.17	0.44	1.33	1.00	1.01
Cholesterol	1.04	1.00	1.04	0.35	1.36	1.00	0.59
2-Methyltetrols	4.57	1.00	157.76	0.80	0.11	1.00	6.23

Note: ‘Highway-12’, ‘Campus-12’, ‘Campus-24’, and ‘YRK-24’ denote 12-hr highway, 12-hr campus, 24-hr campus, and 24-hr Yorkville filter-based field samples, respectively; ‘S’ and ‘W’ indicate summer and winter seasons, respectively; ‘nd’, not detected; [a] normalized to the measurements of Campus-S12; [b] normalized to the measurements of Campus-S24; [c] normalized to the measurements of Campus-W12. Units in the table: ng/ng.

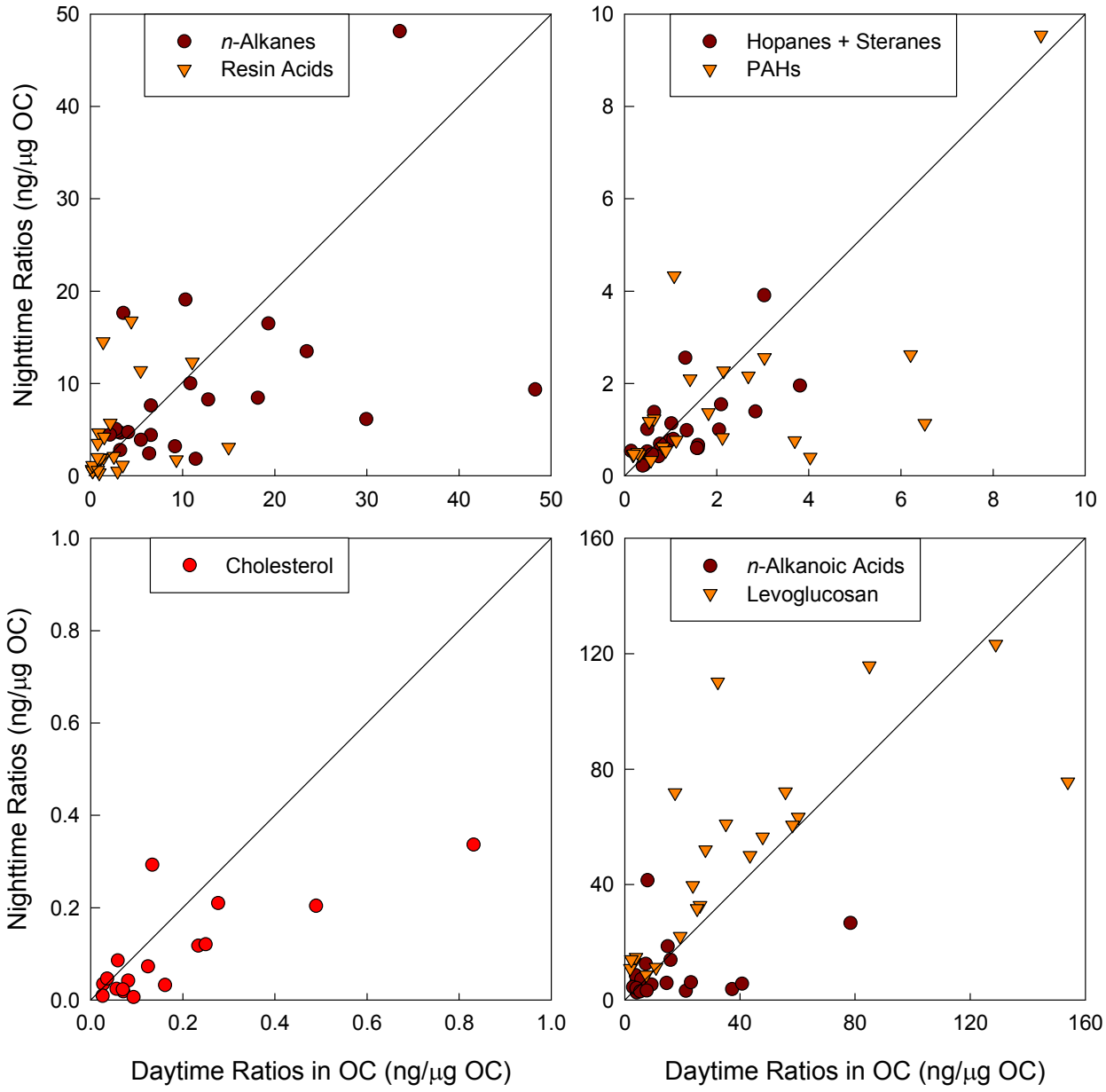

Figure 2.2. 'Nighttime' vs. 'Daytime' primary organic compounds in $PM_{2.5}$ measured at the roadside site and the campus site in the summer and the winter. All ambient concentrations of organic compounds are normalized to associated measured OC.

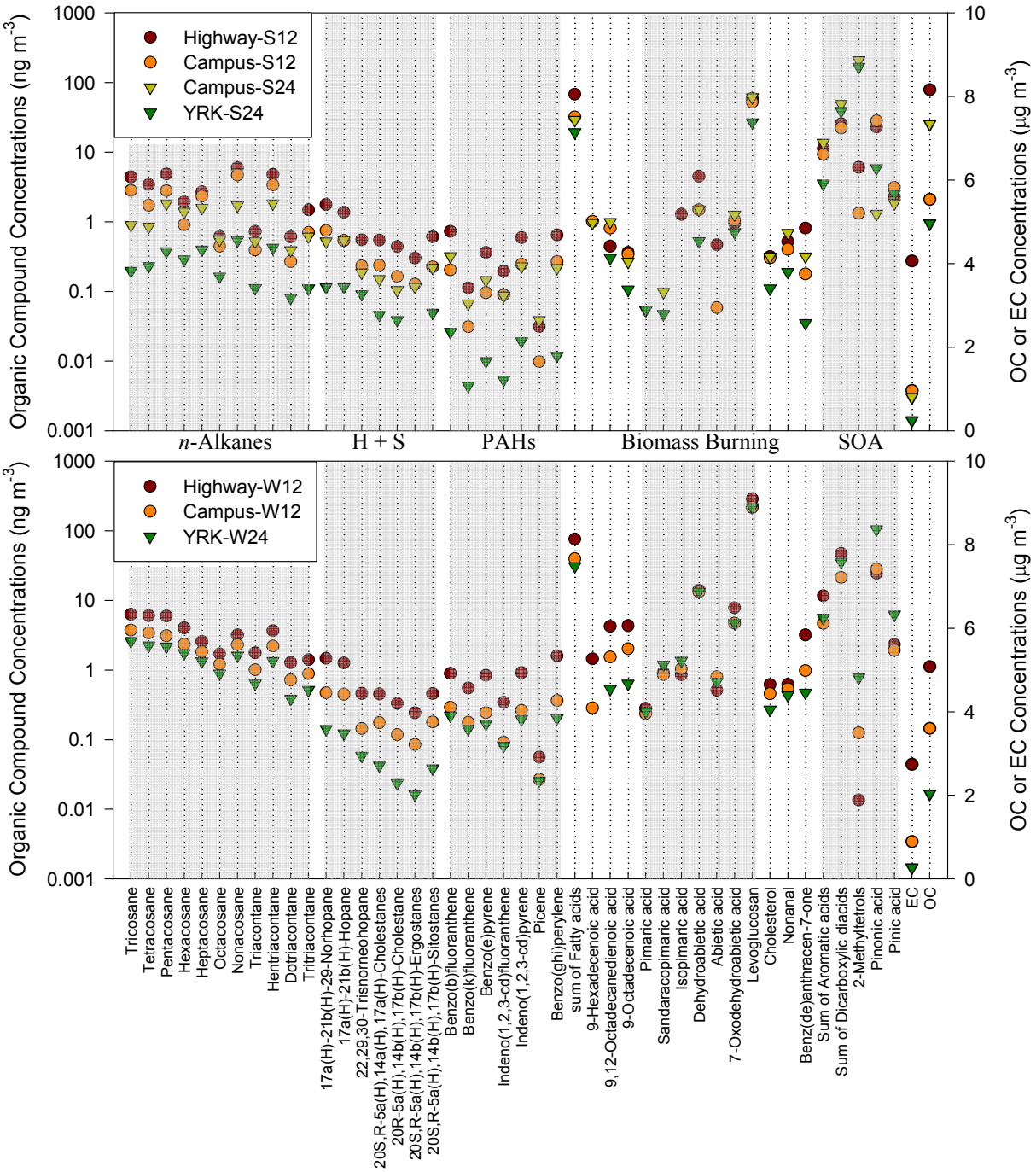

Figure 2.3. Mean ambient concentrations of individual organic compounds in $PM_{2.5}$ at the three sampling sites (Highway, Georgia Tech campus and Yorkville (YRK)) and the two seasons (summer 2005 and winter 2006). 'S12', 'S24', 'W12', and 'W24' denote 12-hr summer (June), 24-hr summer (July), 12-hr winter (January), and 24-hr winter (January) samples, respectively. 'H + S' denotes hopanes and steranes. 'Biomass Burning' and 'SOA' indicate the organic tracers of biomass burning and SOA, respectively. Note that a log scale is used on the left axis.

2.3.4 Source Profiles for On-Road Vehicle Emissions

The measurements and discussion above suggest that one can estimate an on-road vehicle emission source profile, recognizing the inherent limitations, uncertainties and required assumptions. A first assumption is that the overwhelming majority of automotive-related primary organic compounds are due to mobile sources at the roadside site. This is reasonable given that the monitor is adjacent to the highway, that the nearby campus site is not so directly impacted, and that there are significant site differences for automotive-related $PM_{2.5}$ constituents. For example, EC, an indicator of mobile source emissions, drops by about 80% from the roadside site to the campus site in both seasons. The second assumption is that both the roadside and the campus sites are simultaneously impacted by a regional mix from other major sources as the two sites are only about 400 m apart and organic tracers of non-mobile sources are observed at similar levels, e.g., levoglucosan and cholesterol, tracers of wood combustion and meat cooking, respectively, did not show significant differences between the two sites (Tables 2.1 and 2.2). Furthermore, organic markers of SOA (*cis*-pinonic acid, pinic acid, aromatic acids and dicarboxylic acids) varied little. A third assumption is that atmospheric processing does not significantly alter individual compounds between emission and sampling at the roadside and the campus site.

The on-road mobile source primary OC (POC) profile (f_i) is calculated by subtracting the on-campus concentration of individual species i, C_i(campus), from the concentration at the highway, C_i(highway), and dividing by the difference in OC (POC_{mobile}):

$$f_i = \frac{C_i(\text{Highway}) - C_i(\text{Campus})}{OC(\text{Highway}) - OC(\text{Campus})} = \frac{\Delta C_i}{POC_{mobile}}, \quad (2.1)$$

Table 2.3. Source Composition Profiles Estimated for the On-Road Mobile Emissions and from Previous Mobile Source Lab Tests (unit: ng/μg OC for organic compounds; μg/μg OC for EC)

Species	Summer [a]	Winter [b]	Mobile_1 [c]	Mobile_2 [d]
Element Carbon	1.208 ± 0.435	1.070 ± 0.443	1.406 ± 0.120	1.835 ± 0.159
Pentacosane	1.558 ± 1.952	4.025 ± 3.733	1.164 ± 0.189	0.259 ± 0.038
Hexacosane	0.769 ± 1.186	2.544 ± 2.786	1.762 ± 0.292	0.090 ± 0.019
Heptacosane	0.432 ± 0.541	1.245 ± 1.532	0.979 ± 0.154	0.040 ± 0.010
Octacosane	0.129 ± 0.122	0.771 ± 1.205	0.414 ± 0.059	0.041 ± 0.007
Nonacosane	1.156 ± 1.112	1.681 ± 1.814	0.237 ± 0.037	0.138 ± 0.033
Triacontane	0.220 ± 0.188	0.996 ± 1.190	0.000 ± 0.001	0.000 ± 0.001
Hentriacontane	1.064 ± 0.894	2.115 ± 2.042	0.000 ± 0.001	0.057 ± 0.011
Dotriacontane	0.196 ± 0.079	0.707 ± 0.804	0.000 ± 0.001	0.019 ± 0.003
Tritriacontane	0.459 ± 0.306	0.780 ± 0.822	0.000 ± 0.001	0.004 ± 0.001
20S,R-5α(H),14β(H),17β(H)-Cholestanes	0.115 ± 0.063	0.233 ± 0.172	0.332 ± 0.063	0.046 ± 0.006
20R-5α(H),14α(H),17α(H)-Cholestane	0.101 ± 0.061	0.179 ± 0.109	0.233 ± 0.044	0.036 ± 0.007
20S,R-5α(H),14β(H),17β(H)-Ergostanes	0.074 ± 0.028	0.138 ± 0.079	0.290 ± 0.052	0.025 ± 0.003
20S,R-5α(H),14β(H),17β(H)-Sitostanes	0.143 ± 0.061	0.233 ± 0.162	0.279 ± 0.051	0.082 ± 0.012
22,29,30-Trisnorneohopane	0.127 ± 0.075	0.252 ± 0.167	0.258 ± 0.047	0.039 ± 0.007
17α(H)-21β(H)-29-Norhopane	0.365 ± 0.159	0.806 ± 0.468	0.635 ± 0.107	0.129 ± 0.024
17α(H)-21β(H)-Hopane	0.320 ± 0.127	0.659 ± 0.418	0.708 ± 0.121	0.136 ± 0.026
Benzo(k)fluoranthene	0.050 ± 0.030	0.410 ± 0.341	0.061 ± 0.013	0.121 ± 0.023
Benzo(b)fluoranthene	0.307 ± 0.212	0.677 ± 0.568	0.069 ± 0.014	0.154 ± 0.030
Benzo(e)pyrene	0.160 ± 0.104	0.640 ± 0.549	0.071 ± 0.015	0.215 ± 0.042
Indeno(1,2,3-cd)fluoranthene	0.079 ± 0.062	0.264 ± 0.229	0.053 ± 0.011	0.000 ± 0.001
Indeno(1,2,3-cd)pyrene	0.243 ± 0.170	0.685 ± 0.585	0.171 ± 0.034	0.118 ± 0.024
Benzo(ghi)perylene	0.286 ± 0.225	1.248 ± 1.038	0.000 ± 0.001	0.428 ± 0.085
Benz(de)anthracen-7-one	0.387 ± 0.362	2.445 ± 2.120	0.000 ± 0.001	0.107 ± 0.018
n-Alkanoic acids (C_{14}-C_{30})	23.803 ± 23.458	53.180 ± 69.677	4.446 ± 0.715	2.186 ± 0.300

Note: [a] source composition profiles where individual organic compounds are normalized to the on-road primary OC mass estimated in the summer; [b] source composition profiles where individual organic compounds are normalized to the on-road primary OC mass estimated in the winter; [c] combined mobile source composition profiles based on the gasoline- and diesel-powered vehicle emission profiles tested by Schauer et al. [*Schauer et al.*, 1999b; 2002b]; [d] combined mobile source composition profiles based on the gasoline- and diesel-powered vehicle emission profiles tested by Lough et al. [*Lough et al.*, 2007]. The species with fractions significantly less than one standard deviation from zero are not shown in the table.

The above f_i is calculated separately for each 12-hr sampling period in the summer and the winter. On the other hand, no significant difference is observed between day and night in traffic types passing through the roadside site [*Kall and Guensler*, 2007], implying relatively consistent diurnal source composition profiles from on-road mobile emissions. Finally, the on-road mobile source profiles are created using the seasonal (summer or winter) mean of f_i (Table 2.3). Uncertainties in these source profiles could be caused by propagation of uncertainties in field sampling and lab measurement. An overall uncertainty in each f_i was calculated by propagating the reported uncertainties associated with the measured OC and individual organic compounds. In particular, the uncertainty in GC/MS quantified organic compounds was approximately ±20% (one standard deviation) on average [*Zheng et al.*, 2002]. However, associated standard deviations of the seasonal mean (summer or winter) f_i are used in the source profiles, recognizing that the propagating uncertainties are smaller than the standard deviations. A specific consideration in using this profile is that the freeway is dominated by light duty vehicle traffic, and that heavy duty vehicles are limited to those with local delivery. Through traffic of heavy duty vehicles is routed to a perimeter road approximately 18 km away.

In this study, two on-road mobile source profiles are approximated corresponding to the measurements in the summer and the winter, and show seasonal differences (Table 2.3). In the winter, on-road mobile emission fractions (ng/μg OC) of *n*-alkanes, hopanes, steranes, PAHs and *n*-alkanoic acids increase by 2.0, 1.1, 0.8, 3.5 and 1.2 times compared to the ones in the summer, respectively, implying either higher emissions of these tracers from on-road mobile sources in the cold season or significant decay in organic tracers in the warm season. In addition, gas-particle partitioning is a potential reason for increased

particulate fractions of these organic tracers in the winter [*Robinson et al.*, 2007]. However, the emission fraction of EC in the winter, 1.07, is only slightly lower than the value in the summer, 1.21. The results suggest that atmospheric decay and/or gas-particle partitioning may play a role in the seasonal variations of mobile source profiles and seasonal impacts should be considered in source apportionment using receptor models. Given the observed changes, source contributions of mobile sources (especially gasoline vehicle exhaust) are subject to underestimation in summer or overestimation in winter without application of season-specific profiles. Furthermore, the comparison indicates that EC, hopanes and steranes are preferred tracers of mobile sources in source apportionment due to their relatively seasonal stability in the atmosphere.

Significant differences are found between the on-road mobile source profiles developed in this work and those measured previously in the lab (Table 2.3; Figure 2.4). Lab-based profiles are calculated using the mixture of observed vehicle types (passenger vehicles, small trucks, large trucks and buses) on the I–75/85 highway [*Kall and Guensler*, 2007] and $PM_{2.5}$ emission factors from the Mobile6 model (version 6.2.0.3). Gasoline- and diesel-related emission ratios are obtained for OC, EC, and $PM_{2.5}$ by assuming all passenger vehicles and half of small trucks are gasoline vehicles while large trucks, buses and the other half of small trucks are diesel vehicles. These emissions-weighted fractions were combined with previous gasoline- and diesel-powered vehicle emission profiles measured by Schauer et al. [*Schauer et al.*, 1999b; 2002b] and Lough et al [*Lough et al.*, 2007], respectively, leading to two different mobile source profiles, Mobile_1 and Mobile_2.

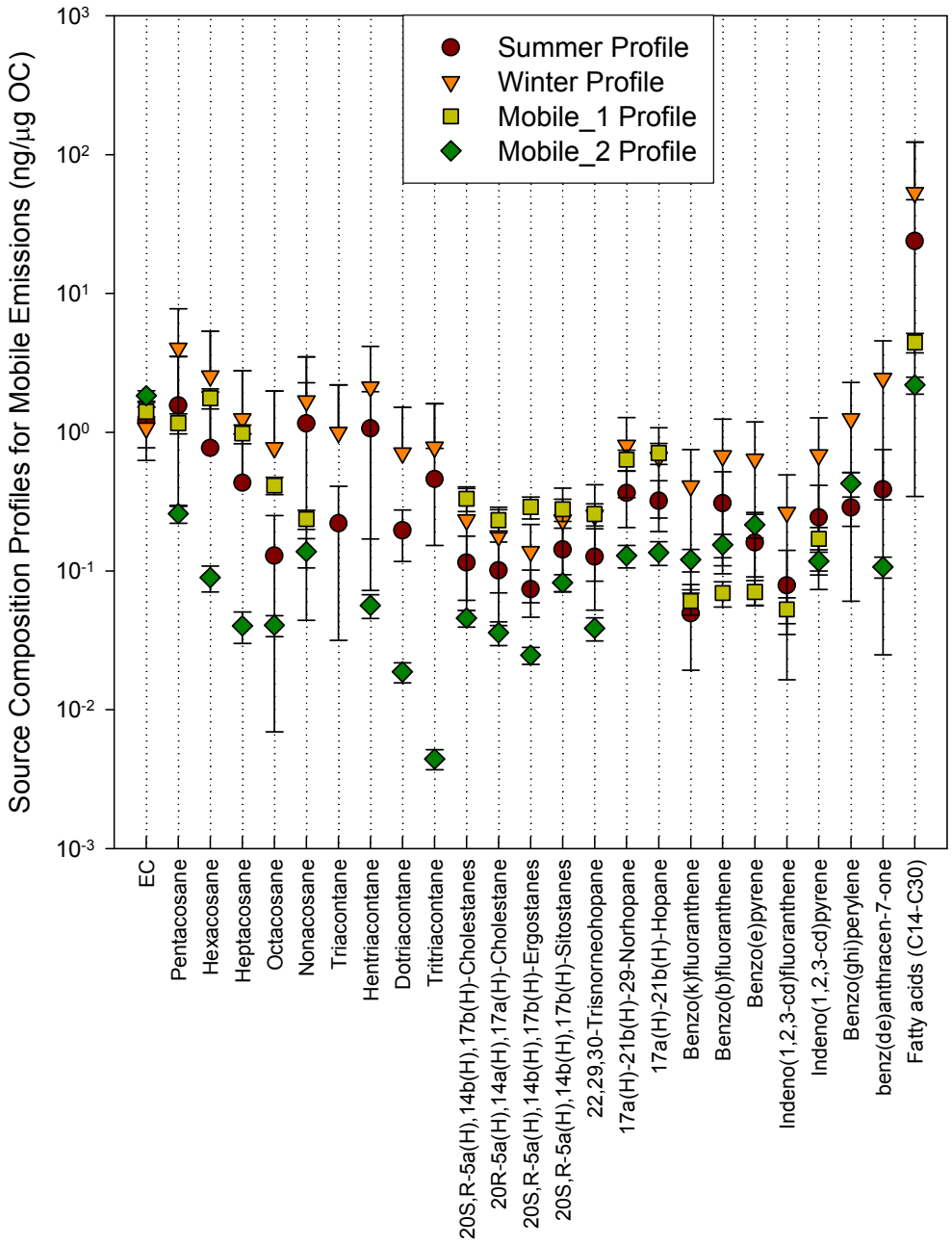

Figure 2.4. Calculated summer and winter source composition profiles for on-road mobile emissions in this study and two combined mobile emission source profiles, Mobile_1 and Mobile_2, which are built by integrating previous gasoline- and diesel-powered vehicle emission profiles measured by Schauer et al. [*Schauer et al.*, 1999b; 2002b] and Lough et al. [*Lough et al.*, 2007], respectively. The profiles are composed of individual species fractions, normalized to OC. The unit is ng/µg OC for all organic compounds, and µg/µg OC for EC. Log scale is used and error bars are shown.

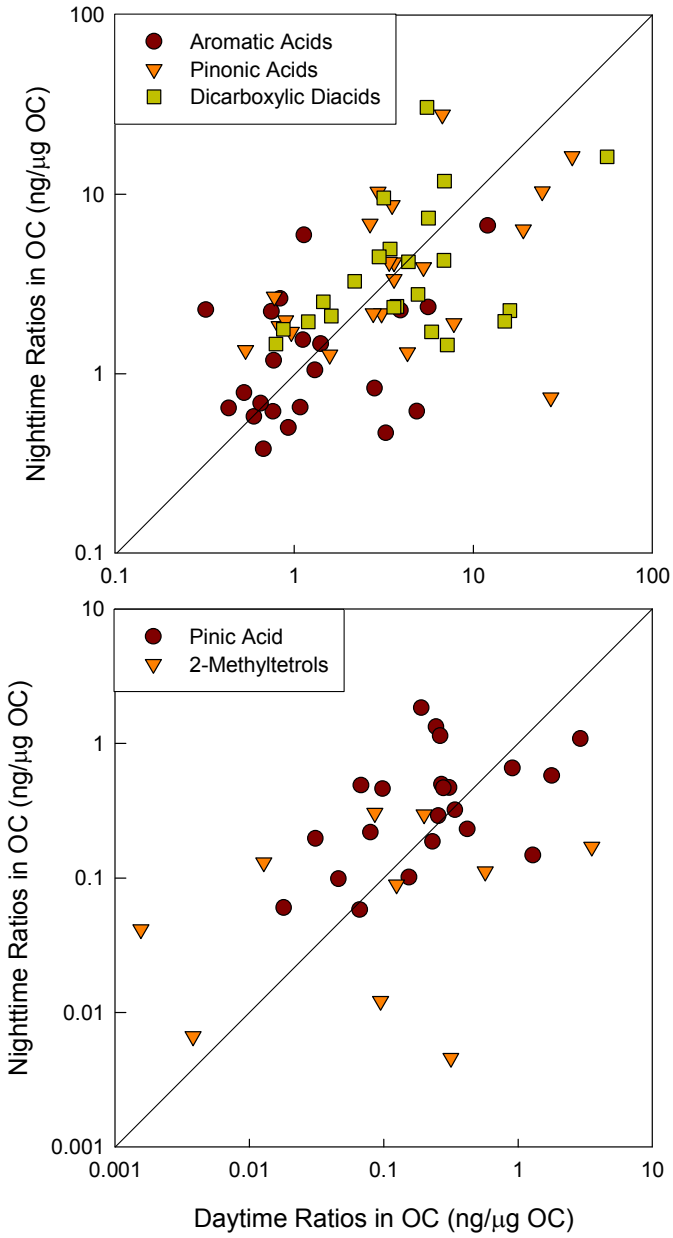

Figure 2.5. 'Nighttime' vs. 'Daytime' SOA organic tracers measured at the roadside site and the campus site in the summer and the winter. All ambient concentrations are normalized to associated measured OC in the plots. Note that a log scale is used.

The comparisons show that *n*-alkanes, hopanes, steranes, and PAHs abundances differ significantly while EC is similar (Table 2.3; Figure 2.4). For relatively light molecular-weight *n*-alkanes (C_{25}–C_{28} homologues), emission fractions of the estimated

profile are comparable to those of Mobile_1, but significantly higher than Mobile_2. Estimated fractions are higher than both Mobile_1 and Mobile_2 for high molecular-weight *n*-alkanes (C_{29}–C_{34} homologues). Emission fractions of hopanes and steranes are consistently lower than those of Mobile_1, but higher than Mobile_2. For PAHs, comparisons between these source profiles do not show any clear trend, but the winter profile is usually found to be highest. Such differences suggest that location- and season-specific profiles should be developed, and that actual on-road mobile emissions (or the impact of dilution and cooling process) differ significantly from lab tests. On the other hand, the uncertainties of species are large in the calculated source profiles.

2.3.5 Organic SOA Tracers

Unlike primary organic compounds, there is no distinct day–night variation observed for secondary organic tracers, including 2-methyltetrols, dicarboxylic diacids, aromatic acids, *cis*-pinonic acid, and pinic acid (Figure 2.5).

A high linear correlation (overall r^2=0.98) is observed for the two isomers of 2-methyltetrols with 2-methylerythritol/2-methylthreitol ratios of 2.2 and 1.7 in the summer and the winter, respectively (Figure 2.6). These ratios are comparable to the values of 2.1 [*Ding et al.*, 2008] and 1.7 [*Xia and Hopke*, 2006] obtained previously in the eastern and southeastern U.S. 2-methyltetrols are measured much higher in the summer while levels in the winter are near or below the detection limit. Higher temperatures and light intensity in the summer enhance both emissions of isoprene [*Lamb et al.*, 1987] and photochemical reaction. Compared with June 2005, 2-methyltetrols are observed to be higher in July. One reason is that the average concentration of isoprene increased by about 2 times in July, and ozone is high as well. Chamber studies suggest that ozonolysis of isoprene is

important for formation of these SOA species [*Kleindienst et al.*, 2007b]. In contrast, little 2-methylterols are found in the winter given low temperatures, weak solar radiation and defoliation of deciduous trees.

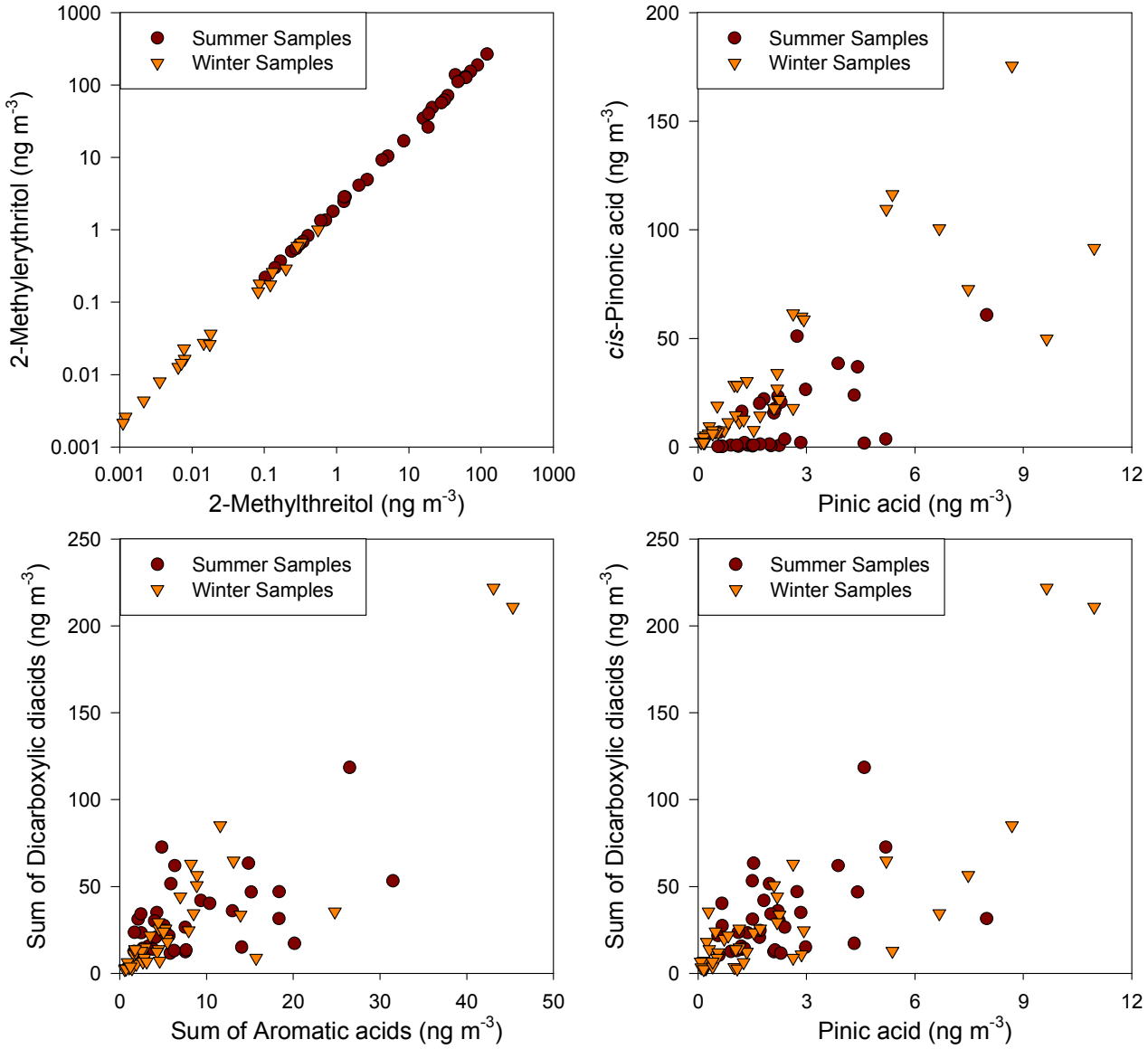

Figure 2.6. Scatter plots of SOA organic tracers (2-methyltetrols, dicarboxylic diacids, aromatic, *cis*-pinonic and pinic acids) measured in the summer and the winter. A log scale is used in (a). 2-methyltetrols indicates the sum of 2-methylthreitol and 2-methylerythritol in $PM_{2.5}$.

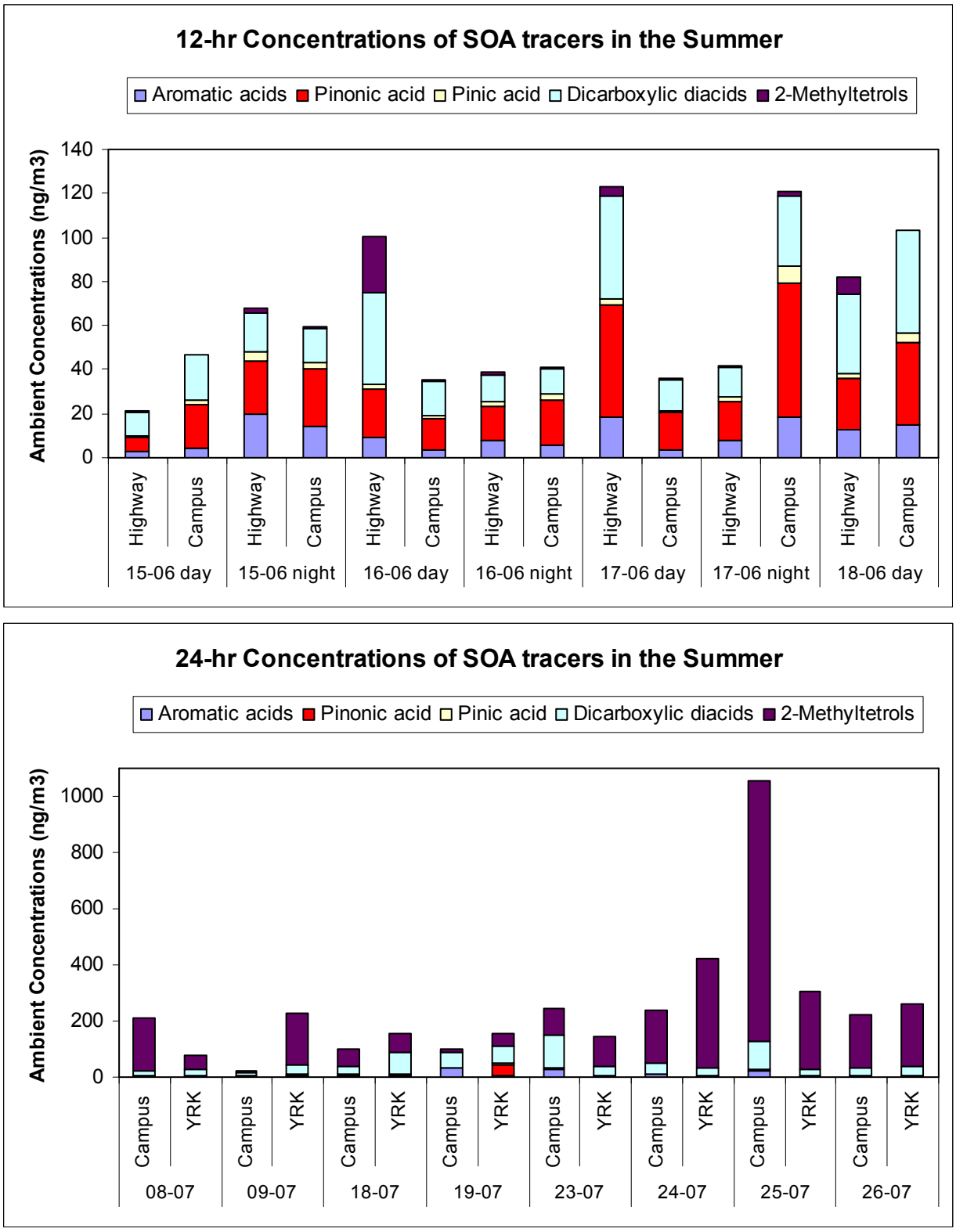

Figure 2.7. Spatial and daily variations of SOA organic tracers in the summer time.

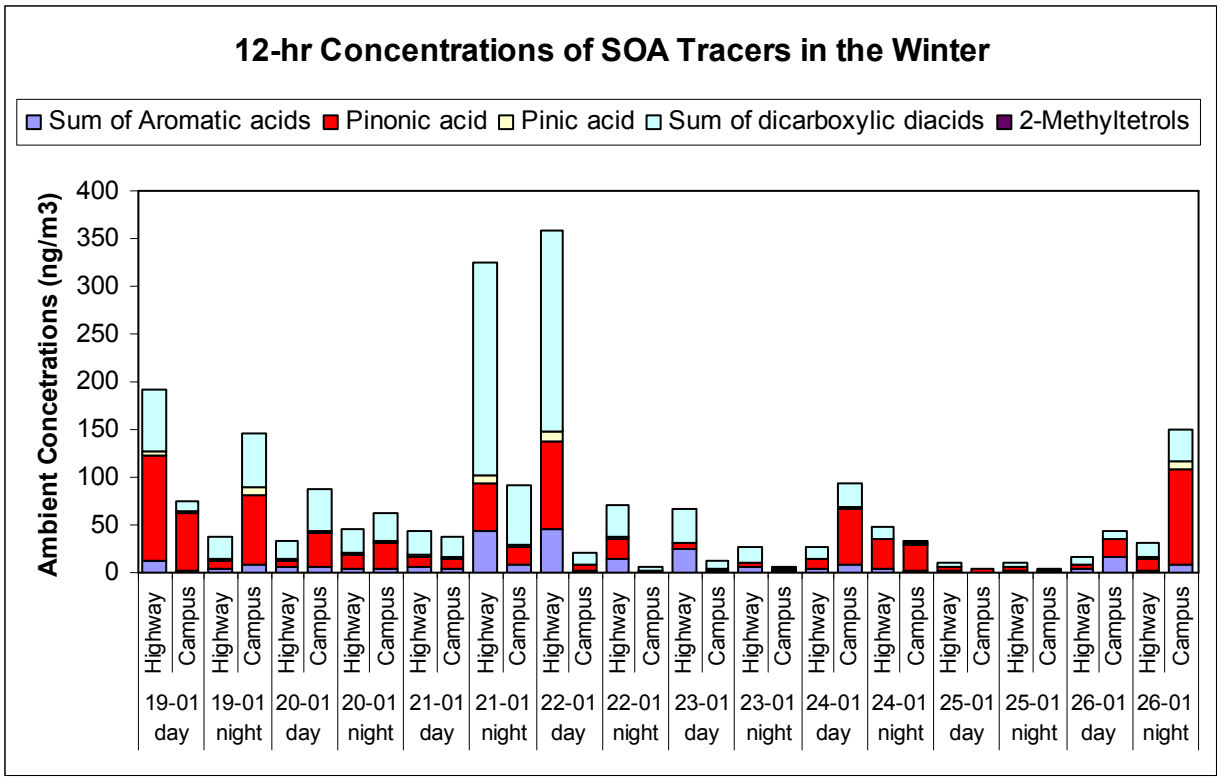

Figure 2.8. Spatial and daily variations of SOA tracers in the winter time.

Unlike 2-methyltetrols, *cis*-pinonic acid and pinic acid concentrations are highest in the winter (Table 2.1; Figures 2.7 and 2.8). One reason is that emissions of monoterpenes do not decrease as much as isoprene in the winter, and depend not only on temperatures but also on biophysical processes in conifer trees [*Lamb et al.*, 1987] that are plentiful in the Southeast and account for over half of the forests [*Geron et al.*, 2000]. Prescribed burning, prevalent from winter through spring in this region, can also enhance emissions of monoterprenes as well as formation of particulate SOA tracers even in cold weather [*Hu et al.*, 2008; *Yan et al.*, 2008a]. A further hypothesis is that gas-particle partitioning of *cis*-pinonic acid and pinic acid is very sensitive to ambient temperatures,

and lower temperatures lead to greater partitioning to the condensed phase, which is supported by negative correlation between *cis*-pinonic and pinic acids vs. ambient temperature in the summer (Figure 2.9). Sheehan and Brown found that a decrease of temperature by 10 ^{0}C might result in 150% increases in SOA yield [*Sheehan and Bowman*, 2001]. This study found little correlation between 2-methyltetrols with *cis*-pinonic or pinic acid (not shown in figure), implying different origins and formation paths for the two kinds of biogenic SOA tracers. *cis*-Pinonic acid and pinic acid exhibit very similar patterns in both seasons, suggesting the same sources, formation pathways, and properties in the atmosphere (Figure 2.6).

Aromatic and dicarboxylic acids show more complicated spatial and seasonal variations. Higher concentrations are measured at the highway, implying vehicular emissions probably are a significant source or there is rapid formation/condensation of particle phase aromatic acids and dicarboxylic acids (Table 2.1, Figures 2.7 and 2.8). The former is further supported by the winter measurements that display much larger reductions in ambient concentrations for both aromatic acids and dicarboxylic acids from the roadside site to the campus site. The results also exhibit a strong correlation (overall r^2=0.67, $p<0.001$) between aromatic acids and dicarboxylic acids, implying similar origins and atmospheric properties (Figure 2.6). The correlation (overall r^2=0.55, $p<0.001$) between pinic acid and dicarboxylic acids suggests that the two types of organic compounds might have similar dynamics. Therefore, atmospheric processing of biogenic or anthropogenic VOCs are both likely sources of dicarboxylic acids. In contrast, there is little correlation between 2-methyltetrols and dicarboxylic acids. .

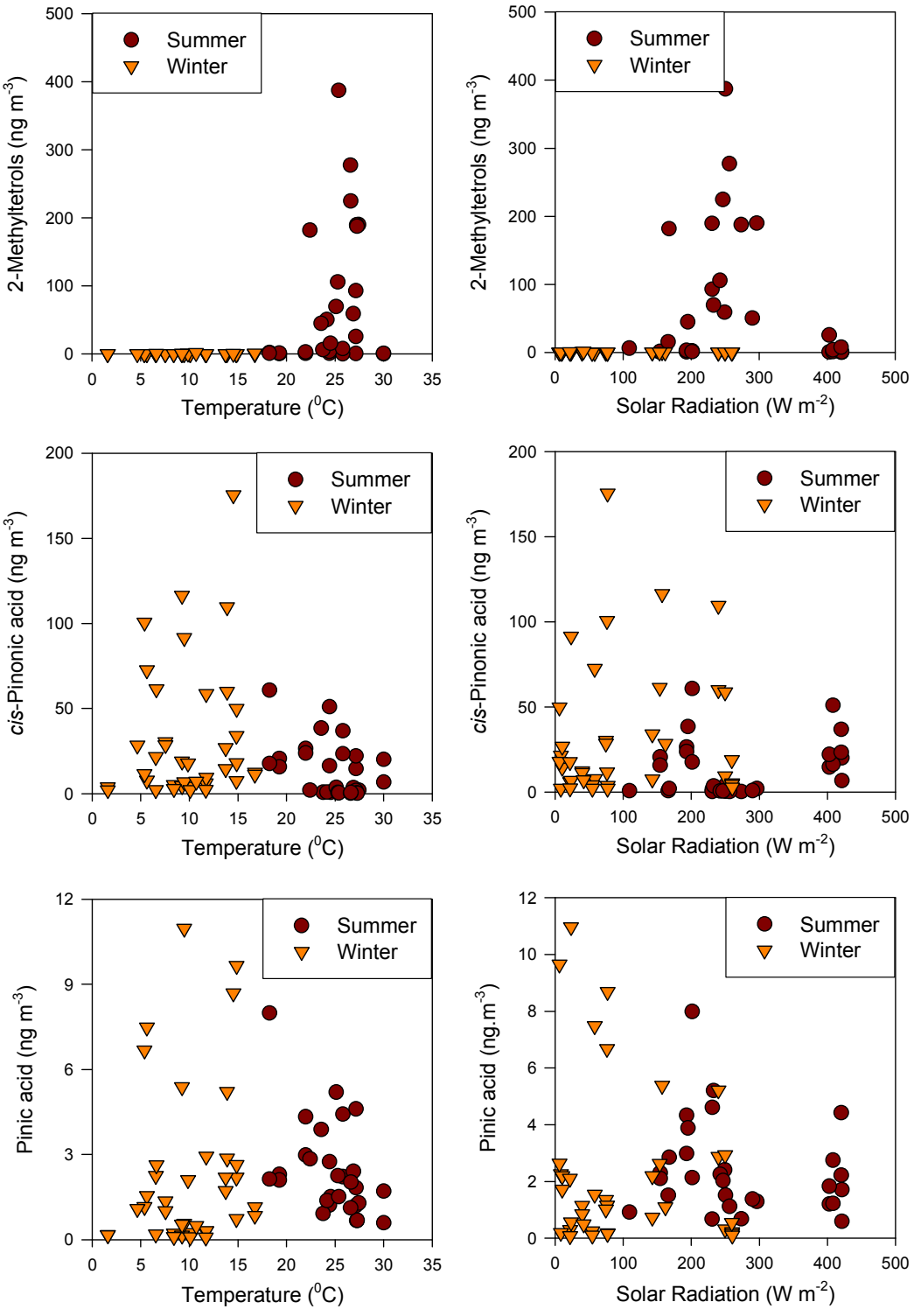

Figure 2.9. SOA tracers (2-methyltetrols, *cis*-pinonic acid and pinic acid) vs. meteorological variables (temperature and solar radiation) for both the summer and winter.

Acknowledgments

This work was funded in part by U.S. Environmental Protection Agency STAR grants (R832159, R828976 and R831076). We thank Georgia Power for their support. The authors acknowledge Drs. Yingjun Chen and Liping Yu for their assistance in organic tracer analysis, and Atmospheric Research & Analysis, Inc. for their help on field sampling and meteorological measurements. We also thank Dr. Sangil Lee, Charles Evan Cobb, Santosh Chandru, and Hyeon Kook Kim for assistance in field sampling and lab experiments.

CHAPTER 3

CHARACTERIZATION OF AIRBORNE $PM_{2.5}$ AT ROADSIDE, URBAN AND RURAL SITES IN THE SUMMER AND THE WINTER

(Bo Yan, Mei Zheng, Yongtao Hu, Amy P. Sullivan, Rodney J. Weber, Sangil Lee, Charles Evan Cobb, Santosh Chandru, Hyeon Kook Kim, Eric S. Edgerton, and Armistead G. Russell. *Environmental Science & Technology*, in preparation)

Abstract

In summer 2005 and winter 2006, 12-hr and 24-hr $PM_{2.5}$ filter samples were collected from three sites: two from urban Atlanta, GA (one site adjacent to a freeway and another 400 m away), and one at a rural site. Detailed $PM_{2.5}$ composition was investigated including OC, EC, WSOC, ionic species and trace metals, as well as their day–night, seasonal and spatial variations. Particulate organic matter (OM) was estimated through mass balance analysis of gravimetric $PM_{2.5}$, and the OM/OC ratio is found to depend on season and location. OM, sulfate and ammonium are major components of $PM_{2.5}$ in both seasons and significantly higher in the summer; whereas nitrate is important only in the winter. Sulfate dominates $PM_{2.5}$ in the summer, particularly on haze days. Homogeneous distributions of WSOC reflect impacts from secondary organic aerosols (SOA). Much higher concentrations of automotive-related species are detected at the roadside, including OC, EC, iron and copper. Season-specific on-road mobile source primary $PM_{2.5}$ profiles were developed by using differences in individual species

concentrations between the roadside site and the nearby on-campus site, and differ from in-use mobile source profiles measured in the lab.

3.1 Introduction

Airborne fine particulate matter ($PM_{2.5}$) has been linked to adverse human health effects, visibility reduction, and climate change [*Buseck and Posfai*, 1999; *Horvath*, 1993; *Pope et al.*, 2002] with growing focus on health effects from roadway-related exposures [*Escamilla-Nunez et al.*, 2008; *Sarnat et al.*, 2008]. Typically, the major contributors of $PM_{2.5}$ include mobile source emissions, biomass burning, and secondary sources with anthropogenic and biogenic nature in origin. The air quality in Atlanta, GA and surrounding metropolitan region, which is located in the southeastern U.S and populated by over 5.4 million residents, is of particular interest due to high emissions from mobile sources, biomass burning, coal-fired power plants and biogenic volatile organic compounds (VOC), with vigorous photochemical processes as well. This region is still struggling to attain the National Ambient Air Quality Standards (NAAQS), and ranked among the most polluted urban areas in the country. In 2007, for example, the 24-hr $PM_{2.5}$ and 8-hr O_3 levels in Atlanta exceeded the NAAQS on 24 and 29 days, respectively [*Georgia EPD*, 2007].

Effective strategies to control airborne $PM_{2.5}$ require understanding $PM_{2.5}$ chemical composition. Although previous studies have reported $PM_{2.5}$ composition in the Atlanta area and the southeastern U.S [*Baumann et al.*, 2003; *Edgerton et al.*, 2005; 2006; *Hansen et al.*, 2003], little research has explored a detailed composition of $PM_{2.5}$, which is dominated by direct on-road vehicular emissions, and day vs. night attributes of

urban $PM_{2.5}$. Moreover, local source composition profiles of mobile emissions, a major source of primary $PM_{2.5}$, have not been developed in the southeastern U.S. As a result, source profiles tested elsewhere in laboratory (e.g., in California [*Cooper et al.*, 1987; *Lough et al.*, 2007; *Schauer et al.*, 1999b; 2002b] and Colorado [*Watson et al.*, 1998]) were used in source apportionment studies in this area [*Lee et al.*, 2007; *Marmur et al.*, 2005]. This may cause errors in source contributions estimated by receptor models. The dilution and cooling processes applied in the present laboratory emission tests cannot represent real-world atmospheric mixing well, and would result in bias in the source profiles tested in lab [*Donahue et al.*, 2006; *Lipsky and Robinson*, 2006]. Seasonal variations of mobile source compositions have been proposed due to cold start of vehicles and gas-particle partitioning [*Lough et al.*, 2005a; *Robinson et al.*, 2007]. To examine the $PM_{2.5}$ composition directly impacted by on-road emissions and to assess in-use mobile source profiles for different seasons in the southeast U.S., field experiments were performed in urban Atlanta, adjacent to a freeway (roadside) and 400 m away, as well as at a rural site, with focus on on-road emissions, regional transport, secondary source effects and seasonal variations of $PM_{2.5}$ composition.

A detailed composition of $PM_{2.5}$ organic matter measured in the same study has been presented in another paper that compares the roadside, urban and rural levels of primary and secondary organic molecular markers in $PM_{2.5}$ and develops season-specific on-road mobile source profiles for primary organic carbon (OC) [*Yan et al.*, 2009c]. This paper is directed at other components in $PM_{2.5}$, including total OC, water-soluble OC (WSOC), elemental carbon (EC), ionic species and trace metals.

3.2 Experimental Section

3.2.1 Field Sampling

Details of the field sampling are described elsewhere, including samplers, sampling sites, seasons and periods [*Yan et al.*, 2009c]. Briefly, $PM_{2.5}$ filter samples were collected by high-volume (Hi-Vol) particulate samplers and three-channel particulate composition monitors (PCM) at three sites (Figure 2.1): (1) a roadside site by an interstate highway; (2) an urban site on the Georgia Institute of Technology campus, 400 m away from the roadside site; (3) a rural site at Yorkville (YRK), GA, 55 km northwest of the metro Atlanta. The roadside site is 3 m away from the I-75/85 freeway in Midtown Atlanta that carries about 280,000 vehicles per day [*Georgia DOT*, 2006], 97% of which are light duty, gasoline-powered vehicles [*Kall and Guensler*, 2007]. The Yorkville site is a rural sampling site of the Southeastern Aerosol Research and Characterization Experiment (SEARCH) air quality monitoring network [*Hansen et al.*, 2003]. Furthermore, these sites were complemented by a SEARCH site (the Jefferson Street (JST), 2 km southwest of Georgia Tech), four sites from the Assessment of Spatial Aerosol Composition in Atlanta (ASACA) [*Butler et al.*, 2003], and multiple routine monitors around Atlanta (Figure 2.1).

Hi-Vol samplers (flow rate: 1.13 m^3 min^{-1}) used pre-baked quartz microfibre filters (8 x 10 in), and PCM samplers (flow rate: 16.7 L min^{-1}) had diffusion denuders followed by pre-baked quartz microfibre filters in one channel and pre-weighed Teflon filters (47 mm) in the other two channels. Field sampling was carried out during two seasons: summer (June-July, 2005) and winter (January 2006). In the summer study, 12-hr (10am–10pm–10am) back-to-back sampling was conducted simultaneously at both the

roadside site and the campus site on June 15-18, 2005, and 24-hr (10am–10am) measurements were taken simultaneously at both the campus site and the Yorkville site on non-rainy days on July 8-26, 2005. In the winter study, 12-hr back-to-back filter samples were taken simultaneously on January 19-26, 2006 both at the roadside site and the campus site and 24-hr sampling was conducted at Yorkville. The reasons for selecting the sampling time of 10am–10pm–10am were explained previously [*Yan et al.*, 2009c].

3.2.2 Chemical Analysis

$PM_{2.5}$ mass was determined gravimetrically using both Teflon PCM filters after 24-hr equilibration in a temperature- and humidity-controlled clean room. Next, water-soluble ionic species (sulfate, nitrate, ammonium, sodium, chloride, potassium, etc.) were measured from one Teflon filter with ion chromatography (IC, Dionex), and the other Teflon filter was analyzed for trace metals by X-ray fluorescence (XRF) at the Desert Research Institute (DRI). Quartz filters from both the Hi-Vol sampler and the PCM were analyzed for OC and EC using thermal optical transmittance (TOT, Sunset Lab). WSOC and particulate organic compounds were measured from the Hi-Vol quartz filters with a total organic carbon (TOC, Sievers) analyzer and gas chromatography/mass spectrometry (GC/MS, Agilent), respectively. The $PM_{2.5}$ composition analysis methods are described elsewhere [*Baumann et al.*, 2003; *Lee et al.*, 2005a; *Sullivan and Weber*, 2006; *Weber et al.*, 2007; *Yan et al.*, 2009c; *Zheng et al.*, 2002].

3.2.3 Trace Gas and Meteorological Data

Trace gases (O_3, SO_2, CO, NO_x and NO_y) and meteorological data (temperature, solar radiation, relative humidity, precipitation, and light scattering coefficient) were measured at the Yorkville site by the SEARCH air quality monitoring network, but not at

the roadside and campus sites. A SEARCH site (the Jefferson Street (JST), 2 km southwest of Georgia Tech) provides complementary data for the roadside and campus sites. The field measurement methods in the SEARCH network are described by Hansen et al. and Edgerton et al. [*Edgerton et al.*, 2006; *Hansen et al.*, 2003].

3.3 Results and Discussion

3.3.1 $PM_{2.5}$ Composition

Much higher ambient $PM_{2.5}$ concentrations are observed in the summer. On average, $PM_{2.5}$ concentrations are 22.7±3.3 and 16.4±1.5 μg m^{-3} at the roadside and campus sites in June 2005, respectively, and 28.8±14.6 and 24.5±12.0 μg m^{-3} at the campus and Yorkville sites in July 2005 (Table 3.1). Three consecutive haze days (July 24–26, 2005) were captured at both the campus and the Yorkville sites, resulting in high $PM_{2.5}$ levels in the July sampling events. In the winter, $PM_{2.5}$ concentrations decrease to 14.8±5.2, 11.3±5.3 and 7.6±3.2 μg m^{-3} at the roadside, campus and Yorkville sites, respectively (Table 3.1).

OC, ammonium and sulfate are major components of $PM_{2.5}$ in both seasons, making up 36/34%, 8.3/7.0% and 20/14% of the $PM_{2.5}$ mass at the roadside site in the summer/winter, respectively, 30/32%, 12/7.3% and 31/11% at the campus site, and 23/28%, 14/10% and 36/20% at the Yorkville site. Nitrate is a seasonally major component of $PM_{2.5}$, accounting for 11%, 17% and 28% of the $PM_{2.5}$ mass in the winter at the roadside, campus and Yorkville sites, respectively, but contributes little in the summer (Figure 3.1). Fine soil is a significant constituent of the urban $PM_{2.5}$, accounting for about 10% and 7.5% of the $PM_{2.5}$ mass at the roadside and campus sites, respectively,

but soil components are minor at the rural site, making up about 2% of $PM_{2.5}$ in both seasons. Here, fine soil, that is, crustal material, is calculated using [*Malm et al.*, 1994]:

$$[\text{Soil}] = 2.2 \times [\text{Al}] + 2.49 \times [\text{Si}] + 1.63 \times [\text{Ca}] + 2.42 \times [\text{Fe}] + 1.94 \times [\text{Ti}] \quad (3.1)$$

EC, mostly emitted by mobile sources, accounts for 18% of the $PM_{2.5}$ mass at the roadside site in both seasons and below 8% at the campus site, 400 m away. At the rural site, EC is a minor component, contributing 1.5/3.6% of the $PM_{2.5}$ mass in the summer/winter, respectively. In Figure 3.1, the 'Others' term is a mix of other ionic species (chloride, sodium, etc.), other metals (manganese, copper, zinc, arsenic, selenium, bromine, tin, antimony, barium, etc.) as well as other elements other than carbon (such as oxygen, nitrogen, sulfur and hydrogen) in particulate organic matter (OM).

To assess OM mass in $PM_{2.5}$, historically, a factor of 1.4 has been widely used to convert OC to OM [*White and Roberts*, 1977]. Recently, the OM/OC factors of 1.6 and 2.1 have been proposed for urban and rural areas by Turpin and Lim [*Turpin and Lim*, 2001], and the ratio of 2.0 has been approximated by EI-Zanan et al. [*El-Zanan et al.*, 2009]. In this study, the OM/OC ratio is calculated by mass balance analysis of gravimetric $PM_{2.5}$, as shown below:

$$\frac{\text{OM}}{\text{OC}} = \frac{[\text{PM}_{2.5}] - \left([\text{EC}] + [\text{NH}_4^+] + [\text{NO}_3^-] + [\text{SO}_4^{2-}] + [\text{Soil}] + [\text{other elements}]\right)}{[\text{OC}]} \quad (3.2)$$

where 'other elements' includes other ions and non-soil metals. This OM/OC ratio is likely overestimated without subtracting particle-bound water from $PM_{2.5}$ mass and without including oxygen in non-soil metal oxides. Uncertainties in the OM/OC ratios could be caused by propagation of various uncertainties in field sampling (e.g., flowrate) and lab measurement (e.g., instrument, method). An overall uncertainty in each OM/OC ratio was calculated by propagating the reported uncertainties associated with all

individual measurements [*El-Zanan et al.*, 2009]. However, associated standard deviations of the mean OM/OC ratios (location- or season-specific) are used below, because the propagating uncertainties are significantly smaller than the standard deviations. Our results indicate that the OM/OC ratio is season and location dependent, increasing from 1.5±0.4 (summer) to 1.9±0.5 (winter) at the campus site and decreasing from 2.1±0.2 (summer) to 1.4±0.3 (winter) at Yorkville (computed from Table 3.1). At the roadside site, the OM/OC ratio varies little in both seasons and the value of 1.2±0.3 agrees well with a previous study on mobile emissions [*Engelbrecht*, 2003]. Calculated from measured OC with these ratios, OM is found to contribute 42/45%, 40/60%, and 42/48% of the $PM_{2.5}$ mass in the summer/winter at the roadside, campus, and rural sites, respectively. As the dominant component of $PM_{2.5}$ in this area, OM has been investigated previously for detailed chemical composition as well as day–night, seasonal and spatial comparison [*Yan et al.*, 2009c].

3.3.2 $PM_{2.5}$ Composition on Haze Days

Haze is characterized by intense scattering and absorption of light in the presence of aerosols, and is of concern in the southeastern U.S, especially during summer where high level $PM_{2.5}$ concentrations tend to occur [*Brewer and Adlhoch*, 2005]. Compared to the non-haze days, the average daily $PM_{2.5}$ concentrations increase by 1.5 and 1.3 times on the haze days at the campus and Yorkville sites, respectively, and reach 46 and 38 μg m^{-3}, reducing visibility regionwide (Table 3.2). The associated light scattering coefficients, b_{scat}, increase from $6.1x10^{-5}$ and $4.7x10^{-5}$ m^{-1} on the non-haze days to $20x10^{-5}$ and $14x10^{-5}$ m^{-1} on the haze days at the urban (JST) and rural (YRK) sites, respectively.

Table 3.1. Average Concentrations and Standard Divisions of $PM_{2.5}$ Components at the Three Sampling Sites (unit: μg m^{-3})

$PM_{2.5}$ Component	Highway Roadside		Georgia Tech. Campus			Yorkville (YRK)	
	Summer-12	Winter-12	Summer-12	Summer-24	Winter-12	Summer-24	Winter-24
Ions							
Sodium	0.021 ± 0.032	0.054 ± 0.065	0.033 ± 0.031	0.119 ± 0.054	0.109 ± 0.095	0.021 ± 0.024	0.092 ± 0.117
Ammonium	1.892 ± 0.641	1.028 ± 0.603	1.680 ± 0.480	3.717 ± 2.494	0.822 ± 0.505	3.425 ± 1.782	0.768 ± 0.443
Potassium	0.053 ± 0.025	0.029 ± 0.024	0.020 ± 0.017	0.047 ± 0.022	0.023 ± 0.024	0.040 ± 0.011	0.019 ± 0.017
Calcium	0.077 ± 0.145	0.000 ± 0.000	0.000 ± 0.000	0.041 ± 0.059	0.336 ± 0.664	0.000 ± 0.000	0.052 ± 0.134
Acetate	0.025 ± 0.019	0.046 ± 0.031	0.023 ± 0.032	0.049 ± 0.043	0.060 ± 0.058	0.028 ± 0.018	0.021 ± 0.025
Formate	0.031 ± 0.013	0.034 ± 0.027	0.036 ± 0.038	0.085 ± 0.071	0.073 ± 0.122	0.050 ± 0.037	0.041 ± 0.048
Chloride	0.002 ± 0.006	0.038 ± 0.030	0.026 ± 0.019	0.008 ± 0.009	0.034 ± 0.040	0.001 ± 0.004	0.013 ± 0.024
Nitrate	0.194 ± 0.213	1.622 ± 2.271	1.216 ± 1.652	0.816 ± 1.026	1.946 ± 3.305	0.088 ± 0.051	2.156 ± 2.452
Sulfate	4.551 ± 1.619	2.014 ± 1.007	4.359 ± 1.455	10.241 ± 7.065	1.269 ± 0.922	9.770 ± 5.804	1.516 ± 0.853
Oxalate	0.148 ± 0.055	0.078 ± 0.048	0.143 ± 0.038	0.245 ± 0.102	0.069 ± 0.086	0.206 ± 0.066	0.081 ± 0.069
Trace Metals							
Sodium	0.016 ± 0.043	0.000 ± 0.000	0.001 ± 0.004	0.045 ± 0.078	0.000 ± 0.001	0.106 ± 0.106	0.005 ± 0.014
Magnesium	0.011 ± 0.029	0.000 ± 0.000	0.016 ± 0.028	0.020 ± 0.024	0.002 ± 0.006	0.021 ± 0.032	0.000 ± 0.000
Aluminum	0.155 ± 0.086	0.055 ± 0.031	0.074 ± 0.039	0.134 ± 0.099	0.054 ± 0.043	0.064 ± 0.052	0.028 ± 0.025
Silicon	0.220 ± 0.124	0.081 ± 0.042	0.171 ± 0.101	0.243 ± 0.145	0.064 ± 0.064	0.103 ± 0.091	0.027 ± 0.018
Phosphorous	0.108 ± 0.062	0.061 ± 0.057	0.071 ± 0.053	0.127 ± 0.119	0.050 ± 0.042	0.119 ± 0.132	0.032 ± 0.011
Sulfur	1.960 ± 1.233	0.713 ± 0.388	1.193 ± 0.824	2.919 ± 2.657	0.643 ± 0.412	2.393 ± 3.028	0.540 ± 0.368
Chlorine	0.001 ± 0.002	0.011 ± 0.011	0.003 ± 0.003	0.001 ± 0.002	0.007 ± 0.018	0.000 ± 0.000	0.002 ± 0.003
Potassium	0.069 ± 0.049	0.021 ± 0.025	0.061 ± 0.040	0.066 ± 0.033	0.038 ± 0.056	0.041 ± 0.025	0.021 ± 0.035
Calcium	0.167 ± 0.072	0.044 ± 0.091	0.133 ± 0.036	0.101 ± 0.049	0.161 ± 0.224	0.028 ± 0.012	0.015 ± 0.037
Titanium	0.020 ± 0.010	0.010 ± 0.008	0.014 ± 0.005	0.013 ± 0.004	0.004 ± 0.004	0.006 ± 0.003	0.001 ± 0.001
Vanadium	0.000 ± 0.000	0.000 ± 0.000	0.000 ± 0.000	0.000 ± 0.000	0.000 ± 0.000	0.000 ± 0.000	0.000 ± 0.000
Manganese	0.005 ± 0.005	0.009 ± 0.004	0.005 ± 0.004	0.003 ± 0.003	0.008 ± 0.004	0.001 ± 0.002	0.000 ± 0.001
Iron	0.448 ± 0.094	0.352 ± 0.152	0.173 ± 0.046	0.200 ± 0.048	0.101 ± 0.068	0.056 ± 0.026	0.017 ± 0.012

Nickel	0.000 ± 0.000	0.000 ± 0.000	0.001 ± 0.001	0.002 ± 0.004	0.000 ± 0.001	0.000 ± 0.000	0.000 ± 0.001
Copper	0.054 ± 0.012	0.020 ± 0.009	0.007 ± 0.008	0.015 ± 0.018	0.012 ± 0.006	0.007 ± 0.007	0.006 ± 0.005
Zinc	0.015 ± 0.005	0.023 ± 0.006	0.015 ± 0.020	0.018 ± 0.012	0.051 ± 0.063	0.004 ± 0.005	0.009 ± 0.009
Arsenic	0.000 ± 0.000	0.000 ± 0.000	0.000 ± 0.000	0.000 ± 0.001	0.000 ± 0.000	0.000 ± 0.000	0.000 ± 0.000
Selenium	0.000 ± 0.000	0.000 ± 0.000	0.000 ± 0.000	0.000 ± 0.000	0.000 ± 0.000	0.000 ± 0.000	0.000 ± 0.000
Bromine	0.002 ± 0.003	0.001 ± 0.001	0.000 ± 0.000	0.003 ± 0.003	0.001 ± 0.002	0.000 ± 0.001	0.002 ± 0.002
Antimony	0.006 ± 0.009	0.002 ± 0.004	0.005 ± 0.009	0.000 ± 0.000	0.006 ± 0.007	0.010 ± 0.007	0.000 ± 0.000
Barium	0.010 ± 0.018	0.015 ± 0.012	0.009 ± 0.016	0.008 ± 0.009	0.003 ± 0.006	0.012 ± 0.014	0.000 ± 0.000
Mercury	0.000 ± 0.000	0.000 ± 0.000	0.000 ± 0.000	0.000 ± 0.000	0.000 ± 0.000	0.000 ± 0.000	0.000 ± 0.000
Lead	0.000 ± 0.000	0.003 ± 0.004	0.001 ± 0.002	0.002 ± 0.003	0.002 ± 0.004	0.000 ± 0.000	0.002 ± 0.003
OC_PCM	8.161 ± 1.149	5.081 ± 2.518	5.532 ± 0.977	7.338 ± 3.147	3.596 ± 2.781	4.957 ± 1.818	2.119 ± 1.442
EC_PCM	4.065 ± 1.053	2.736 ± 1.341	0.964 ± 0.514	0.795 ± 0.352	0.894 ± 0.744	0.251 ± 0.089	0.271 ± 0.144
EC/OC_PCM	0.507 ± 0.140	0.585 ± 0.210	0.169 ± 0.074	0.113 ± 0.055	0.278 ± 0.133	0.053 ± 0.017	0.173 ± 0.121
OM_PCM	9.603 ± 3.401	6.596 ± 3.681	6.850 ± 1.947	11.630 ± 4.820	6.741 ± 3.629	10.389 ± 4.390	3.638 ± 2.506
OC_Hi-Vol	11.412 ± 1.265	8.394 ± 3.195	8.472 ± 1.156	8.514 ± 3.201	4.452 ± 2.240	6.211 ± 2.124	2.952 ± 1.751
EC_Hi-Vol	3.665 ± 0.950	2.636 ± 1.354	0.785 ± 0.469	0.823 ± 0.392	0.559 ± 0.443	0.114 ± 0.052	0.212 ± 0.182
EC/OC_Hi-Vol	0.329 ± 0.106	0.321 ± 0.117	0.090 ± 0.044	0.097 ± 0.044	0.127 ± 0.073	0.019 ± 0.009	0.078 ± 0.057
WSOC_Hi-Vol	4.703 ± 0.770	2.836 ± 1.256	4.300 ± 0.641	5.141 ± 2.239	2.001 ± 1.042	4.916 ± 1.936	1.685 ± 1.098
Soil	2.283 ± 0.750	1.265 ± 0.522	1.248 ± 0.438	1.573 ± 0.691	0.792 ± 0.617	0.591 ± 0.407	0.198 ± 0.108
$PM_{2.5}$	22.680 ± 3.259	14.757 ± 5.244	16.361 ± 1.545	28.828 ± 14.553	11.337 ± 5.337	24.549 ± 11.985	7.599 ± 3.230

Note: 'Summer-12', 'Summer-24', 'Winter-12', and 'Winter-24' denote 12-hr summer (June), 24-hr summer (July), 12-hr winter, and 24-hr winter filter-based field samples, respectively. "OM' indicates calculated organic matter. 'Soil' = (2.2*Al+2.49*Si+1.63*Ca+2.42*Fe+1.94*Ti).

Table 3.2. Comparison of the Field Measurements between the Non-Haze and the Haze Days in July 2005

Measurements	Campus site		Yorkville site	
	Non-Haze	Haze	Non-Haze	Haze
Ammonium (μg m^{-3})	1.963	6.641	2.243	5.395
Acetate (μg m^{-3})	0.030	0.080	0.019	0.044
Formate (μg m^{-3})	0.048	0.147	0.026	0.090
Nitrate (μg m^{-3})	0.993	0.520	0.094	0.078
Sulfate (μg m^{-3})	5.253	18.56	5.861	16.28
Oxalate (μg m^{-3})	0.177	0.359	0.167	0.271
OC_PCM (μg m^{-3})	5.235	10.84	3.815	6.860
EC_PCM (μg m^{-3})	0.692	0.969	0.244	0.262
EC/OC_PCM	0.127	0.090	0.061	0.038
OM-Calculated (μg m^{-3})	8.284	17.21	7.462	15.27
OM/OC-Calculated	1.643	1.590	1.968	2.238
OC_Hi-Vol (μg m^{-3})	6.374	12.08	4.784	8.588
EC_Hi-Vol (μg m^{-3})	0.671	1.076	0.102	0.133
EC/OC_Hi-Vol	0.101	0.089	0.021	0.016
WSOC_Hi-Vol (μg m^{-3})	3.488	7.347	3.505	6.797
Soil (μg m^{-3})	1.355	1.935	0.557	0.648
$PM_{2.5}$ (μg m^{-3})	18.59	45.89	16.50	37.96
Trace Gas				
CO (ppb)	319	432	159	201
SO2 (ppb)	2.56	7.45	1.97	3.51
NO (ppb)	-	-	0.13	0.07
NO_2 (ppb)	-	-	1.54	0.79
NO_y (ppb)	29.7	40.6	2.97	2.37
NO_x/NO_y	-	-	0.56	0.36
Meteorological Data				
Wind speed (m s^{-1})	1.28	1.00	1.98	1.31
Temperature (^oC)	26.0	27.6	24.1	26.2
Relative Humidity (%)	83	71	73	68
Precipitation (mm)	0.48	0.00	0.35	0.00
Solar Radiation (w m^{-2})	210	256	225	251
Scattering Coefficient (x10^{-5} m^{-1})	6.1	20	4.7	14

Note: the values of 'Trace Gas' and 'Meteorological Data' on the campus site in the table come from the measurements on the JST SEARCH site; and '-' denotes data unavailable.

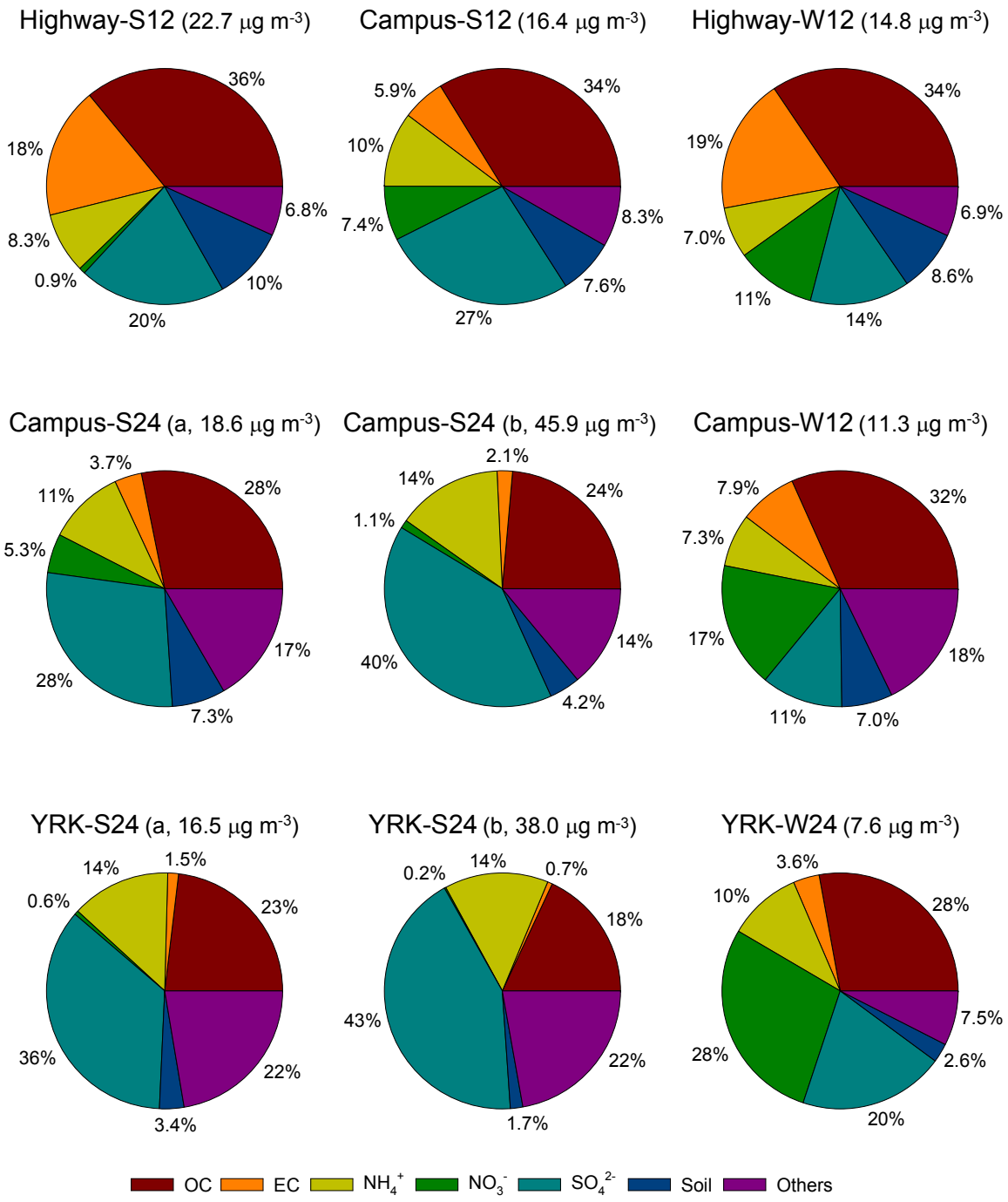

Figure 3.1. Average composition (percentage) of $PM_{2.5}$ (PCM filter samples) at the roadside, the campus and the Yorkville sites in the summer and the winter. 'Highway-12', 'Campus-12', 'Campus-24', and 'YRK-24' denote 12-hr highway, 12-hr campus, 24-hr campus, and 24-hr Yorkville filter-based field samples, respectively; 'S' and 'W' indicate the summer and the winter season, respectively. 'a' and 'b' indicate non-haze and haze samples, respectively.

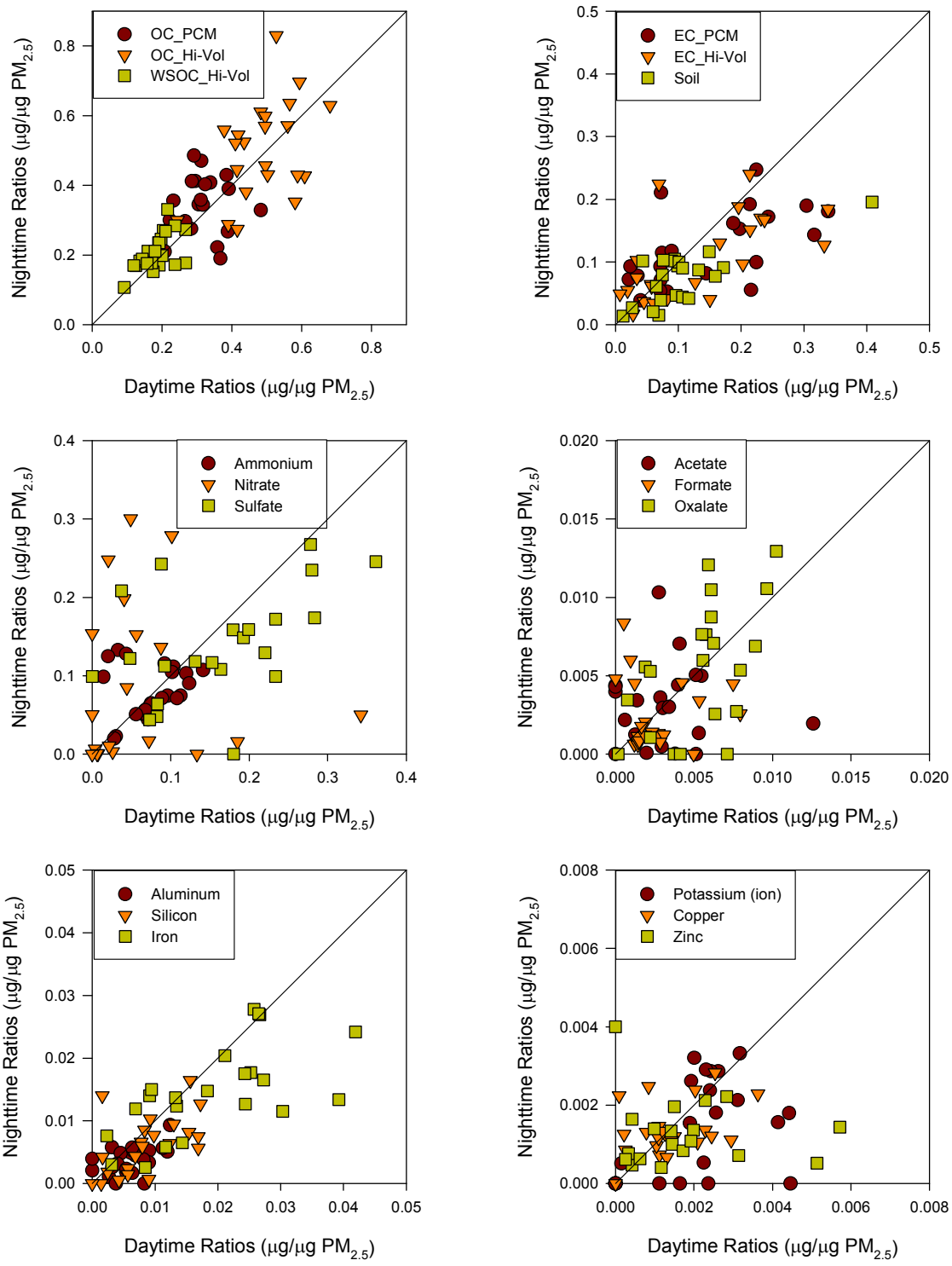

Figure 3.2. 'Nighttime' vs. 'Daytime' $PM_{2.5}$ components (12-hr back-to-back filter samples) measured at the roadside and the campus sites in the two seasons. All ambient concentrations of components are normalized to associated measured $PM_{2.5}$.

Concentrations of particulate OC, ammonium and sulfate at the campus/Yorkville sites are 2.1/1.8, 3.4/2.4, and 3.5/2.8 times higher on the haze days, respectively, and the percentages of both ammonium and sulfate in the $PM_{2.5}$ mass are elevated. In particular, sulfate increase from 28/36% on the non-haze days to 40/43% on the haze days (Figure 3.1). However, the percentages of OC in the $PM_{2.5}$ mass decrease on the haze days at both sites. Similarly, other $PM_{2.5}$ components such as EC and soil increase in concentration on the haze days, but significantly decrease in percentage. At the same time, ambient levels of SO_2 and CO are clearly elevated on the haze days. These suggest sulfate-dominant hazes that are caused by regional transport and local coal-fired power plant emissions. Nitrate decease significantly in both ambient concentration and $PM_{2.5}$ mass percentage, implying that more nitrate exists in gas phase. Little precipitation, lower wind speeds, higher temperatures and stronger solar radiation on the haze days lead to formation and accumulation of high level $PM_{2.5}$ in the stagnant atmosphere and the regionwide hazes, therefore, are due to a combination of meteorology and photochemistry (Table 3.2).

3.3.3 Day–Night Variation of $PM_{2.5}$ Composition

Day–night differences in $PM_{2.5}$ composition were studied by comparing 12-hr daytime concentrations with the surrounding 12-hr nighttime data. The nighttime $PM_{2.5}$ concentrations are slightly higher than the daytime values both at the roadside and the campus sites. To offset impacts from different mixing heights in the day and the night, the data of individual $PM_{2.5}$ components were normalized to the observed total $PM_{2.5}$. Our results do not display significant day–night variations for most $PM_{2.5}$ components including OC, sulfate, ammonium, and roadway emission-related constituents, e.g., EC, soil, iron, copper, and zinc (Figure 3.2). This suggests a relatively consistent mix of

major primary sources in the day and the night. In contrast, a significant day–night difference is observed for nitrate with ratios of 0.06±0.08 μg/μg $PM_{2.5}$ in the day vs. 0.17±0.27 μg/μg $PM_{2.5}$ in the night, implying that condensation of gas-phase nitrate in $PM_{2.5}$ is sensitive to ambient temperature. Lower temperatures at night lead to the formation of more particulate nitrate.

3.3.4 Spatial and Seasonal Comparison of $PM_{2.5}$ Composition

There are distinct spatial variations for $PM_{2.5}$ composition during both seasons (Table 3.1; Figure 3.3). The highest concentrations of automotive-related $PM_{2.5}$ components are found at the roadside site, including OC, EC, iron and copper. Their concentrations are significantly lower at the nearby campus site and are much lower at Yorkville. On average, the roadside concentrations of OC, EC, iron and copper are about 1.5, 3.6, 3.0, and 4.5 times the campus concentrations in both seasons, and the campus is 1.7, 3.3, 5.0, and 2.0 times the Yorkville, respectively (Table 3.3). In particular, EC drops by over 70% from the roadside site to the campus site while OC drops by about 30% between the same sites, suggesting a dramatic decrease of on-road emission impacts with distance away from the highway. However, zinc, manganese and lead do not show similar spatial differences. Fine soil-related components such as aluminum, silicon, calcium and titanium are usually higher at the roadside, especially in the summer, and are much lower at the rural site.

Spatial analysis of organic molecular markers indicates that there is no significant difference between the roadside and the campus sites for major nonautomotive-related primary OM sources such as meat cooking, wood combustion and vegetative detritus [*Yan et al.*, 2009c]. Ammonium and sulfate vary little between the same sites in both

seasons, and their urban concentrations are close to the rural levels, suggesting a combined impact from atmospheric secondary processing and regional transport on ammonium and sulfate. Regional dispersion and similar thermodynamics may lead to comparable data between the urban and the rural sites for particulate nitrate in the winter.

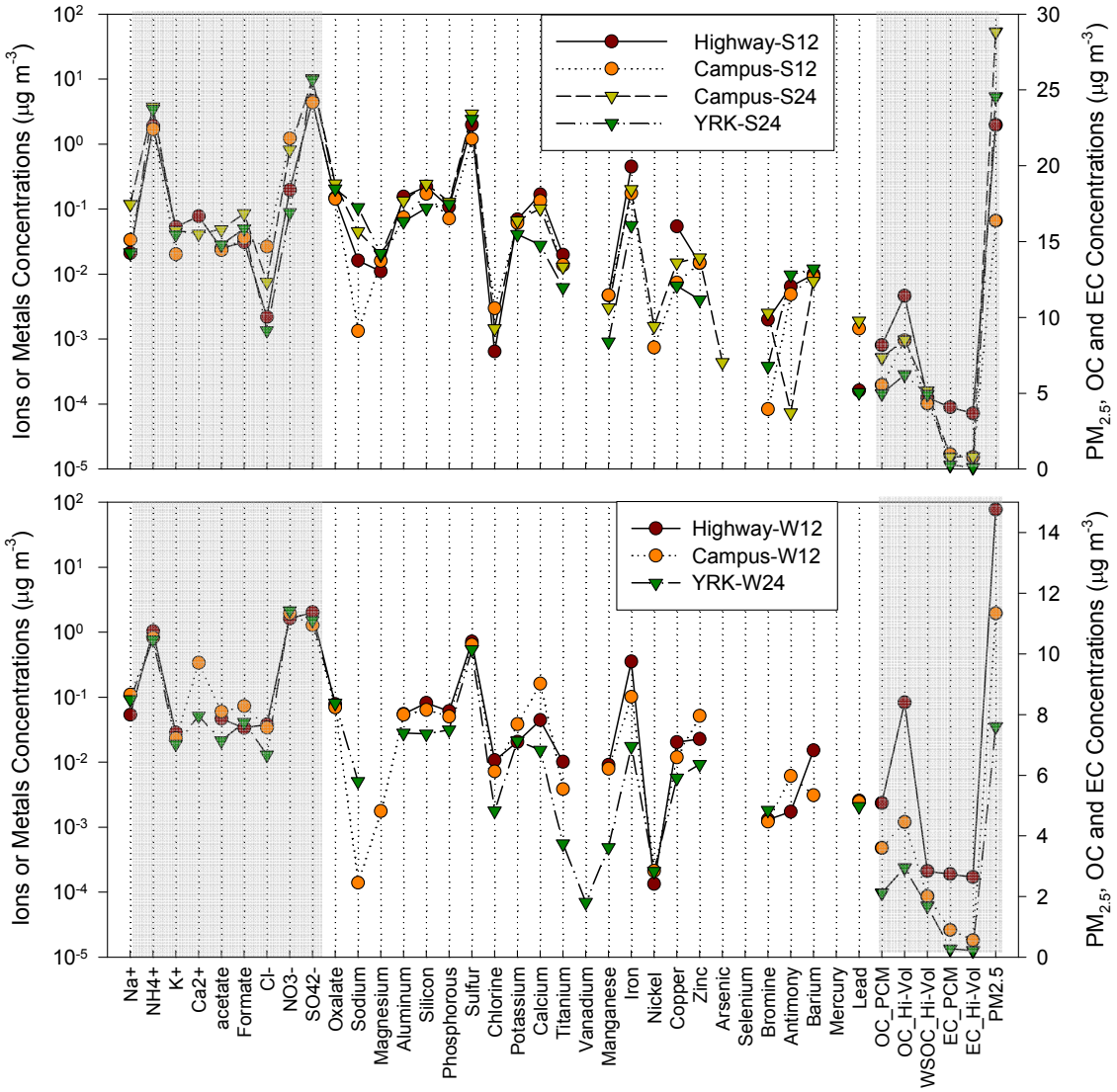

Figure 3.3. Mean concentrations of $PM_{2.5}$ components at the three sampling sites (Roadside, Georgia Tech campus and Yorkville (YRK)) and the two seasons (summer 2005 and winter 2006). 'S12', 'S24', 'W12', and 'W24' denote 12-hr summer, 24-hr summer, 12-hr winter, and 24-hr winter samples, respectively. Log scale is used.

Table 3.3. Average Concentrations of $PM_{2.5}$ Components Normalized to the Georgia Tech Campus Values (Campus-S12 or -S24)

$PM_{2.5}$ Components	Highway-S12	Campus-S12	Campus-S24	YRK-S24	Highway-W12	Campus-W12	YRK-W24
Na^+	0.62	1.00	3.55	0.18	0.49	1.00	0.85
NH_4^+	1.13	1.00	2.21	0.92	1.25	1.00	0.94
K^+	2.63	1.00	2.32	0.87	1.23	1.00	0.82
Ca^{2+}	-	-	-	0.00	0.00	1.00	0.15
Acetate	1.09	1.00	2.10	0.58	0.78	1.00	0.36
Formate	0.86	1.00	2.36	0.59	0.46	1.00	0.56
Cl^-	0.08	1.00	0.29	0.18	1.12	1.00	0.38
NO_3^-	0.16	1.00	0.67	0.11	0.83	1.00	1.11
SO_4^{2-}	1.04	1.00	2.35	0.95	1.59	1.00	1.19
Oxalate	1.04	1.00	1.72	0.84	1.12	1.00	1.17
Sodium	12.16	1.00	33.86	2.35	0.00	1.00	36.36
Magnesium	0.69	1.00	1.25	1.05	0.00	1.00	0.00
Aluminum	2.10	1.00	1.82	0.48	1.02	1.00	0.52
Silicon	1.29	1.00	1.42	0.42	1.28	1.00	0.43
Phosphorous	1.52	1.00	1.79	0.93	1.22	1.00	0.63
Sulfur	1.64	1.00	2.45	0.82	1.11	1.00	0.84
Chlorine	0.22	1.00	0.49	0.00	1.48	1.00	0.25
Potassium	1.13	1.00	1.08	0.62	0.54	1.00	0.56
Calcium	1.26	1.00	0.76	0.27	0.27	1.00	0.09
Titanium	1.44	1.00	0.94	0.48	2.64	1.00	0.14
Vanadium	-	-	-	-	-	-	-
Manganese	0.99	1.00	0.65	0.30	1.14	1.00	0.06
Iron	2.59	1.00	1.16	0.28	3.47	1.00	0.17
Nickel	0.00	1.00	2.13	0.00	0.63	1.00	0.99
Copper	7.28	1.00	2.03	0.44	1.72	1.00	0.48
Zinc	0.99	1.00	1.20	0.23	0.44	1.00	0.18
Arsenic	-	-	-	0.00	-	-	-
Bromine	23.85	1.00	30.27	0.15	1.08	1.00	1.51
Antimony	1.32	1.00	0.02	132.47	0.28	1.00	0.00
Barium	1.09	1.00	0.87	1.53	4.90	1.00	0.00
Lead	0.11	1.00	1.32	0.08	1.05	1.00	0.86
OC_PCM	1.48	1.00	1.33	0.68	1.41	1.00	0.59
EC_PCM	4.22	1.00	0.83	0.32	3.06	1.00	0.30
EC/OC_PCM	3.00	1.00	0.67	0.47	2.11	1.00	0.62
OC_Hi-Vol	1.35	1.00	1.00	0.73	1.89	1.00	0.66
EC_Hi-Vol	4.67	1.00	1.05	0.14	4.72	1.00	0.38
EC/OC_Hi-Vol	3.67	1.00	1.08	0.19	2.53	1.00	0.62
WSOC-Hi-Vol	1.09	1.00	1.20	0.96	1.42	1.00	0.84
$PM_{2.5}$	1.39	1.00	1.76	0.85	1.30	1.00	0.67
Soil	1.83	1.00	1.26	0.38	1.60	1.00	0.25
OMA_PCM	1.48	1.00	1.33	0.68	1.41	1.00	0.59

Note: ‘Highway-12’, ‘Campus-12’, ‘Campus-24’, and ‘YRK-24’ denote 12-hr highway, 12-hr campus, 24-hr campus, and 24-hr Yorkville filter-based field samples, respectively; ‘S’ and ‘W’ indicate summer and winter seasons, respectively; ‘-’ denotes data unavailable.

$PM_{2.5}$ composition is characterized by seasonal differences (Table 3.1). Significantly higher OC, sulfate and ammonium are measured in the summer as a result of strong photochemical processes and high VOC emissions. The summer concentration of nitrate is much less than the winter. There is no significant seasonal difference for EC at the campus and the rural sites. However, the summer EC is higher than the winter at the roadside site, probably due to resuspended road dust which is enriched in EC. This is supported by the fact that concentrations of fine soil components are significantly higher in the summer. However, concentrations of water-soluble potassium (K^+) are lower in the winter when more biomass burning activities occur, implying that potassium is not a unique tracer of biomass burning emissions [*Fine et al.*, 2001].

3.3.5 Source Profiles for On-Road Vehicle Emissions

The discussion above suggests that an on-road vehicle $PM_{2.5}$ emission source profile can be derived under three assumptions. The first assumption is that the overwhelming majority of automotive-related primary $PM_{2.5}$ components are due to mobile sources at the roadside. The second one is that atmospheric processing does not significantly impact individual species between emission and sampling at the roadside and campus sites. The two assumptions are reasonable given that the monitor is adjacent to the roadside and that the nearby campus site is not directly impacted, observing significant drops in concentrations of automotive-related $PM_{2.5}$ constituents (Tables 3.1 and 3.3). The third assumption is that both the roadside and the campus sites are simultaneously impacted by a regional mix from other major sources and secondary sources. This is supported by the proximity of the two sites as well as the similar levels of

sulfate and the organic tracers of non-mobile sources [*Yan et al.*, 2009c]. These assumptions can be expressed as follows:

$$PM_{regional}(\text{roadside}) = PM_{regional}(\text{campus}) \tag{3.3}$$

$$C_{i,regional}(\text{roadside}) = C_{i,regional}(\text{campus}) \tag{3.4}$$

$$f_i = \frac{C_i(\text{roadside}) - C_{i,regional}(\text{roadside})}{PM(\text{roadside}) - PM_{regional}(\text{roadside})} = \frac{C_{i,mobile}(\text{roadside} \rightarrow \text{campus})}{PPM_{mobile}(\text{roadside} \rightarrow \text{campus})} \tag{3.5}$$

where PM and C_i are concentrations of $PM_{2.5}$ and individual species i, respectively; f_i stands for the on-road mobile source primary $PM_{2.5}$ (PPM) profile; and PPM_{mobile} (roadside→campus) denotes the on-road mobile-emitted primary $PM_{2.5}$ at the campus site, which is dispersed directly from the roadside. The on-road mobile source profile f_i is calculated by subtracting the on-campus concentration of individual species from the concentration at the roadside site and dividing by the difference in $PM_{2.5}$ (PPM_{mobile}):

$$f_i = \frac{\Delta C_{i,mobile}}{PPM_{mobile}} = \frac{C_i(\text{roadside}) - C_i(\text{campus})}{PM(\text{roadside}) - PM(\text{campus})} \tag{3.6}$$

The above f_i is created separately for each 12-hr sampling period in the summer and the winter. Finally, the on-road mobile primary $PM_{2.5}$ source profiles are built by the seasonal mean of f_i (Table 3.4; Figure 3.4). Associated standard deviations of the seasonal mean f_i (summer or winter) are used in the source profiles, recognizing that the propagating uncertainties are smaller than the standard deviations. [*Yan et al.*, 2009c] A specific consideration in using this profile is that the freeway is dominated by light duty vehicle traffic (97%, by traffic volume), and that heavy duty vehicles are limited to those with local delivery. Heavy duty vehicles bypassing this city are contained to a perimeter road approximately 18 km away, contributing to the regional background.

Table 3.4. $PM_{2.5}$ Source Composition Profiles Estimated for the On-Road Mobile Emissions and from Previous Mobile Source Lab Tests (unit: μg/μg $PM_{2.5}$)

$PM_{2.5}$ Component	Summer [a]	Winter [b]	Mobile_1 [c]	Mobile_2 [d]	NFRAQS [e]	EPA Speciate [f]
OC	0.38854 ± 0.13236	0.50677 ± 0.26181	0.44475 ± 0.01826	0.55222 ± 0.08676	0.42348 ± 0.04968	0.45082 ± 0.06937
EC	0.48212 ± 0.28498	0.51614 ± 0.25545	0.27995 ± 0.01772	0.57160 ± 0.07402	0.57525 ± 0.06954	0.42631 ± 0.07226
Sulfate	0.03971 ± 0.03946	0.30269 ± 0.23993	0.00360 ± 0.00081	0.01248 ± 0.00970	0.01047 ± 0.00406	0.02423 ± 0.00484
Ammonium	0.04729 ± 0.03635	0.07049 ± 0.06581	0.00241 ± 0.00036	0.00428 ± 0.00412	0.00000 ± 0.00749	0.00000 ± 0.00001
Aluminum	0.01624 ± 0.00756	0.00070 ± 0.01403	0.00026 ± 0.00049	0.00016 ± 0.00023	0.00131 ± 0.00362	0.00058 ± 0.00010
Silicon	0.01692 ± 0.01226	0.00528 ± 0.01545	0.00285 ± 0.00014	0.00506 ± 0.00044	0.00817 ± 0.01345	0.00061 ± 0.00009
Potassium	0.00514 ± 0.00417	0.00195 ± 0.00434	0.00000 ± 0.00030	0.00032 ± 0.00034	0.00012 ± 0.00102	0.00000 ± 0.00001
Calcium	0.00804 ± 0.00508	0.00000 ± 0.09341	0.00030 ± 0.00026	0.00390 ± 0.00060	0.00817 ± 0.00111	0.00013 ± 0.00003
Titanium	0.00123 ± 0.00203	0.00122 ± 0.00242	0.00000 ± 0.00102	0.00004 ± 0.00003	0.00004 ± 0.00455	0.00007 ± 0.00001
Iron	0.04748 ± 0.02633	0.06873 ± 0.02593	0.00023 ± 0.00003	0.00144 ± 0.00086	0.00820 ± 0.00106	0.00101 ± 0.00020
Copper	0.00721 ± 0.00352	0.00179 ± 0.00109	0.00003 ± 0.00003	0.00024 ± 0.00010	0.00023 ± 0.00037	0.00756 ± 0.00151
Zinc	0.00000 ± 0.00314	0.00000 ± 0.01699	0.00043 ± 0.00003	0.00430 ± 0.00195	0.00634 ± 0.00068	0.00731 ± 0.00143

Note: [a] source composition profiles where individual organic compounds are normalized to the on-road primary OC mass estimated in the summer; [b] source composition profiles where individual organic compounds are normalized to the on-road primary OC mass estimated in the winter; [c] combined mobile source composition profiles based on the gasoline- and diesel-powered vehicle emission profiles tested by Schauer et al. [*Schauer et al.*, 1999b; 2002b]; [d] combined mobile source composition profiles based on the gasoline- and diesel-powered vehicle emission profiles tested by Lough et al. [*Lough et al.*, 2007]. [e] combined mobile source composition profiles based on the gasoline- and diesel-powered vehicle emission profiles provided in NFRAQS [*Watson et al.*, 1998]; [f] combined mobile source composition profiles based on the gasoline- and diesel-powered vehicle emission profiles provided in EPA SPECIATE 4.0 [*Cooper et al.*, 1987]. The species with fractions significantly less than one standard deviation from zero are not shown in the table.

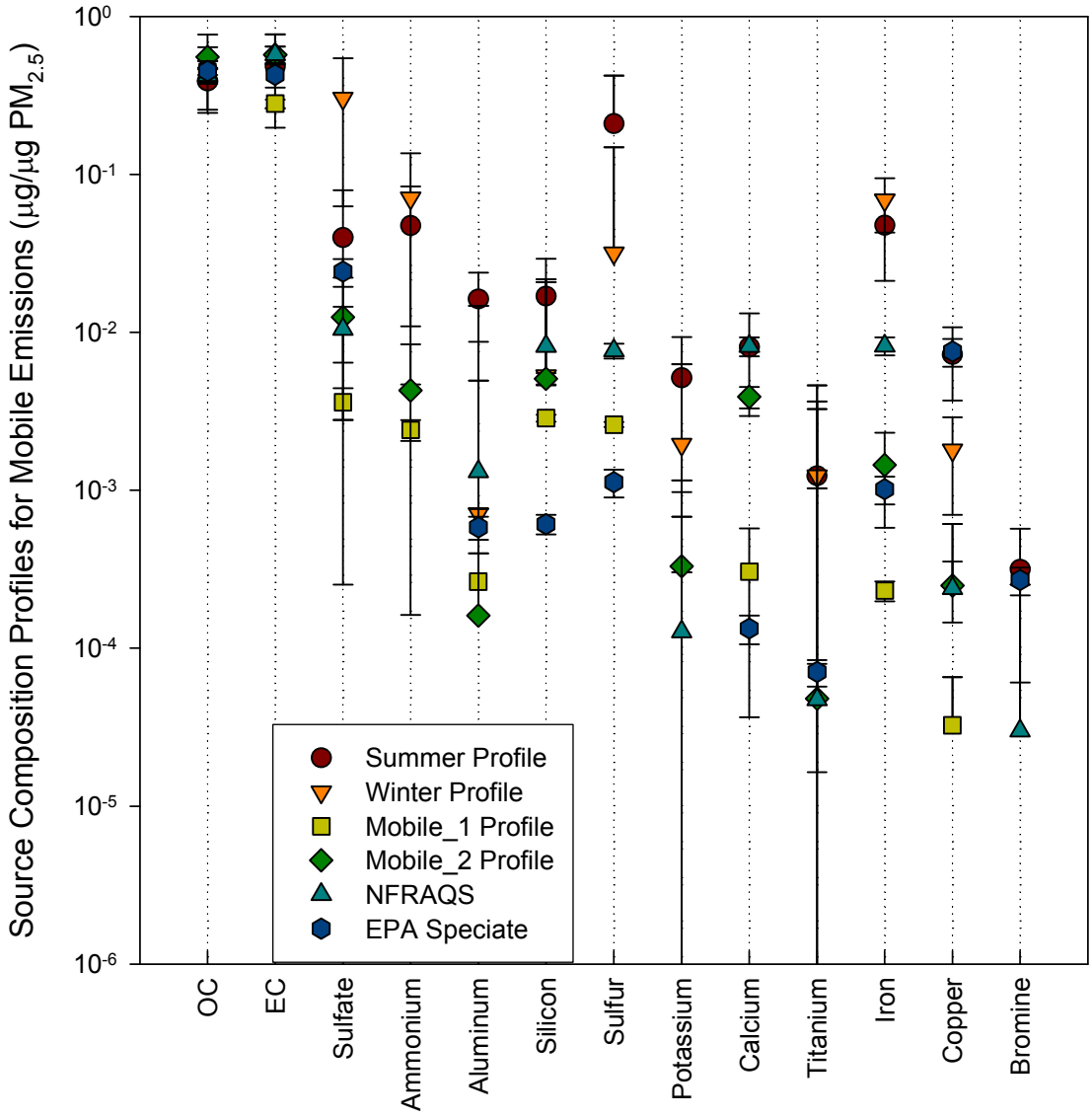

Figure 3.4. Calculated summer and winter $PM_{2.5}$ source composition profiles for on-road mobile emissions in this study and two combined mobile emission source profiles, Mobile_1 and Mobile_2, which are built by integrating previous gasoline- and diesel-powered vehicle emission profiles measured by Schauer et al. [*Schauer et al.*, 1999b; 2002b] and Lough et al. [*Lough et al.*, 2007], respectively. 'NFRAQS' and 'EPA SPECIATE' indicate the emission profiles tested in North Front Range Air Quality Study and EPA SPECIATE 4.0 database, respectively. The profiles are composed of individual species fractions, normalized to $PM_{2.5}$. Log scale is used and error bars are shown.

In this study, two on-road mobile emission source profiles are approximated from the summer and winter measurements, and the results show a significant seasonal difference between the two profiles. The winter season has a significant higher fraction of OC in $PM_{2.5}$ while the EC fraction is slightly higher. There are several possible reasons for the differences, including higher emission factors of fine OC from on-road mobile sources in the cold season, lower gas-particle partitioning of organic matter in the warm season, and meteorological impacts [*Pankow*, 1987; *Robinson et al.*, 2007]. Given the observed discrepancies, contributions of mobile sources are subject to underestimation in summer or overestimation in winter without application of seasonal-specific profiles. A further implication is that the contribution split between gasoline vehicle and diesel vehicle exhausts would be impacted by application of season-specific OC/EC ratios in source profiles. The fractions of sulfate, ammonium, and iron are higher in the winter source profile, whereas aluminum, silicon, sulfur, potassium, calcium and copper are higher in the summer source profile. It is more interesting that the fractions of zinc, manganese and antimony are not significantly different from zero in $PM_{2.5}$ in both source profiles, even though they have been proposed elsewhere as metal tracers for roadway-related emissions such as emissions of fuel, motor oil and additives (zinc dithiophosphate), tailpipe emissions of motor oil, tire wear, and brake wear ([*Lough et al.*, 2005b; *Ning et al.*, 2008] and references therein). This implies that there probably exist other important sources for these elements so that emissions of these sources either overwhelm on-road emissions of the elements in both sites or only significantly increase the ambient levels at the campus site. For example, zinc can also be emitted by metal process industry. This study indicates that application of these elements in receptor

models is probably limited given that the unknown major sources were not included in source apportionment modeling. The comparison also indicates that EC and iron are preferred inorganic tracers of mobile sources in source apportionment due to their abundance and seasonal stability.

The two on-road mobile primary $PM_{2.5}$ source profiles developed in this work were further compared with those measured previously in the lab. The lab-based profiles were calculated using observed vehicle types (passenger vehicles, small trucks, large trucks and buses) on the I-75/85 highway [*Kall and Guensler*, 2007] and $PM_{2.5}$ emission factors from the Mobile6 model (version 6.2.0.3). Gasoline- and diesel-related emission ratios were obtained for OC, EC, and $PM_{2.5}$ by assuming all passenger vehicles and a half of small trucks are gasoline vehicles while large trucks, buses and another half of small trucks are diesel vehicles. These emissions-weighted fractions were combined with previous gasoline- and diesel-powered vehicle emission profiles measured by Schauer et al. [*Schauer et al.*, 1999b; 2002b], Lough et al. [*Lough et al.*, 2007], Watson et al. [*Watson et al.*, 1998], and Cooper et al. [*Cooper et al.*, 1987], respectively, creating four different lab-based mobile source profiles, Mobile_1, Mobile_2, NFRAQS, and EPA SPECIATE.

The comparisons show that OC and EC are comparable, but other $PM_{2.5}$ components differ (Table 3.4; Figure 3.4). The lowest OC fraction, 0.389, is found in the summer source profile, and the value in the winter profile is 0.507, similar to the average OC of the four lab-based profiles, 0.468. The EC fractions in the summer and the winter profiles, 0.482 and 0.516, are higher than the average EC of the four lab-based profiles, 0.463. The levels of ammonium, sulfate, titanium, and iron are significantly higher than

those derived from the lab-based profiles. The fractions of aluminum and silicon in the winter profile are comparable to the others, but much higher in the summer profile. Copper in the summer profile is similar to the one in the EPA SPECIATE profile. In contrast, nitrate, manganese and zinc, which are tested in each of the lab-based source profiles, are not statistically significant in our real-world source profiles. Such differences suggest that source profiles are location specific and the actual on-road mobile emissions (or the impact of dilution and cooling process) differ significantly from the lab tests. On the other hand, the uncertainties of individual species would be large in the source profiles in the presence of other unknown important sources for $PM_{2.5}$ components at the roadside or the campus sites. Furthermore, the on-road source profiles here actually include contribution from road dust.

3.3.6 WSOC in Total OC

A significant fraction of total OC is WSOC, which is correlated to oxygenated organic compounds and has been proposed as an indicator of secondary organic aerosol (SOA) and biomass burning contributions in airborne $PM_{2.5}$ [*Kondo et al.*, 2007; *Sullivan et al.*, 2006]. Summer time spatial variations of WSOC at the three sampling sites have been discussed partially previously, and the results suggest that anthropogenic sources probably play a role in the formation of SOA in this region in the absence of biomass burning emissions [*Weber et al.*, 2007]. Here, further research is focused on exploring both seasonal and spatial distributions of WSOC in fine particulate OC. Note that both WSOC and total OC presented below are measured from Hi-Vol filter samples.

The summer concentrations of WSOC, on average, are roughly 2 times the winter, accounting for 41% and 51% of OC at the roadside and the campus sites in June 2005,

respectively, and 60% and 79% at the campus and the Yorkville sites in July 2005 (Table 3.1). On the haze days, WSOC concentrations are about 2 times those on the non-haze days at both the campus and the Yorkville sites, and their percentages in total OC increased by 6% (Table 3.2). In the winter, the levels of WSOC decrease to 34%, 45% and 57% of OC at the roadside, the campus and the Yorkville sites, respectively. Although WSOC is also emitted by biomass burning, much higher WSOC in the summer suggests formation of more SOA in the atmosphere, supported by strong correlations between WSOC and OC or secondary tracers such as sulfate, ammonium, and SOA tracers (e.g., dicarboxylic acids, 2-methyltetrols, *cis*-pinonic acid and pinic acid) (Table 3.5). This is further supported by the fact that WSOC is not correlated to levoglucosan, an organic tracer of biomass burning, in the summer. The ratios of WSOC/levoglucosan measured in this research are 109–182 in the summer and 10–15 in the winter at the urban and rural sites. On the other hand, WSOC/levoglucosan ratios of biomass burning emissions measured in the Atlanta area are 9.1 and 6.4 for the aged prescribed burning plume and wildfire plume, respectively [*Lee et al.*, 2008; *Yan et al.*, 2008a; *Yan et al.*, 2009a]. Thus, it can be estimated that biomass burning contributes less than 8% of WSOC in the summer and over 60% of WSOC in the winter, given that levoglucosan is a unique organic tracer of biomass burning and relatively stable in the atmosphere [*Fraser and Lakshmanan*, 2000; *Simoneit et al.*, 1999]. In other words, an overwhelming majority of WSOC in $PM_{2.5}$ is SOA in the summer, and there may be a significant SOA fraction in OC even in the winter. This is supported by the significant correlation coefficients between WSOC and SOA tracers in the summer and the winter (Table 3.5).

Spatially, WSOC concentrations decrease slightly from the roadside site to the campus site and then to Yorkville in both seasons, revealing regionally homogeneous contributions from SOA and biomass burning emissions (Table 3.1). In the winter, biomass burning is a major source of OC and WSOC over this region, and exhibits little spatial variation, as shown by associated organic tracers, levoglucosan and resin acids [*Yan et al.*, 2009c]. There is no solid evidence that either anthropogenic or biogenic sources play a predominant role in SOA formation over this area. WSOC is correlated with both aromatic acids (1,2-, 1,3-, and 1,4-benzenedicarboxylic acid), tracers of mobile sources and anthropogenic secondary sources [*Fraser et al.*, 2003a; *Schauer et al.*, 2002a], and biogenic SOA tracers, *cis*-pinonic acid, pinic acid and 2-methyltetrols (Table 3.5). These imply that there are complex sources and photochemical paths to form WSOC and SOA in the atmosphere, which cannot be elucidated well by the current knowledge about organic compounds linked to SOA.

In addition, our study found that ambient WSOC can come from the sources other than SOA and biomass burning emission. In the on-road mobile source summer and winter profiles developed in this research, WSOC approximately makes up about 15±12% and 21±10% of total primary OC emitted by on-road motor vehicles (not shown in figures), respectively. That suggests mobile source is probably a minor contributor of WSOC especially in the winter, possibly due to direct emissions of polar organic compounds from motor vehicles, contribution of resuspended road dust or fast formation/condensation of anthropogenic SOA at the roadside.

Table 3.5 Correlation Coefficients between WSOC and Other $PM_{2.5}$ Components

$PM_{2.5}$ Components	Correlation Coefficient (P-value)						
	Highway-S12	Campus-S12	Campus-S24	YRK-S24	Highway-W12	Campus-W12	YRK-W24
Ammonium	0.26 (0.58)	0.41 (0.37)	**0.95 (0.00)**	**0.96 (0.00)**	0.35 (0.19)	0.34 (0.19)	0.32 (0.48)
Sulfate	0.23 (0.63)	0.25 (0.59)	**0.96 (0.00)**	**0.99 (0.00)**	0.32 (0.23)	**0.49 (0.05)**	0.49 (0.27)
OC_Hi-Vol	**0.83 (0.02)**	**0.72 (0.07)**	**0.97 (0.00)**	**0.99 (0.00)**	**0.89 (0.00)**	**0.87 (0.00)**	**0.99 (0.00)**
EC_Hi-Vol	-0.28 (0.55)	0.10 (0.84)	**0.88 (0.01)**	0.41 (0.36)	0.24 (0.37)	0.29 (0.29)	**0.85 (0.02)**
Levoglucosan	0.37 (0.41)	0.24 (0.60)	0.60 (0.15)	**0.97 (0.00)**	**0.77 (0.00)**	**0.82 (0.00)**	**0.94 (0.00)**
1,2-Benzenedicarboxylic acid	0.07 (0.88)	**0.89 (0.01)**	0.34 (0.46)	**-0.74 (0.06)**	0.08 (0.78)	0.22 (0.42)	0.62 (0.14)
1,4-Benzenedicarboxylic acid	-0.10 (0.83)	0.30 (0.51)	0.54 (0.21)	-0.59 (0.17)	0.11 (0.68)	**0.59 (0.02)**	0.48 (0.27)
1,3-Benzenedicarboxylic acid	-0.33 (0.47)	**0.86 (0.01)**	0.32 (0.48)	-0.63 (0.13)	0.06 (0.83)	**0.89 (0.00)**	**0.89 (0.01)**
cis-Pinonic acid	-0.28 (0.55)	**0.71 (0.08)**	-0.62 (0.14)	**-0.75 (0.05)**	-0.02 (0.95)	**0.47 (0.07)**	**0.67 (0.10)**
Pinic acid	-0.04 (0.93)	**0.69 (0.09)**	-0.07 (0.89)	-0.63 (0.13)	0.20 (0.47)	**0.67 (0.01)**	0.56 (0.20)
Sum of dicarboxylic diacids	-0.10 (0.83)	**0.96 (0.00)**	0.42 (0.35)	-0.47 (0.28)	0.21 (0.43)	**0.88 (0.00)**	**0.73 (0.06)**
2-Methyltetrols	-0.02 (0.97)	**0.88 (0.01)**	0.66 (0.11)	0.64 (0.12)	0.30 (0.25)	0.13 (0.62)	-0.24 (0.61)
BioSOA	-0.23 (0.62)	**0.74 (0.06)**	0.65 (0.11)	0.63 (0.13)	0.00 (0.99)	**0.48 (0.06)**	0.66 (0.11)
Hopanes	0.35 (0.45)	-0.04 (0.93)	0.49 (0.27)	-0.38 (0.40)	0.14 (0.60)	0.31 (0.24)	0.47 (0.29)
Steranes	0.32 (0.49)	-0.18 (0.70)	-0.23 (0.62)	**-0.67 (0.10)**	0.08 (0.76)	0.23 (0.40)	**-0.68 (0.09)**
Isoprene	0.16 (0.74)	0.05 (0.92)	**0.83 (0.02)**	n/a	n/a	n/a	n/a

Note: 'BioSOA' represents the sum of 2-methyltetrols, cis-pinonic acid and pinic scid; 'S12', 'S24', 'W12', and 'W24' denote 12-hr summer (June, 2005), 24-hr summer (July, 2005), 12-hr winter (January, 2006), and 24-hr winter (January, 2006) filter-based field samples, respectively; "n/a', not available; Significant figures (i.e., P-value is equal to or less than 0.10) are shown in bold type.

Acknowledgments

This work was funded in part by the U.S. Environmental Protection Agency STAR grants (R832159, R828976 and R831076). We would like to thank Georgia Power (Southern Company) for their support of work at the Laboratory for Atmospheric Modeling, Diagnostics, and Analysis (LAMDA) at Georgia Institute of Technology in this study area. The authors acknowledge Atmospheric Research & Analysis, Inc. for their help with the field sampling and meteorological measurements. We also thank Xiaolu Zhang for assistance with the WSOC lab measurements.

CHAPTER 4

SOURCE APPORTIONMENT OF $PM_{2.5}$ ORGANIC CARBON AND SOA IMPACT: SPATIAL AND TEMPORAL VARIATIONS

(Bo Yan, Mei Zheng, Yongtao Hu, Amy P. Sullivan, Rodney J. Weber, Eric S. Edgerton, and Armistead G. Russell. *Environmental Science & Technology*, in preparation)

Abstract

Source apportionment of $PM_{2.5}$ and organic carbon was performed using the molecular marker-based chemical mass balance (CMB-MM) model. Contributions of major primary sources were calculated, including diesel vehicle exhaust, gasoline vehicle exhaust, biomass burning, meat cooking, road dust, and vegetative detritus. Their seasonal and spatial variations are also discussed. The CMB-MM estimated contributions of roadway-related emissions (sum of diesel vehicle exhaust, gasoline vehicle exhaust, and road dust) were evaluated at the roadside site using the differences in the total organic carbon (OC) measured between the roadside site and the nearby campus site. This research in particular focused on assessing the secondary OC (SOC) contribution using four different approaches: (1) the CMB-MM model; (2) the elemental carbon (EC) tracer method; (3) the water-soluble organic carbon (WSOC) method; (4) the secondary organic tracer method. Fraction boundaries of SOC in total OC were estimated at the roadside, the campus and the rural sites for the summer and the winter.

4.1 Introduction

Fine particulate matter ($PM_{2.5}$) has been associated with adverse health effects [*Dockery et al.*, 1993; *Pope et al.*, 2002], and sources of airborne $PM_{2.5}$ appear to be of particular interest [*Sarnat et al.*, 2008]. To explore composition and sources of $PM_{2.5}$, 12-hr and 24-hr $PM_{2.5}$ filter samples were collected in summer 2005 and winter 2006 from three field sites in Georgia (Figure 2.1): two from urban Atlanta, GA (one site right next to a freeway and another 400 m away), and one at a rural site located at Yorkville (YRK), 55 km northwest of the metropolitan Atlanta. Detailed $PM_{2.5}$ composition was investigated including organic carbon (OC), elemental carbon (EC), water-soluble OC (WSOC), ionic species, trace metals, and a number of solvent-extractable organic compounds with particular focus on on-road emissions, regional transport and secondary organic aerosol (SOA) effects [*Yan et al.*, 2009c; *Yan et al.*, 2009d].

Organic matter is one of major components in ambient $PM_{2.5}$ in the southeastern U.S, accounting for up to 80% of the $PM_{2.5}$ mass in previous studies [*Hansen et al.*, 2003; *Turpin et al.*, 2000] or 40–60% in this research [*Yan et al.*, 2009d]. As a complex mixture of many organic compounds, particulate organic matter can be either emitted directly by primary sources or formed from photochemical processes in the atmosphere. Unfortunately, only a small fraction of organic matter in aerosols can be characterized quantitatively on the molecular level by current speciation methodologies, such as gas chromatography/mass spectrometry (GC/MS) [*Zheng et al.*, 2002]. In this research, 3–15% of total organic mass was quantified, with the majority of $PM_{2.5}$ organic matter characterized as unextractable and nonelutable in GC/MS [*Yan et al.*, 2009c; *Yan et al.*, 2009d]. Fortunately, this small fraction of elutable compounds contain species which can

be used as tracers for major sources of primary OC, and then major source contributions to $PM_{2.5}$ and organic aerosols can be calculated by source apportionment modeling with organic tracers measured in extractable and elutable fraction.

One of most popular approaches to calculate source contributions for organic aerosols and $PM_{2.5}$ is the organic molecular marker-based chemical mass balance (CMB-MM) air quality model. This method was first developed by Schauer et al. (1996) through introducing organic molecular markers, some of which are reasonably unique tracers for specific sources, to the regular inorganic species-based CMB model [*Schauer et al.*, 1996], and have been widely applied in source apportionment studies [*Docherty et al.*, 2008; *Fraser et al.*, 2003b; *Subramanian et al.*, 2007; *Zheng et al.*, 2002; *Zheng et al.*, 2005]. Typically, CMB-MM is used to apportion source contributions to primary OC (POC) in $PM_{2.5}$, which is emitted directly from primary sources, such as mobile sources, biomass burning, and meat cooking. Source contributions to secondary OC (SOC) cannot be obtained directly through CMB-MM modeling, but is usually estimated by the difference between measured total OC and POC identified by CMB-MM [*Schauer et al.*, 1996; *Zheng et al.*, 2002]. This would lead to large uncertainties when the estimated POC is greatly biased owing to lack of local and representative emission source profiles in the methodology. Recent studies indicated that CMB-MM source apportionment results are sensitive to the emission source profiles applied in the model [*Lough and Schauer*, 2007; *Robinson et al.*, 2006c; *Subramanian et al.*, 2006; 2007]. Moreover, the mobile source profiles newly developed in Atlanta, GA were found to be significantly different from those tested in the laboratories elsewhere [*Yan et al.*, 2009c]. It is very hard to effectively assess those modeled contributions from primary and secondary sources without

knowledge of real-world emissions and formation of ambient $PM_{2.5}$. This research provides an opportunity to directly evaluate CMB-MM performance in $PM_{2.5}$ source apportionment for both primary sources and SOC by comparing OC measurements with CMB-MM results at the roadside and the nearby campus sites.

SOC is a major component of total OC, especially in summer when vigorous photochemical processing, together with enhanced volatile organic compound (VOC) emissions, promotes formation of secondary organic aerosols (SOA) in the atmosphere. In the southeastern U.S and California, 30–80% of the total OC in summer is estimated as SOC with different approaches [*Hildemann et al.*, 1993; *Turpin and Huntzicker*, 1995; *Zheng et al.*, 2007]. However, very few studies have assessed uncertainties or errors associated with SOC estimates. The current knowledge about atmospheric formation, condensation/partition, and composition of SOA is still very poor, and no direct measurement of SOA is available. Thus, SOC estimates are primarily performed indirectly. Other than the CMB-MM approach, the EC tracer method is widely applied to separate SOC from POC based on a large set of ambient OC/EC observations in the same location [*Chu*, 2005; *Turpin and Huntzicker*, 1995]. Recent studies also propose using WSOC as an indicator of SOC since it usually correlated to SOA formation, especially in summer [*Kondo et al.*, 2007; *Miyazaki et al.*, 2006; *Weber et al.*, 2007]. Furthermore, new developments on smog chamber irradiation experiments provide a different approach, called the secondary organic tracer method, which was used to estimate major source contributions to fine SOC originating from some prevalent gaseous precursors, such as isoprene and monoterpene [*Edney et al.*, 2005; *Kleindienst et al.*, 2007a; *Offenberg et al.*, 2007].

In order to identify and quantify the impacts of specific emission sources on air quality in the metropolitan Atlanta and surrounding areas, the CMB-MM approach was used for source apportionment of fine organic carbon and $PM_{2.5}$ at the roadside, urban and rural sites in the summer and the winter. As a focus of active research, mobile source contributions identified by CMB-MM were compared to the measured OC from the roadside and the nearby campus sites. Intercomparisons of SOC estimates from the four approaches described above provide helpful information for evaluating CMB-MM performance and better understanding SOA compositions in $PM_{2.5}$.

4.2 Methods

4.2.1 The CMB-MM Model

The CMB air quality model depends on a variety of assumptions: 1) that compositions of source emissions are constant over the period of ambient and source sampling; 2) that chemical species are relatively stable and conservative during transport from emissions to the receptor; 3) that major sources contributing to the receptor are included in the model; 4) that the number of source categories is less than the number of chemical species; 5) that source profiles are linearly independent on each other (without collinear problems); and 6) that measurement uncertainties are random, uncorrelated, and normally distributed [*U.S.EPA*, 2004]. Mathematically, the fundamental principle of CMB can be expressed as:

$$C_{ik} = \sum_{j=1}^{m} a_{ij} S_{jk} + e_{ik} \qquad i = 1, 2, \ldots\ldots, n \qquad (4.1)$$

where C_{ik} is the ambient concentration of chemical species i at a specific receptor site k; a_{ij} is the fraction of chemical species i in the OC (or $PM_{2.5}$) emission from source j, also called source profile abundances; S_{jk} is the contribution of source j to the OC (or $PM_{2.5}$) concentration at the receptor site k; and e_{ik} is the error term.

Molecular marker-based source profiles applied to the CMB-MM model were obtained from previous source emission tests including medium-duty diesel truck exhaust [*Hildemann et al.*, 1991; *Schauer et al.*, 1999b], combined gasoline vehicle exhaust of catalyst- and noncatalyst-equipped gasoline-powered vehicles [*Schauer et al.*, 2002b], combined wood combustion in the southeastern states [*Fine et al.*, 2002], meat cooking [*Schauer et al.*, 1999a], Alabama paved road dust [*Schauer*, 1998; *Zheng et al.*, 2002], natural gas combustion [*Hildemann et al.*, 1991; *Rogge et al.*, 1993b], and vegetative detritus [*Hildemann et al.*, 1991; *Rogge et al.*, 1993a]. Recent studies indicate that CMB-MM source apportionment results are sensitive to the emission source profiles applied in the model [*Lough and Schauer*, 2007; *Robinson et al.*, 2006c; *Sheesley et al.*, 2007; *Subramanian et al.*, 2006; 2007]. Moreover, the on-road mobile source profiles that were newly developed in Atlanta not only show seasonal variation but also significantly differ from those tested in the laboratories elsewhere [*Yan et al.*, 2009c]. Therefore, application of these lab-created source profiles in the CMB-MM model could result in biases or uncertainties of source apportionment results in this research.

Fitting species applied to CMB-MM include aluminum (Al), silicon (Si), OC, EC, and molecular markers such as *n*-alkanes, branched alkanes, hopanes, steranes, polycyclic aromatic hydrocarbons (PAHs), cholesterol, and levoglucosan. These molecular markers are recommended as tracers for specific emission sources based on source tests [*Schauer*

et al., 1996; *Schauer and Cass*, 2000; *Simoneit et al.*, 1999]. Chemical stabilities of these fitting species during local transportation in the atmosphere have been tested [*Fraser and Lakshmanan*, 2000; *Schauer et al.*, 1996].

Through CMB-MM modeling, several major primary sources are apportioned to OC, and the sum of these sources represents POC, recognizing the inherent limitations, uncertainties and required assumptions. Then, an upper bound of SOC, namely, 'Other OC' or 'unidentified OC' in CMB-MM that probably includes unknown or unidentified primary sources, can be approximated by [*Schauer et al.*, 1996; *Subramanian et al.*, 2007; *Zheng et al.*, 2002]

$$\mathrm{POC} \approx \sum_{j=1}^{m} \mathrm{S_j(Primary)}, \qquad j = 1,2,\ldots,m \tag{4.2}$$

$$\mathrm{SOC} \approx \text{'Other } OC\text{' or 'unidentified OC'} = \mathrm{OC_{tot}} - \mathrm{POC} \tag{4.3}$$

where 'S_j' is the contribution of primary source j to the OC concentration, and 'OCtot' represents the total measured OC.

4.2.2 The EC Tracer Method

Ambient EC is considered a good tracer of primary OC generated from combustion sources [*Cabada et al.*, 2004; *Turpin and Huntzicker*, 1995]. A few relationships are built among primary OC, secondary OC and EC as follows:

$$\mathrm{OC_{pri}} = \mathrm{OC_{nc}} + \left(\frac{\mathrm{OC}}{\mathrm{EC}}\right)_{\mathrm{pri}} \times \mathrm{EC} \tag{4.4}$$

$$\mathrm{OC_{sec}} = \mathrm{OC_{tot}} - \mathrm{OC_{pri}} \tag{4.5}$$

where 'OC_{pri}', 'OC_{sec}', 'OC_{tot}' and 'OC_{nc}' represent 'primary OC', 'secondary OC', 'total measured OC' and 'non-combustion OC', respectively. The key of the EC tracer method

is to estimate OC_{nc} and $(OC/EC)_{pri}$ from measured OC and EC data. Statistically, these values can be derived from linear regression analysis of measured OC vs. EC under a consistent and dominant influence from primary source emissions. OC_{nc} is usually assumed to be negligible or small, and can be estimated by an intercept of regression line, and $(OC/EC)_{pri}$ can be approximated as a slope of regression line [*Saylor et al.*, 2006]. However, the approximation is too rough if we include all observations in the same linear regression model to estimate OC_{nc} and $(OC/EC)_{pri}$ since many OC measurements actually contain large and inconsistent secondary OC. Therefore, previous studies propose that OC observations, which are within the lowest 5–10% of OC/EC ratios or collected on a cold and cloudy winter when photochemical activities are not active, are most likely dominated by primary carbonaceous emissions [*Lim and Turpin*, 2002; *Yu et al.*, 2007].

In this research, a different statistical methodology is introduced to analyze probability distribution attributes of measured OC/EC data at different locations. The cut-off point of $(OC/EC)_{pri}$ is not arbitrarily set as the lowest 5–10% of OC/EC ratios or based solely on special winter samples, but is estimated using the data that are characterized both by the lowest OC/EC ratios and the similar probability distribution mode (e.g., normal distribution). The same OC/EC probability distribution is assumed to reflect a consistent mix of similar primary emission sources in $PM_{2.5}$. Here, probability plots of OC/EC ratios through the summer and the winter were conducted for each sampling site (Figure 4.1). Excluding those outliers, the data groups with both the lowest OC/EC ratio and linear distribution (90% confidence interval) were picked out for regression analysis. For example, the data with the probability of 5–50%, 5–40% and below 40% can meet our criteria at the roadside, campus and rural sites, respectively.

These data mostly come from the winter samples, taking 8 out of 11 roadside samples, 9 out of 12 campus samples, and all 6 rural samples. Then, sample linear regression fitting were performed to find associated slopes and intercepts at different sites, as shown in Figure 4.2. As described previously, slopes of the linear regression fitting lines are approximated as $(OC/EC)_{pri}$, which were then used to calculate OC_{pri} (or POC) and OC_{sec} (or SOC) using equations 4.4 and 4.5. Note that OC_{nc} was neglected in this research since only negative and small intercepts were obtained by the fitting model above for all sampling sites. Note that uncertainties are likely caused in this method by the fact that both the summer and winter measurements were combined and used in the same statistical model without considering seasonal variations of primary emissions and source categories owing to lack of field observations in each season. In addition, this method can only describe an average situation of primary and secondary OC for a large set of observations with significant daily or seasonal variations, e.g., many negative SOC estimates in the winter.

4.2.3 The WSOC Method

Correlated to oxygenated organic compounds, WSOC makes up a significant fraction of total OC and has been regarded as an indicator of secondary organic aerosol (SOA) and biomass burning emissions in airborne $PM_{2.5}$ [*Kondo et al.*, 2007; *Sullivan et al.*, 2006; *Weber et al.*, 2007]. The effects of biomass burning contribution need to be excluded from the total measured WSOC when it used as a surrogate of SOC. In this research, biomass burning derived WSOC is calculated from measured levoglucosan, a unique and relatively stable organic tracer of biomass burning emissions [*Fraser and Lakshmanan*, 2000; *Simoneit et al.*, 1999]. The ratios of WSOC/levoglucosan in biomass

burning emissions have been measured in Georgia, i.e., 9.1±2.9 and 4.5–6.8 for aged prescribed burning plume, and wildfire plumes at different distances downwind from the wildfires, respectively [*Lee et al.*, 2008; *Yan et al.*, 2008a; *Yan et al.*, 2009b]. The average ratio of 6.7±1.9 is used to calculate biomass burning caused WSOC ($WSOC_{biomass\ burning}$) from observed levoglucosan concentrations ($C_{levoglucosan}$). So, SOC (or WSOC_adj) can be computed as below:

$$SOC \approx WSOC_{measured} - WSOC_{biomass\ burning} \tag{4.6}$$

$$WSOC_{biomass\ burning} = \left(WSOC/levoglucosan\right)_{emission} \times C_{levoglucosan} \tag{4.7}$$

Note that this WSOC methodology tends to underestimate SOC in $PM_{2.5}$. Firstly, the above WSOC/levoglucosan ratios are overestimated with respect to primary biomass burning plumes because some WSOC here are formed secondarily. Biogenic VOCs emissions can enhance formation of SOC during the fire events, which has not been subtracted from total measured WSOC. Secondly, not all SOC in $PM_{2.5}$ are water-soluble. It was reported that 6–19% of oxygenated organic carbon (OOC) is water-insoluble between summer and winter in Tokyo, respectively [*Kondo et al.*, 2007]. Therefore, WSOC, after subtracting associated biomass burning effects, is likely to reflect the lower bound of the SOC estimate. It should be acknowledged that uncertainties could be caused by biases in the WSOC/levoglucosan ratios, which were measured in aged prescribed burning and wildfire plumes which occurred in this area and are used to represent the seasonal-average mix of various biomass burning emissions in the atmosphere, e.g., residential and commercial wood combustion.

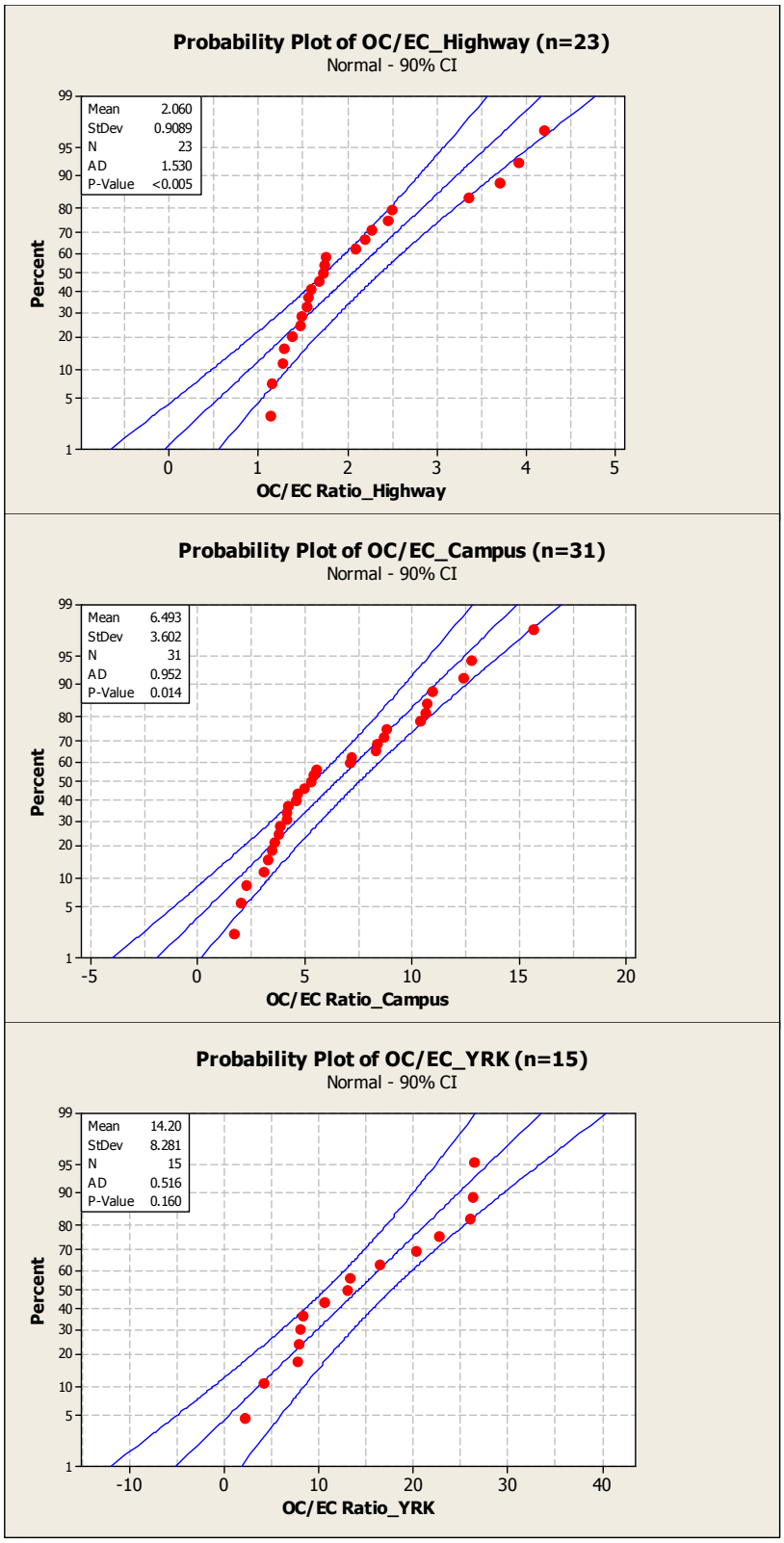

Figure 4.1. Probability plots of measured OC/EC ratios during the summer and the winter at the roadside, the campus and the Yorkville (YRK) sites.

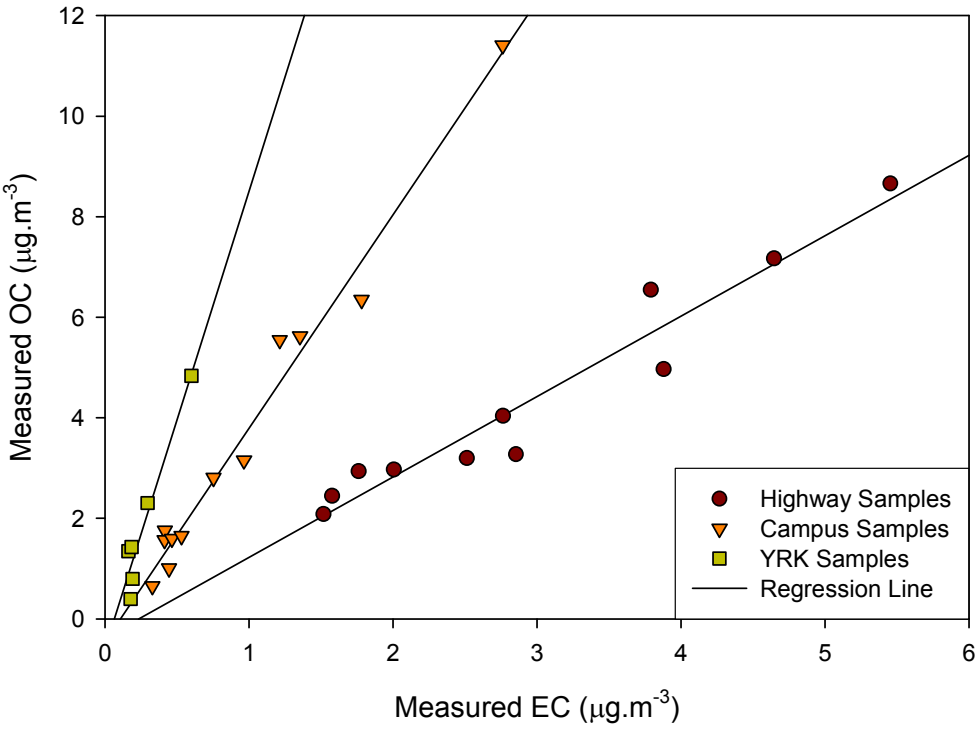

Figure 4.2. Scatter plots and linear regression fitting of the measured OC and EC with the lowest OC/EC ratios at the three sampling sites. The non-intercept fitting equations are shown as follows: a) OC_{pri}=1.4924×EC at the roadside site; b) OC_{pri}=3.9377×EC at the campus site; c) OC_{pri}=7.4377×EC at the Yorkville (YRK) site.

4.2.4 The Secondary Organic Tracer Method

Related to the two most abundant biogenic VOC emissions, isoprene and monoterpene, some SOA tracers have been identified and quantified, such as 2-methyltetrols (oxidation products of isoprene), *cis*-pinonic acid and pinic acid (oxidation products of monoterpene) [*Claeys et al.*, 2004a; *Claeys et al.*, 2004b; *Kavouras et al.*, 1998; *Yu et al.*, 1999b]. Together with developments in smog chamber irradiation and field studies, these identified SOA tracers provide us an additional path to understand composition of atmospheric SOA. The secondary organic tracer method has recently been used to estimate individual SOA sources under the assumption that SOA mass fractions

measured in the laboratory are same as those formed in the atmosphere [*Edney et al.*, 2005; *Kleindienst et al.*, 2007a; *Lewandowski et al.*, 2008; *Offenberg et al.*, 2007]. Following this method, contributions of specific secondary sources to OC, [monoterpene SOC] or [isoprene SOC], were approximated in this study using a few fixed conversion ratios of organic tracer to SOC concentrations, which were measured in the above laboratory studies. These calculations are shown below:

$$[\text{monoterpene SOC}] = \frac{[\text{cis–Pinonic acid}] + [\text{Pinic acid}]}{F_{SOC}(\text{monoterpene})} \quad (4.8)$$

$$[\text{isoprene SOC}] = \frac{[\text{2–Methyltetrols}]}{F_{SOC}(\text{isoprene})} \quad (4.9)$$

where 'F_{SOC}(monoterpene)' and 'F_{SOC}(isoprene) represent the ratios of monoterpene-derived and isoprene-derived secondary organic tracers (i.e., sum of *cis*-pinonic and pinic acids, and 2-methyltetrols) to the yielded SOC concentrations in the laboratories, respectively. In this research, the Fsoc ratios of 0.148±0.037 and 0.041±0.020 are used for isoprene and monoterpenes, respectively, assuming that these secondary organic compounds are relatively unique to their biogenic gaseous precursors [*Edney et al.*, 2005; *Kleindienst et al.*, 2007a]. However, atmospheric formation and fate of SOA are so complicated and least understood so far that the chamber irradiation-derived secondary organic tracer method can only provide preliminary estimates of SOC contributions in ambient $PM_{2.5}$ with a high degree of uncertainties.

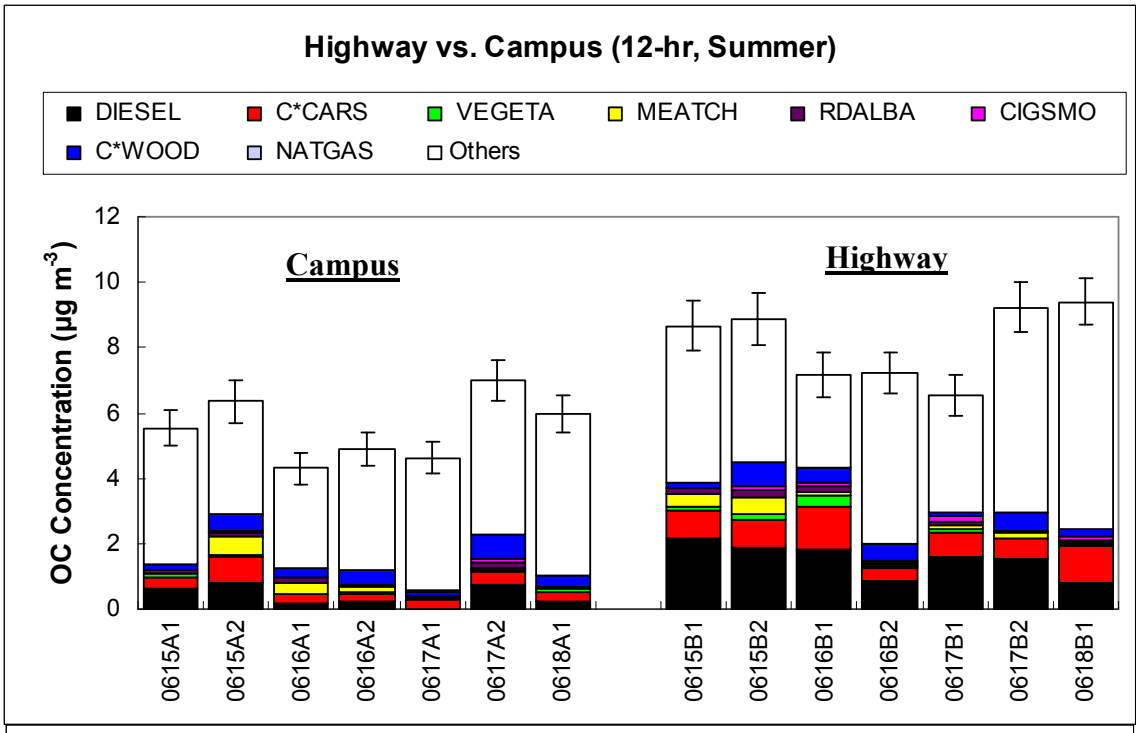

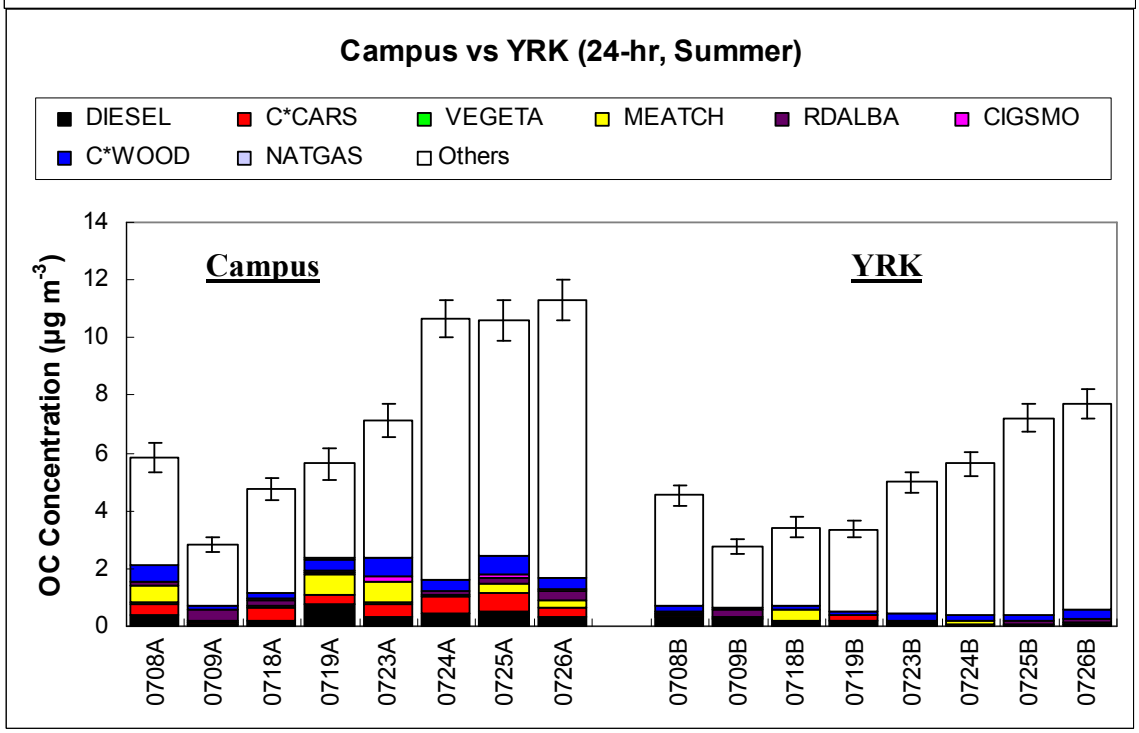

Figure 4.3. Source contributions to fine OC at the three sampling sites in summer 2005. '1' and '2' denote daytime and nighttime 12-hr samples, respectively. 'DIESEL'–diesel vehicle exhaust, 'C*CARS'–gasoline vehicle exhaust, 'VEGETA'–vegetative detritus, 'MEATCH'–meat cooking, 'RDALBA'–road dust, 'CIGSMO'–cigarette smoke, 'C*WOOD'–wood combustion, 'NATGAS'–natural gas combustion, 'Others'–other OC (or unidentified OC). Error bars are shown.

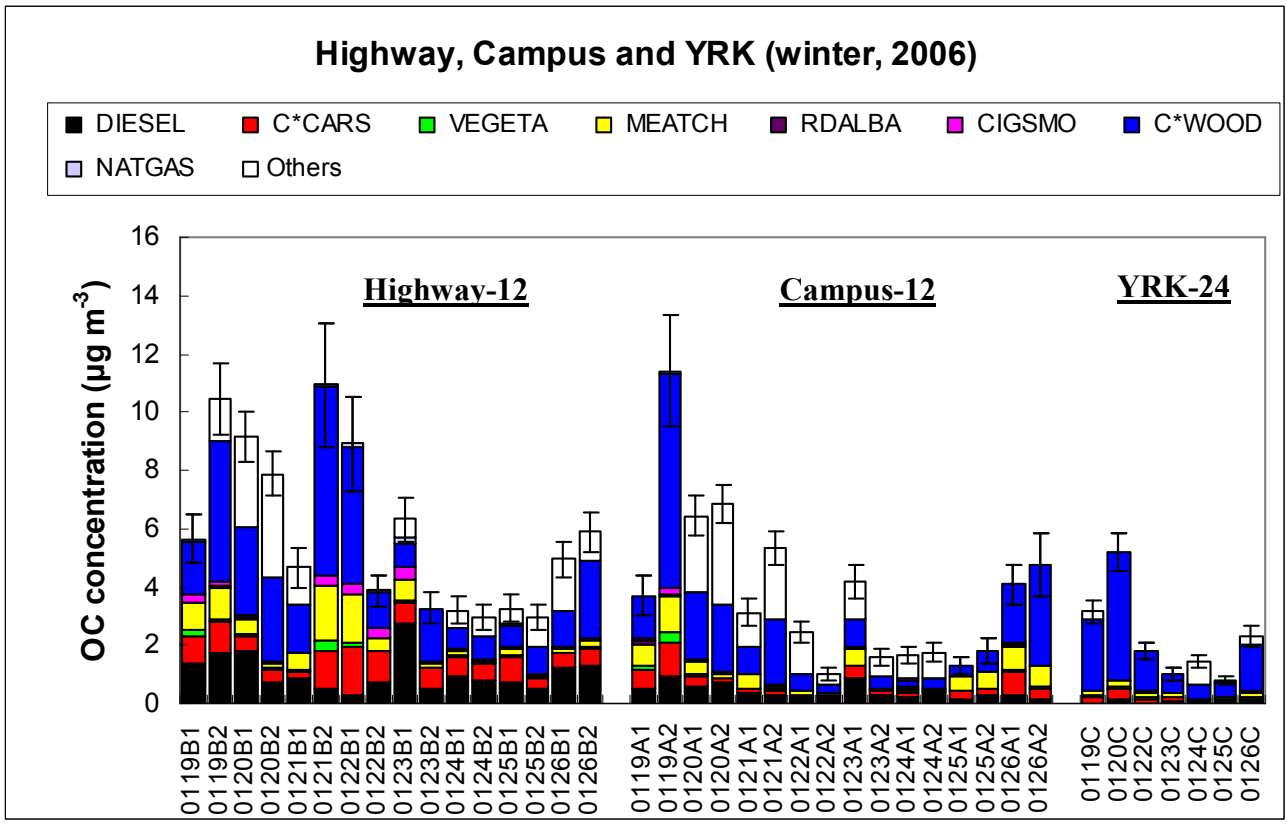

Figure 4.4. Source contributions to fine OC at the three sampling sites in winter 2006. '1' and '2' denote daytime and nighttime 12-hr samples, respectively, and 'B', 'A' and 'C' represent the roadside, the campus and the Yorkville (YRK) sites. Error bars are shown.

4.3 Results and Discussion

4.3.1 Source Apportionment of Fine OC

Up to eight primary sources of fine OC were identified by CMB-MM modeling, including diesel vehicle exhaust, gasoline vehicle exhaust, meat cooking, biomass burning, road dust, natural gas combustion, cigarette smoke, and vegetative detritus (Tables B.1 and B.2; Figures 4.3 and 4.4). Our CMB-MM results show both spatial and seasonal differences of primary source contributions for fine OC. At the two urban sites, mobile source (sum of diesel and gasoline vehicle exhausts) is the largest contributor of

primary OC in the summer, contributing 2.4 and 0.77 μg m^{-3} (or 71% and 46%) of the total identified OC (or approximated POC as discussed above) at the roadside and the campus sites, respectively (Figure 4.3). At the same time, the average OC/EC ratio at the roadside site is 3.3 times lower than that at the campus site, corresponding to a large drop in EC of over 70% [*Yan et al.*, 2009d]. In particular, diesel vehicle emissions contribute 1.5 and 0.39 μg m^{-3} (or 46% and 24%) of POC at the roadside and the campus sites in the summer, respectively, and gasoline vehicle emissions contribute 0.84 and 0.38 μg m^{-3} or (26% and 23%) of POC. Much more primary OC is apportioned to diesel vehicle emissions at the roadside site even though 97% of vehicles driving on the freeway are light-duty and gasoline-powered [*Kall and Guensler*, 2007], implying that on-road diesel vehicles have a remarkable impact on $PM_{2.5}$ emissions. Emission control of diesel vehicles exhaust is probably more important for local air quality improvement.

Meat cooking, biomass burning, road dust, and cigarette smoke are the other significant primary OC sources at the two urban sites with slight spatial variations, suggesting similar local emissions or homogeneous transport background for these primary sources at both the roadside and the campus sites (Figure 4.3). At the rural site (Yorkville or YRK), much lower primary source contributions are found. Mobile emissions are the largest primary source in the summer, contributing 0.21 μg m^{-3} (or 38%) of POC. Biomass burning, meat cooking, and road dust are the other significant sources at the rural site, whereas no cigarette smoke source is identified. In the summer, natural gas combustion is not a significant source at either the urban site or the rural site.

In the winter, source contributions of biomass burning increased greatly and surpassed all the other primary OC sources at each site, suggesting that intensive biomass

burning activities occurred regionally in cold weather, including residential, commercial and prescribed burning (Figure 4.4). On average, biomass burning contributes 2.3, 1.6, and 1.6 μg m^{-3} (or 46%, 56% and 53%) of POC in the winter at the roadside, the campus, and the rural sites, respectively. Thus significant influence of biomass burning is clearly across this region. Contributions of meat cooking also increased in the winter at all sites based on elevated ambient concentrations of cholesterol, a unique organic tracer of meat cooking. This is probably due to combination of more indoor activities and reduced atmospheric dispersion in the winter. The contributions of mobile sources, the second largest source of primary OC in the winter, varied slightly between summer and winter. This is consistent with ambient measurements of hopanes, steranes, PAHs, and EC, which are unique organic tracers or major components of mobile emissions. The trend is different from previous studies in the southeastern U.S., which report much higher source contributions from gasoline-powered vehicles in the winter [*Zheng et al.*, 2002; *Zheng et al.*, 2007].

Contributions from road dust also exhibit seasonal differences, being higher in the summer corresponding to higher levels of Al and Si, two major components of road dust. In the summer, the average concentrations of Al and Si were 2.2 and 3.4 times those in the winter. A previous study also found a similar seasonal trend for Al and Si in this region [*Zheng et al.*, 2007]. Warm weather and dry conditions in the summer may be conducive to road dust reentrainment by passing vehicles [*Fraser et al.*, 2003b]. Higher summer concentrations of Al and Si are also likely caused by long-range transport of African dusts, which are thought to be carried to the southeastern U.S. by the summer trade winds [*Prospero et al.*, 2001]. As minor primary sources, cigarette smoke and

vegetative detritus did not show significant seasonal variations. In addition, source contributions from natural gas combustion increased significantly at the urban sites in the winter, reflecting enhanced emissions from residential heating activities relaying on natural gas combustion (Figures 4.3 and 4.4)

It is common to find that total measured OC mass is not completely identified by the CMB-MM model, especially in summer samples (Figures 4.3 and 4.4). On average, the identified primary sources can explain 26.2% and 98.8% of the measured OC in the summer and the winter, respectively. These unidentified OC mass, namely 'Other OC', can consist of three terms: unidentified POC, SOC and propagated uncertainties. In the winter, 'Other OC', on average, accounts for 1% of the total OC, whereas it takes over 70% in the summer, implying SOA play a role in this observed seasonal variations. The fraction of 'Other OC', about 70% in the total measured OC, is similar to what was found in previous studies [*Zheng et al.*, 2007].

4.3.2 Source Apportionment of $PM_{2.5}$

From the fine OC source apportionment results above, source contributions to $PM_{2.5}$ mass were computed using $OC/PM_{2.5}$ ratios measured in previous source emission tests. Sulfate, nitrate and ammonium from secondary atmospheric formation were calculated directly from their ambient concentrations by subtracting the associated amounts emitted from primary sources, which are very small. Detailed source contributions from secondary sulfate, nitrate, and ammonium for $PM_{2.5}$ have been shown and discussed in another article [*Yan et al.*, 2009d]. The focus of this study is on source apportionment of fine organic matter.

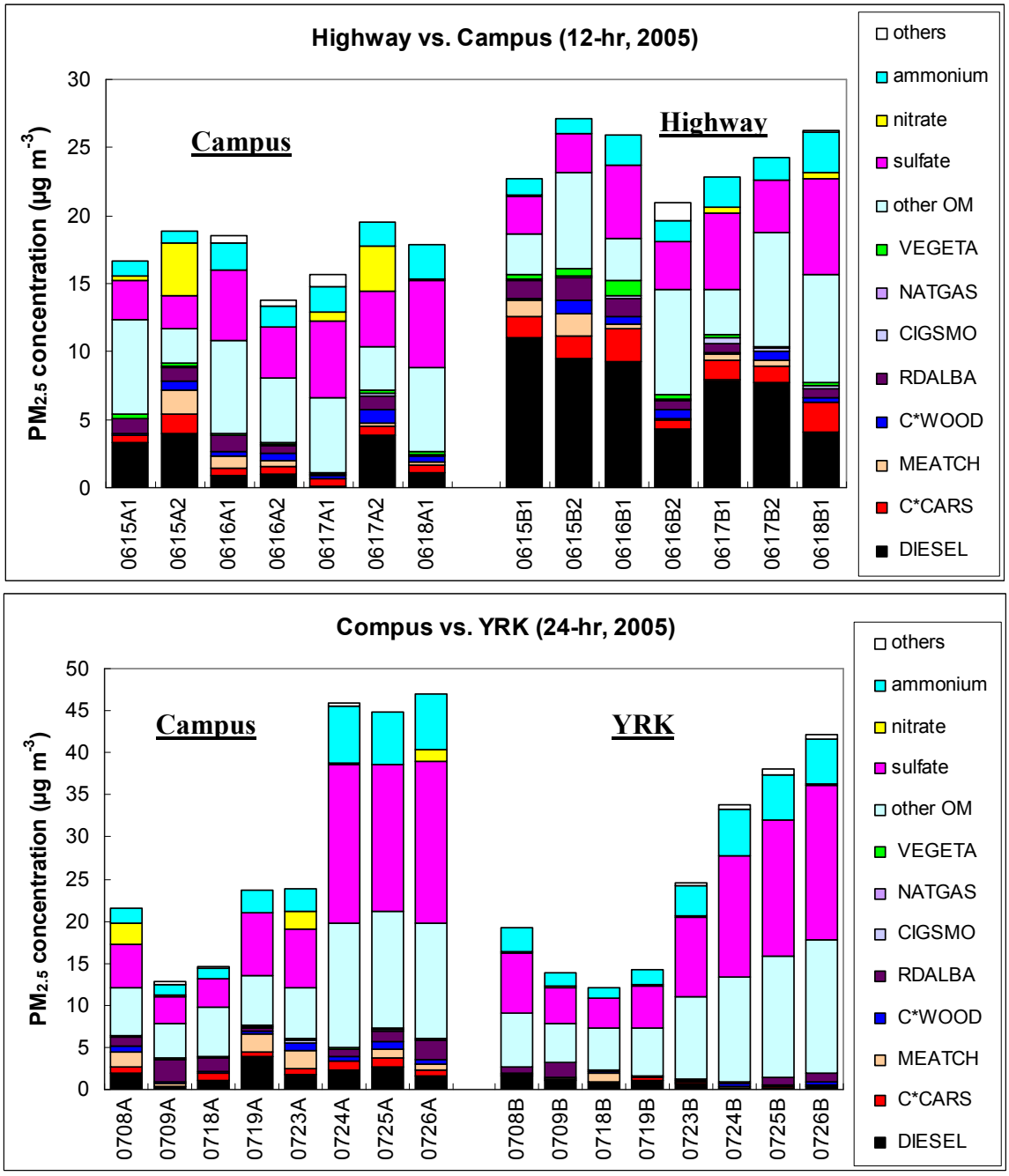

Figure 4.5. Source contributions to $PM_{2.5}$ at the three sampling sites in summer 2005. '1' and '2' denote daytime and nighttime 12-hr samples, respectively. 'DIESEL'–diesel vehicle exhaust, 'C*CARS'–gasoline vehicle exhaust, 'MEATCH'–meat cooking, 'C*WOOD'–wood combustion, 'RDALBA'–road dust, 'CIGSMO'–cigarette smoke, 'NATGAS'–natural gas combustion, 'VEGETA'–vegetative detritus, 'other OM'–other organic matter (converted from 'other OC'), 'Others'–other or unidentified $PM_{2.5}$.

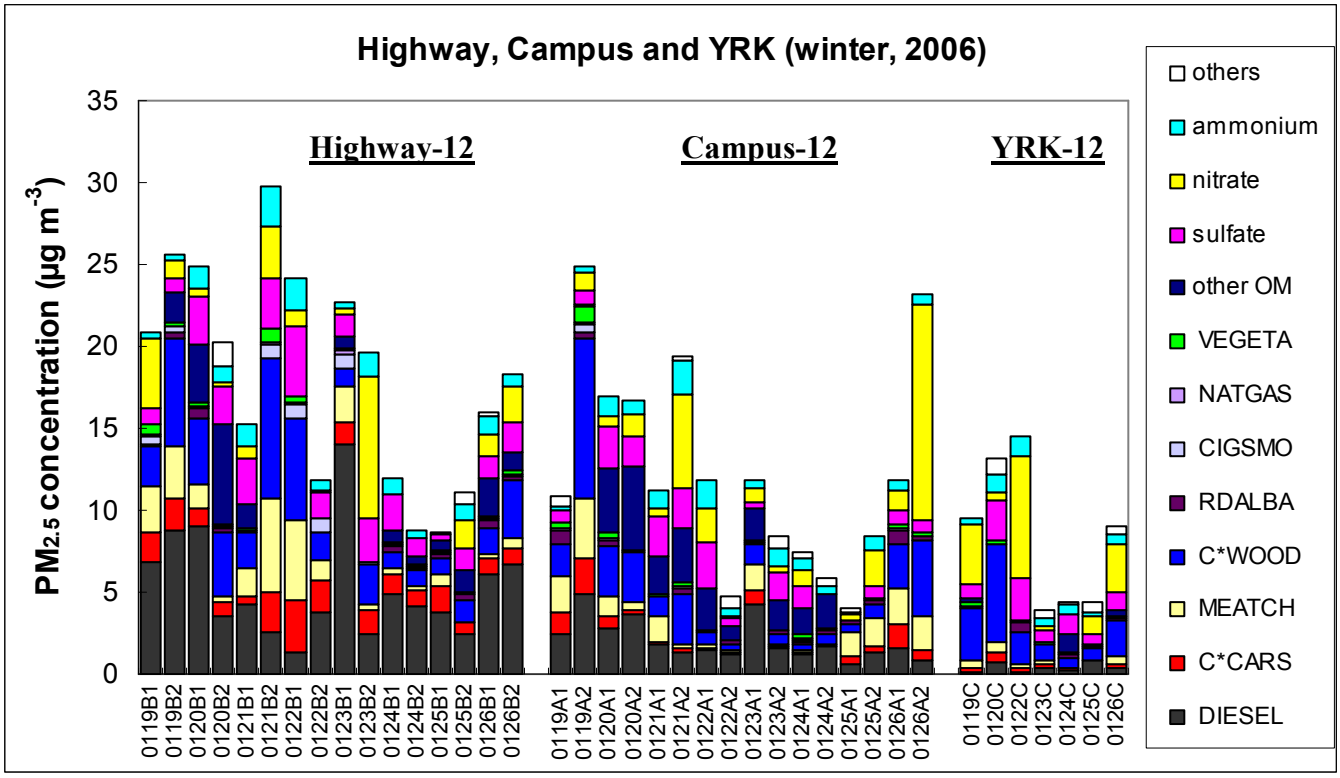

Figure 4.6. Source contributions to $PM_{2.5}$ at the three sampling sites in winter 2006. '1' and '2' denote daytime and nighttime 12-hr samples, respectively, and 'B', 'A' and 'C' represent the roadside, the campus and the Yorkville (YRK) sites. 'DIESEL'–diesel vehicle exhaust, 'C*CARS'–gasoline vehicle exhaust, 'MEATCH'–meat cooking, 'C*WOOD'–wood combustion, 'RDALBA'–road dust, 'CIGSMO'–cigarette smoke, 'NATGAS'–natural gas combustion, 'VEGETA'–vegetative detritus, 'other OM'–other organic matter (converted from 'other OC'), 'Others'–other or unidentified $PM_{2.5}$.

Our results indicate that mobile source, meat cooking, biomass burning, and road dust are major primary sources to $PM_{2.5}$ mass (Tables B.3 and B.4; Figures 4.5 and 4.6). At the urban sites, mobile source contributed 9.3 and 2.7 µg m^{-3} (or about 37% and 12%) of the total identified $PM_{2.5}$ mass on average in the summer at the roadside and the campus sites, respectively, whereas the average contributions decreased slightly at the

two sites with values of 6.7 and 2.6 μg m^{-3} (or 37% and 22%) of the total identified $PM_{2.5}$ mass. In both seasons, contributions from diesel vehicle exhausts were significantly higher than those from gasoline vehicle exhausts at the urban sites. At the rural site, mobile source contributions were much lower with values of 0.86 and 0.65 μg m^{-3} (or 4% and 8%) of the total identified $PM_{2.5}$ mass in the summer and winter, respectively. As a typical urban source, meat cooking contributed 0.68 and 1.4 μg m^{-3} (or 2.9% and 9.6%) of the identified $PM_{2.5}$ mass in the summer and the winter, respectively. Source contributions from biomass burning and road dust exhibited different seasonal variation patterns. At the urban sites, biomass burning and road dust contributed 0.52 and 0.94 μg m^{-3} (or 2.2% and 3.9%) of the identified $PM_{2.5}$ mass in the summer, respectively, whereas contributed 2.6 and 0.24 μg m^{-3} (or 18% and 1.8%) in the winter. No significant seasonal variation of source contributions is observed for cigarette smoke and vegetative detritus. In addition, natural gas combustion is identified only in the winter at the urban sites.

Secondary sources also play important roles in composition of ambient $PM_{2.5}$ at this area, especially in the summer, including secondary sulfate, nitrate, ammonium, and 'Other OM' ('other organic matter', which is converted from CMB-MM-estimated 'Other OC' by associated OM/OC ratios obtained in this research [*Yan et al.*, 2009d]). With relatively small spatial variations, these secondary sources usually show regional transport attributes. On average, secondary sulfate, nitrate, ammonium and 'Other OM' contributed 7.4, 0.55, 2.7, and 7.4 μg m^{-3} (or 31%, 2.4%, 11%, and 31%) of the total identified $PM_{2.5}$ mass in the summer, respectively. In the winter, their average contributions are 1.5, 1.8, 0.85, and 1.2 μg m^{-3} (or 14%, 19%, 7.9%, and 9.1%) of the identified $PM_{2.5}$ mass, respectively.

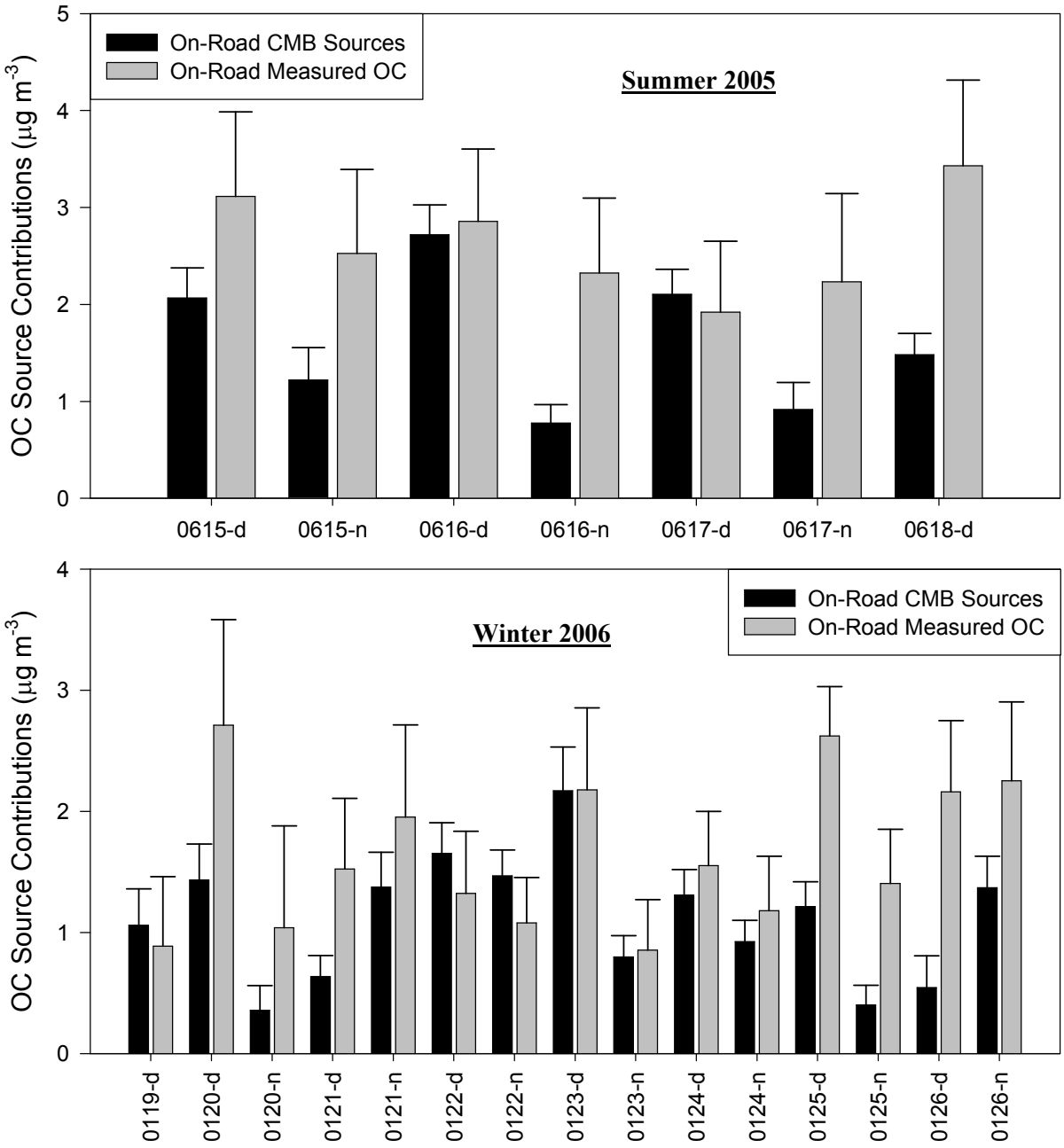

Figure 4.7. Comparison between the CMB-MM-calculated on-road OC source contribution (sum of the roadside diesel vehicle exhaust, gasoline vehicle exhaust, and road dust minus sum of the campus diesel vehicle exhaust, gasoline vehicle exhaust, and road dust) and the measured on-road total OC (the roadside OC minus the campus OC). 'd' and 'n' indicate daytime and nighttime 12-hr sample, respectively. Error bars are shown.

4.3.3 Evaluation of CMB-MM Modeling and Estimated SOC in $PM_{2.5}$

In this research, the measured total OC was used to directly assess the CMB-MM modeling results. Given that the contributions from non-roadway related primary sources and SOA varied little between the roadside and the nearby campus sites, the roadside OC minus the campus OC should be close to the OC directly emitted by the on-road sources (diesel vehicle exhaust, gasoline vehicle exhaust, and road dust). This is reasonable recognizing that there are similar spatial distributions in non-roadway related organic tracers across both sites [*Yan et al.*, 2009c] and in the CMB-MM results for meat cooking, biomass burning, cigarette smoke, and vegetative detritus (Tables B.1 and B.2; Figures 4.3 and 4.4). Therefore, the CMB-MM-estimated roadway-related source contributions can be evaluated by differences in the measured OC between the two sites. Our comparison shows that CMB-MM usually underestimated the contributions from on-road emissions at the roadside site by average values of 1.02±0.77 and 0.40±0.82 μg m^{-3} in the summer and the winter, respectively (Figure 4.7). This implies that 'Other OC' or 'unidentified OC', which calculated by the CMB-MM model, is likely the upper bound of the SOC estimate considering the underestimation of POC as well as possible existence of unknown primary OC sources in CMB-MM modeling. This SOC estimate was assessed by comparing CMB-MM-calculated 'Other OC' with secondary organic tracers as well as SOC determined by other methods.

Figure 4.8 show the correlation between secondary organic tracers and estimated 'Other OC'. The CMB-MM-estimated 'Other OC' is found significantly correlated with ambient sulfate (r^2=0.64) and ammonium (r^2=0.66) in the summer. This suggests 'Other OC' probably consists of secondary organic sources, which can be attributed to similar

atmospheric formation and condensation/partition processes as secondary sulfate and ammonium. In the winter, 'Other OC' was statistically zero on many samples even though sulfate and ammonium were still detected. However, no significant correlation is found between 'Other OC' and secondary organic tracers, such as biogenic secondary tracers (*cis*-pinonic acid, pinic acid and 2-methyltetrols) and multiple secondary tracers (aromatic and dicarboxylic acids) even in the summer. One possible explanation is that composition of 'Other OC' or SOC could be complicated by various anthropogenic and biogenic sources and impacted by numerous factors, e.g., temperature, humidity, solar radiation, emissions. The amounts of identified organic tracers are only part of SOA sources and did not accurately represent all source attributes of SOA in the atmosphere.

Scatter plots in Figure 4.9 show the correlationships between CMB-MM-estimated 'Other OC' with the total measured OC, EC Tracer_SOC (estimated by the EC tracer method), and WSOC_adj (WSOC subtracting biomass burning effects). 'Other OC' is significantly correlated with total OC and EC Tracer_SOC (r^2=0.73 and 0.72, respectively) in the summer. 'Other OC' is also significantly correlated with WSOC_adj (r^2=0.58 and 0.55 in the summer and the winter, respectively). These suggest that CMB-MM-calculated 'Other OC' is probably dominated by SOC. However, CMB-MM-estimated "Other OC' is not always comparable to the EC tracer-estimated SOC in the winter. It might be caused by the errors of both the two methods, which would be relatively larger in the winter due to small SOC fractions in the total OC. Possible overestimations of identified primary OC in sources of biomass burning and meat cooking by CMB-MM can also offset some impacts from SOC in the winter.

Fraction boundaries of the SOC estimates in the total measured OC were described in the method section with the CMB-MM-calculated 'Other OC' as the upper bound of the SOC estimate and with the WSOC_adj as the lower bound. Our results indicate that 38–59%, 51–74%, and 74–87% of the total OC were SOC in the summer at the roadside, the campus, and the Yorkville sites, respectively, whereas 13–17%, 18–27%, and about 12% of the total OC were contributed by SOA in the winter (Figures 4.10 and 4.11). The SOC fractions estimated by the EC tracer method are found to be comparable to the WSOC_adj values.

4.3.4 Source Contributions for SOA

The above comparison suggests that SOC is the dominant component of ambient OC in the summer. However, we can still not distinguish impacts from anthropogenic and biogenic secondary sources. An organic tracer method was then applied to estimate source contributions from isoprene and monoterpene, two predominant biogenic emissions at the southeastern U.S.

Results indicate that these biogenic secondary organic sources usually take a significant faction of measured OC, especially in the summer (Figures 4.12 and 4.13). At the urban sites, isoprene-originated and monoterpene-originated secondary sources were estimated to contribute on average 7.5% and 8.2% of the total OC, respectively. In the June samples, isoprene-originated and monoterpene-originated sources contributed 0.023 and 0.85 μg m^{-3} (or 0.3% and 12%) of the total measured OC, respectively, whereas they contributed 1.4 and 0.10 μg m^{-3} (or 20% and 1.3%) in the July samples. At the rural site, isoprene-originated and monoterpene-originated sources, on average, contributed 1.1 and 0.25 μg m^{-3} (or 23% and 5.1%) of the total measured OC in the July samples. These

values are comparable to the urban site in the same period, suggesting a similarly homogeneous emission background level over this area.

However, large discrepancies can be found between total measured OC and total estimated OC, which is equal to the CMB-MM-estimated POC plus the organic tracer method-estimated biogenic SOC. In the summer, the measured OC is usually much bigger than the estimated OC for four possible reasons: 1) the first direct one lies in the fact that anthropogenic SOC is not included in the total OC, which is important for sites close to anthropogenic emissions such as highway; 2) the fixed mass factions of SOC from the chamber experiments may not be able to represent real-world atmospheric processes of these tracers with seasonal variations; 3) the composition of SOA in the atmosphere is not well known and complicated such that some important secondary sources were probably missed, especially anthropogenic sources; and 4) dynamic processes in the atmosphere can impact the fate of ambient aerosols in many unexpected ways. The results from the winter samples indicated how difficult it is to understand these complex processes through any simplified and laboratory-derived model or method. In the winter, a few source contributions originating from monoterpenes were observed with high levels at the rural site, and the relative ratios (or Fsoc ratios) between *cis*-pinonic acid and pinic acid were found to differ from those in the summer (Figures 2.6-2.8). Therefore, it is suspect to elucidate such a complicated and dynamic process with this kind of method since we still know little about these formations. Future research in this area should focus on studying formation and composition of SOC, in particular.

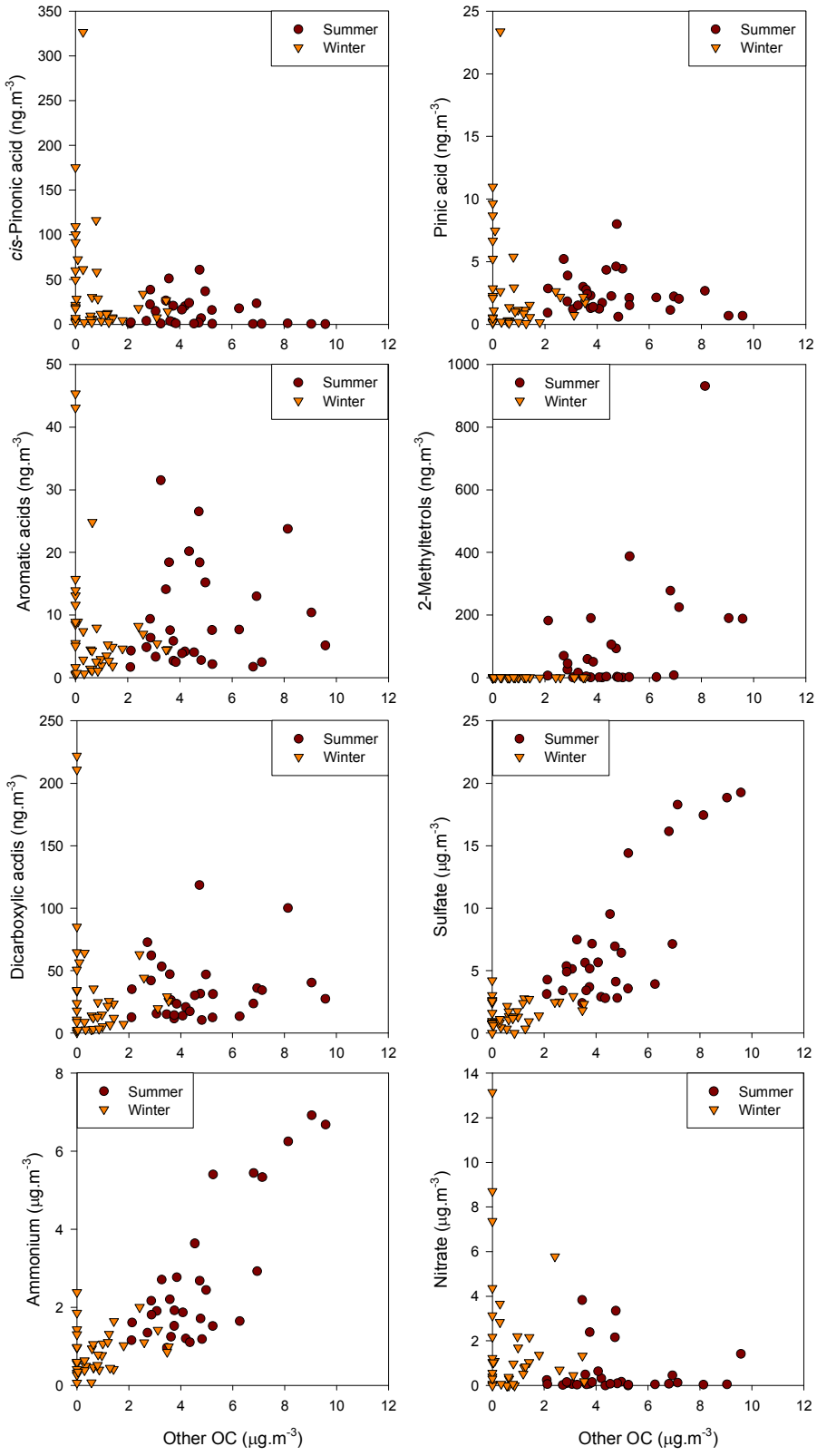

Figure 4.8. Scatter plots of Other OC and tracers (*cis*-pinonic acid, pinic acid, aromatic acids, 2-methyltetrols, dicarboxylic acids, sulfate, nitrate, and ammonium) of secondary sources for $PM_{2.5}$.

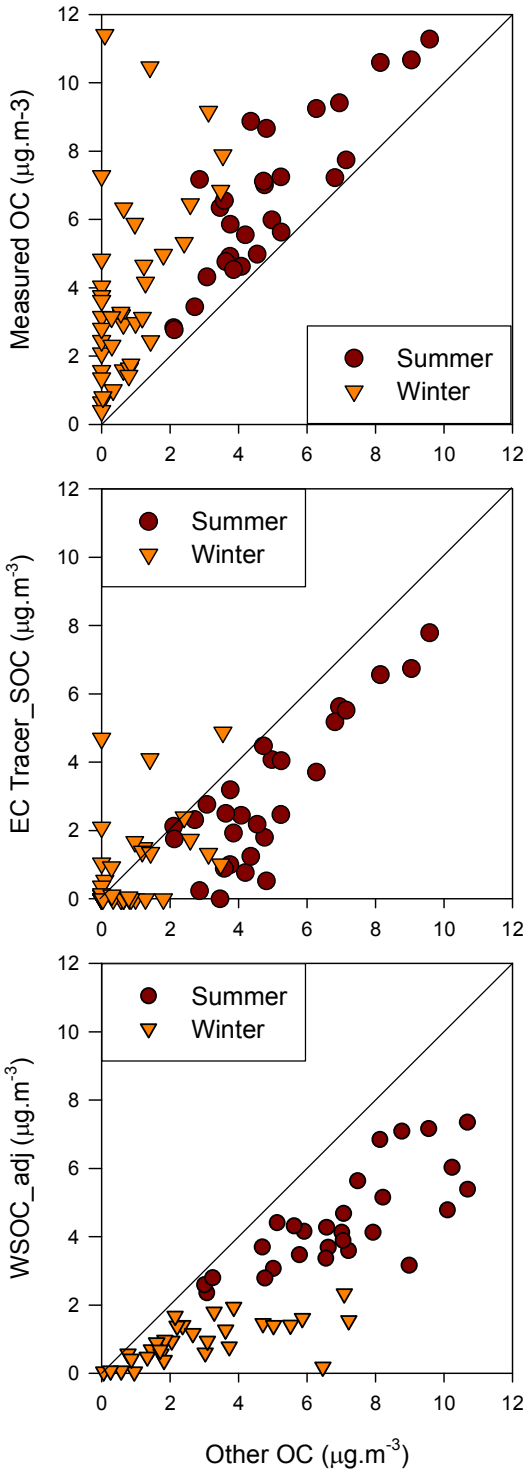

Figure 4.9. Scatter plots of 'Other OC' in the CMB-MM model, SOC estimated by the EC tracer method, and WSOC adjusted by subtracting biomass burning effect.

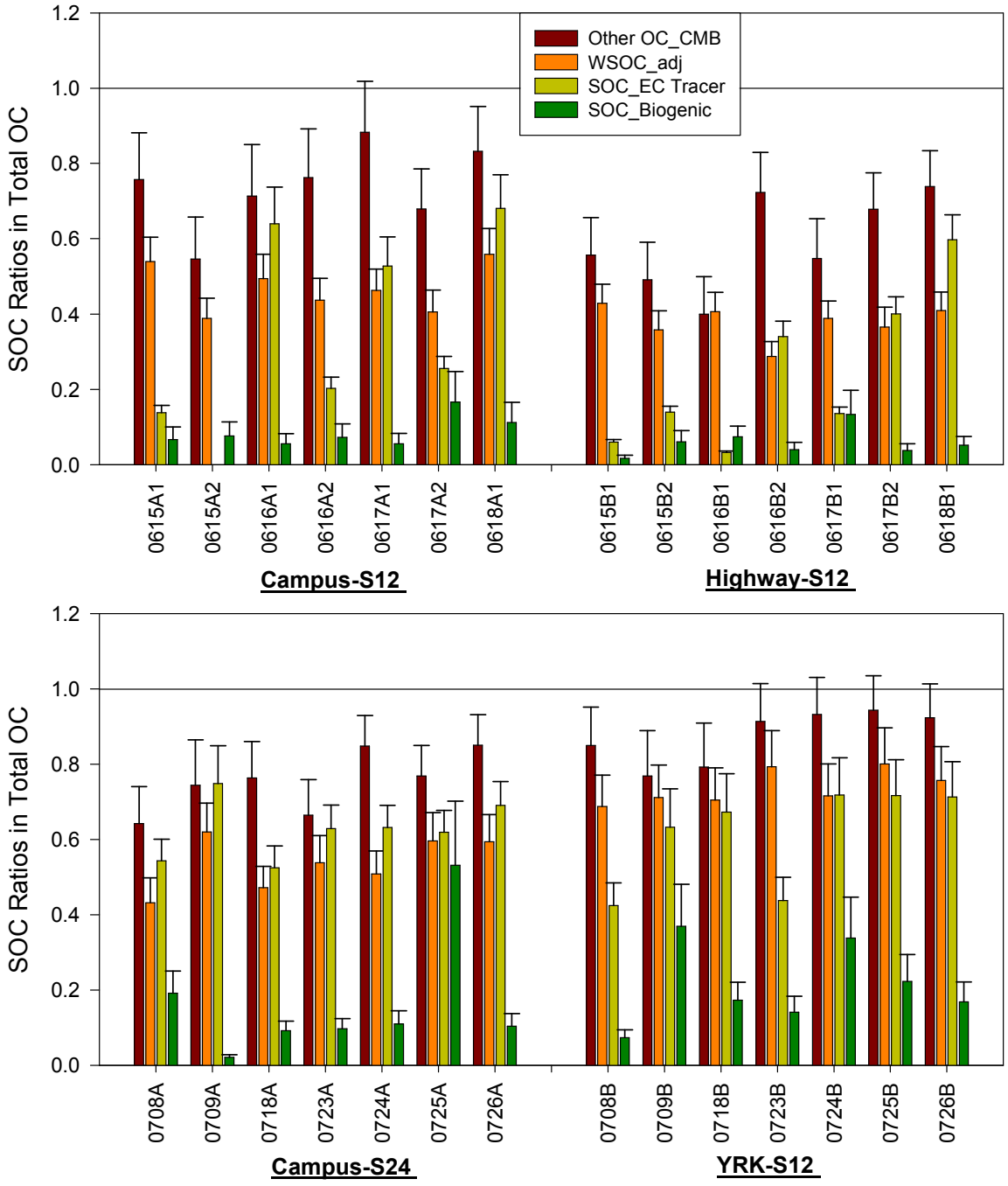

Figure 4.10. Ratios of SOC in the total measured OC in summer 2005 at the three sampling sites. Error bars are shown.

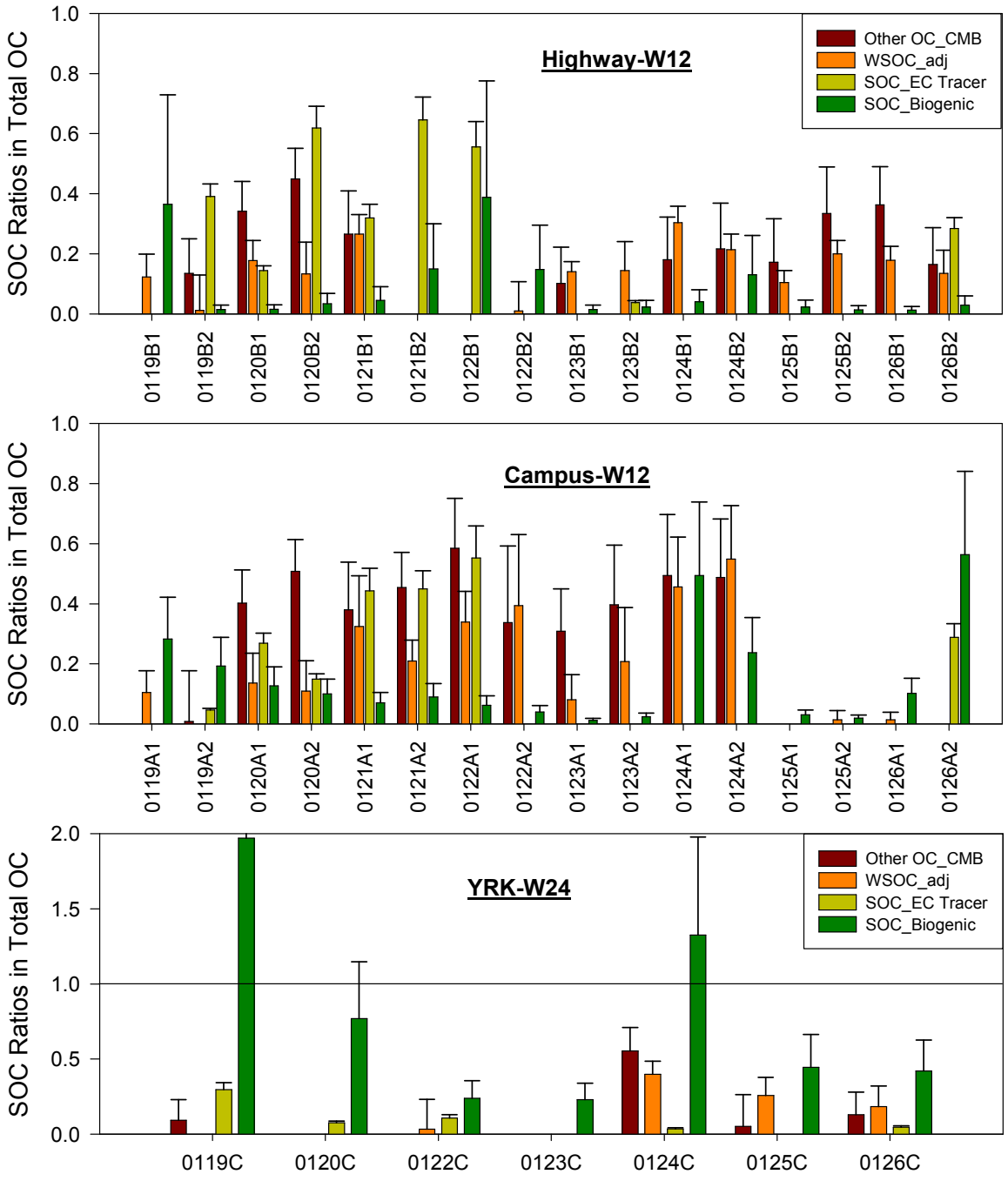

Figure 4.11. Ratios of SOC in the total measured OC in winter 2006 at the three sampling sites. Error bars are shown.

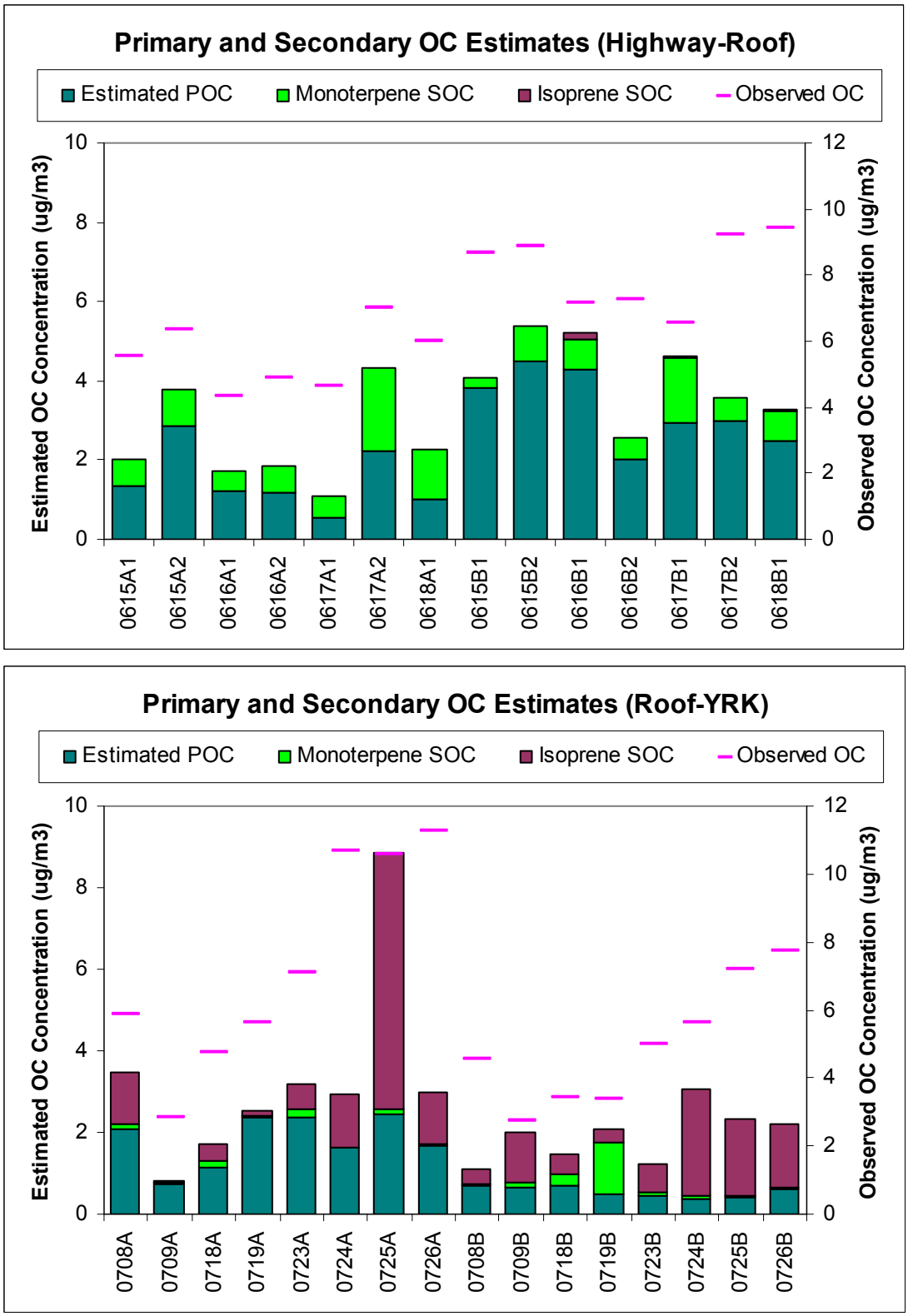

Figure 4.12. Estimated primary and secondary OC by CMB-MM and organic tracer methods in summer 2005.

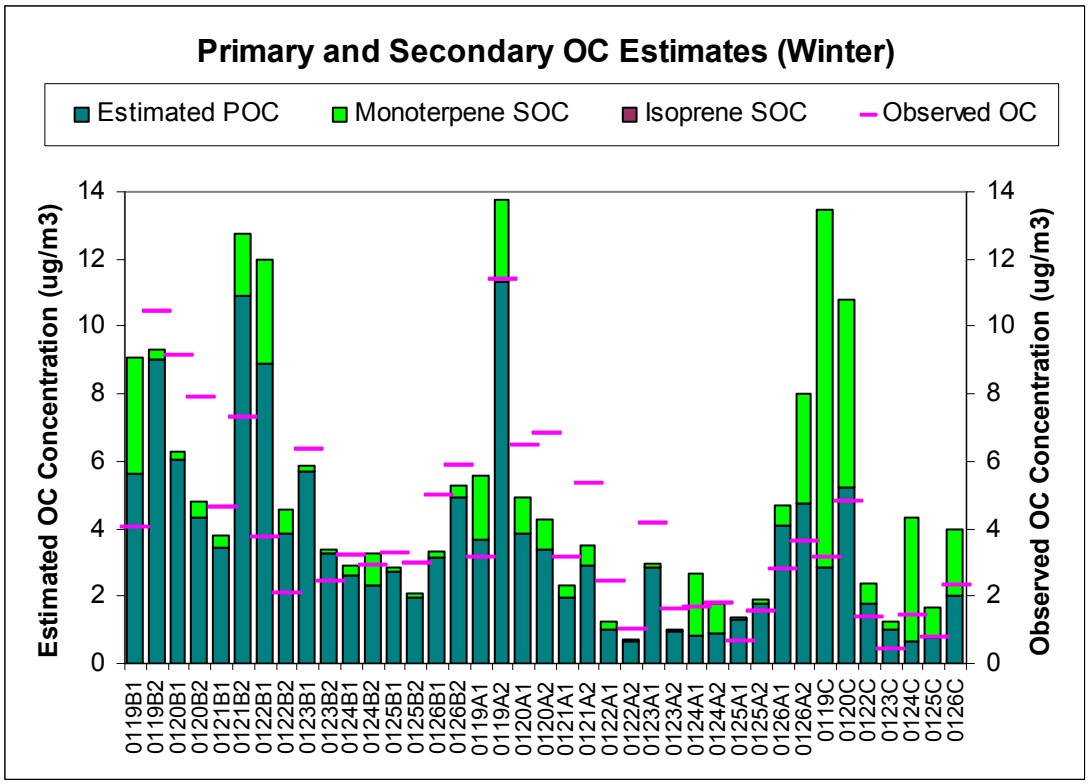

Figure 4.13. Estimated primary and secondary OC by the CMB-MM and organic tracer methods in winter 2006.

Acknowledgments

This work was funded in part by the U.S. Environmental Protection Agency STAR grants (R832159, R828976 and R831076). We would like to thank Georgia Power (Southern Company) for their support of work in the Laboratory for Atmospheric Modeling, Diagnostics, and Analysis (LAMDA) at Georgia Institute of Technology in this study area. The authors also acknowledge Drs. Xing Ding, Yingjun Chen, and Liping Yu for assistance with the organic tracer analysis, and Atmospheric Research & Analysis, Inc. for help with the field sampling and meteorological measurements. We also thank Dr. Sangil Lee, Charles Evan Cobb, Santosh Chandru, and Hyeon Kook Kim for assistance in the field sampling and lab experiments.

CHAPTER 5

ORGANIC COMPOSITION OF CARBONACEOUS AEROSOLS IN AN AGED PRESCRIBED FIRE PLUME

(Bo Yan, Mei Zheng, Yongtao Hu, Sangil Lee, Hyeon Kook Kim, and Armistead G. Russell. *Atmospheric Chemistry and Physics*, 8, 6381–6394, 2008)

Abstract

Aged smoke from a prescribed fire (dominated by conifers) impacted Atlanta, GA on February 28th, 2007 and dramatically increased hourly ambient concentrations of $PM_{2.5}$ and organic carbon (OC) up to 140 and 72 μg m^{-3}, respectively. It was estimated that over 1 million residents were exposed to the smoky air lasting from the late afternoon to midnight. To better understand the processes impacting the aging of fire plumes, a detailed chemical speciation of carbonaceous aerosols was conducted by gas chromatography/mass spectrometry (GC/MS) analysis. Ambient concentrations of many organic species (levoglucosan, resin acids, retene, *n*-alkanes and *n*-alkanoic acids) associated with wood burning emission were significantly elevated on the event day. Levoglucosan increased by a factor of 10, while hopanes, steranes, cholesterol and major polycyclic aromatic hydrocarbons (PAHs) did not show obvious increases. Strong odd over even carbon number predominance was found for *n*-alkanes versus even over odd predominance for *n*-alkanoic acids. Alteration of resin acids during transport from burning sites to monitors is suggested by the observations. Our study also suggests that

large quantities of biogenic volatile organic compounds (VOCs) and semivolatile organic compounds (SVOCs) were released both as products of combustion and unburned vegetation heated by the fire. Higher leaf temperature can stimulate biogenic VOC and SVOC emissions, which enhanced formation of secondary organic aerosols (SOA) in the atmosphere. This is supported by elevated ambient concentrations of secondary organic tracers (dicarboxylic acids, 2-methyltetrols, pinonic acid and pinic acid). An approximate source profile was built for the aged fire plume to help better understand evolution of wood smoke emission and for use in source impact assessment.

5.1 Introduction

Wildland fire (wild fire and prescribed burning) is estimated to contribute about 20% of total fine particulate matter ($PM_{2.5}$) emissions in the United States [*EPA*, 2000]. In 2006, a total of 96,385 wildland fires were reported to burn 39,958 square kilometers, 125% above the 10-year average [*NIFC*, 2007]. Among these forests, 11,010 square kilometers were treated with prescribed fires, which is 1,659 square kilometers above last year's total and is the second highest since 1998 [*NIFC*, 2007]. Such large and increasing emission contributions are of concern to air quality managers, particularly in areas near or above the applicable air quality standards. For example, the prescribed fires on February 28th, 2007 in Georgia and later the Georgia-Florida wildfires lasting from April through May severely impacted Atlanta, Georgia with thick wood smoke [*Hu et al.*, 2008; *Lee et al.*, 2008]. During such events, hourly concentrations of $PM_{2.5}$ increased by over 100 μg m^{-3}.

Previous studies have shown that the major component of $PM_{2.5}$ from forest burning events is organic carbon (OC), accounting for 30-70% of $PM_{2.5}$ mass [*Nopmongcol et al.*, 2007; *Robinson et al.*, 2004; *Ward et al.*, 2006]. However, detailed data speciating OC in $PM_{2.5}$ impacted by wildland fires is sparse, and even less data is available for aged plumes. During the February 28th, 2007 event, OC reached 72 μg m^{-3} at 6 p.m. and contributed approximately 51% of the ambient $PM_{2.5}$ in Atlanta, GA [*Lee et al.*, 2008]. This smoke event provides an opportunity to characterize OC in such carbonaceous aerosols, further understand processes impacting the aging of fire plumes, and estimate the composition of prescribed fire-derived $PM_{2.5}$ for source apportionment studies.

In this study, detailed GC/MS speciation of carbonaceous aerosols, along with receptor modeling, is used to quantify impacts from the biomass burning plume, although some other techniques can provide information about aerosol composition and source impacts as well. For example, aerosol mass spectrometer (AMS) is increasingly used to determine real-time size distribution and chemical composition of non-refractory submicron inorganic and organic aerosols [*Allan et al.*, 2003; *Canagaratna et al.*, 2007; *Jimenez et al.*, 2003]. Recently, this method has been used to estimate source contributions from biomass burning through quantitatively characterizing hydrocarbon-like and oxygenated organic aerosols [*Cottrell et al.*, 2008; *DeCarlo et al.*, 2008; *Zhang et al.*, 2005]. GC/MS allows identification and quantification of hundreds of organic compounds from ambient $PM_{2.5}$, including *n*-alkanes, hopanes, steranes, alkanoic acids, alkanedioic acids, PAHs, resin acids, and others (syringols, levoglucosan, cholesterol, 2-methyltetrols, etc.). Some of these compounds are reasonably unique tracers for certain

sources and are widely used to track specific sources of carbonaceous aerosols. Similar sets of organic species have also been measured for source emissions. Together, they can be used to quantify source impacts on ambient $PM_{2.5}$.

Source impacts from biomass burning are usually traced through a few organic tracers including levoglucosan, resin acids, syringols and retene. As a pyrolysis product of cellulose in wood biopolymers, levoglucosan has been considered a particularly useful molecular marker of biomass burning [*Simoneit et al.*, 1999]. With its large emission abundance and reasonable thermal stability in the atmosphere, levoglucosan is frequently used to assess air quality impacts from biomass burning [*Fraser and Lakshmanan*, 2000; *Schauer and Cass*, 2000]. Resin acids are thermal alteration products of coniferous wood resins and emitted exclusively from softwood burning (various pines, firs, etc.) [*Rogge et al.*, 1998; *Simoneit et al.*, 1993; *Standley and Simoneit*, 1994]. In contrast, hardwood combustion produces much higher quantities of syringols [*Hawthorne et al.*, 1988; *Hawthorne et al.*, 1989]. Although PAHs are emitted from multiple combustion processes of fuels (biomass, natural gas, diesel and gasoline) and ubiquitous in the atmosphere, retene, a thermal alteration of abietane compounds (resin diterpenoids), is considered as an organic tracer specific for coniferous wood burning [*Ramdahl*, 1983].

Other primary sources can be also linked to some specific organic tracers. Hopanes and steranes are emitted from both gasoline-powered vehicle and diesel-powered vehicle [*Simoneit*, 1985; *Zielinska et al.*, 2004]. They have been widely used as molecular markers of vehicular emissions in source apportionment of $PM_{2.5}$ and OC [*Fraser et al.*, 2003b; *Schauer et al.*, 1996; *Zheng et al.*, 2002; *Zheng et al.*, 2006b; *Zheng et al.*, 2007]. Cholesterol, found in animal fats and oils, is thought as an excellent

molecular marker of meat cooking emission [*Rogge et al.*, 1991]. Vegetative detritus emissions are characterized by high-molecular weight *n*-alkanes with pronounced odd over even carbon number predominance [*Rogge et al.*, 1993a].

In addition to primary components of $PM_{2.5}$, secondary organic aerosol (SOA) formation can result from gaseous emissions of isoprenoids (isoprene and monoterpene) [*Claeys et al.*, 2004a; *Kavouras et al.*, 1998]. A few biogenic SOA species have been identified and quantified including 2-methyltetrols (oxidation products of isoprene), pinonic acid and pinic acid (oxidation products of monoterpene) [*Claeys et al.*, 2004a; *Claeys et al.*, 2004b; *Yu et al.*, 1999a; *Yu et al.*, 1999b]. Although dicarboxylic acids (alkanedioic acids and dicarboxylic aromatic acids) can be emitted from various primary sources (mobile emission, meat cooking, etc.), previous studies suggested that atmospheric photochemical formation is probably the main source of these dicarboxylic acids [*Fine et al.*, 2004b; *Fraser et al.*, 2003a; *Schauer et al.*, 2002a].

Here, we collected $PM_{2.5}$ filter samples before, during and after the February 28th, 2007 prescribed fire episode impacting Atlanta, GA and analyzed organic composition of carbonaceous aerosols using GC/MS. We further capitalize on the quantified organic tracers to better understand the evolution of wood smoke from wildland fires.

5.2 Method Description

5.2.1 Ambient Sampling

Daily $PM_{2.5}$ samples were collected on 47 mm quartz fiber filters with particulate composition monitors (PCM) at the Assessment of Spatial Aerosol Composition in Atlanta (ASACA) sites [*Butler et al.*, 2003]. These sites are located in the Atlanta metro

area about 80 km downwind from the February 28th, 2007 prescribed fires and were impacted directly by the smoke plume. The 24-hr daily samples were analyzed for organic carbon/elemental carbon (OC/EC), metals and ions using thermal optical transmittance (TOT), X-ray fluorescence (XRF) and ion chromatography (IC), respectively. Details of ambient sampling, chemical measurements and particle compositions are described elsewhere [*Baumann et al.*, 2003; *Lee et al.*, 2005a; *Lee et al.*, 2008].

5.2.2 Organic Speciation

Due to the low air volumes sampled, OC mass on a single PCM filter is usually not enough for organic tracer analysis. Therefore, three composite PCM samples (named 'Before_Fire', 'Event' and 'After_Fire') were prepared as below. 'Before_Fire' was composed of 6 PCM filters from three ASACA sites for the two days before the smoke day. 'Event' was composed of 3 PCM filters collected at the same sites on February 28th, the day most directly impacted. 'After_Fire' was composed of 7 PCM filters from the same sites within the three days after the smoke day. The three composite samples along with a composite field blank were analyzed for organic compounds in $PM_{2.5}$ using a standardized method described elsewhere [*Nolte et al.*, 2002; *Zheng et al.*, 2002; *Zheng et al.*, 2006b]. Briefly, each filter composite was spiked with deuterated internal standard (IS) mixtures and then successively extracted using hexane and benzene/isopropanol (2:1, v/v). After filtering, extracts were concentrated with rotary evaporation followed by blowdown under pure nitrogen. Half of each concentrated extract was then derivatized with diazomethane to convert organic acids to their methyl esters. These methylated extracts were analyzed by GC/MS along with authentic standards. To quantify polar

organic compounds (levoglucosan, cholesterol and 2-methyltetrols), underivatized remains of concentrated extracts were silylated with BSTFA (N, O-bis(trimethylsilyl)acetamide) to convert polar compounds to trimethylsilyl (TMS) derivatives. After one hour reaction at 70 ºC, these silylated extracts were analyzed using GC/MS along with authentic standards.

5.3 Results and Discussion

Our results show that the observed 24-hr average OC concentration jumped from 3.5 to 17.7 μg m^{-3} on the event day, accounting for more than 70% (when converted to organic matter by a factor of 1.5 [*Lee et al.*, 2008]) of the total 24-hr average $PM_{2.5}$ mass of 37 μg m^{-3}. Major sources of carbonaceous aerosols are traced using variations of their associated organic tracers.

5.3.1 Organic Tracers of Biomass Burning

During the smoke, large increases were observed for biomass burning tracers (levoglucosan, resin acids, retene, etc.). Levoglucosan was detected in all ambient samples as the most abundant organic compound (Figure 5.1). Before and after the smoke event, the observed levoglucosan concentrations were 114 and 145 ng m^{-3}, respectively. On the event day, the levoglucosan concentration increased dramatically to 1210 ng m^{-3} and contributed 7% of the total OC, suggesting that the wood burning emission impact was 10 times higher on the event day than the non-smoke days. Along with levoglucosan, concentrations of resin acids also increased, especially dehydroabietic acid and 7-oxodehydroabietic acid, increasing to 42 and 19 ng m^{-3}, approximately 9 and 23 times higher respectively than the levels before the burning day. Unlike levoglucosan, their

ambient concentrations remained elevated after the fires (Figure 5.2). To elucidate the processes occurring during transport, comparisons between wood burning source emissions and ambient data are conducted here. Ratios of major resin acids to levoglucosan were calculated and compared for both ambient data and a few source emissions from prominent softwood species in the southern United States (Table 5.1). In the softwood source emissions, abietic acid and dehydroabietic acid generally account for the majority of resin acids, about 58% and 32% respectively on average, while 7-oxodehydroabietic acid is minor. However, dehydroabietic acid and 7-oxodehydroabietic acid constituted a major fraction of the observed resin acids, about 65% and 29% respectively, in the ambient sample impacted by the fires. This comparison provides evidence that dehydroabietic acid and 7-oxodehydroabietic acid are being formed from other resin acids (i.e. diterpenoids) during the 3-4 hour (around 80 km travel distance) transport from the burning sites to the monitors. Note that further alterations of dehydroabietic acid and 7-oxodehydroabietic acid exist, leading to their ratios to levoglucosan being variable over time during transport. Previous studies have also proposed that dehydroabietic acid and 7-oxodehydroabietic acid can be formed through oxidation processes of other resin acids (i.e. abietic acids), resulting in accumulated concentrations in the atmosphere [*Oros and Simoneit*, 2001; *Rogge et al.*, 1993e]. Although most PAHs did not show significant elevation in ambient concentrations during the event day, retene, a potential softwood burning tracer, increased by around 12 and 7 times, respectively compared to before and after the fire, and predominated among all PAHs (Figure 5.2).

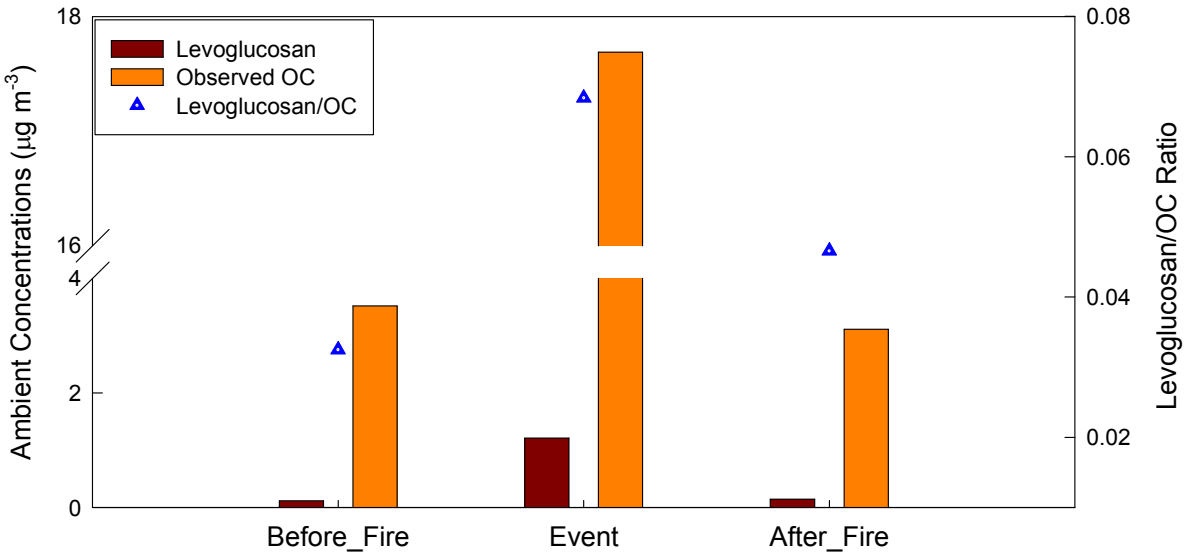

Figure 5.1. 24-hr average ambient concentrations of OC and levoglucosan observed before, during and after the event day at Atlanta area, GA.

Table 5.1. Ratios of Major Resin Acids to Levoglucosan in Source Emissions and Ambient Samples

Compounds	Softwood Emissions					Ambient Samples		
	Loblolly Pine [a]	Slash Pine [a]	White pine [b]	Hemlock [b]	Balsam fir [b]	Before_Fire	Smoke	After_Fire
Pimaric acid	0.069	0.029	0.008	0.001	0.001	0.001	0.000	0.002
Sandaracopimaric acid	0.013	0.011	0.026	0.002	0.001	0.003	0.001	0.011
Dehydroabietic acid	0.339	0.141	0.149	0.017	0.028	0.041	0.034	0.248
Abietic acid	0.801	0.056	0.391	0.021	0.240	0.001	0.000	0.002
Abieta-6,8,11,13,15-pentae-18-oic acid	0.007	0.003	0.005	0.000	0.002	0.000	0.000	0.000
Abieta-8,11,13,15-tetraen-18-oic acid	0.021	0.000	0.010	0.001	0.003	0.001	0.001	0.001
7-Oxodehydroabietic acid	0.009	0.004	0.005	0.001	0.000	0.007	0.015	0.042

Note: [a] softwood species tested by Fine et al. [*Fine et al.*, 2002]; [b] softwood species tested by Fine et al. [*Fine et al.*, 2001].

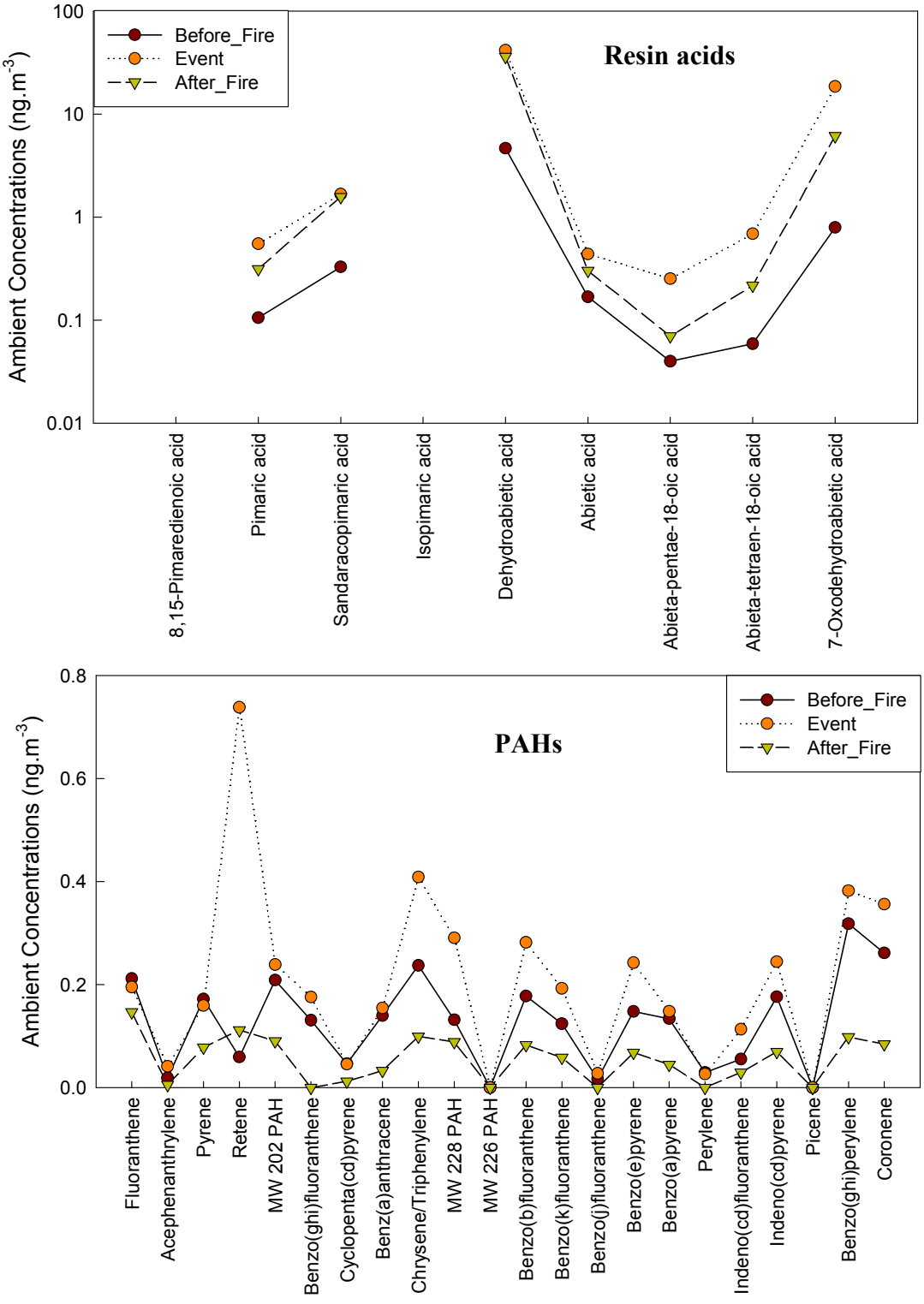

Figure 5.2. 24-hr average concentrations of resin acids and PAHs observed before, during and after the event day at Atlanta area, GA.

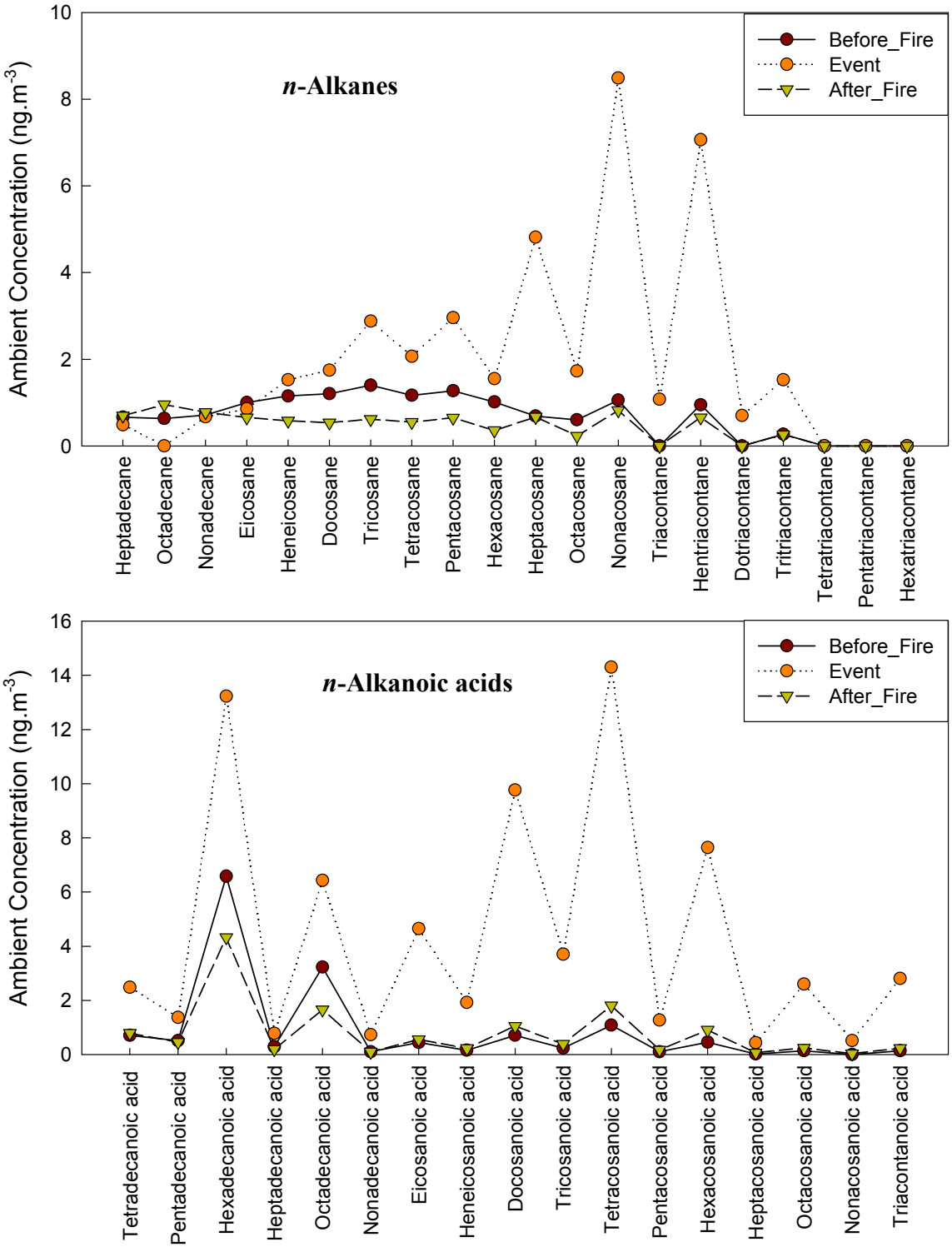

Figure 5.3. 24-hr average concentrations of *n*-alkanes and *n*-alkanoic acids observed before, during and after the event day at Atlanta area, GA.

n-alkanes and *n*-alkanoic acids identified in this study ranged from C_{17} to C_{36} and from C_{14} to C_{30}, respectively (Figure 5.3). Generally, *n*-alkanes are associated with plant wax and fossil fuel contributions, depending on carbon numbers. To approximately compare source impacts from plant wax versus fossil fuel combustion, the carbon preference index (CPI) measuring carbon number predominance in homologous compound series is calculated [*Mazurek and Simoneit*, 1984; *Oros et al.*, 2006]. In the samples before and after the fire, *n*-alkanes only show a slight odd carbon number predominance with CPIs of 1.4 and 1.7, respectively. However, *n*-alkanes exhibited distinctly strong odd carbon number predominance (CPI=3.1, carbon number maximum C_{max}=29) on the event day, reflecting a major contribution from plant waxes. Likewise, *n*-alkanoic acids had a strong even carbon number predominance on the event day (CPI=5.7, C_{max}=24). The concentration of even-over-odd carbon number series on the event day was 50 ng m^{-3}, much larger than those before and after the event (12 and 10 ng m^{-3}, respectively). Thus, a dominant contribution from plant waxes is suggested. These compounds are considered natural products of epicuticular waxes and internal lipid substances in leaf surfaces and emitted as vegetative detritus or through direct thermal volatilization [*Rogge et al.*, 1993a; *Simoneit*, 2002]. Higher leaf temperatures presumably lead to volatilization of these high-molecular weight organic compounds, which can then condense into the particle phase in the atmosphere. This result indicates that such waxes are not unique tracers for vegetative detritus when wildland fires also significantly impact air quality.

5.3.2 Other Primary Organic Tracers

Non-biomass organic molecular markers were also analyzed as indicators of other major primary sources. Vehicular engine exhaust and meat cooking are the two other major sources of primary organic carbon in the Atlanta urban area [*Lee et al.*, 2007; *Liu et al.*, 2005; *Marmur et al.*, 2005; *Zheng et al.*, 2007]. The before, during and after concentrations of hopanes and steranes, both organic markers for internal combustion engine emissions, did not show significant variation, i.e. 1.7, 1.7 and 1.0 ng m^{-3} (Figure 5.4). Cholesterol, an organic tracer of meat cooking, did not exhibit major variation as well (Figure 5.5). Both suggest that primary sources other than prescribed fire have similar influences on Atlanta, GA before, during and after the event day. This point has further foundation from prior studies, which have shown that there is a significant increase in OC within Atlanta compared with a more rural site (e.g., Yorkville, GA) by analyzing regional EC and OC levels from the Southeastern Aerosol Research and Characterization (SEARCH) network [*Edgerton et al.*, 2005; *Hansen et al.*, 2003; *Zheng et al.*, 2006b]. Furthermore, the sampling sites used here are spread out around metro Atlanta and capture the urban mix of primary sources. By compositing the filters, the results are relatively insensitive to changes in wind direction. On the other hand, very large increases in continuous $PM_{2.5}$ and OC values were observed when the plume, which originated in a rural area, hit the urban monitors in Atlanta [*Lee et al.*, 2008]. These increases are consistent with those increases measured on the filters, and overwhelmed the background in this area. On the event day, $PM_{2.5}$ increased by 23.9 μg m^{-3} (over 60%) while OC increased by 14.2 μg m^{-3} (over 80%). Biomass burning-related organic tracers (levoglucosan, resin acids and retene) increased by 7-23 times. In addition, Community Multi-scale Air Quality (CMAQ) modeling showed that the timing of the increase in OC

is consistent with when the prescribed fire plume impacted Atlanta [*Hu et al.*, 2008]. These points strongly support that vehicular sources and meat cooking emissions are not responsible for the large increase in $PM_{2.5}$ and OC on the event day, and that the greatly increased carbonaceous aerosol concentrations during the smoke episode are from prescribed fires. Source apportionment results calculated using organic molecular marker-based chemical mass balance (CMB-MM) model also indicate significant increases of prescribed burning emissions on the event day, but not for other major primary sources (i.e. vehicular source and meat cooking) (Table 5.2). Moreover, about 43% of the total observed OC can not be explained by primary source contributions, suggesting that secondary organic aerosol (SOA) is also a significant contributor to the increased OC.

5.3.3 Secondary Organic Tracers

Our results for secondary organic tracers indicate that additional biogenic SOA were formed during the February 28th, 2007 fire episode. 2-methyltetrols, secondary organic products of isoprene, were detected only on the smoke plume day with a concentration of 0.8 ng m^{-3} (Figure 5.5). Pinonic acid and pinic acid, photo-oxidation products of monoterpenes, increased from 2.9 and 1.2 ng m^{-3} to 5.0 and 3.1 ng m^{-3}, respectively, from the day prior to the fire through the smoke day (Figure 5.5). Additionally, elevated dicarboxylic acids (alkanedioic acids and dicarboxylic aromatic acids) provided supportive evidence of increased SOA formation in the atmosphere. They are further considered here products of biogenic emissions enhanced by the fire since significant increases were not found in anthropogenic emissions (i.e. vehicular source and meat cooking). The sums of dicarboxylic acids were 7.5, 51, 8.4 ng m^{-3} before, during

and after the event, respectively. There are three possible hypotheses relating to the large increases in these dicarboxylic acids. The most direct one is that precursors of these compounds are associated with prescribed fire emissions. As stated previously, emissions of biogenic VOC and SVOC (isoprenes, terpenes, sesquiterpenes, alcohols, esters, carbonyls, acids, etc.) would be enhanced by either wood combustion process or increasing leaf temperature. Emissions of isoprenoids (isoprene and monoterpene) have been observed to be higher during forest fires due to increased temperatures [*Alessio et al.*, 2004]. A previous study also suggests that leaf temperatures rising from 25 to 35 ºC would increase biogenic VOC and SVOC emissions by 4 and 1.5 times from isoprene-emitting deciduous trees and terpene-emitting conifers, respectively [*Lamb et al.*, 1987]. The second hypothesis is that the dramatic increase in OC mass can enhance formation of SOA due to increased partitioning of these diacids to the particle phase. However, unless there is a significant chemical affinity between OC and the compounds, such a shift is not expected to be so large (less than 10% of enhancement in SOA) [*Nopmongcol et al.*, 2007; *Odum et al.*, 1996]. The third hypothesis is that enhanced photo-oxidation occurred. The observed increase of ozone in the plume is indicative that this effect might exist, but would be limited since ozone increased about 50% (from around 60 to 90 ppb), significantly less than the increase in dicarboxylic acids (8 times higher). Therefore, among the three hypotheses above, the evidence strongly supports that biomass burning is a major contributor to precursors of dicarboxylic acids. Results of air quality modeling and measurement of water soluble organic carbon (WSOC) provide further supporting evidence [*Hu et al.*, 2008; *Lee et al.*, 2008].

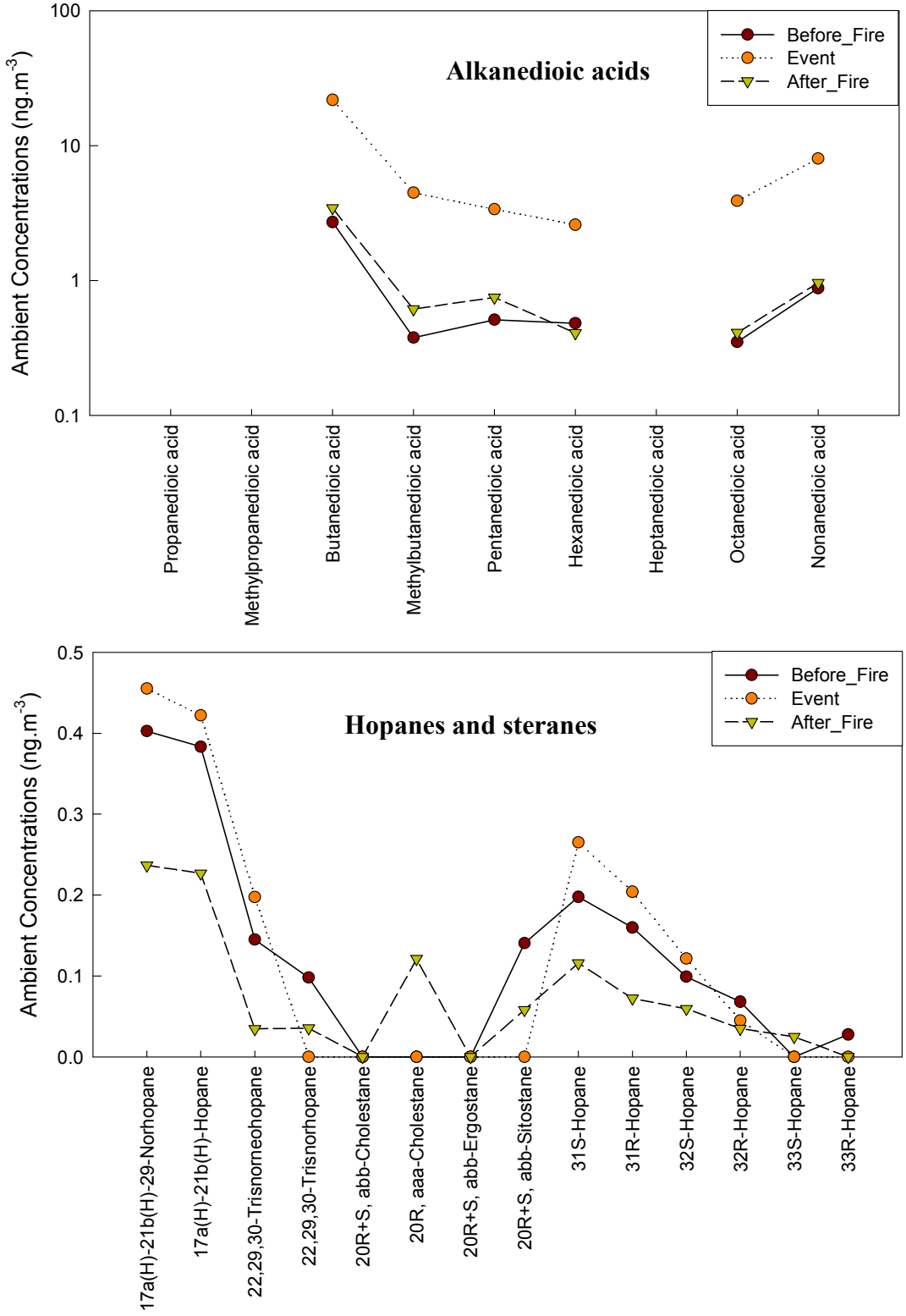

Figure 5.4. 24-hr average concentrations of alkanedioic acids, hopanes and steranes observed before, during and after the event day at Atlanta area, GA.

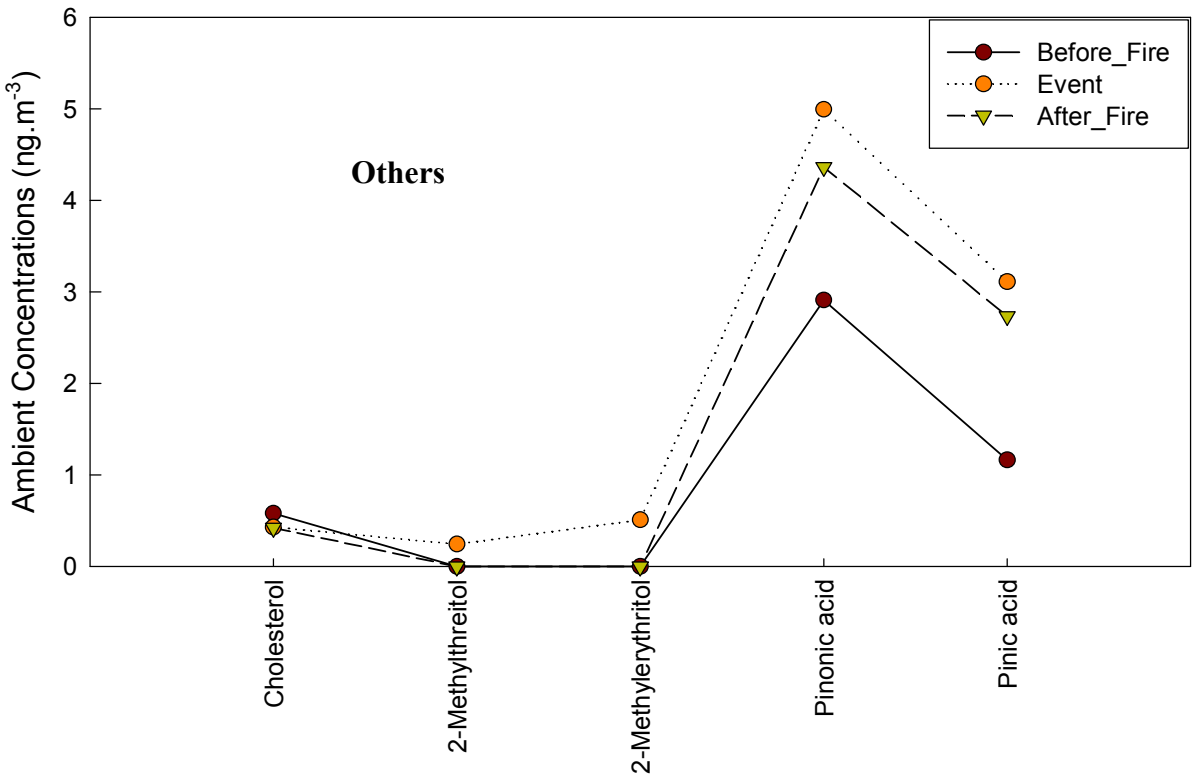

Figure 5.5. 24-hr average concentrations of other compounds (cholesterol, 2-methyltetrols, pinonic acid and pinic acid) observed before, during and after the event day at Atlanta area, GA.

Table 5.2. Source Contributions to Organic Carbons in $PM_{2.5}$ (unit: µg m^{-3})

Samples	Diesel Vehicle Exhaust	Gasoline Vehicle Exhaust	Vegetative Detritus	Meat Cooking	Road Dust	Nature Gas Combustion	Prescribed Wood Burning	Others
Before_Fire	0.691 ± 0.105	0.202 ± 0.055	0.013 ± 0.006	0.467 ± 0.225	0.004 ± 0.004	0.008 ± 0.003	1.137 ± 0.331	0.996
Event	0.808 ± 0.186	0.209 ± 0.117	0.090 ± 0.044	0.373 ± 0.194	N/A [a]	N/A	8.676 ± 1.851	7.530
After_Fire	0.247 ± 0.068	0.107 ± 0.029	0.011 ± 0.005	0.297 ± 0.146	0.003 ± 0.002	0.001 ± 0.002	0.952 ± 0.228	1.490

Note: [a] 'N/A' indicates that this source was not identified in the ambient sample.

5.3.4 Source Profiles for an Aged Plume

Capturing the fire event provides information to assess the source composition profiles of an aged prescribed fire plume. The above discussions indicate that the large increases in $PM_{2.5}$, OC and associated chemical species on the event day are a direct contribution from prescribed fire emissions. From this result, associated aged source profiles can be derived. Here, two approximate source composition profiles were developed for the aged biomass burning plume by considering differences between the before_event day (non-fire event impacted) and the event day, designated 'aged_plume profile' and 'primary_plume profile'. 'Aged_plume profile' is constituted by fractions of individual chemical species (increased concentrations) in the total increased (fire-caused total) $PM_{2.5}$ mass, i.e. 23.9 μg m^{-3}, on the event day (Table 5.3). This profile contains chemical compositions of the aged plume, but is not the primary $PM_{2.5}$ source profile due to large quantities of SOA in aerosol from the fire emissions. 'Primary_plume profile' is then calculated using fractions of individual chemical species (increased concentrations) in the fire-caused primary $PM_{2.5}$ mass where the estimated fire-caused secondary organic carbon (SOC) was subtracted from the fire-caused total $PM_{2.5}$ mass on the event day (Table 5.3). The fire-caused SOC on the event was estimated based on the CMB-MM modeling results and measured EC/OC ratios. Briefly, the CMB-MM apportionment results indicate that prescribed fires contributed approximately 1.1 and 8.7 μg m^{-3} to the total primary OC before and on the event day, respectively (Table 5.2). The difference, 7.6 μg m^{-3}, is attributed to the plumes. Results here find that the total, primary plus secondary, impact of the plumes on OC is 14.2 μg m^{-3}, suggesting that 6.6 μg m^{-3} (47% of the fire-caused total OC) comes from enhanced SOC. A comparable SOC fraction in

the fire-caused total OC was also estimated using the EC/OC ratio method. In the aged plume, the fire-caused EC/OC ratio is 0.039 while a value of 0.065 has been measured for prescribed burning emissions in Georgia [*Lee et al.*, 2005a]. The lower EC/OC ratio suggests SOA formation in the aged plume. Using those ratios, SOC is calculated to account for 40% of the fire-caused total OC. Averaging the two, 44% of fire-caused total OC is taken as SOC during the event, and the fire-caused primary OC (POC_{fc}) is then estimated by:

$$POC_{fc} = OC(\text{fire}-\text{caused}) \times (1 - f_{SOC}) = [OC(\text{event}) - OC(\text{before}-\text{event})] \times (1 - f_{SOC}) \quad (5.1)$$

where f_{soc} is the estimated SOC fraction in the fire-caused total OC. Similarly, the amount of fire_caused primary $PM_{2.5}$ (PPM_{fc}) is calculated as:

$$PPM_{fc} = [PM(\text{event}) - PM(\text{before}-\text{event})] - OC(\text{fire}-\text{caused}) \times f_{SOC} \quad (5.2)$$

Finally, fractions of individual species (f_i) in fire_caused primary $PM_{2.5}$ are found as:

$$f_i = \frac{C_i(\text{event}) - C_i(\text{before}-\text{event})}{PPM_{fc}} \quad (5.3)$$

where C_i is the ambient concentration of individual chemical species in $PM_{2.5}$ that are viewed as being dominated by primary emissions. An overall uncertainty of each chemical species in the two plume source profiles was calculated by propagating uncertainties associated with the observed OC, estimated SOC fraction and measured chemical species (i.e. organic compounds, EC, ions and trace metals). Note that additional uncertainties would be caused in estimation of SOC due to uncertainties of the CMB-MM results and biases of the applied OC/EC ratios which are obtained from another prescribed burning plume in this area.

Our study indicates that the 'primary_plume profile' derived from the fire event is comparable with the prescribed burning emission profile measured by Lee et al. (2005) for some organic compounds, but significantly different for others (Table 5.3 and Figure 5.6). In the aged fire plume, levoglucosan accounts for 14% of primary OC, comparable to 9.5% in the profile of Lee et al. (2005). Most *n*-alkanes also show comparable levels for the two source profiles. Hopanes and steranes were not significant in either set. The ratio of water-soluble potassium (K^+)/OC in the 'primary_plume profile' is 0.0067, lower than the values in Lee et al. (0.011) and in Fine et al. (0.012 on average), but comparable to the average ratio of 0.0058 from foliar fuel combustion [*Fine et al.*, 2004a; *Hays et al.*, 2002; *Lee et al.*, 2005a]. However, significant differences were found for the fractions of PAHs, resin acids, *n*-alkanoic acid and dicarboxylic acids, suggesting aging of fire smoke after a 3-4 hour travel distance. Lee et al. (2005) measured higher abundances for many PAHs and resin acids, implying direct combustion is the main contributor of these compounds and significant chemical alteration occurs during transport, especially for resin acids. In contrast, the aged plume has distinctly higher dicarboxylic acids (alkanedioic acids and dicarboxylic aromatic acids) fractions. Enhanced SOA formation in the atmosphere from the fire is suggested by these secondary indicators. The profile comparison between prescribed fire source emission and aged plume is useful to understand evolution of wood smoke during transport and to assess the organic species applied in CMB-MM modeling. Impacts from aging process of smoke plume should be considered in source apportionment methodology using CMB model, i.e. selection of fitting species.

5.4 Conclusions

Large increases in $PM_{2.5}$ and OC in Atlanta caused by an aged prescribed fire plume through direct burning emissions and formation of secondary organic aerosols was captured by a system of monitors. Organic tracers of biomass burning, levoglucosan, resin acids and retene, exhibited sharp increases in concentrations during the episode. Observed resin acids and retene indicated predominant softwood (conifers) burning. Increases in resin acids were accompanied by high levels of dehydroabietic acids and 7-oxodehydroabietic acids, mainly formed during transport. Carbon number predominance for *n*-alkanes (odd over even) and *n*-alkanoic acids (even over odd) suggested that emissions from heat-exposed vegetation are important as one of major sources for increasing OC, especially secondary OC. Secondary organic tracers were observed with significantly higher ambient concentrations, providing further support for biogenic SOA formation. These data allow estimating source profiles for aged fire plumes, which can be used for improving source apportionment of wood burning by CMB modeling.

Acknowledgements

This work was funded in part by the U.S. Environmental Protection Agency STAR grants (R832159, R828976 and R831076). We would like to thank Georgia Power (Southern Company) for their support of work in Laboratory for Atmospheric Modeling, Diagnostics, and Analysis (LAMDA) at Georgia Institute of Technology in this study area. The authors also acknowledge the helpful forest information provided by Dr. Di Tian.

Table 5.3. Source Composition Profiles from The Aged Plume on The Event and The Previous Prescribed Burning Emission (unit: ng/μg $PM_{2.5}$)

Compound	Aged Plume [a]	PPM_{fc} [b]	Lee et al. [c]	Compound	Aged Plume [a]	PPM_{fc} [b]	Lee et al. [c]
	Fraction [d] ± std [e]	Fraction ± std	Fraction ± std		Fraction ± std	Fraction ± std	Fraction ± std
***n*-alkanes**							
Tetracosane	0.038 ± 0.021	0.051 ± 0.028	0.084 ± 0.053	Triacontane	0.045 ± 0.012	0.061 ± 0.016	0.117 ± 0.072
Pentacosane	0.071 ± 0.029	0.096 ± 0.040	0.151 ± 0.095	Hentriacontane	0.256 ± 0.073	0.347 ± 0.102	0.174 ± 0.105
Hexacosane	0.023 ± 0.016	0.031 ± 0.022	0.137 ± 0.091	Dotriacontane	0.029 ± 0.008	0.040 ± 0.011	0.000 ± 0.001
Heptacosane	0.173 ± 0.050	0.234 ± 0.069	0.151 ± 0.114	Tritriacontane	0.053 ± 0.016	0.071 ± 0.022	0.054 ± 0.048
Octacosane	0.047 ± 0.017	0.064 ± 0.024	0.070 ± 0.042	Tetratriacontane	0.000 ± 0.001	0.000 ± 0.001	0.000 ± 0.001
Nonacosane	0.311 ± 0.088	0.422 ± 0.123	0.486 ± 0.295				
Branch-alkanes							
iso-Nonacosane	0.000 ± 0.001	0.000 ± 0.001	0.000 ± 0.001	iso-Hentriacontane	0.000 ± 0.001	0.000 ± 0.001	0.000 ± 0.001
anteiso-Triacontane	0.000 ± 0.001	0.000 ± 0.001	0.000 ± 0.001				
Hopanes							
17α(H)-21β(H)-29-Norhopane	0.002 ± 0.005	0.003 ± 0.007	0.000 ± 0.001	22R,17α(H),21β(H)-Homohopane	0.002 ± 0.002	0.003 ± 0.003	0.000 ± 0.001
17α(H)-21β(H)-Hopane	0.002 ± 0.005	0.002 ± 0.006	0.000 ± 0.001	22S,17α(H),21β(H)-Bishomohopane	0.001 ± 0.001	0.001 ± 0.002	0.000 ± 0.001
22,29,30-Trisnorneohopane	0.002 ± 0.002	0.003 ± 0.003	0.000 ± 0.001	22R,17α(H),21β(H)-Bishomohopane	0.000 ± 0.001	0.000 ± 0.001	0.000 ± 0.001
22,29,30-Trisnorhopane	0.000 ± 0.001	0.000 ± 0.001	0.000 ± 0.001	22S,17α(H),21β(H)-Trishomohopane	0.000 ± 0.001	0.000 ± 0.001	0.000 ± 0.001
22S,17α(H),21β(H)-Homohopane	0.003 ± 0.003	0.004 ± 0.004	0.000 ± 0.001	22R,17α(H),21β(H)-Trishomohopane	0.000 ± 0.001	0.000 ± 0.001	0.000 ± 0.001
Steranes							
20S,R-5α(H),14β(H),17β(H)-Cholestanes	0.000 ± 0.001	0.000 ± 0.001	0.000 ± 0.001	20S,R-5α(H),14β(H),17β(H)-Ergostanes	0.000 ± 0.001	0.000 ± 0.001	0.000 ± 0.001
20R-5α(H),14α(H),17α(H)-Cholestane	0.000 ± 0.001	0.000 ± 0.001	0.000 ± 0.001	20S,R-5α(H),14β(H),17β(H)-Sitostanes	0.000 ± 0.001	0.000 ± 0.001	0.000 ± 0.001
PAHs							
Fluoranthene	0.000 ± 0.001	0.000 ± 0.001	0.054 ± 0.031	Benzo(j)fluoranthene	0.000 ± 0.001	0.001 ± 0.001	0.008 ± 0.005
Acephenanthrylene	0.001 ± 0.001	0.001 ± 0.001	0.017 ± 0.011	Benzo(e)pyrene	0.004 ± 0.002	0.005 ± 0.003	0.030 ± 0.017
Pyrene	0.000 ± 0.001	0.000 ± 0.001	0.064 ± 0.036	Benzo(a)pyrene	0.001 ± 0.002	0.001 ± 0.002	0.018 ± 0.010
Retene	0.028 ± 0.008	0.039 ± 0.011	0.210 ± 0.127	Perylene	0.000 ± 0.001	0.000 ± 0.001	0.002 ± 0.002
Benzo(ghi)fluoranthene	0.002 ± 0.002	0.003 ± 0.003	0.059 ± 0.052	Indeno(1,2,3-cd)fluoranthene	0.002 ± 0.001	0.003 ± 0.002	0.000 ± 0.001
Cyclopenta(cd)pyrene	0.000 ± 0.001	0.000 ± 0.001	0.174 ± 0.106	Indeno(1,2,3-cd)pyrene	0.003 ± 0.003	0.004 ± 0.003	0.044 ± 0.027

Benz(a)anthracene	0.001 ± 0.002	0.001 ± 0.002	0.048 ± 0.027	Picene	0.000 ± 0.001	0.000 ± 0.001	0.000 ± 0.001
Chrysene/Triphenylene	0.007 ± 0.004	0.010 ± 0.006	0.059 ± 0.033	Benzo(ghi)perylene	0.003 ± 0.004	0.004 ± 0.006	0.022 ± 0.012
Benzo(b)fluoranthene	0.004 ± 0.003	0.006 ± 0.004	0.030 ± 0.017	Coronene	0.004 ± 0.004	0.005 ± 0.005	0.004 ± 0.003
Benzo(k)fluoranthene	0.003 ± 0.002	0.004 ± 0.003	0.025 ± 0.014				
Resin Acids							
8,15-Pimaredienoic acid	0.000 ± 0.001	0.000 ± 0.001	0.000 ± 0.001	Abietic acid	0.011 ± 0.004	0.015 ± 0.006	0.000 ± 0.001
Pimaric acid	0.019 ± 0.006	0.025 ± 0.008	1.486 ± 0.826	Abieta-6,8,11,13,15-pentae-18-oic acid	0.009 ± 0.003	0.012 ± 0.004	0.000 ± 0.001
Sandaracopimaric acid	0.056 ± 0.017	0.076 ± 0.024	0.000 ± 0.001	Abieta-8,11,13,15-tetraen-18-oic acid	0.026 ± 0.007	0.036 ± 0.010	0.000 ± 0.001
Isopimaric acid	0.000 ± 0.001	0.000 ± 0.001	1.783 ± 0.999	7-Oxodehydroabietic acid	0.743 ± 0.198	1.006 ± 0.277	0.000 ± 0.001
Dehydroabietic acid	1.546 ± 0.433	2.092 ± 0.605	20.07 ± 11.45				
Aromatic Acids							
1,2-Benzenedicarboxylic acid	0.119 ± 0.036	0.160 ± 0.050	0.009 ± 0.006	1,3-Benzenedicarboxylic acid	0.029 ± 0.011	0.039 ± 0.015	0.000 ± 0.001
1,4-Benzenedicarboxylic acid	0.044 ± 0.021	0.059 ± 0.028	0.005 ± 0.005				
Alkanoic Acids							
Tetradecanoic acid	0.074 ± 0.025	0.100 ± 0.034	1.209 ± 0.743	Tricosanoic acid	0.145 ± 0.039	0.196 ± 0.055	0.394 ± 0.227
Pentadecanoic acid	0.036 ± 0.014	0.049 ± 0.019	0.384 ± 0.245	Tetracosanoic acid	0.554 ± 0.151	0.750 ± 0.211	2.984 ± 1.740
Hexadecanoic acid	0.278 ± 0.132	0.377 ± 0.181	4.055 ± 2.338	Pentacosanoic acid	0.049 ± 0.013	0.066 ± 0.019	0.231 ± 0.133
Heptadecanoic acid	0.021 ± 0.008	0.028 ± 0.011	0.149 ± 0.091	Hexacosanoic acid	0.301 ± 0.081	0.408 ± 0.114	2.212 ± 1.282
Octadecanoic acid	0.134 ± 0.064	0.182 ± 0.088	1.351 ± 0.811	Heptacosanoic acid	0.017 ± 0.005	0.023 ± 0.006	0.085 ± 0.051
Nonadecanoic acid	0.026 ± 0.008	0.036 ± 0.011	0.294 ± 0.187	Octacosanoic acid	0.103 ± 0.028	0.140 ± 0.039	0.595 ± 0.350
Eicosanoic acid	0.176 ± 0.049	0.238 ± 0.068	0.720 ± 0.437	Nonacosanoic acid	0.022 ± 0.006	0.029 ± 0.008	0.101 ± 0.065
Heneicosanoic acid	0.074 ± 0.020	0.100 ± 0.028	0.174 ± 0.101	Triacontanoic acid	0.112 ± 0.030	0.152 ± 0.042	0.484 ± 0.314
Docosanoic acid	0.379 ± 0.103	0.514 ± 0.144	1.076 ± 0.638				
Alkenoic Acids							
9-Hexadecenoic acid	0.000 ± 0.001	0.000 ± 0.001	0.306 ± 0.227	9-Octadecenoic acid	0.000 ± 0.001	0.000 ± 0.001	1.469 ± 0.881
9,12-Octadecanedienoic acid	0.000 ± 0.001	0.000 ± 0.001	1.357 ± 0.921				
Alkanedioic Acids							
Propanedioic acid	0.000 ± 0.001	0.000 ± 0.001	0.000 ± 0.001	Hexanedioic acid	0.088 ± 0.026	0.120 ± 0.037	0.016 ± 0.013
Methylpropanedioic acid	0.000 ± 0.001	0.000 ± 0.001	0.000 ± 0.001	Heptanedioic acid	0.000 ± 0.001	0.000 ± 0.001	0.018 ± 0.016
Butanedioic acid	0.801 ± 0.227	1.084 ± 0.317	0.239 ± 0.153	Octanedioic acid	0.149 ± 0.041	0.201 ± 0.057	0.036 ± 0.028
Methylbutanedioic acid	0.172 ± 0.047	0.232 ± 0.066	0.000 ± 0.001	Nonanedioic acid	0.299 ± 0.084	0.404 ± 0.117	0.156 ± 0.101

Pentanedioic acid	0.120 ± 0.035	0.162 ± 0.048	0.049 ± 0.032				
Others							
Nonanal	0.013 ± 0.009	0.017 ± 0.012	0.000 ± 0.001	Benz(de)anthracen-7-one	0.004 ± 0.002	0.005 ± 0.003	0.0000 ± 0.0001
Sinapyl aldehyde	0.000 ± 0.001	0.000 ± 0.001	0.000 ± 0.001	3,5-Dimethoxy-4-hydroxyacetophenone	0.028 ± 0.007	0.037 ± 0.010	0.0000 ± 0.0001
Acetonylsyringol	0.058 ± 0.018	0.079 ± 0.025	0.000 ± 0.001	Levoglucosan	45.91 ± 12.69	62.15 ± 17.75	57.09 ± 32.38
Coniferyl aldehyde	0.000 ± 0.001	0.000 ± 0.001	0.000 ± 0.001	Cholesterol	0.000 ± 0.001	0.000 ± 0.001	0.000 ± 0.001
Propionylsyringol	0.000 ± 0.001	0.000 ± 0.001	0.000 ± 0.001				
OC	593.9 ± 180.2	450.2 ± 250.6	602.5 ± 185.2	Cl^-	0.44 ± 0.09	0.59 ± 0.13	5.27 ± 2.89
EC	23.0 ± 12.4	31.1 ± 17.0	39.2 ± 11.3	NH_4^+	13.12 ± 4.43	17.76 ± 6.13	1.07 ± 1.08
Al	0.000 ± 0.001	0.000 ± 0.001	0.229 ± 0.426	NO_3^-	19.31 ± 5.18	26.14 ± 7.26	4.40 ± 2.99
Si	0.289 ± 0.228	0.391 ± 0.309	0.186 ± 0.258	SO_4^{2-}	13.80 ± 8.57	18.68 ± 11.68	2.45 ± 1.12
K^+	2.23 ± 0.50	3.01 ± 0.72	6.49 ± 4.35				

Note: [a] source composition profiles where individual chemical species are normalized to the fire-caused total $PM_{2.5}$ mass on the event day; [b] source composition profiles where individual chemical species are normalized to the fire-caused primary $PM_{2.5}$ mass estimated on the event day; [c] source composition profiles from the prescribed burning emission in Georgia [*Lee et al.*, 2005a]; [d] fraction of chemical species in the associated $PM_{2.5}$ mass (ng/μg $PM_{2.5}$); [e] standard deviation.

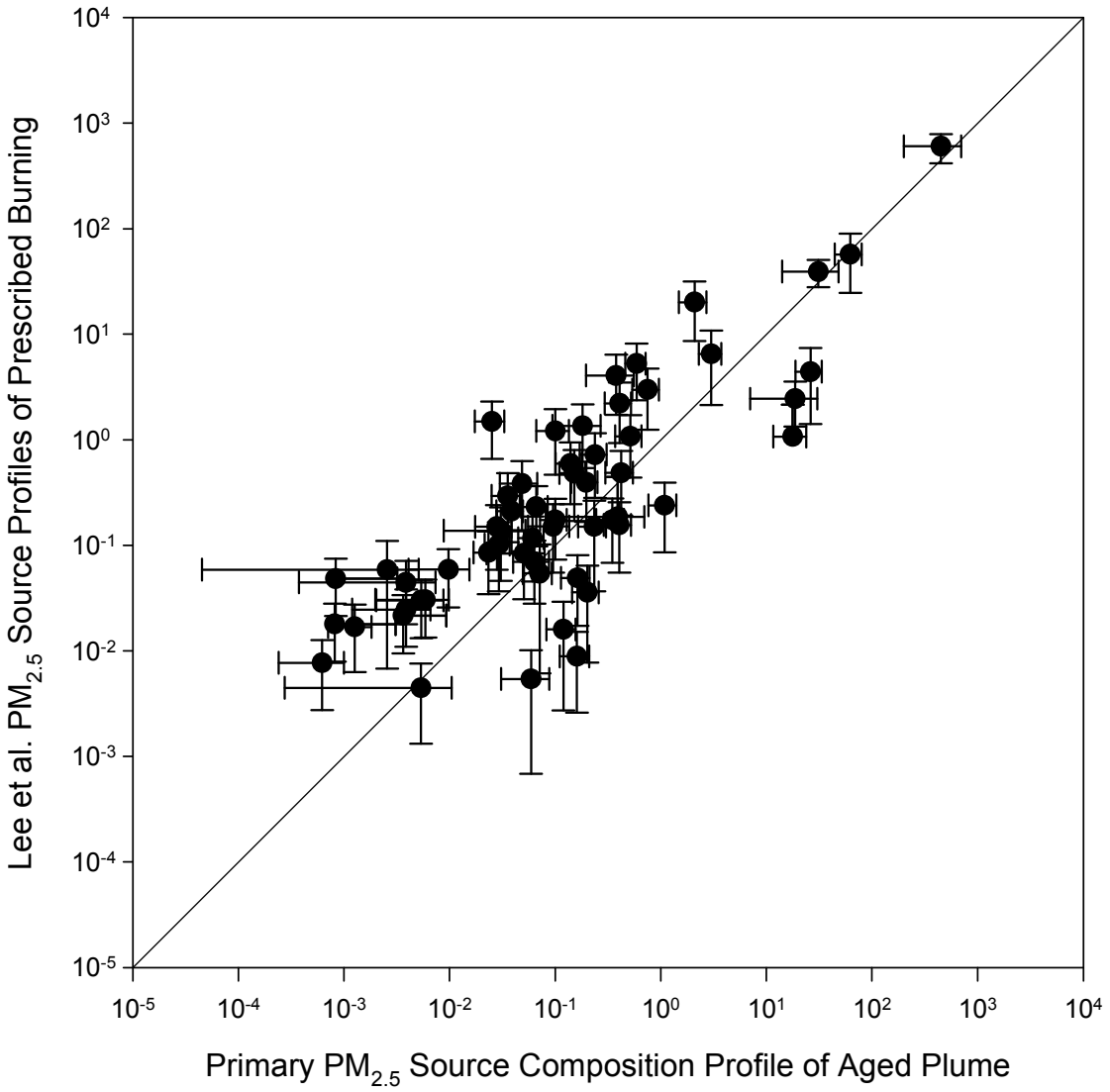

Figure 5.6. Comparison between source composition profiles developed from the aged biomass burning plume on the event and the prescribed burning emission measured by Lee et al. (2005). The profiles are composed of individual species fractions, normalized to primary $PM_{2.5}$ mass. A log-log scale is used.

CHAPTER 6

DETAILED CHEMICAL CHARACTERIZATION AND AGING OF WILDFIRE AEROSOLS IN THE SOUTHEASTERN U.S

(Bo Yan, Yongtao Hu, Xiaolu Zhang, Di Tian, Sivaraman Balachandran, Hyeon Kook Kim, Rodney J. Weber, Mei Zheng, and Armistead G. Russell. *Journal of Geophysical Research-Atmospheres*, in preparation)

Abstract

In April of 2007, a major wildfire originated in the Okefenokee National Wildlife Refuge in Georgia, and over next two months spread across the Georgia-Florida border. Burning out about 388,017 aces of wildland, the fire led to dozens of hazy days over states in the southeastern U.S. The wildfire-derived $PM_{2.5}$ was characterized at three sampling sites at different distances downwind of the fire origin for detailed chemical composition, including organic carbon (OC), elemental carbon (EC), water-soluble OC (WSOC), ionic species, trace metals, and solvent-extractable organic compounds.

The highest increases in hourly and 24-hr $PM_{2.5}$ were observed to reach over 340 and 100 μg m^{-3}, respectively, on the smoke days. Wildfire-derived $PM_{2.5}$ was dominated by organic matter, making up 60-85% of the $PM_{2.5}$ mass. Significant increases were found for biomass burning tracers (levoglucosan, resin acids, retene, etc.), *n*-alkanes, *n*-alkanoic acids, as well as some inorganic species, such as water-soluble potassium (K^+), ammonium (NH_4^+), nitrate (NO_3^-), sulfate (SO_4^{2-}), and EC. The ratios of levoglucosan vs. inorganic indicators of biomass burning (K^+ and EC) did not show significant decreases

from the wildfire origin to the monitors 400 km downwind. However, resin acids are subject to alteration in the atmosphere. It is interesting to note that hopanes increased significantly during wildfire smoke events, implying that ambient hopanes, unique organic tracers of mobile source, can also be produced by thermal alteration of biogenic hopanoid precursors. The source profiles for aged wildfire plumes were developed and can be used for improving source apportionment of biomass burning by CMB modeling.

Secondary organic tracers, 2-methyltetrols and pinic acid, were observed with significantly higher concentrations at the downwind sites, providing further support for enhanced formation of biogenic SOA. However, *cis*-pinonic acid, another photo-oxidation product of monoterpenes, did not show significant increase. In addition, elevated aromatic and aliphatic diacids were observed at all downwind sites, suggesting that they are not only secondarily created from anthropogenic emissions but also formed from or enhanced by wildfire-derived biogenic emissions in the atmosphere.

6.1 Introduction

Biomass burning is a major source of fine particulate matter ($PM_{2.5}$) in the atmosphere on both regional and global scales, and has significant impacts on air quality, visibility, human health and climate [*Bond et al.*, 2004; *Hobbs et al.*, 1997; *Lighty et al.*, 2000; *Penner et al.*, 1992; *Reid et al.*, 2005]. It is estimated that wildland fire, including wildfires and prescribed burning, contributes about 20% of total $PM_{2.5}$ emissions in the United States [*U.S. EPA*, 2000]. In 2007, a total of 85,705 wildland fires were reported nationally to have burned 9,328,045 acres, over 60% of which were caused by wildfires [*NIFC*, 2008]. The frequency and intensity of wildfire are expected to increase in the

future as a result of climate change, which is elevating spring and summer temperatures [*Flannigan et al.*, 1998; *Westerling et al.*, 2006].

Such large and increasing emission contributions are of concern to affected areas, especially those with large populations and local related air pollutant concentrations near or above the applicable air quality standards. For instance, the Big Turnaround Complex (BTC) wildfire, originating in the Okefenokee National Wildlife Refuge in Georgia and spreading across the Georgia–Florida border, resulted in elevated pollutant levels from April through June 2007. This massive wildfire burned about 390,000 aces of saw palmettos, titis, gallberry hollies, scrubs and varied pines. Ranked the 11th largest wildfire in U.S. since 1997 and the largest fire for the US Fish & Wildlife Service outside Alaska [*NIFC*, 2008], the fire led to dozens of hazy days over Georgia, Florida, Alabama and parts of neighboring states. It was estimated that millions of residents in this region were exposed to the unhealthy air for hours or even days. For example, thick wildfire smoke plumes hit the metropolitan Atlanta, GA and surrounding areas several times within one month (May 2007), resulting in ambient $PM_{2.5}$ concentrations of up to 76 μg m^{-3} (24-hr average) and 365 μg m^{-3} (1-hr average).

Previous studies on biomass burning have often concentrated on residential and commercial wood combustion, e.g., fireplace and woodstove wood combustion [*Fine et al.*, 2002; 2004a; *Hays et al.*, 2003; *Schauer et al.*, 2001], as well as agricultural biomass burning [*Hays et al.*, 2002]. Recently, chemical composition and air quality impacts of prescribed burning emissions have been investigated, especially in the southern states where prescribed burning is applied increasingly in agriculture and wildland management [*Lee et al.*, 2008; *Yan et al.*, 2008a]. However, detailed data speciating fine organic

carbon (OC) and $PM_{2.5}$ impacted by wildfires is sparse, especially in the southern states, and even less data is available for both fresh and aged plumes originated from the same wildfire event. Consequently, the aging process of specific organic tracers during long-range transport is not well known for wildfire emissions, even though it is critical for air quality management as well as application and assessment of molecular marker based receptor models in source apportionment [*Robinson et al.*, 2006b]. Here, the Okefenokee wildfire plumes were captured by downwind monitors at different distances away from the fire origin. This provides an opportunity to further understand atmospheric processes impacting the aging of fire plumes, assess formation of secondary organic aerosol (SOA) enhanced by wildfires, and approximate source composition profiles of wildfire emissions for use in future source apportionment.

In this study, chemical composition of aerosols was characterized on days heavily impacted by the plume from the BTC wildfire, and contrasted against days less directly impacted. Routine observations of $PM_{2.5}$ composition include OC, elemental carbon (EC), ions, and trace metals. As the major component of $PM_{2.5}$ from biomass burning emissions, fine OC is further characterized by gas chromatography/mass spectrometry (GC/MS) analysis for detailed composition of organic compounds including *n*-alkanes, hopanes, steranes, *n*-alkanoic acids, alkanedioic acids, polycyclic aromatic hydrocarbons (PAHs), resin acids, and others (syringols, levoglucosan, cholesterol, 2-methyltetrols, etc.). Some of these compounds are reasonably used as to track specific sources of carbonaceous aerosols.

Source impacts from biomass burning, in particular, were traced through a few organic molecular markers including levoglucosan, resin acids, syringols and retene.

Levoglucosan is considered a particularly useful tracer of biomass burning [*Simoneit et al.*, 1999], and is frequently used for source impact studies because of its large emission abundance and reasonable thermal stability in the atmosphere [*Fraser and Lakshmanan*, 2000; *Schauer and Cass*, 2000]. Resin acids are thermal alteration products of coniferous wood resins and emitted exclusively from softwood burning (various pines, firs, etc.) [*Rogge et al.*, 1998; *Simoneit et al.*, 1993; *Standley and Simoneit*, 1994]. In contrast, hardwood combustion produces much higher quantities of syringols [*Hawthorne et al.*, 1988; *Hawthorne et al.*, 1989]. Although PAHs are emitted from multiple combustion processes of fuels (biomass, natural gas, diesel and gasoline) and ubiquitous in the atmosphere, retene, a thermal alteration of abietane compounds (resin diterpenoids), is considered as an organic tracer for coniferous wood burning [*Ramdahl*, 1983]. Potassium (K), an important inorganic tracer of biomass burning, is widely applied because of its abundant fraction in emissions [*Hays et al.*, 2002; *Kim et al.*, 2003; *Schauer et al.*, 2001]. Along with receptor modeling, these tracers were used to quantify source impacts of biomass burning on $PM_{2.5}$. Their aging processes during transport were investigated by comparing these organic tracers with EC and a few other inorganic species.

6.2 Experimental Section

6.2.1 Ambient Aerosol Sampling

Filter samples from a variety of ambient air monitoring networks were utilized (Figure 6.1). Daily $PM_{2.5}$ samples were collected on 47 mm filters by particulate composition monitors (PCM) at the Assessment of Spatial Aerosol Composition in Atlanta (ASACA) sites [*Butler et al.*, 2003]. Three ASACA urban sites (Fire Station #8

(FS8), Fort McPherson (FT), and South Dekalb (SD)) are located in metropolitan Atlanta, about 400 km away from the wildfires in Okefenokee National Wildlife Refuge. Hourly $PM_{2.5}$ was also measured in the metropolitan Atlanta and surrounding areas at the Southeastern Aerosol Research and Characterization (SEARCH) sites [*Hansen et al.*, 2003], as well as at the U.S. Environmental Protection Agency's (EPA) State and Local Air Monitoring Station (SLAMS) sites [*Demerjian*, 2000]. In Bibb County, GA, about 120 km southeast of Atlanta or 280 km northwest of the wildfires, 24-hr $PM_{2.5}$ samples were collected by PCM every 6 days at a Speciation Trends Network (STN) site (Allied Chemicals, Macon) [*Chu et al.*, 2004], and hourly data was measured at a nearby SLAMS site (Macon Southeast). In Coffee County, GA, about 60 km northwest of the wildfires, 24-hr $PM_{2.5}$ was collected every 6 days at a STN site (Douglas). Just inside the Okefenokee National Wildlife Refuge, an Interagency Monitoring of Protected Visual Environments (IMPROVE) monitor was sampling 24-hr $PM_{2.5}$ every 3 days [*Eldred et al.*, 1997]. In April and May of 2007, the ambient air monitors in the metropolitan Atlanta area captured the wildfire plumes on May 16, May 22, and May 27. The air monitors in Bibb County captured one heavy smoke plume on May 12, and the one in the Coffee site was impacted by smoke plumes several times (Table 6.1).

The 24-hr filter samples collected from the ASACA sites were individually analyzed for OC/EC, trace metals, and ions using thermal optical transmittance (TOT), X-ray fluorescence (XRF) and ion chromatography (IC), respectively [*Baumann et al.*, 2003; *Lee et al.*, 2005a; *Lee et al.*, 2008]. Chemical composition (OC, EC, ions and trace metals) of 24-hr ambient $PM_{2.5}$ collected at the STN and IMPROVE sites were measured by RTI international and Crocker Nuclear Laboratory in UC Davis, respectively. Note

that the data of $PM_{2.5}$ mass and trace metals is not available for a few smoke samples collected at the Okefenokee site due to overloading.

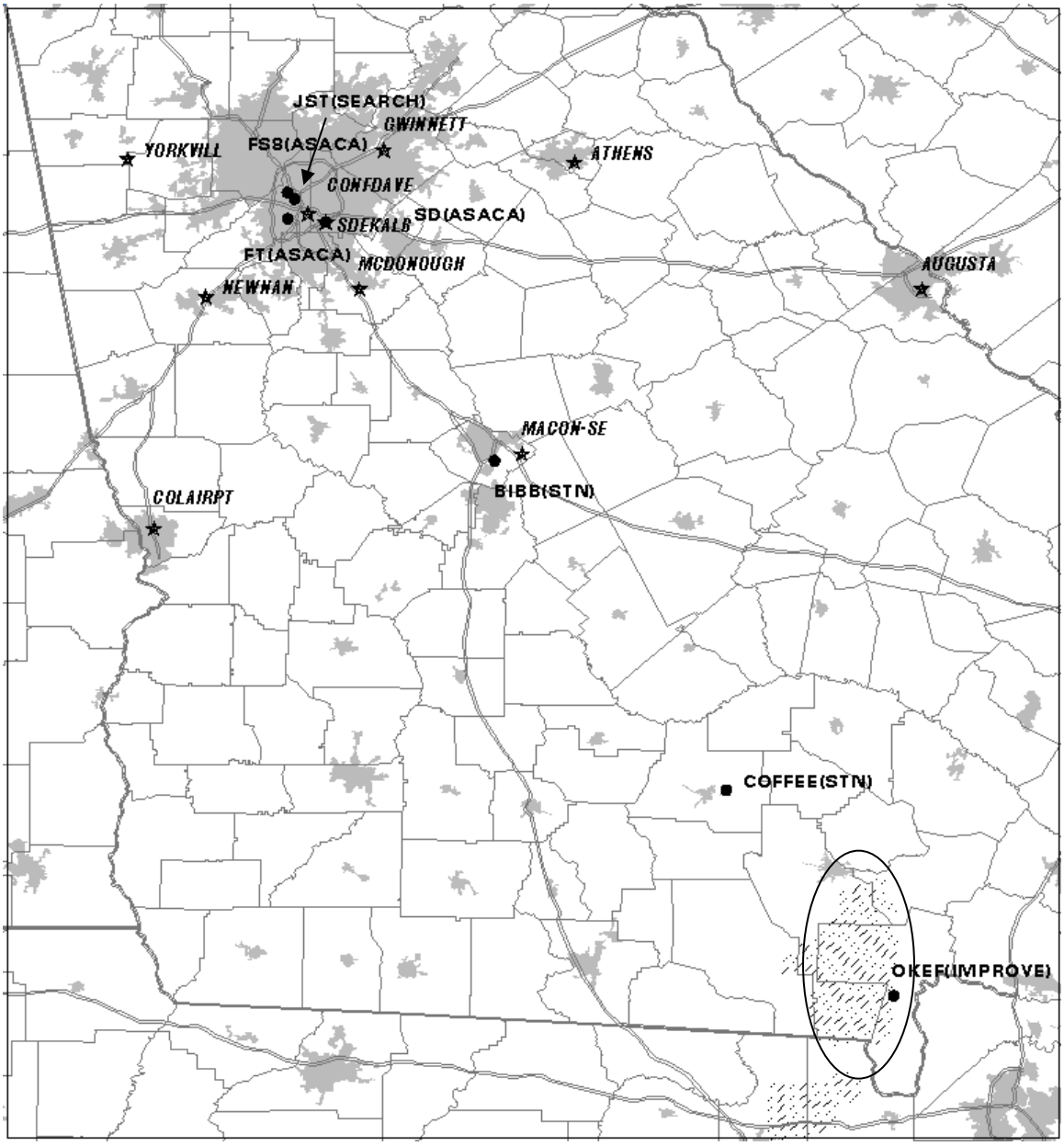

Figure 6.1. Ambient air monitors in metropolitan Atlanta, Georgia and southern Georgia impacted by the wildfire plumes. FS8, FT and SD are the ASACA sites; Bibb and Coffee are the STN sites; OKEF is an IMPROVE site; JST is an SEARCH site; and the others are the SLAMS sites. The Okefenokee wildfires area is circled (lower right corner).

Table 6.1. ASACA and STN Composite PCM Non-Smoke and Smoke Samples Used for GC/MS Organic Tracer analysis

Composite Samples	Combination Sites	Combination Sampling Date	$PM_{2.5}$ (μg.m-3)	OC (μg.m-3)	EC (μg.m-3)	OC/EC
ASACA Samples						
NonSmoke-1	FS8, FT, SD	05/14 - 05/15	14.9	4.09	0.74	5.54
Smoke-1	FS8, FT, SD	5/16/2007	25.0	10.3	1.25	8.24
NonSmoke-2	FS8, FT, SD	05/17 - 05/19	10.8	2.56	0.62	4.10
Smoke-2	FS8, FT, SD	5/22/2007	53.6	25.3	2.10	12.07
NonSmoke-3	FS8, FT, SD	05/24 - 05/25	10.0	3.22	0.75	4.27
Smoke-3	FS8, FT, SD	5/27/2007	46.2	22.7	1.68	13.50
NonSmoke-4	FS8, FT, SD	05/28 - 05/29	14.6	3.41	0.65	5.22
STN Samples						
NonSmoke-Bibb	Bibb	04/18, 04/30, 05/06, 05/18, 05/24	16.2	5.21	0.75	6.95
Smoke-Bibb	Bibb	5/12/2007	117	62.8	1.22	51.5
NonSmoke-Coffee	Coffee	03/31, 04/06, 04/12, 05/24, 05/30	10.8	3.54	0.31	11.4
Smoke-Coffee	Coffee	04/18, 04/24, 04/30, 05/06, 05/12/07	19.9	7.38	0.55	13.4

Note: 'FS8', 'FT' and 'SD' denote the ASACA urban sites at Fire Station #8, Fort McPherson and South Dekalb, respectively. 'Bibb' and 'Coffee' indicate the STN sites at Bibb county and Coffee county, GA, respectively.

6.2.2 Organic Speciation Using GC/MS and IC

Owing to low air volumes, OC mass on a single PCM filter is usually not enough for GC/MS organic tracer analysis. Therefore, individual PCM filters from the ASACA and the STN sites were combined as a few non-smoke and smoke samples (Table 6.1). These composite samples, along with composite field blanks, were analyzed for solvent-extractable organic compounds in $PM_{2.5}$ using a standardized GC/MS method described previously [*Nolte et al.*, 2002; *Yan et al.*, 2008a; *Zheng et al.*, 2002; *Zheng et al.*, 2006b]. The ASACA and STN filters were also measured for water-soluble OC (WSOC) with a

Total Organic Carbon (TOC) analyzer (Sievers Model 800 Turbo, Boulder, CO) [*Sullivan et al.*, 2004]. Additionally, quartz filters from the STN sites were further analyzed for levoglucosan with the IC method [*Engling et al.*, 2006].

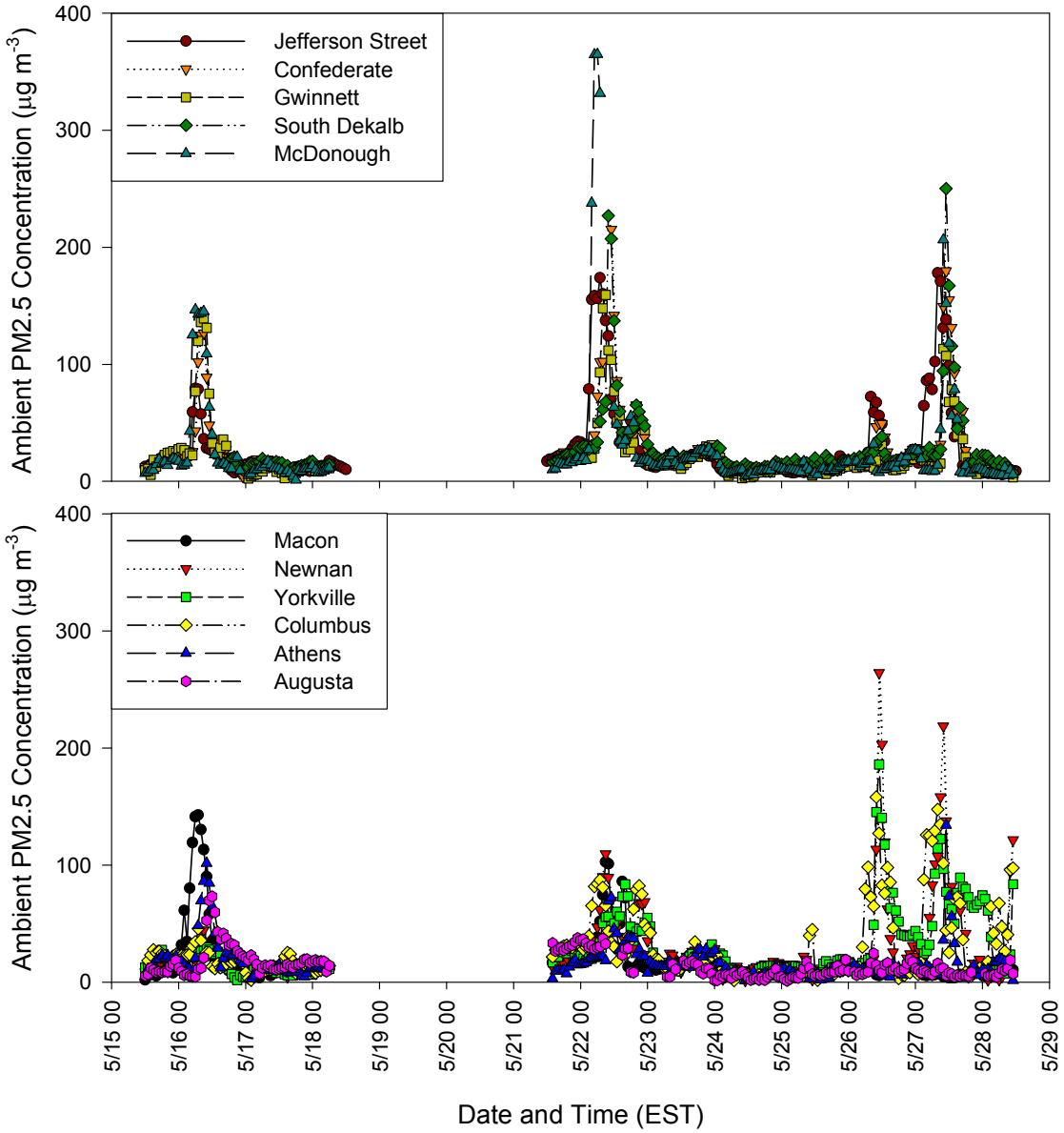

Figure 6.2. Hourly ambient concentrations of $PM_{2.5}$ observed in the metropolitan Atlanta, GA and surrounding areas during the wildfire episodes.

6.3 Results and Discussion

6.3.1 Ambient $PM_{2.5}$ and OC

Between May 15-28, 2007, the metropolitan Atlanta and nearby areas were impacted by wildfire smoke plumes a few times. Large increases of hourly $PM_{2.5}$ were observed by many monitors in this region (Figure 6.2). The highest increase (over 340 μg m^{-3}) in hourly $PM_{2.5}$ occurred at MacDonough on May 22, following by increases of over 240 and 230 μg m^{-3} in Newnan on May 26 and South Dekalb on May 27, respectively. Three of these smoke events were captured by the ASACA air monitors (FS8, FT, and SD) (Table 6.1). The 24-hr $PM_{2.5}$ concentrations (three sites combined) jumped from 14.9, 10.8, and 10.0 μg m^{-3} to 25.0, 53.6, and 46.2 μg m^{-3}, respectively, and the 24-hr OC (three sites combined) increased from 4.1, 2.6, and 3.2 μg m^{-3} to 10.3, 25.4, and 22.7 μg m^{-3}, on the smoke days. Wildfire plumes were sampled by the air monitors at the Bibb, Coffee, and Okefenokee sites on or around May 12, 2007. At the Bibb site, hourly $PM_{2.5}$ increased rapidly from 20 to 142 μg m^{-3} within the first hour (10:00 am) when the plume arrived, and peaked at 342 μg m^{-3} by 2:00 pm (Figure 6.3). Correspondingly, the 24-hr $PM_{2.5}$ and OC increased from 16.2 and 5.2 μg m^{-3} to 117 and 62.8 μg m^{-3}, respectively. At the Okefenokee site, tremendously high 24-hr OC (up to 80 μg m^{-3}) were found, contrasting against the average OC of 1.3 μg m^{-3} on non-smoke days (Figure 6.3). Smaller variations were observed at the Coffee site with increases of 9.1 and 3.8 μg m^{-3} in 24-hr $PM_{2.5}$ and OC, respectively. Such large and continuous increases in $PM_{2.5}$ and OC were observed during the same period over these monitors that spread from the Georgia-Florida border to the metropolitan Atlanta area, suggesting direct impacts of wildfire emissions. Our back trajectory modeling indicates that these smoke plumes

originated in the Okefenokee National Wildlife Refuge (Figure D.1). This is supported by regionwide investigations in organic molecular markers and inorganic tracers of major primary sources.

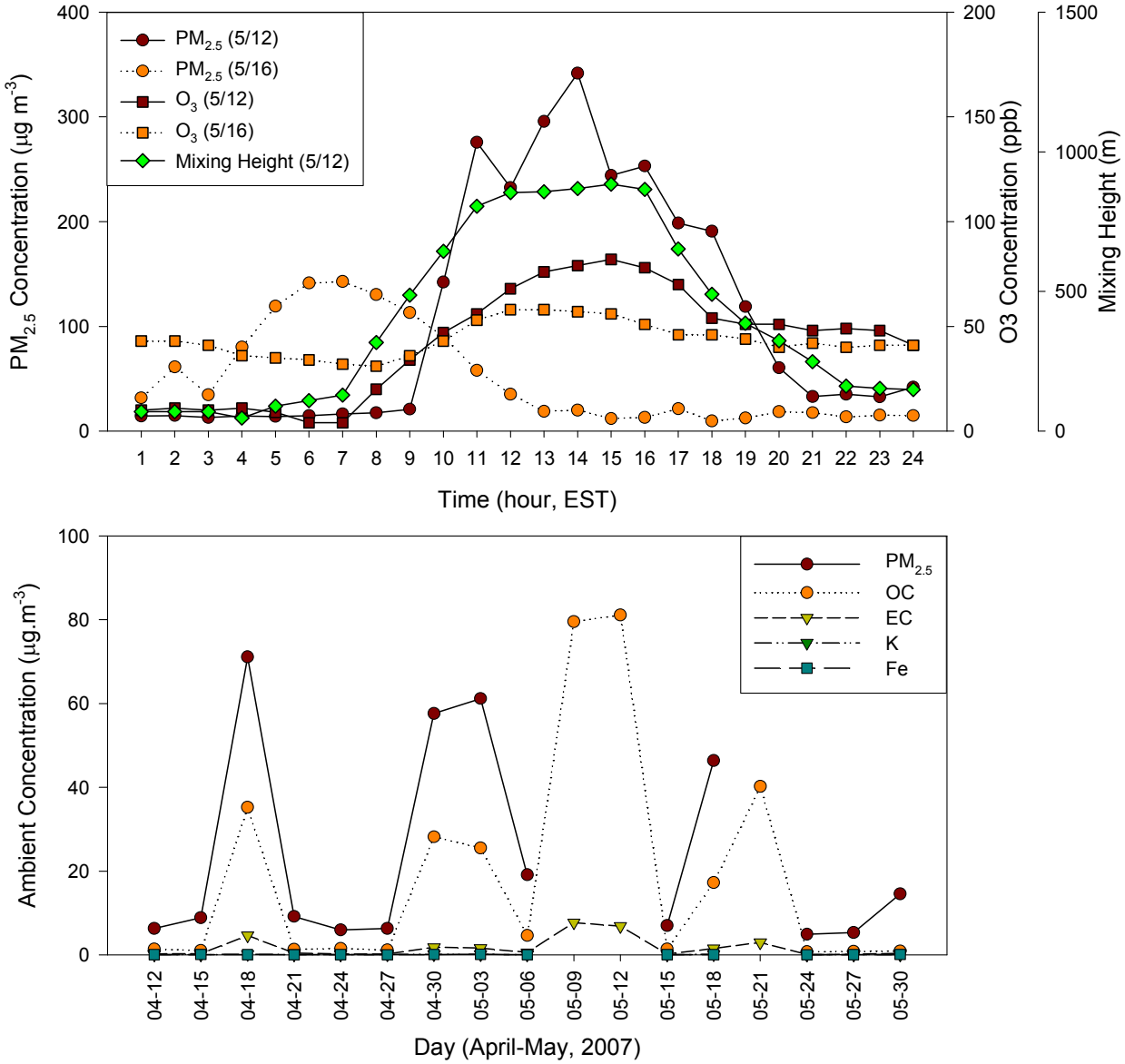

Figure 6.3. Ambient concentrations of $PM_{2.5}$ during the wildfire episodes: (a) hourly $PM_{2.5}$, O_3 and mixing heights (estimated by the NOAA HYSPLIT back trajectory model) at the Bibb site; (b) daily $PM_{2.5}$, OC, EC, K, and Fe at the Okefenokee site.

Table 6.2. Fire-Caused $PM_{2.5}$ Compositions (Cross-Ratios) in the Wildfire Plumes and Previous Studies

Comparison Ratios (µg / µg)	This Wildfire Study				Prescribed [d]	Pine Wood [e]
	Okefenokee [a]	Coffee [b]	Bibb [b]	Atlanta [c]		
OC / $PM_{2.5}$	0.43	0.39	0.49	0.55	0.59	0.53
OM/$PM_{2.5}$	0.65	0.59	0.74	0.83	0.89	0.80
WSOC/OC	n/a [f]	0.61 [g]	0.49	0.47	0.71	n/a
OC / EC	11.3	45.0	66.9	17.3	25.9	38.0
OC / K	304.7	161.9	220.7	461.7	266.8	192.1
K / EC	0.05	0.28	0.30	0.04	0.10	0.20
Fe / EC	0.03	0.16	0.05	0.07	0.03	0.00
Levoglucosan / K	n/a	10.9	26.4	34.5	20.6	52.3
Levoglucosan / EC	n/a	3.03	8.01	1.29	2.00	10.3
Dehydroabietic acid / Levoglucosan	n/a	0.006	0.005	0.027	0.034	0.032
7-oxodehydroabietic acid / Levoglucosan	n/a	0.006	0.003	0.005	0.015	0.002
Abietic Acid / Levoglucosan	n/a	0	0	0	0	0.136

Note: [a] IMPROVE data, and XRF values come from averages of smoke days; [b] STN data, and organic compounds are measured by GC/MS; [c] ASACA data, and organic compounds are measured by GC/MS; [d] Lee et al. (2008) and Yan et al. (2008); [e] Schauer et al. (2001); [f] n/a data is not available; [g] partial filters are selected for averaging.

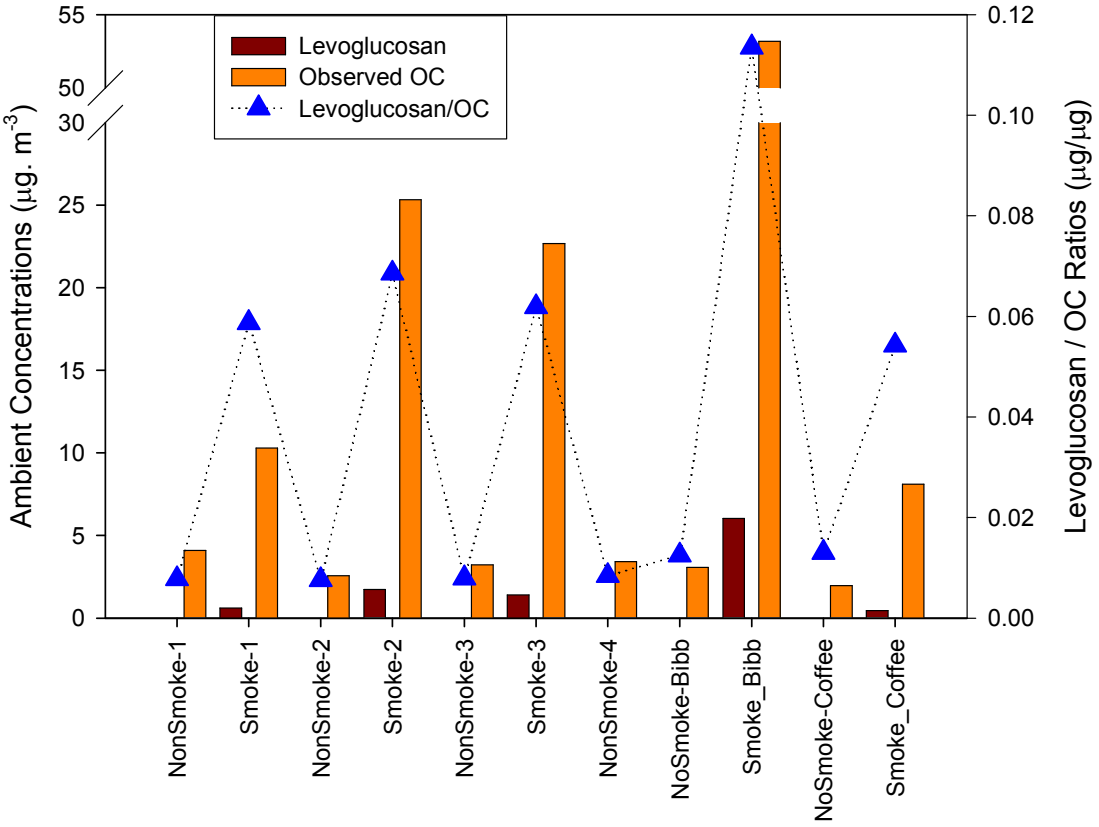

Figure 6.4. 24-hr average ambient concentrations of OC and levoglucosan observed at the metropolitan Atlanta, Bibb, and Coffee sites during the wildfire episodes.

6.3.2 Organic and Inorganic Tracers of Biomass Burning

Results indicate that the major component of $PM_{2.5}$ from wildfire is OC, accounting for 40-55% of the $PM_{2.5}$ mass or 60-85% when converted to organic matter (OM) (using a factor of 1.5 [*Lee et al.*, 2008]) (Table 6.1). On the smoke days, large increases in biomass burning tracers (levoglucosan, resin acids, retene, etc.) were observed. Levoglucosan concentrations increased from 26.4, 41.1 and 21.9 ng m^{-3} to 1248, 6664 and 309 ng m^{-3} at the Atlanta, Bibb, and Coffee sites, respectively, contributing 6%, 11%, and 5% of the total OC (Figure 6.4). Resin acids also increased significantly at the Atlanta and Bibb sites (Figure 6.5). Dehydroabietic acid and 7-oxodehydroabietic acid, two major resin acids in aged wildfire plumes, increased by about 80 and 15 times at the Atlanta sites on the smoke days, respectively, and by 15 and 8 times at the Bibb site. However, no significant increase was found at the Coffee site, implying that the composite smoke sample might be an ambiguous mixture of both fresh and aged plumes.

To elucidate processes occurring during transport, ratios of major resin acids to levoglucosan were calculated and compared (Table 6.2). Abietic acid, the most abundant resin acid in softwood source emissions, was found in very small ratios to levoglucosan, whereas 7-oxodehydroabietic acid, a relatively minor component in source emissions, was several times higher. The ratios of dehydroabietic acid to levoglucosan varied in the ambient samples. This suggests that resin acids, unlike levoglucosan, are subject to alteration in the atmosphere, leading to their ratios to levoglucosan being variable over time during transport. Previous studies have also proposed that dehydroabietic acid and 7-oxodehydroabietic acid can be formed by oxidation processes of other resin acids (e.g.,

abietic acids) [*Oros and Simoneit*, 2001; *Rogge et al.*, 1993e]. In addition, PAHs increased on the smoke days from 0.42, 0.47, and 0.13 ng m^{-3} to 2.2, 2.1, and 0.28 ng m^{-3} at the Atlanta, Bibb and Coffee sites, respectively, and retene increased by 21, 5.8 and 1.8 times (Figure 6.5).

The wildfire emissions also caused large increases in concentrations of *n*-alkanes and *n*-alkanoic acids (Figure 6.6). Ambient *n*-alkanes increased from 4.2, 4.5, and 1.9 ng m^{-3} to 154, 369, and 46 ng m^{-3} at the Atlanta, Bibb and Coffee site, respectively, and *n*-alkanoic acids increased from 19, 4.4, and 5.5 ng m^{-3} to 408, 1007, and 62 ng m^{-3}. Generally, *n*-alkanes are associated with plant wax and fossil fuel contributions, and biomass emission is characterized by odd carbon number predominance [*Mazurek and Simoneit*, 1984; *Oros et al.*, 2006]. In the non-smoke samples, *n*-alkanes only show a slight odd carbon number predominance with carbon number maximum (C_{max}) of 23, 25, and 25 at the Atlanta, Bibb and Coffee sites, respectively. However, *n*-alkanes exhibited distinctly strong odd carbon number predominance (C_{max}=29) on the smoke days. Likewise, *n*-alkanoic acids had a strong even-to-odd carbon number predominance on the smoke days (C_{max}=24). Therefore, a dominant contribution from plant waxes is suggested. These compounds are natural products of epicuticular waxes and internal lipid substances on leaf surfaces and emitted as vegetative detritus (via leaf surface abrasion) or through direct thermal volatilization [*Rogge et al.*, 1993a; *Simoneit*, 2002]. Higher leaf temperatures presumably lead to volatilization of these high-molecular weight organic compounds, which can then condense into the particle phase in the atmosphere. This result indicates that such waxes are not unique tracers for vegetative detritus when wildland fires also significantly impact air quality [*Yan et al.*, 2008a].

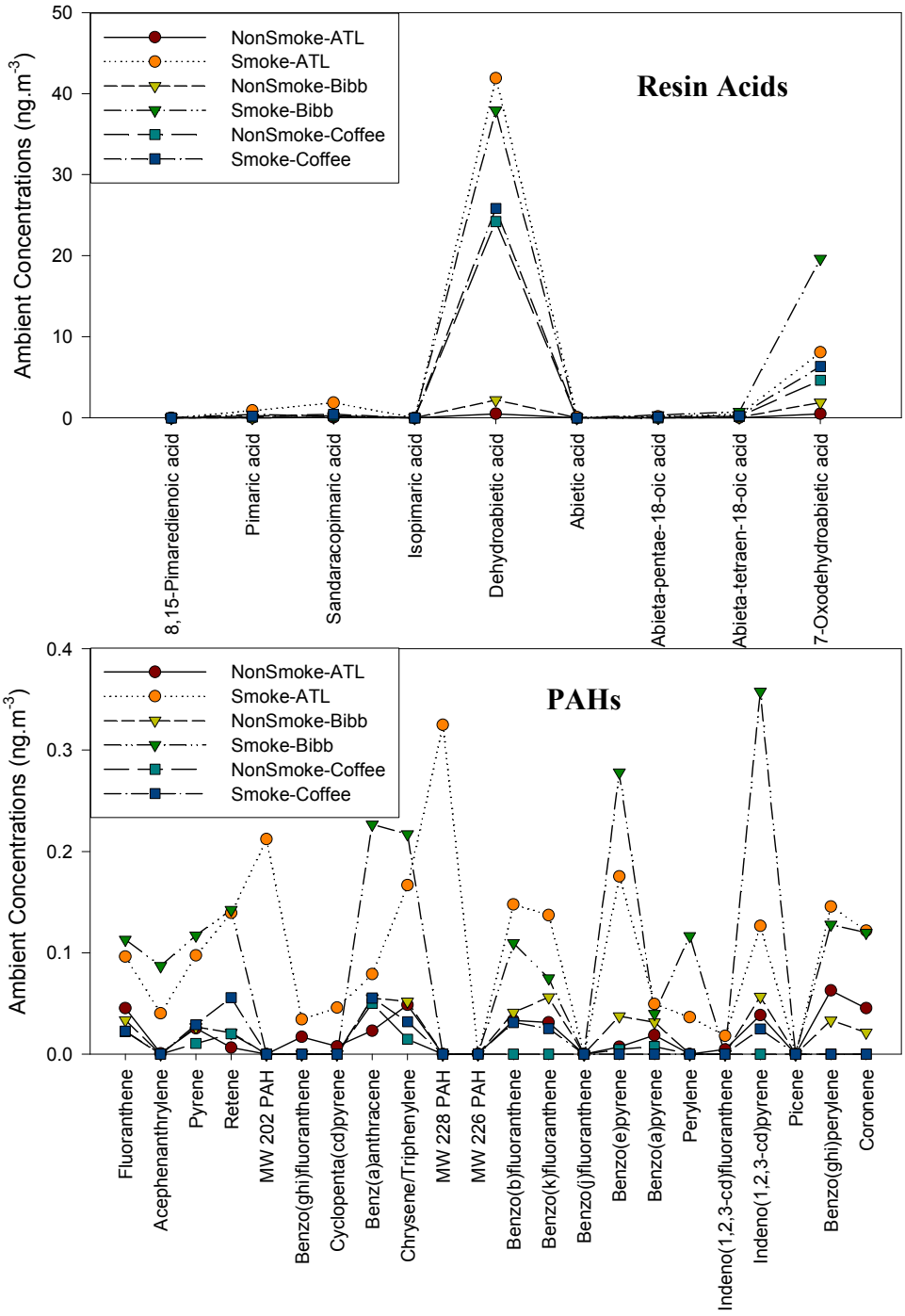

Figure 6.5. 24-hr average concentrations of resin acids and PAHs observed at the metropolitan Atlanta, Bibb, and Coffee sites during the wildfire episodes.

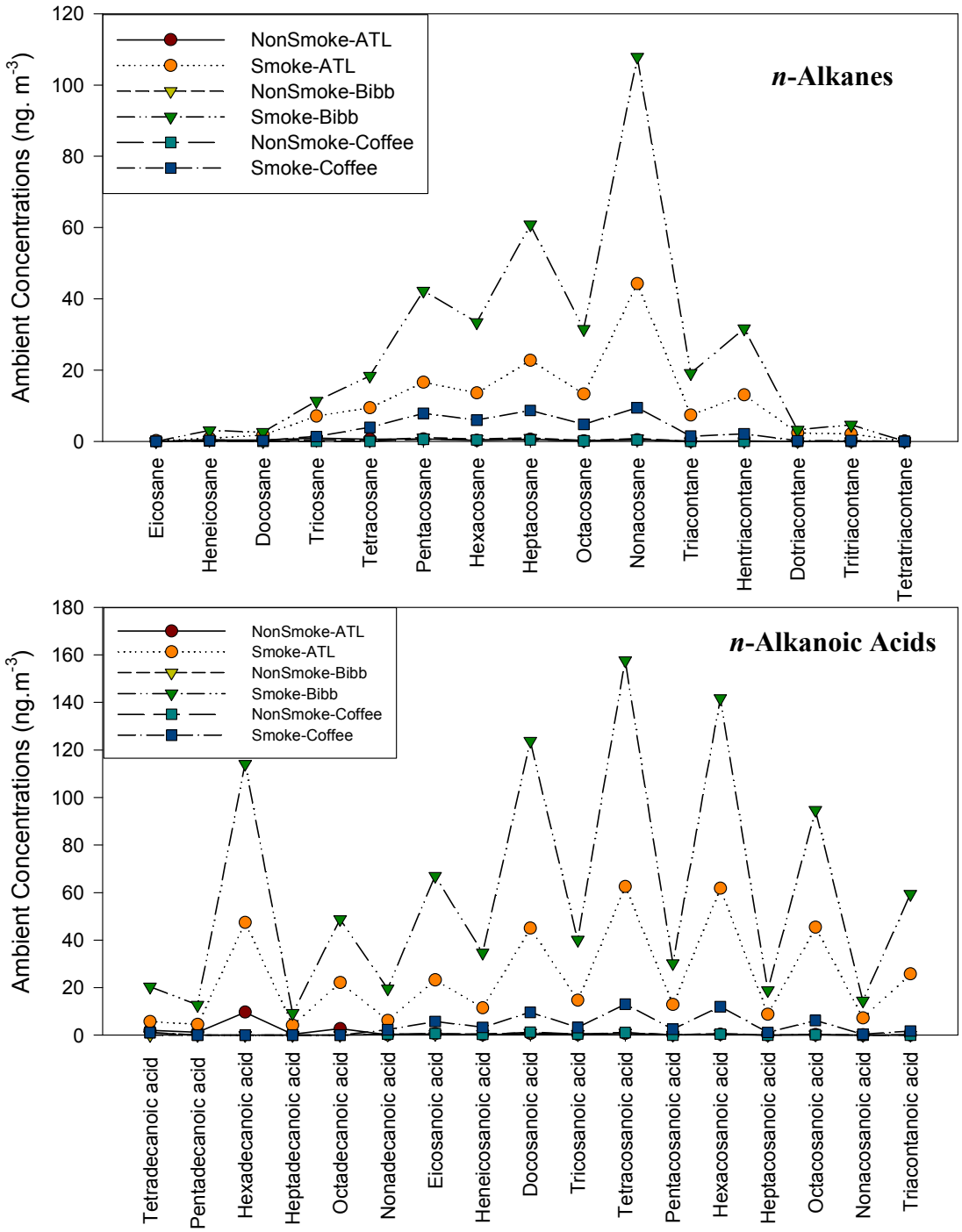

Figure 6.6. 24-hr average concentrations of *n*-alkanes and *n*-alkanoic acids observed at the metropolitan Atlanta, Bibb, and Coffee sites during the wildfire episodes.

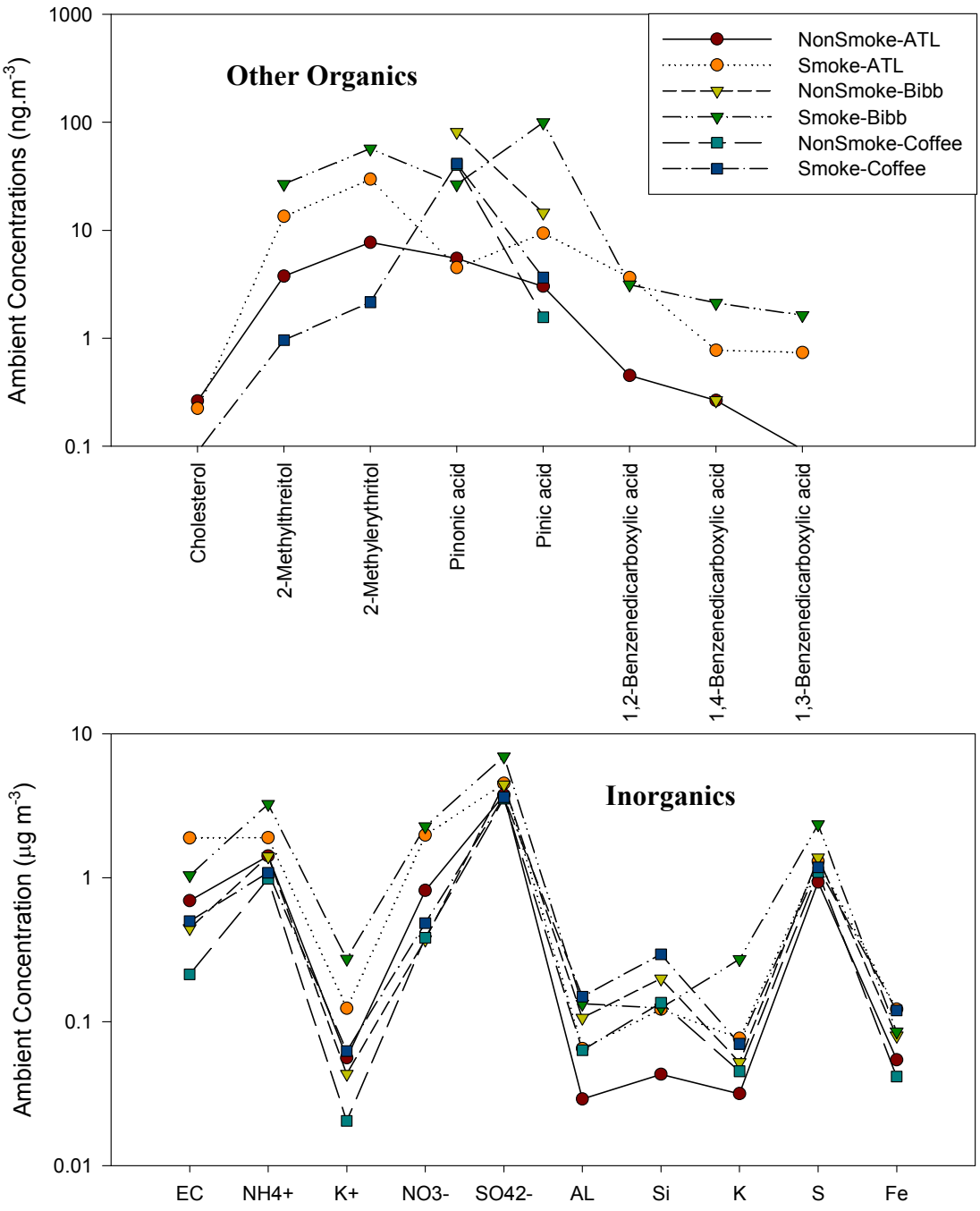

Figure 6.7. 24-hr average concentrations of other organic compounds (cholesterol, 2-methyltetrols, *cis*-pinonic acid, pinic acid, and aromatic acids) and some inorganic components (EC, ions and trace metals) observed at the metropolitan Atlanta, Bibb, and Coffee sites during the wildfire episodes. Log scale is applied for Y axis.

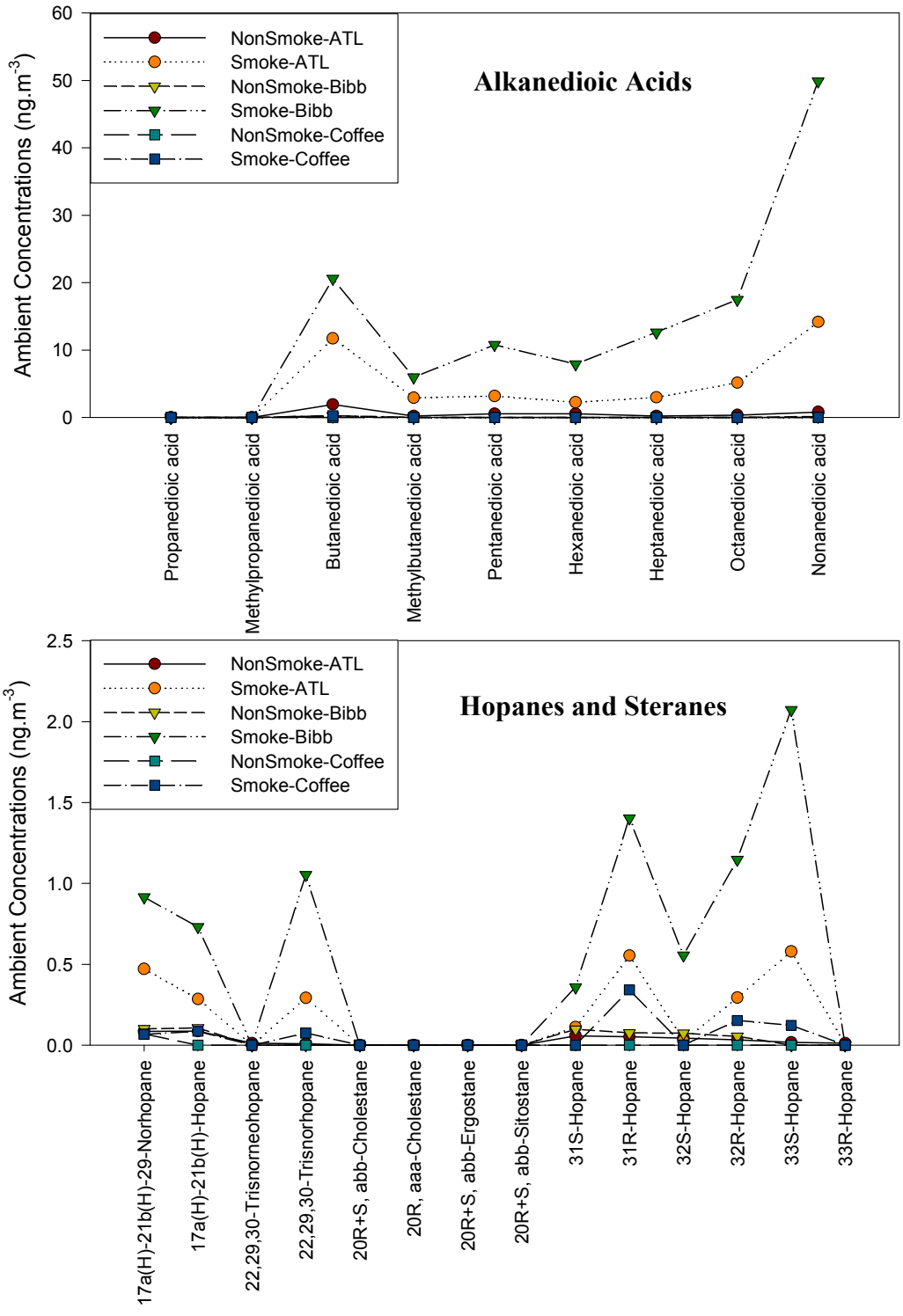

Figure 6.8. 24-hr average concentrations of alkanedioic acids, hopanes and steranes observed at the metropolitan Atlanta, Bibb, and Coffee sites during the wildfire episodes.

The wildfire emissions also led to significant increases in ambient concentrations of some inorganic species such as potassium (K), ammonium (NH_4^+), nitrate (NO_3^-), sulfate (SO_4^{2-}) and EC (Figure 6.7). During the smoke events, potassium, an inorganic tracer of biomass burning, increased from 0.03, 0.05, and 0.05 μg m^{-3} to 0.08, 0.27 and 0.07 μg m^{-3} at the Atlanta, Bibb and Coffee sites, respectively, and EC increased from 0.69, 0.45, and 0.21 μg m^{-3} to 1.9, 1.0 and 0.50 μg m^{-3} at the same time.

6.3.3 Other Primary Organic Tracers

Non-biomass organic molecular markers were also analyzed as indicators of other major primary sources. Meat cooking and vehicular engine exhaust are the two other major sources of primary organic carbon in urban areas [*Lee et al.*, 2007; *Liu et al.*, 2005; *Marmur et al.*, 2005; *Zheng et al.*, 2007]. Cholesterol, an organic tracer of meat cooking, did not exhibit significant variation at the Atlanta sites, and was near or below detection limits at the Bibb and Coffee sites on the event days (Figure 6.7). Steranes, organic markers for mobile emissions, were not detected in filters from any monitor, whereas hopanes, also molecular markers of vehicle emissions, were measured to be significantly higher on the event days, increasing from 0.40, 0.51, and 0.07 ng m^{-3} to 2.6, 8.2, and 0.84 ng m^{-3} at the Atlanta, Bibb, and Coffee sites, respectively (Figure 6.8). There is not any evidence either that contributions of mobile emissions varied significantly over the smoke affected area during the event days or that coal combustion emissions in this region could lead to significantly high levels in ambient hopanes [*Oros and Simoneit*, 2000]. Wildfire emissions are the most likely sources of the elevated hopanes, which are about 10 times higher than the levels on the non-smoke events. Similarly, hopanes were also found to significantly increase on the prescribed burning smoke event that occurred

on February 28, 2007 [*Yan et al.*, 2008a]. These interesting observations are further supported by previous studies. They proposed that 17β(H),21β(H)-hopanes or other biogenic hopanoid precursors produced by microbiota and some higher plants can thermally alter or mature under high temperatures to 17α(H),21β(H)-hopanes, organic tracers of vehicular emissions as well as the compounds measured in this research [*Standley and Simoneit*, 1987]. On the other hand, 17α(H),21β(H)-hopanes have not ever been reported to be detected in previous emission tests of residential and commercial wood combustion [*Fine et al.*, 2002; 2004a; *Rogge et al.*, 1998; *Schauer et al.*, 2001], implying that these combustion processes cannot result in such thermal alteration of 17β(H),21β(H)-hopanes with biological nature in origin. Therefore, our results indicate that such hopanes likely are not unique organic tracers for mobile sources when emission impacts of wildland fires are significant. Impacts of elevated hopanes should be considered for wildland fire smoke events; otherwise contributions of mobile sources, especially gasoline vehicle exhausts, would be overestimated at that time by receptor models (Table D.2).

Very large increases in continuous $PM_{2.5}$ and OC measurements were also observed when the wildfire plumes hit the urban monitors at the Atlanta, Bibb and Coffee sites. These increases are consistent with those increases measured on the PCM filters, and overwhelmed typical levels, especially at the Atlanta and Bibb sites. On the smoke events, $PM_{2.5}$ increased by 37, 100 and 9.1 μg m^{-3} (or by 300%, over 600% and 80%) at the Atlanta, Bibb and Coffee sites, respectively, and OC increased by 21, 58 and 4.5 μg m^{-3} (or by over 600%, 1100% and 130%). Biomass burning-related organic tracers (levoglucosan, resin acids and retene) increased by up to 80, 160 and 13 times at the

Atlanta, Bibb and Coffee sites, respectively. Thus, vehicular sources and meat cooking emissions are likely not responsible for the large increase in $PM_{2.5}$ and OC on the event days, and that the greatly increased concentrations are from the wildfire. Source apportionment results calculated using the molecular marker-based chemical mass balance (CMB-MM) model also indicate significant increases in wildfire emissions on the smoke days, but not for other major primary sources (i.e. meat cooking) (Table D.2).

6.3.4 Secondary Organic Tracers

Wildfire emissions can enhance formation of biogenic SOA in the atmosphere [*Hu et al.*, 2008; *Yan et al.*, 2008a]. Here, 2-methyltetrols, secondary organic products of isoprene, on the non-smoke days were detected only at Atlanta (11 ng m-3) (Figure 6.7). However, 2-methyltetrols were detected at all monitors on the event days (43, 84, and 3.1 ng m^{-3} at the Atlanta, Bibb and Coffee sites, respectively). Pinic acid, a photo-oxidation product of monoterpenes, increased from 3.0, 14 and 1.6 ng m^{-3} to 9.4, 99 and 3.6 ng m^{-3} at the Atlanta, Bibb and Coffee sites, respectively, on the event days (Figure 6.7). However, *cis*-pinonic acid, another photo-oxidation product of monoterpenes, did not show significant increases, probably implying different mechanisms of atmospheric formation and fate for pinic acid and *cis*-pinonic acid in aged wildfire plumes. Elevated aromatic and aliphatic diacids were observed at all sites on the event days, providing supportive evidence of increased SOA formation in the atmosphere [*Yan et al.*, 2008a]. Dicarboxylic acids increased from 4.6 and 0.4 ng m^{-3} to 42 and 125 ng m^{-3} on the event days at the Atlanta and Bibb sites, respectively, though less increase was detected at the Coffee site. This suggests that they are not only secondarily created from anthropogenic emissions but also enhanced by wildfire-derived biogenic emissions in the atmosphere.

Table 6.3. Source Composition Profiles Approximated from The Wildfire Plumes and from The Previous Prescribed Burning Emissions (ng/µg $PM_{2.5}$)

Compound	Wildfire Aged Plume [a] (Fraction [f] ± std [g])			Wildfire PPM_{fc} [b] (Fraction [f] ± std [g])			Pre-burning Aged Plume [c]	Pre-burning PPM_{fc} [d]	Lee et al. [e]
	Atlanta	Bibb	Coffee	Atlanta	Bibb	Coffee			
***n*-alkanes**									
Tetracosane	0.2370 ± 0.0859	0.1800 ± 0.0445	0.4275 ± 0.1570	0.2928 ± 0.1062	0.3442 ± 0.0851	0.6758 ± 0.2482	0.0375 ± 0.0208	0.0508 ± 0.0284	0.0836 ± 0.0528
Pentacosane	0.4273 ± 0.1344	0.4097 ± 0.1022	0.7926 ± 0.2986	0.5280 ± 0.1661	0.7832 ± 0.1954	1.2530 ± 0.4720	0.0706 ± 0.0294	0.0956 ± 0.0404	0.1506 ± 0.0954
Hexacosane	0.3553 ± 0.1050	0.3262 ± 0.0810	0.6093 ± 0.2286	0.4390 ± 0.1298	0.6236 ± 0.1548	0.9632 ± 0.3614	0.0225 ± 0.0159	0.0305 ± 0.0217	0.1374 ± 0.0913
Heptacosane	0.5934 ± 0.2217	0.5957 ± 0.1477	0.9086 ± 0.3384	0.7332 ± 0.2740	1.1387 ± 0.2823	1.4363 ± 0.5349	0.1728 ± 0.0497	0.2339 ± 0.0693	0.1505 ± 0.1137
Octacosane	0.3519 ± 0.1156	0.3111 ± 0.0766	0.5074 ± 0.1877	0.4348 ± 0.1429	0.5948 ± 0.1464	0.8022 ± 0.2967	0.0470 ± 0.0171	0.0637 ± 0.0236	0.0695 ± 0.0416
Nonacosane	1.1737 ± 0.4038	1.0654 ± 0.2626	0.9891 ± 0.3683	1.4503 ± 0.4990	2.0365 ± 0.5020	1.5635 ± 0.5822	0.3115 ± 0.0881	0.4217 ± 0.1231	0.4860 ± 0.2950
Triacontane	0.1956 ± 0.0610	0.1902 ± 0.0466	0.1541 ± 0.0566	0.2417 ± 0.0754	0.3636 ± 0.0892	0.2437 ± 0.0895	0.0451 ± 0.0116	0.0610 ± 0.0164	0.1168 ± 0.0715
Hentriacontane	0.3435 ± 0.0951	0.3147 ± 0.0772	0.2266 ± 0.0832	0.4245 ± 0.1175	0.6016 ± 0.1476	0.3582 ± 0.1316	0.2561 ± 0.0731	0.3467 ± 0.1020	0.1737 ± 0.1054
Dotriacontane	0.0631 ± 0.0170	0.0318 ± 0.0078	0.0139 ± 0.0051	0.0779 ± 0.0210	0.0607 ± 0.0149	0.0219 ± 0.0080	0.0292 ± 0.0075	0.0395 ± 0.0106	0.0000 ± 0.0001
Tritriacontane	0.0552 ± 0.0202	0.0460 ± 0.0113	0.0213 ± 0.0078	0.0683 ± 0.0249	0.0880 ± 0.0215	0.0336 ± 0.0123	0.0527 ± 0.0156	0.0713 ± 0.0217	0.0542 ± 0.0480
Tetratriacontane	0.0000 ± 0.0001	0.0000 ± 0.0001	0.0000 ± 0.0001	0.0000 ± 0.0001	0.0000 ± 0.0001	0.0000 ± 0.0001	0.0000 ± 0.0001	0.0000 ± 0.0001	0.0000 ± 0.0001
Branch-alkanes									
iso-Nonacosane	0.0000 ± 0.0001	0.0000 ± 0.0001	0.0000 ± 0.0001	0.0000 ± 0.0001	0.0000 ± 0.0001	0.0000 ± 0.0001	0.0000 ± 0.0001	0.0000 ± 0.0001	0.0000 ± 0.0001
anteiso-Triacontane	0.0000 ± 0.0001	0.0000 ± 0.0001	0.0000 ± 0.0001	0.0000 ± 0.0001	0.0000 ± 0.0001	0.0000 ± 0.0001	0.0000 ± 0.0001	0.0000 ± 0.0001	0.0000 ± 0.0001
iso-Hentriacontane	0.0000 ± 0.0001	0.0000 ± 0.0001	0.0000 ± 0.0001	0.0000 ± 0.0001	0.0000 ± 0.0001	0.0000 ± 0.0001	0.0000 ± 0.0001	0.0000 ± 0.0001	0.0000 ± 0.0001
Hopanes									
17α(H)-21β(H)-29-Norhopane	0.0103 ± 0.0033	0.0080 ± 0.0021	0.0000 ± 0.0001	0.0127 ± 0.0041	0.0154 ± 0.0041	0.0000 ± 0.0001	0.0022 ± 0.0051	0.0029 ± 0.0069	0.0000 ± 0.0001
17α(H)-21β(H)-Hopane	0.0053 ± 0.0042	0.0062 ± 0.0017	0.0093 ± 0.0034	0.0065 ± 0.0052	0.0118 ± 0.0032	0.0147 ± 0.0054	0.0016 ± 0.0047	0.0021 ± 0.0064	0.0000 ± 0.0001
22,29,30-Trisnorneohopane	0.0000 ± 0.0001	0.0000 ± 0.0001	0.0000 ± 0.0001	0.0000 ± 0.0001	0.0000 ± 0.0001	0.0000 ± 0.0001	0.0022 ± 0.0020	0.0029 ± 0.0028	0.0000 ± 0.0001
22,29,30-Trisnorhopane	0.0075 ± 0.0049	0.0104 ± 0.0025	0.0081 ± 0.0030	0.0093 ± 0.0060	0.0200 ± 0.0049	0.0129 ± 0.0047	0.0000 ± 0.0001	0.0000 ± 0.0001	0.0000 ± 0.0001
22S,17α(H),21β(H)-Homohopane	0.0014 ± 0.0012	0.0025 ± 0.0008	0.0000 ± 0.0001	0.0018 ± 0.0015	0.0049 ± 0.0015	0.0000 ± 0.0001	0.0028 ± 0.0028	0.0038 ± 0.0038	0.0000 ± 0.0001
22R,17α(H),21β(H)-Homohopane	0.0134 ± 0.0098	0.0132 ± 0.0033	0.0375 ± 0.0137	0.0166 ± 0.0121	0.0252 ± 0.0064	0.0592 ± 0.0217	0.0018 ± 0.0021	0.0025 ± 0.0029	0.0000 ± 0.0001
22S,17α(H),21β(H)-Bishomohopane	0.0000 ± 0.0001	0.0048 ± 0.0013	0.0000 ± 0.0001	0.0000 ± 0.0001	0.0091 ± 0.0024	0.0000 ± 0.0001	0.0009 ± 0.0013	0.0012 ± 0.0017	0.0000 ± 0.0001
22R,17α(H),21β(H)-Bishomohopane	0.0069 ± 0.0022	0.0108 ± 0.0027	0.0166 ± 0.0061	0.0086 ± 0.0027	0.0207 ± 0.0052	0.0263 ± 0.0096	0.0000 ± 0.0001	0.0000 ± 0.0001	0.0000 ± 0.0001
22S,17α(H),21β(H)-Trishomohopane	0.0150 ± 0.0054	0.0206 ± 0.0050	0.0133 ± 0.0049	0.0186 ± 0.0067	0.0394 ± 0.0096	0.0211 ± 0.0077	0.0000 ± 0.0001	0.0000 ± 0.0001	0.0000 ± 0.0001
22R,17α(H),21β(H)-Trishomohopane	0.0000 ± 0.0001	0.0000 ± 0.0001	0.0000 ± 0.0001	0.0000 ± 0.0001	0.0000 ± 0.0001	0.0000 ± 0.0001	0.0000 ± 0.0001	0.0000 ± 0.0001	0.0000 ± 0.0001
Steranes									
20S,R-5α(H),14β(H),17β(H)-Cholestanes	0.0000 ± 0.0001	0.0000 ± 0.0001	0.0000 ± 0.0001	0.0000 ± 0.0001	0.0000 ± 0.0001	0.0000 ± 0.0001	0.0000 ± 0.0001	0.0000 ± 0.0001	0.0000 ± 0.0001

20R-5α(H),14α(H),17α(H)-Cholestane	0.0000 ± 0.0001	0.0000 ± 0.0001	0.0000 ± 0.0001	0.0000 ± 0.0001	0.0000 ± 0.0001	0.0000 ± 0.0001	0.0000 ± 0.0001	0.0000 ± 0.0001	0.0000 ± 0.0001
20S,R-5α(H),14β(H),17β(H)-Ergostanes	0.0000 ± 0.0001	0.0000 ± 0.0001	0.0000 ± 0.0001	0.0000 ± 0.0001	0.0000 ± 0.0001	0.0000 ± 0.0001	0.0000 ± 0.0001	0.0000 ± 0.0001	0.0000 ± 0.0001
20S,R-5α(H),14β(H),17β(H)-Sitostanes	0.0000 ± 0.0001	0.0000 ± 0.0001	0.0000 ± 0.0001	0.0000 ± 0.0001	0.0000 ± 0.0001	0.0000 ± 0.0001	0.0000 ± 0.0001	0.0000 ± 0.0001	0.0000 ± 0.0001
PAHs									
Fluoranthene	0.0013 ± 0.0015	0.0007 ± 0.0002	4.6574 ± 0.0006	0.0016 ± 0.0019	0.0015 ± 0.0004	7.3620 ± 0.0011	0.0000 ± 0.0001	0.0000 ± 0.0001	0.0539 ± 0.0310
Acephenanthrylene	0.0010 ± 0.0002	0.0008 ± 0.0002	0.0000 ± 0.0001	0.0013 ± 0.0003	0.0016 ± 0.0004	0.0000 ± 0.0001	0.0009 ± 0.0004	0.0012 ± 0.0005	0.0168 ± 0.0105
Pyrene	0.0019 ± 0.0007	0.0008 ± 0.0002	0.0020 ± 0.0009	0.0023 ± 0.0009	0.0017 ± 0.0005	0.0032 ± 0.0014	0.0000 ± 0.0001	0.0000 ± 0.0001	0.0643 ± 0.0363
Retene	0.0035 ± 0.0023	0.0012 ± 0.0003	0.0039 ± 0.0017	0.0043 ± 0.0028	0.0023 ± 0.0006	0.0062 ± 0.0028	0.0284 ± 0.0077	0.0385 ± 0.0108	0.2102 ± 0.1267
Benzo(ghi)fluoranthene	0.0004 ± 0.0010	0.0000 ± 0.0001	0.0000 ± 0.0001	0.0005 ± 0.0012	0.0000 ± 0.0001	0.0000 ± 0.0001	0.0018 ± 0.0018	0.0025 ± 0.0025	0.0585 ± 0.0517
Cyclopenta(cd)pyrene	0.0010 ± 0.0009	0.0000 ± 0.0001	0.0000 ± 0.0001	0.0012 ± 0.0012	0.0000 ± 0.0001	0.0000 ± 0.0001	0.0000 ± 0.0001	0.0000 ± 0.0001	0.1740 ± 0.1058
Benz(a)anthracene	0.0014 ± 0.0006	0.0017 ± 0.0005	0.0005 ± 0.0016	0.0018 ± 0.0007	0.0032 ± 0.0010	0.0009 ± 0.0026	0.0006 ± 0.0017	0.0008 ± 0.0023	0.0482 ± 0.0268
Chrysene/Triphenylene	0.0031 ± 0.0020	0.0016 ± 0.0005	0.0018 ± 0.0009	0.0039 ± 0.0025	0.0031 ± 0.0009	0.0029 ± 0.0015	0.0071 ± 0.0041	0.0097 ± 0.0056	0.0589 ± 0.0332
Benzo(j)fluoranthene	0.0030 ± 0.0012	0.0006 ± 0.0002	0.0034 ± 0.0012	0.0037 ± 0.0015	0.0013 ± 0.0004	0.0053 ± 0.0019	0.0004 ± 0.0002	0.0006 ± 0.0003	0.0077 ± 0.0049
Benzo(e)pyrene	0.0028 ± 0.0011	0.0001 ± 0.0001	0.0027 ± 0.0010	0.0035 ± 0.0014	0.0003 ± 0.0003	0.0043 ± 0.0015	0.0039 ± 0.0024	0.0053 ± 0.0033	0.0300 ± 0.0168
Benzo(a)pyrene	0.0000 ± 0.0001	0.0000 ± 0.0001	0.0000 ± 0.0001	0.0000 ± 0.0001	0.0000 ± 0.0001	0.0000 ± 0.0001	0.0006 ± 0.0016	0.0008 ± 0.0022	0.0179 ± 0.0100
Perylene	0.0045 ± 0.0014	0.0023 ± 0.0006	0.0000 ± 0.0001	0.0055 ± 0.0017	0.0045 ± 0.0012	0.0000 ± 0.0001	0.0000 ± 0.0001	0.0000 ± 0.0001	0.0023 ± 0.0015
Indeno(1,2,3-cd)fluoranthene	0.0008 ± 0.0008	0.0000 ± 0.0001	0.0000 ± 0.0001	0.0010 ± 0.0010	0.0001 ± 0.0001	0.0000 ± 0.0001	0.0024 ± 0.0011	0.0033 ± 0.0015	0.0000 ± 0.0001
Indeno(1,2,3-cd)pyrene	0.0009 ± 0.0003	0.0011 ± 0.0002	0.0000 ± 0.0001	0.0012 ± 0.0004	0.0022 ± 0.0005	0.0000 ± 0.0001	0.0028 ± 0.0025	0.0038 ± 0.0034	0.0444 ± 0.0265
Picene	0.0003 ± 0.0003	0.0000 ± 0.0001	0.0000 ± 0.0001	0.0004 ± 0.0004	0.0000 ± 0.0001	0.0000 ± 0.0001	0.0000 ± 0.0001	0.0000 ± 0.0001	0.0000 ± 0.0001
Benzo(ghi)perylene	0.0023 ± 0.0007	0.0029 ± 0.0008	0.0027 ± 0.0009	0.0029 ± 0.0009	0.0057 ± 0.0015	0.0042 ± 0.0015	0.0026 ± 0.0041	0.0036 ± 0.0056	0.0215 ± 0.0120
Benzo(b)fluoranthene	0.0000 ± 0.0001	0.0000 ± 0.0001	0.0000 ± 0.0001	0.0000 ± 0.0001	0.0000 ± 0.0001	0.0000 ± 0.0001	0.0043 ± 0.0028	0.0059 ± 0.0039	0.0304 ± 0.0170
Benzo(k)fluoranthene	0.0022 ± 0.0019	0.0009 ± 0.0002	0.0000 ± 0.0001	0.0027 ± 0.0024	0.0017 ± 0.0005	0.0000 ± 0.0001	0.0028 ± 0.0019	0.0038 ± 0.0026	0.0245 ± 0.0136
Coronene	0.0020 ± 0.0013	0.0009 ± 0.0002	0.0000 ± 0.0001	0.0025 ± 0.0017	0.0018 ± 0.0005	0.0000 ± 0.0001	0.0039 ± 0.0037	0.0053 ± 0.0051	0.0044 ± 0.0031
Resin Acids									
8,15-Pimaredienoic acid	0.0000 ± 0.0001	0.0000 ± 0.0001	0.0000 ± 0.0001	0.0000 ± 0.0001	0.0000 ± 0.0001	0.0000 ± 0.0001	0.0000 ± 0.0001	0.0000 ± 0.0001	0.0000 ± 0.0001
Pimaric acid	0.0236 ± 0.0071	0.0040 ± 0.0010	0.0140 ± 0.0067	0.0292 ± 0.0087	0.0077 ± 0.0019	0.0221 ± 0.0106	0.0185 ± 0.0055	0.0251 ± 0.0077	1.4856 ± 0.8256
Sandaracopimaric acid	0.0487 ± 0.0183	0.0014 ± 0.0004	0.0214 ± 0.0130	0.0602 ± 0.0226	0.0026 ± 0.0009	0.0338 ± 0.0205	0.0558 ± 0.0169	0.0756 ± 0.0235	0.0000 ± 0.0001
Isopimaric acid	0.0000 ± 0.0001	0.0000 ± 0.0001	0.0000 ± 0.0001	0.0000 ± 0.0001	0.0000 ± 0.0001	0.0000 ± 0.0001	0.0000 ± 0.0001	0.0000 ± 0.0001	1.7830 ± 0.9994
Dehydroabietic acid	1.1087 ± 0.6578	0.3553 ± 0.0908	0.1791 ± 0.7790	1.3701 ± 0.8129	0.6791 ± 0.1737	0.2832 ± 1.2314	1.5456 ± 0.4331	2.0923 ± 0.6051	20.073 ± 11.450
Abietic acid	0.0026 ± 0.0009	0.0000 ± 0.0001	0.0000 ± 0.0001	0.0032 ± 0.0012	0.0000 ± 0.0001	0.0000 ± 0.0001	0.0112 ± 0.0043	0.0152 ± 0.0059	0.0000 ± 0.0001
Abieta-6,8,11,13,15-pentae-18-oic acid	0.0046 ± 0.0019	0.0034 ± 0.0008	0.0111 ± 0.0041	0.0057 ± 0.0024	0.0065 ± 0.0016	0.0177 ± 0.0065	0.0088 ± 0.0025	0.0120 ± 0.0036	0.0000 ± 0.0001
Abieta-8,11,13,15-tetraen-18-oic acid	0.0115 ± 0.0064	0.0068 ± 0.0017	0.0098 ± 0.0073	0.0142 ± 0.0079	0.0130 ± 0.0033	0.0156 ± 0.0116	0.0263 ± 0.0072	0.0356 ± 0.0101	0.0000 ± 0.0001
7-Oxodehydroabietic acid	0.2031 ± 0.1149	0.1766 ± 0.0466	0.1855 ± 0.1811	0.2510 ± 0.1420	0.3375 ± 0.0891	0.2933 ± 0.2863	0.7430 ± 0.1978	1.0058 ± 0.2773	0.0000 ± 0.0001

Aromatic Acids									
1,2-Benzenedicarboxylic acid	0.0854 ± 0.0320	0.0310 ± 0.0076	0.0000 ± 0.0001	0.1056 ± 0.0396	0.0594 ± 0.0145	0.0000 ± 0.0001	0.1185 ± 0.0359	0.1604 ± 0.0499	0.0088 ± 0.0062
1,4-Benzenedicarboxylic acid	0.0136 ± 0.0047	0.0183 ± 0.0049	0.0022 ± 0.0009	0.0168 ± 0.0058	0.0351 ± 0.0095	0.0035 ± 0.0015	0.0436 ± 0.0207	0.0591 ± 0.0284	0.0054 ± 0.0047
1,3-Benzenedicarboxylic acid	0.0171 ± 0.0058	0.0162 ± 0.0039	0.0000 ± 0.0001	0.0212 ± 0.0071	0.0310 ± 0.0076	0.0000 ± 0.0001	0.0286 ± 0.0112	0.0387 ± 0.0154	0.0000 ± 0.0001
Alkanoic Acids									
Tetradecanoic acid	0.0991 ± 0.0646	0.2020 ± 0.0495	0.0057 ± 0.0309	0.1224 ± 0.0799	0.3861 ± 0.0947	0.0090 ± 0.0489	0.0741 ± 0.0248	0.1004 ± 0.0343	1.2089 ± 0.7432
Pentadecanoic acid	0.0868 ± 0.0439	0.1262 ± 0.0309	0.0000 ± 0.0001	0.1073 ± 0.0543	0.2412 ± 0.0591	0.0000 ± 0.0001	0.0359 ± 0.0135	0.0486 ± 0.0187	0.3838 ± 0.2446
Hexadecanoic acid	1.0115 ± 0.3344	1.1357 ± 0.2786	0.0000 ± 0.0001	1.2499 ± 0.4133	2.1708 ± 0.5326	0.0000 ± 0.0001	0.2784 ± 0.1320	0.3769 ± 0.1808	4.0548 ± 2.3375
Heptadecanoic acid	0.0987 ± 0.0371	0.0915 ± 0.0224	0.0000 ± 0.0001	0.1220 ± 0.0458	0.1750 ± 0.0429	0.0000 ± 0.0001	0.0207 ± 0.0077	0.0280 ± 0.0106	0.1494 ± 0.0907
Octadecanoic acid	0.5218 ± 0.2002	0.4848 ± 0.1189	0.0000 ± 0.0001	0.6448 ± 0.2474	0.9268 ± 0.2274	0.0000 ± 0.0001	0.1343 ± 0.0642	0.1818 ± 0.0879	1.3508 ± 0.8111
Nonadecanoic acid	0.1616 ± 0.0573	0.1921 ± 0.0475	0.2011 ± 0.0799	0.1997 ± 0.0709	0.3672 ± 0.0909	0.3179 ± 0.1263	0.0262 ± 0.0075	0.0355 ± 0.0105	0.2941 ± 0.1870
Eicosanoic acid	0.6087 ± 0.2042	0.6622 ± 0.1631	0.5565 ± 0.2127	0.7521 ± 0.2524	1.2657 ± 0.3119	0.8797 ± 0.3363	0.1761 ± 0.0487	0.2383 ± 0.0681	0.7198 ± 0.4371
Heneicosanoic acid	0.3024 ± 0.0922	0.3407 ± 0.0842	0.3277 ± 0.1239	0.3737 ± 0.1139	0.6513 ± 0.1609	0.5180 ± 0.1958	0.0740 ± 0.0202	0.1002 ± 0.0283	0.1739 ± 0.1009
Docosanoic acid	1.1883 ± 0.3530	1.2230 ± 0.3015	0.9106 ± 0.3513	1.4683 ± 0.4362	2.3377 ± 0.5764	1.4395 ± 0.5554	0.3794 ± 0.1031	0.5136 ± 0.1444	1.0757 ± 0.6382
Tricosanoic acid	0.3885 ± 0.1099	0.3956 ± 0.0975	0.3061 ± 0.1177	0.4800 ± 0.1359	0.7561 ± 0.1865	0.4838 ± 0.1861	0.1450 ± 0.0392	0.1963 ± 0.0548	0.3941 ± 0.2273
Tetracosanoic acid	1.6559 ± 0.5810	1.5589 ± 0.3841	1.3102 ± 0.4944	2.0462 ± 0.7179	2.9798 ± 0.7343	2.0710 ± 0.7816	0.5537 ± 0.1509	0.7496 ± 0.2112	2.9835 ± 1.7399
Pentacosanoic acid	0.3398 ± 0.0931	0.2996 ± 0.0737	0.2712 ± 0.0996	0.4199 ± 0.1151	0.5728 ± 0.1409	0.4288 ± 0.1575	0.0488 ± 0.0133	0.0660 ± 0.0186	0.2308 ± 0.1332
Hexacosanoic acid	1.6456 ± 0.5646	1.4040 ± 0.3455	1.2655 ± 0.4698	2.0334 ± 0.6977	2.6836 ± 0.6604	2.0004 ± 0.7427	0.3011 ± 0.0811	0.4077 ± 0.1136	2.2120 ± 1.2819
Heptacosanoic acid	0.2326 ± 0.0674	0.1876 ± 0.0460	0.1187 ± 0.0436	0.2875 ± 0.0833	0.3586 ± 0.0880	0.1877 ± 0.0689	0.0172 ± 0.0046	0.0233 ± 0.0064	0.0850 ± 0.0506
Octacosanoic acid	1.2118 ± 0.4211	0.9404 ± 0.2311	0.6621 ± 0.2448	1.4974 ± 0.5204	1.7974 ± 0.4418	1.0467 ± 0.3870	0.1031 ± 0.0276	0.1395 ± 0.0387	0.5953 ± 0.3501
Nonacosanoic acid	0.1914 ± 0.0519	0.1444 ± 0.0354	0.0352 ± 0.0129	0.2365 ± 0.0642	0.2760 ± 0.0677	0.0557 ± 0.0204	0.0216 ± 0.0056	0.0292 ± 0.0078	0.1014 ± 0.0647
Triacontanoic acid	0.6879 ± 0.1869	0.5897 ± 0.1448	0.1908 ± 0.0700	0.8501 ± 0.2310	1.1272 ± 0.2768	0.3016 ± 0.1108	0.1119 ± 0.0299	0.1516 ± 0.0419	0.4837 ± 0.3137
Alkenoic Acids									
9-Hexadecenoic acid	0.0000 ± 0.0001	0.0000 ± 0.0001	0.0000 ± 0.0001	0.0000 ± 0.0001	0.0000 ± 0.0001	0.0000 ± 0.0001	0.0000 ± 0.0001	0.0000 ± 0.0001	0.3058 ± 0.2272
9,12-Octadecanedienoic acid	0.0000 ± 0.0001	0.0000 ± 0.0001	0.0000 ± 0.0001	0.0000 ± 0.0001	0.0000 ± 0.0001	0.0000 ± 0.0001	0.0000 ± 0.0001	0.0000 ± 0.0001	1.3574 ± 0.9208
9-Octadecenoic acid	0.0011 ± 0.0146	0.0000 ± 0.0001	0.0000 ± 0.0001	0.0014 ± 0.0181	0.0000 ± 0.0001	0.0000 ± 0.0001	0.0000 ± 0.0001	0.0000 ± 0.0001	1.4690 ± 0.8808
Alkanedioic Acids									
Propanedioic acid	0.0000 ± 0.0001	0.0000 ± 0.0001	0.0000 ± 0.0001	0.0000 ± 0.0001	0.0000 ± 0.0001	0.0000 ± 0.0001	0.0000 ± 0.0001	0.0000 ± 0.0001	0.0000 ± 0.0001
Methylpropanedioic acid	0.0000 ± 0.0001	0.0000 ± 0.0001	0.0000 ± 0.0001	0.0000 ± 0.0001	0.0000 ± 0.0001	0.0000 ± 0.0001	0.0000 ± 0.0001	0.0000 ± 0.0001	0.0000 ± 0.0001
Butanedioic acid	0.2618 ± 0.1111	0.2026 ± 0.0500	0.0274 ± 0.0100	0.3235 ± 0.1373	0.3873 ± 0.0957	0.0433 ± 0.0159	0.8009 ± 0.2267	1.0842 ± 0.3165	0.2388 ± 0.1533
Methylbutanedioic acid	0.0724 ± 0.0199	0.0592 ± 0.0145	0.0000 ± 0.0001	0.0895 ± 0.0246	0.1133 ± 0.0278	0.0000 ± 0.0001	0.1716 ± 0.0470	0.2323 ± 0.0658	0.0000 ± 0.0001
Pentanedioic acid	0.0698 ± 0.0218	0.1072 ± 0.0263	0.0000 ± 0.0001	0.0863 ± 0.0270	0.2049 ± 0.0502	0.0000 ± 0.0001	0.1198 ± 0.0347	0.1622 ± 0.0484	0.0489 ± 0.0317
Hexanedioic acid	0.0455 ± 0.0171	0.0786 ± 0.0193	0.0000 ± 0.0001	0.0562 ± 0.0212	0.1504 ± 0.0369	0.0000 ± 0.0001	0.0882 ± 0.0264	0.1195 ± 0.0367	0.0159 ± 0.0132

Heptanedioic acid	0.0741 ± 0.0203	0.1257 ± 0.0308	0.0000 ± 0.0001	0.0916 ± 0.0251	0.2402 ± 0.0589	0.0000 ± 0.0001	0.0000 ± 0.0001	0.0000 ± 0.0001	0.0180 ± 0.0159
Octanedioic acid	0.1283 ± 0.0351	0.1738 ± 0.0426	0.0000 ± 0.0001	0.1586 ± 0.0434	0.3322 ± 0.0815	0.0000 ± 0.0001	0.1487 ± 0.0409	0.2013 ± 0.0572	0.0358 ± 0.0280
Nonanedioic acid	0.3580 ± 0.0979	0.4949 ± 0.1216	0.0000 ± 0.0001	0.4424 ± 0.1209	0.9459 ± 0.2325	0.0000 ± 0.0001	0.2986 ± 0.0835	0.4043 ± 0.1167	0.1558 ± 0.1006
Others									
Nonanal	0.0385 ± 0.0119	0.0170 ± 0.0045	0.0130 ± 0.0089	0.0475 ± 0.0147	0.0326 ± 0.0087	0.0207 ± 0.0140	0.0125 ± 0.0088	0.0170 ± 0.0120	0.0000 ± 0.0001
Sinapyl aldehyde	0.0000 ± 0.0001	0.0000 ± 0.0001	0.0000 ± 0.0001	0.0000 ± 0.0001	0.0000 ± 0.0001	0.0000 ± 0.0001	0.0000 ± 0.0001	0.0000 ± 0.0001	0.0000 ± 0.0001
Acetonylsyringol	0.0990 ± 0.0283	0.0439 ± 0.0107	0.0193 ± 0.0071	0.1223 ± 0.0349	0.0840 ± 0.0206	0.0305 ± 0.0112	0.0581 ± 0.0181	0.0786 ± 0.0252	0.0000 ± 0.0001
Coniferyl aldehyde	0.0000 ± 0.0001	0.0000 ± 0.0001	0.0000 ± 0.0001	0.0000 ± 0.0001	0.0000 ± 0.0001	0.0000 ± 0.0001	0.0000 ± 0.0001	0.0000 ± 0.0001	0.0000 ± 0.0001
Propionylsyringol	0.0000 ± 0.0001	0.0000 ± 0.0001	0.0000 ± 0.0001	0.0000 ± 0.0001	0.0000 ± 0.0001	0.0000 ± 0.0001	0.0000 ± 0.0001	0.0000 ± 0.0001	0.0000 ± 0.0001
Benz(de)anthracen-7-one	0.0022 ± 0.0031	0.0000 ± 0.0001	0.0000 ± 0.0001	0.0027 ± 0.0039	0.0000 ± 0.0001	0.0000 ± 0.0001	0.0036 ± 0.0023	0.0049 ± 0.0032	0.0000 ± 0.0001
3,5-Dimethoxy-4-hydroxyacetophenone	0.0262 ± 0.0073	0.0259 ± 0.0063	0.0000 ± 0.0001	0.0324 ± 0.0091	0.0496 ± 0.0121	0.0000 ± 0.0001	0.0275 ± 0.0071	0.0372 ± 0.0100	0.0000 ± 0.0001
Levoglucosan	41.345 ± 12.882	65.892 ± 16.235	31.493 ± 11.847	51.090 ± 15.918	125.94 ± 31.031	49.782 ± 18.727	45.911 ± 12.692	62.151 ± 17.746	57.087 ± 32.377
Cholesterol	0.0000 ± 0.0001	0.0000 ± 0.0001	0.0097 ± 0.0035	0.0000 ± 0.0001	0.0000 ± 0.0001	0.0154 ± 0.0056	0.0000 ± 0.0001	0.0000 ± 0.0001	0.0000 ± 0.0001
OC	553.92 ± 163.75	493.16 ± 87.908	421.75 ± 146.70	684.47 ± 202.35	942.63 ± 168.02	666.66 ± 231.90	593.85 ± 180.15	450.19 ± 250.55	602.50 ± 185.20
EC	32.038 ± 12.934	5.9005 ± 1.4020	31.411 ± 11.370	39.590 ± 15.983	11.278 ± 2.6798	49.652 ± 17.972	22.962 ± 12.421	31.085 ± 16.961	39.200 ± 11.300
Al	0.9649 ± 1.0369	0.2630 ± 0.1733	9.4590 ± 3.4167	1.1924 ± 1.2813	0.5028 ± 0.3313	14.952 ± 5.4008	0.0000 ± 0.0001	0.0000 ± 0.0001	0.2290 ± 0.4260
Si	2.1068 ± 1.5913	0.0000 ± 0.0001	17.420 ± 6.4365	2.6034 ± 1.9664	-1.418 ± -0.490	27.537 ± 10.174	0.2889 ± 0.2276	0.3911 ± 0.3094	0.1860 ± 0.2580
K^+	1.8192 ± 1.4678	2.2894 ± 0.4263	6.3130 ± 2.1819	2.2480 ± 1.8138	4.3760 ± 0.8149	9.9791 ± 3.4490	2.2261 ± 0.5044	3.0135 ± 0.7159	6.4900 ± 4.3500
Cl^-	-2.935 ± -1.968	n/a	n/a	-3.627 ± -2.432	n/a	n/a	0.4355 ± 0.0898	0.5895 ± 0.1287	5.2700 ± 2.8900
NH_4^+	12.854 ± 20.519	18.297 ± 4.3770	11.163 ± 16.438	15.883 ± 25.355	34.974 ± 8.3661	17.646 ± 25.984	13.119 ± 4.4281	17.760 ± 6.1272	1.0700 ± 1.0800
NO_3^-	31.216 ± 22.683	18.916 ± 3.5333	11.061 ± 7.5825	38.573 ± 28.030	36.157 ± 6.7535	17.485 ± 11.985	19.310 ± 5.1844	26.141 ± 7.2624	4.4000 ± 2.9900
SO_4^{2-}	20.250 ± 53.971	25.077 ± 8.9620	9.1869 ± 55.877	25.022 ± 66.692	47.932 ± 17.129	14.521 ± 88.325	13.800 ± 8.5722	18.682 ± 11.680	2.4500 ± 1.1200

Note: [a] source composition profiles where individual chemical species are normalized to the fire-caused total $PM_{2.5}$ mass on the wildfire days; [b] source composition profiles where individual chemical species are normalized to the fire-caused primary $PM_{2.5}$ mass estimated on the wildfire day; [c] source composition profiles, normalized to the fire-caused total $PM_{2.5}$ mass, from the prescribed fire in Georgia (Yan et al., 2008); [b] source composition profiles, normalized to the fire-caused primary $PM_{2.5}$ mass, from the prescribed fire in Georgia (Yan et al., 2008); e source composition profiles from the prescribed burning emission in Georgia [*Lee et al.*, 2005a]; [f] fraction of chemical species in the associated $PM_{2.5}$ mass (ng/μg $PM_{2.5}$); [g] standard deviation.

6.3.5 Source Profiles for Aged Plumes

Capturing the wildfire events provides information to develop source composition profiles of wildfire plumes and to further assess aging processes of wildfire-derived organic tracers. The above discussions indicate that the large increases in $PM_{2.5}$, OC and associated chemical species on the smoke days are a direct contribution from wildfire emissions. From this result, associated source profiles for aged wildfire $PM_{2.5}$ were derived. Here, two approximate source composition profiles were developed for each monitor for the aged wildfire plumes by considering differences between the non-smoke and smoke days, designated 'aged_plume profile' and 'primary_plume profile'. 'Aged_plume profile' contains fractions of individual chemical species (increased concentrations) in the total increased (fire-caused total) $PM_{2.5}$ mass, i.e. 37, 100, and 9.1 μg m^{-3} at the Atlanta, Bibb and Coffee sites, respectively (Table D.1). This profile contains chemical compositions of the aged plume, but is not the primary $PM_{2.5}$ source profile due to large quantities of SOA in the aerosols from fire emissions. The 'Primary_plume profile' was then calculated using fractions of individual chemical species (increased concentrations) in the fire-caused primary $PM_{2.5}$ mass where the estimated fire-caused secondary organic carbon (SOC) was subtracted from the fire-caused total $PM_{2.5}$ mass on the event day (Table 6.3). The fire-caused SOC on the event days was estimated using measured OC/EC ratios. In the aged plumes, the fire-caused OC/EC ratios are 17.3, 66.9 and 45, whereas a value of 11.3 was measured at the Okefenokee site. To estimate primary OC/EC ratios in the wildfire emissions, the smoke plumes captured at the Okefenokee site are thought to be fresh or un-age. This is reasonable given this site is next to the wildfire and overwhelmingly dominated by fresh

wildfire emissions (Figure 6.3). The lower OC/EC ratios observed at the downwind sites suggest SOA formation in the aged plumes, assuming wildfire-caused ambient EC did not vary significantly during atmospheric transport. Using those ratios, SOCs are calculated to account for 34%, 83% and 75% of the fire-caused total OCs at the Atlanta, Bibb and Coffee sites, respectively. The fire-caused primary OC (POC_{fc}) is then estimated by

$$POC_{fc} = OC\left(\text{fire}-\text{caused}\right)\times\left(1-f_{SOC}\right) = \left[OC\left(\text{smoke}\right)-OC\left(\text{non}-\text{smoke}\right)\right]\times\left(1-f_{SOC}\right) \quad (6.1)$$

where f_{soc} is the estimated SOC fraction in the fire-caused total OC. Similarly, the amount of fire_caused primary $PM_{2.5}$ (PPM_{fc}) is calculated as

$$PPM_{fc} = \left[PM\left(\text{smoke}\right)-PM\left(\text{non}-\text{smoke}\right)\right]-OC\left(\text{fire}-\text{caused}\right)\times f_{SOC} \quad (6.2)$$

Finally, fractions of individual species (f_i) in fire_caused primary $PM_{2.5}$ are calculated as

$$f_i = \frac{C_i\left(\text{smoke}\right)-C_i\left(\text{non}-\text{smoke}\right)}{PPM_{fc}} \quad (6.3)$$

where C_i is the ambient concentration of individual chemical species in $PM_{2.5}$ that are viewed as being dominated by primary emissions. An overall uncertainty of each chemical species in the two plume source profiles was calculated by propagating uncertainties associated with the observed OC, estimated SOC fraction and measured chemical species (i.e. organic compounds, EC, ions and trace metals) (Table D.1). Note that significant uncertainties would be caused in estimation of SOC due to biases of the applied OC/EC ratios, which were obtained from different wildfire plumes probably under different atmospheric conditions.

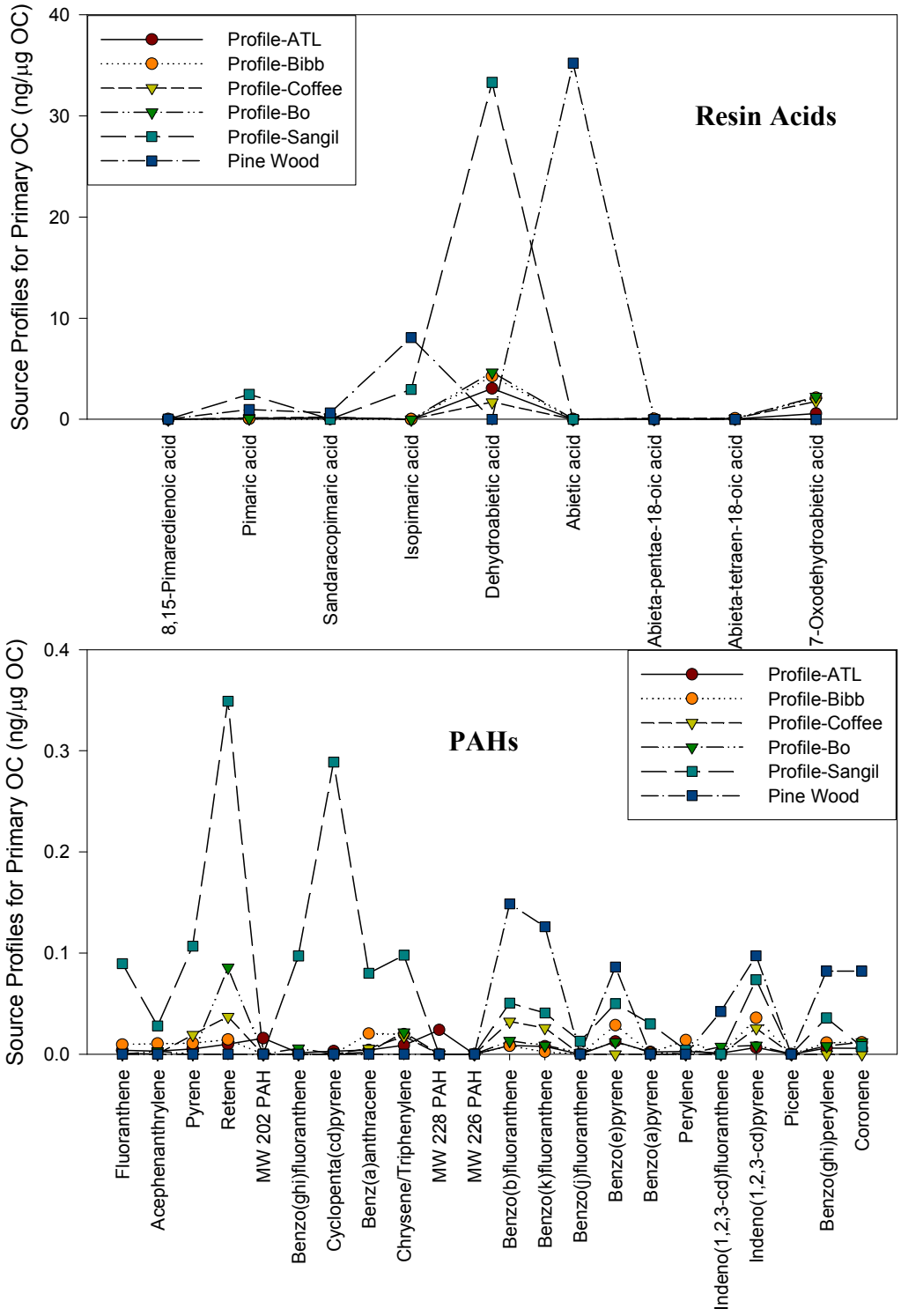

Figure 6.9. Source composition profiles of resin acids and PAHs approximated from the wildfire events and from the previous studies (primary OC normalized).

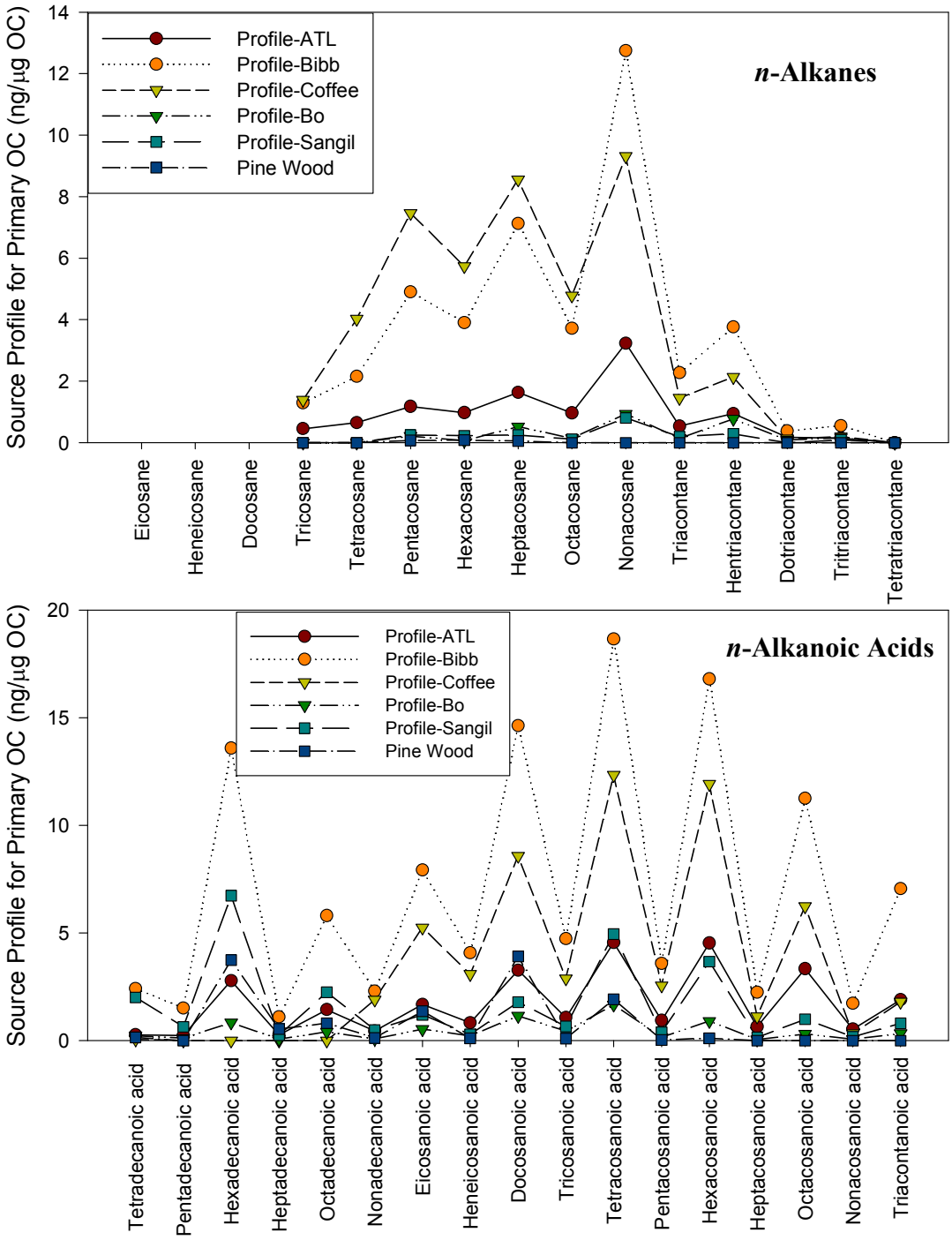

Figure 6.10. Source composition profiles of *n*-alkanes and *n*-alkanoic acids approximated from the wildfire events and from previous studies (primary OC normalized).

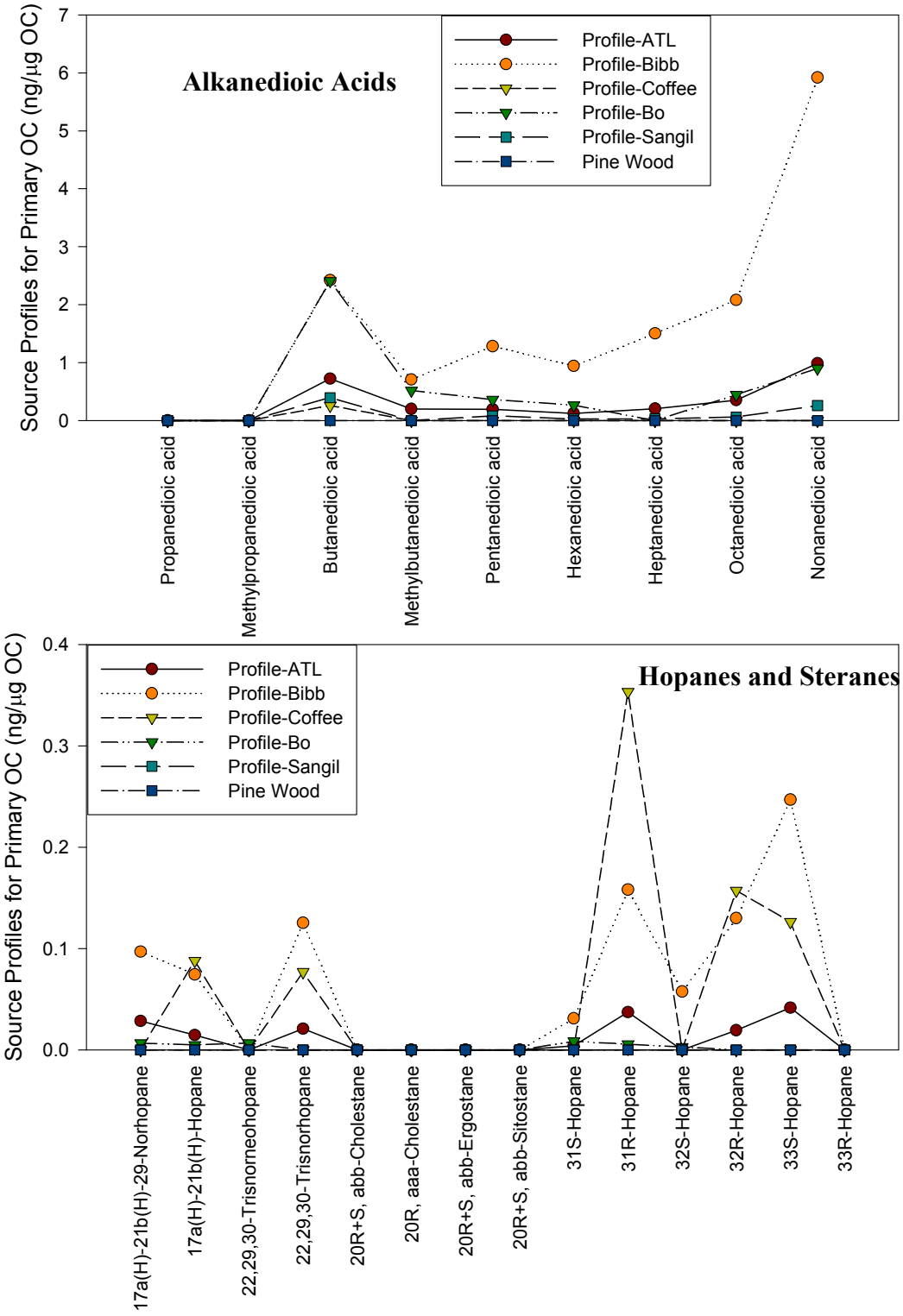

Figure 6.11. Source composition profiles of alkanedioic acids, hopanes, and steranes approximated from the wildfire events and from previous studies (primary OC normalized).

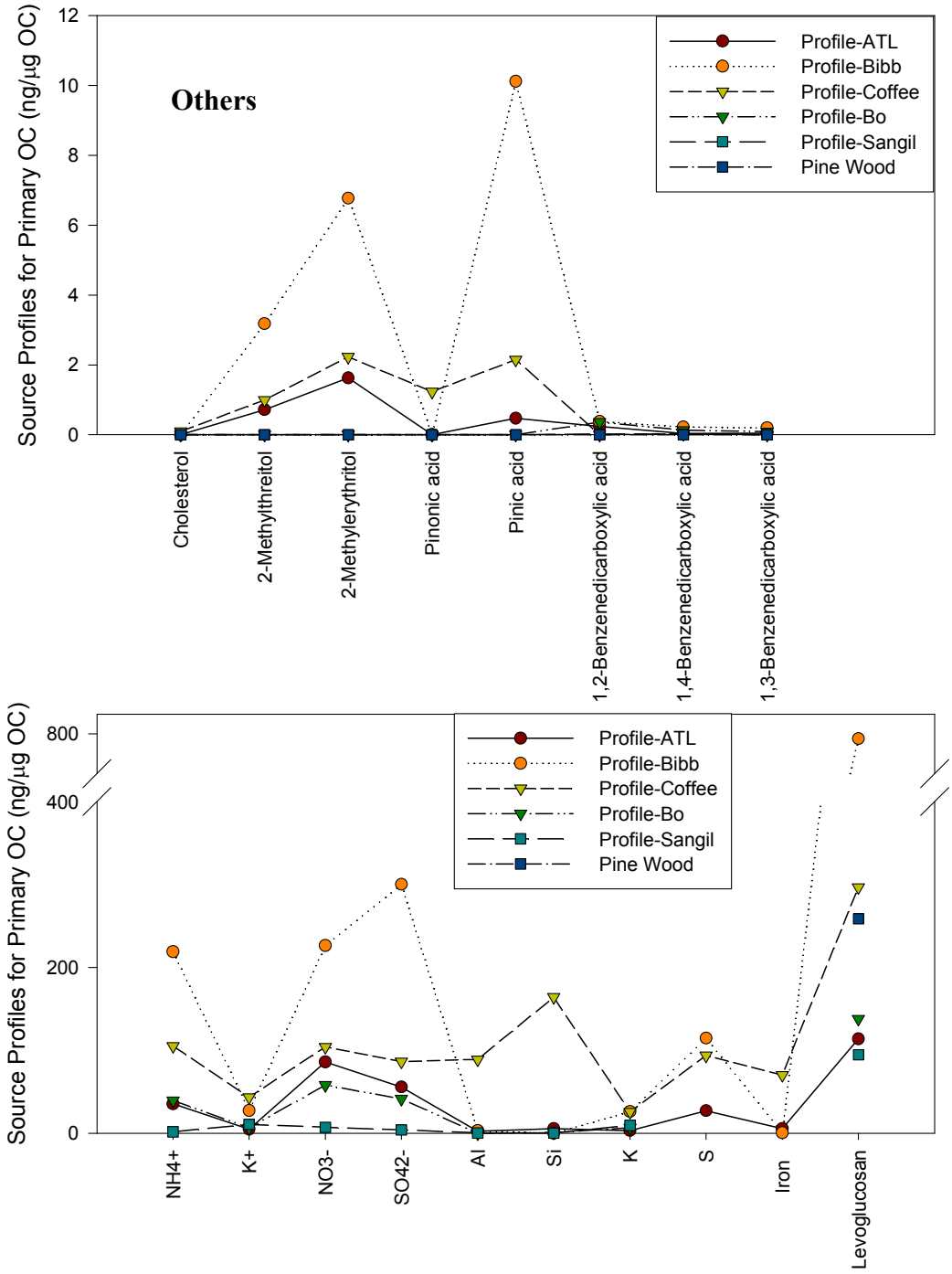

Figure 6.12. Source composition profiles of others, levoglucosan, metals and ions approximated from the wildfire events and from previous studies (primary OC normalized).

The ‘primary_plume profile’ derived from the wildfires is comparable to the aged prescribed burning profile [*Yan et al.*, 2008b], the prescribed burning emission profile [*Lee et al.*, 2005a], and the pine wood emission profile [*Schauer et al.*, 2001], for some organic compounds, but significantly different for other compounds (Table 6.3 and Figures 6.9-6.12). In particular, the aged wildfire profiles at the Atlanta site are more comparable to the previous profiles. In the aged wildfire plumes, levoglucosan accounts for 11% of primary OC in Atlanta, comparable to 14% in the profile of Yan et al. (2008) and 9.5% in the profile of Lee et al. (2005) (Figure 6.12). However, the levoglucosan values at the Bibb and Coffee sites are much higher than the previous ones.

There are a few possible reasons for the differences. Emission factors of wildfires changed during this episode as different biofuels burned or as combustion processes varied (e.g., flaming, smoldering), leading to variable fractions of levoglucosan in the wildfire emissions. Secondly, SOA in the aged wildfire plumes are overestimated at the Bibb and Coffee sites since the measured OC/EC ratios are subject to uncertainties, causing such high ratios of levoglucosan over primary OC. The second one is relatively more probable, considering comparisons of other primary organic tracers. In the aged source profiles, Bibb and Coffee always show significantly higher fractions of *n*-alkanes, *n*-alkanoic acids, and steranes, all of which are believed to be stable molecular markers (Figures 6.10 and 6.11). The ratio of water-soluble potassium (K^+)/OC in the ‘primary_plume profile’ is 0.0050. This is lower than the values in Lee et al. (0.011) and in Fine et al. (0.012 on average), but comparable to the average ratio of 0.0058 from foliar fuel combustion and in Yan et al. (0.0067) [*Fine et al.*, 2004a; *Hays et al.*, 2002; *Lee et al.*, 2005a; *Yan et al.*, 2008b]. Furthermore, significant differences were found for

the fractions of PAHs, resin acids, *n*-alkanoic acid and dicarboxylic acids, suggesting aging of fire smoke after a 12 hour travel distance. Lee et al. [2005] and Schauer et al. [2001] measured higher values in PAHs and resin acids, implying direct combustion is the main contributor of these compounds and significant chemical alteration occurs during transport, especially for resin acids (Figure 6.9). In contrast, the aged plume has distinctly higher aromatic and aliphatic diacids fractions (Figure 6.11). Enhanced SOA formation in the atmosphere from the fire is suggested by these secondary indicators.

The profile comparison between prescribed fire source emissions and the aged plume is useful to understand the evolution of wood smoke during transport and to assess the organic species applied in CMB-MM modeling. Impacts from aging process of the smoke plume should be considered in source apportionment methodology using the CMB model, including selection of fitting species.

Acknowledgements

This work was funded in part by the U.S. Environmental Protection Agency STAR grants (R832159, R828976 and R831076). We would like to thank Georgia Power (Southern Company) for their support of work in Laboratory for Atmospheric Modeling, Diagnostics, and Analysis (LAMDA) at Georgia Institute of Technology in this study area. The authors acknowledge Georgia Environmental Protection Division of the Department of Natural Resources for providing STN field filters and other ambient data to this research. We also thank the assistance from Warren White in Crocker Nuclear Laboratory in UC Davis for IMPROVE data at the Okefenokee Natioanl Wildlife Refuge.

CHAPTER 7

ANALYSIS OF SOURCE APPORTIONMENT APPLICATIONS FOR PM2.5 IN THE SOUTHEAST: INTERCOMPARISON BETWEEN TWO APPROACHES

(Bo Yan, Sangil Lee, Lin Ke, Eric S. Edgerton, Mei Zheng, Armistead G. Russell. *Atmospheric Environment*, in preparation)

Abstract

Chemical mass balance (CMB) modeling has been successfully developed and frequently applied to apportion source contributions to organic carbon (OC) and fine particulate matter ($PM_{2.5}$). Historically, inorganic species are used in CMB (CMB-Regular). More recently, organic molecular markers have been employed (CMB-MM). CMB-Regular and CMB-MM approaches were used and compared in this study for conducting source apportionment of $PM_{2.5}$ data from the Southeastern Aerosol Research and Characterization Study (SEARCH) project. Temporal (winter and summer) and spatial impacts (urban and rural) on source contributions were analyzed. Results indicate a few similarities in source contributions between the two approaches. Secondary sources including secondary sulfate, ammonium, and nitrate contributed the majority of $PM_{2.5}$ mass in the Southeast in both summer (>50%) and winter (>40%). Motor vehicle exhaust and biomass burning are the major primary sources of $PM_{2.5}$ in this area. Motor vehicle exhaust, paved road dust and biomass burning impacts were both calculated using CMB-Regular and CMB-MM. However, the differences of source apportionments between the

two approaches are sometimes rather great. The disagreement is caused by several reasons: (1) fitting species selected; (2) source category identified; (3) source profile applied; (4) model uncertainty.

7.1 Introduction

Effective control strategies for air pollutants require identification and quantification of impacts of specific sources on ambient air quality. As a receptor model, the Chemical Mass Balance (CMB) air quality model has been widely applied for source apportionment of ambient pollutants, especially particulate matter (PM) [*Friedlander*, 1973; *Hopke*, 2003; *Kowalczyk et al.*, 1978; *Miller et al.*, 1972; *Watson*, 1979; *Watson et al.*, 1984; *Watson et al.*, 1990; *Watson et al.*, 1994; *Watson et al.*, 2002].

Based on chemical species mass balance, the CMB air quality model depends on a variety of assumptions: 1) compositions of source emissions are constant over the period of ambient and source sampling; 2) chemical species are relatively stable and conservative during transport from emissions to the receptor; 3) major sources contributing to the receptor are included in the model; 4) the number of source categories is less than the number of chemical species; 5) source profiles are linearly independent of each other (without collinear problems); and 6) measurement uncertainties are random, uncorrelated, and normally distributed [*U.S.EPA*, 2001]. Mathematically, the fundamental principle of CMB can be expressed as:

$$C_{ik} = \sum_{j=1}^{m} a_{ij} S_{jk} + e_{ik} \qquad i = 1,2,.....,n$$

Where c_{ik} is the ambient concentration of chemical species *i* at a specific receptor site *k*; a_{ij} is the fraction of chemical species *i* in the OC (or $PM_{2.5}$) emission from source *j*, also called source profile abundances; s_{jk} is the contribution of source *j* to the OC (or $PM_{2.5}$) concentration at the receptor site *k*; and e_{ik} is error term.

Several methods derived from least square fitting functions have been developed for solving the CMB equations such as ordinary weighted least squares [*Friedlander*, 1973; *Gartrell and Friedlander*, 1975], Britt and Luecke least squares [*Britt and Luecke*, 1973] and effective variance weighted least squares [*Watson et al.*, 1984]. The solution method of effective variance weighted least squares is applied more frequently now as it theoretically yields the most likely solutions to CMB equations using many chemical species, not just chemical tracers in the model. Moreover, uncertainties of source contributions are analytically estimated through integrating precisions of ambient concentrations and source profiles. Chemical species with higher measurement accuracy are given greater weights than those with lower accuracy [*U.S.EPA*, 2001].

Supported by a series of measurement technologies, elemental and ionic species were initially applied in inorganic species-based CMB (CMB-Regular) model to apportion source contributions [*Cass and Mcrae*, 1983; *Chan et al.*, 1999; *Chen et al.*, 2001; *Chow et al.*, 1992; *Chow et al.*, 1995; *Cooper and Watson*, 1980; *Gordon*, 1980; *Hidy and Venkataraman*, 1996; *Ward and Smith*, 2005]. However, the CMB-Regular approach was limited in its ability to distinguish contributions of some important or potentially important sources of OC and $PM_{2.5}$, such as diesel vehicle exhaust and gasoline vehicle exhaust, biomass burning, meat cooking, vegetative detritus, and natural gas combustion. The reason is that these source emissions principally contain organic

compounds and elemental carbon (EC) instead of relatively unique elements. The introduction of molecular markers, some of which are reasonably unique tracers for certain sources, can provide additional information about source impacts so that important sources of OC and $PM_{2.5}$ can be better identified and quantified. With further developments of measurement techniques for ambient organic chemicals [*Nolte et al.*, 2002; *Rogge et al.*, 1991; *Rogge et al.*, 1993a; b; c; d; *Rogge*, 1994], the molecular marker-based CMB (CMB-MM) model has been built and increasingly used for source apportionment in many areas since 1996 [*Fraser et al.*, 2003b; *Schauer et al.*, 1996; *Schauer*, 1998; *Schauer and Cass*, 2000; *Sheesley et al.*, 2004; *Zheng et al.*, 2002; *Zheng et al.*, 2006b; *Zheng et al.*, 2007].

However, the CMB-MM model also has a few disadvantages. More resources and time are needed to measure trace organic compound concentrations, and local source profiles are unavailable in many areas. Chemical stability of organic molecular markers during transport is another concern, particularly under intense photochemical conditions [*Robinson et al.*, 2006a; *Robinson et al.*, 2007]. Unlike organic compounds, elemental species are chemically stable during transport, and their ambient concentrations are routinely measured. Ambient information of such species is more generally available, allowing spatial and temporal variations of source impacts to be calculated using CMB-Regular.

In order to identify and quantify the impacts of specific emission sources on air quality in the southeastern U.S., both the CMB-MM approach and CMB-Regular approach are used here for source apportionment of $PM_{2.5}$. The CMB results calculated from the two approaches can help provide more comprehensive information of major

sources in this region. More importantly, as a focus of active research, intercomparison between the two approaches can be used to evaluate and improve CMB source apportionment applications and to better understand their limitations.

7.2 Methods

7.2.1 Sampling and Measurements

Ambient data used here are from the Southeastern Aerosol Research and Characterization Study (SEARCH) project. Seasonal (winter and summer) and spatial impacts (urban and rural) are studied.

24-hr filter-based samples from July 2001 and January 2002 were collected daily with particle composition monitor (PCM) at SEARCH sites including Jefferson Street in Atlanta, Georgia (JST), Yorkville, Georgia (YRK), N. Birmingham, Alabama (BHM), Centreville, Alabama (CTR), Pensacola, Florida (PNS), and Oak Grove, Mississippi (OAK). During this period, 24-hr filter-based samples were also collected parallel at Jefferson Street in Atlanta with a Hi-Volume $PM_{2.5}$ sampler. Among these SEARCH sites, Jefferson Street, N. Birmingham, and Pensacola are urban sites while Yorkville, Centreville, and Oak Grove are rural sites. Monthly average (daily filter composite) PCM samples from 6 SEARCH sites were used for source apportionment and comparisons as well as the daily high-volume (Hi-Vol) samples from Jefferson Street. The sampling details and species measurements (OC, EC, trace metals and ions) were described in previous papers [*Hansen et al.*, 2003; *Lee et al.*, 2005b]. Organic species in PM2.5 were analyzed with gas chromatography (GC)/mass spectrometry (MS) in Georgia Institute of Technology [*Zheng et al.*, 2002; *Zheng et al.*, 2007].

Ambient measurements in SEARCH and CMB-MM source profiles employed different thermal-optical protocols for carbon analysis (OC/EC): IMPROVE (Interagency Monitoring of Protected Visual Environments) and NIOSH (National Institute of Occupational Safety and Health), respectively. The disagreement of carbon analysis between ambient data and source profiles would bring suspected CMB-MM source apportionments, especially for mobile source, which is greatly depended on ratios of OC/EC. To match with NIOSH-based source profiles, IMPROVE-based ambient OC/EC data had to be converted to NIOSH-based data in advance through comparison between IMPROVE and NIOSH data sets measured on the same SEARCH samples.

NIOSH and IMPROVE methods have been shown to agree with each other for total carbon (TC), sum of OC and EC, but have different splits between OC and EC [*Chow et al.*, 2001; *Chow et al.*, 2004a; *Chow et al.*, 2005]. In this study, a total of 139 Hi-Vol filter-based daily samples was analyzed by both NIOSH and IMPROVE approaches. These samples come from two representative sampling months, January (2004 and 2005) and July (2003 and 2004), and four SEARCH sampling sites, JST, BHM, CTR, and PNS. NIOSH and IMPROVE protocol-based measurements were performed at Georgia Institute of Technology and Desert Research Institute (DRI), respectively. The two data sets were compared for each season and site, and the associated linear regressing equations were conducted and applied to convert IMPROVE-based ambient OC/EC data to simulated NIOSH-based data before CMB-MM modeling. There is not the similar problem in CMB-Regular modeling since the IMPROVE protocol is used in both source profile tests and ambient data measurements.

7.2.2 Source Profiles

CMB-MM source profiles come from previous source emission samplings including medium duty diesel truck exhaust [*Schauer et al.*, 1999b], combined gasoline vehicle exhaust of catalyst-equipped and noncatalyst-equipped gasoline-powered vehicles [*Schauer et al.*, 2002b], biomass burning in the southeastern states [*Fine et al.*, 2002], meat cooking [*Schauer et al.*, 1999a], Alabama paved road dust [*Schauer*, 1998; *U.S.EPA*, 2002; *Zheng et al.*, 2002], natural gas combustion [*Hildemann et al.*, 1991; *Rogge et al.*, 1993b], and vegetative detritus [*Hildemann*, 1991; *Rogge et al.*, 1993a]. The method of NIOSH carbon analysis was used in the emission tests of these source profiles.

CMB-Regular source profiles include motor vehicle exhaust [*Zielinska et al.*, 1998], biomass burning [*Zielinska et al.*, 1998], coal combustion from power plants [*Chow et al.*, 2004b], Alabama paved road dust [*U.S.EPA*, 2002], and cement kilns [*Chow et al.*, 2004b]. The method of IMPROVE carbon analysis was used in the source profile studies except for the Alabama paved road dust.

7.2.3 Fitting Species

Fitting species applied in CMB-MM include aluminum (Al), silicon (Si), OC, EC, and organic molecular markers such as *n*-alkanes, hopanes, steranes, polycyclic aromatic hydrocarbons (PAHs), cholesterol (or nonanal), levoglucosan. These organic molecular markers are recommended for specific emission sources in previous studies [*Cass*, 1998; *Schauer and Cass*, 2000; *Schauer*, 2003; *Simoneit*, 1985; *Simoneit et al.*, 1999]. Both diesel vehicle exhausts and gasoline vehicle exhausts are characterized by high carbon contents, OC and EC, and a few unique organic tracers (hopanes and steranes). Such sources can be distinguished further by different EC/OC ratios and PAHs in CMB-MM

since the diesel vehicle exhaust profile has much higher EC/OC ratio while gasoline vehicles emit more PAHs. Biomass burning is characterized by unique organic tracers, levoglucosan and a few resin acids. Meat cooking is identified by abundant nonanal and unique cholesterol. A few specific *n*-alkanes and PAHs are representative species in the chemical compositions of vegetative detritus and natural gas combustion, respectively. The chemical stabilities of these fitting species during local transportation in atmosphere have been tested [*Schauer et al.*, 1996].

Fitting species applied in CMB-Regular typically include ions (SO_4^{2-}, NO_3^-, NH_4^+), elements (Al, Si, Ca, Fe, K, Se, Cu, As, Ba, Br, Mn, Ti, Zn, Pb), OC and EC. Their different fractions in emission sources provide a possibility to estimate several source contributions in CMB-Regular modeling: (1) motor vehicle: OC, EC, Ba, Zn; (2) road dust: Al, Si, Ca, Fe, OC; (3) biomass burning: K, OC, EC; (4) coal combustion: SO_4^{2-}, Ca, Si, Se, OC; (5) cement kilns: SO_4^{2-}, Ca, Si, Fe, K, and OC [*Chow and Watson*, 2002; *Chow et al.*, 2004b; *Schauer*, 2006].

EPA CMB v8.0 software using effective variance weighted least squares was used to estimate source contributions to OC and PM2.5. A few performance diagnostics were considered in CMB modeling, including χ^2 (target value: 0-4), R^2 (target value: 0.8-1.0), ratio of the calculated to the measured concentration of fitting species (target value: 0.5-2.0), T-Stat (target value: >2.0).

7.3 Results and Discussion

7.3.1 Ambient Data Conversion

An almost perfect agreement on TC (fitting slope = 0.995, intercept = -0.123, R^2 = 0.991) was found between NIOSH-based data and IMPROVE-based data for 139 SEARCH samples. Compared with the IMPROVE protocol, the NIOSH method always lead to larger OC and smaller EC values. Statistical analyses of OC and EC data from the two methods indicated highly correlated linear relationship (Figure 7.1). Notably, the slopes vary with sites and seasons (Figure 7.2). Therefore, the associated linear regression equations were used for converting ambient data between NIOSH and IMPROVE. Here, IMPROVE-based OC/EC measurements were converted to NIOSH-based data with the linear regression functions expressed in Figure 7.2.

7.3.2 Source Categories

For the CMB-MM application, up to seven primary sources of OC and $PM_{2.5}$ were resolved, including diesel vehicle exhaust, gasoline vehicle exhaust, meat cooking, paved road dust, biomass burning, natural gas combustion, and vegetative detritus (Figure 7.3). Other industrial emission sources such as coal combustion and cement kilns were not included due to the lack of organic molecular marker-based profiles.

CMB-Regular resolved three of the primary sources above used in CMB-MM, including motor vehicle exhaust (sum of diesel vehicle and gasoline vehicle exhaust), paved road dust, biomass burning and added industrial sources such as coal combustion and cement kilns (Figure 7.3). CMB-Regular can have trouble separating diesel vehicle exhaust and gasoline vehicle exhaust, biomass burning and meat cooking. Furthermore, appropriate source profiles for natural gas combustion and vegetative detritus are not available for CMB-Regular.

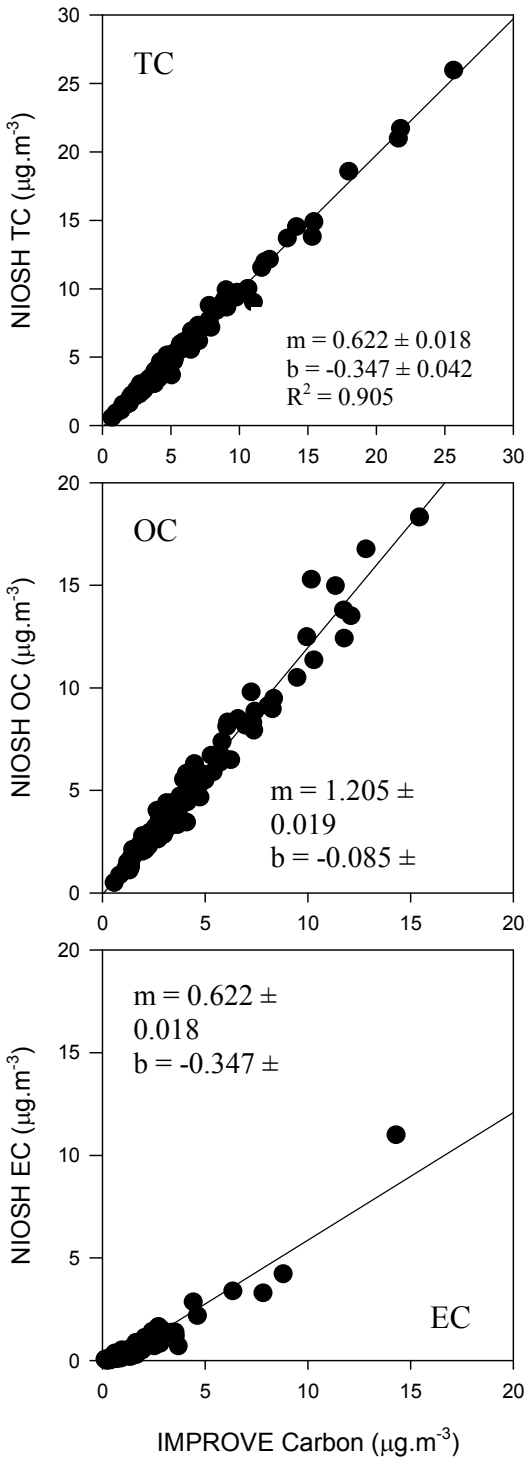

Figure 7.1. Comparison of NIOSH and IMPROVE carbon concentrations for 139 fine particle daily samples from 4 SEARCH sites: JST, BHM, CTR, and PNS.

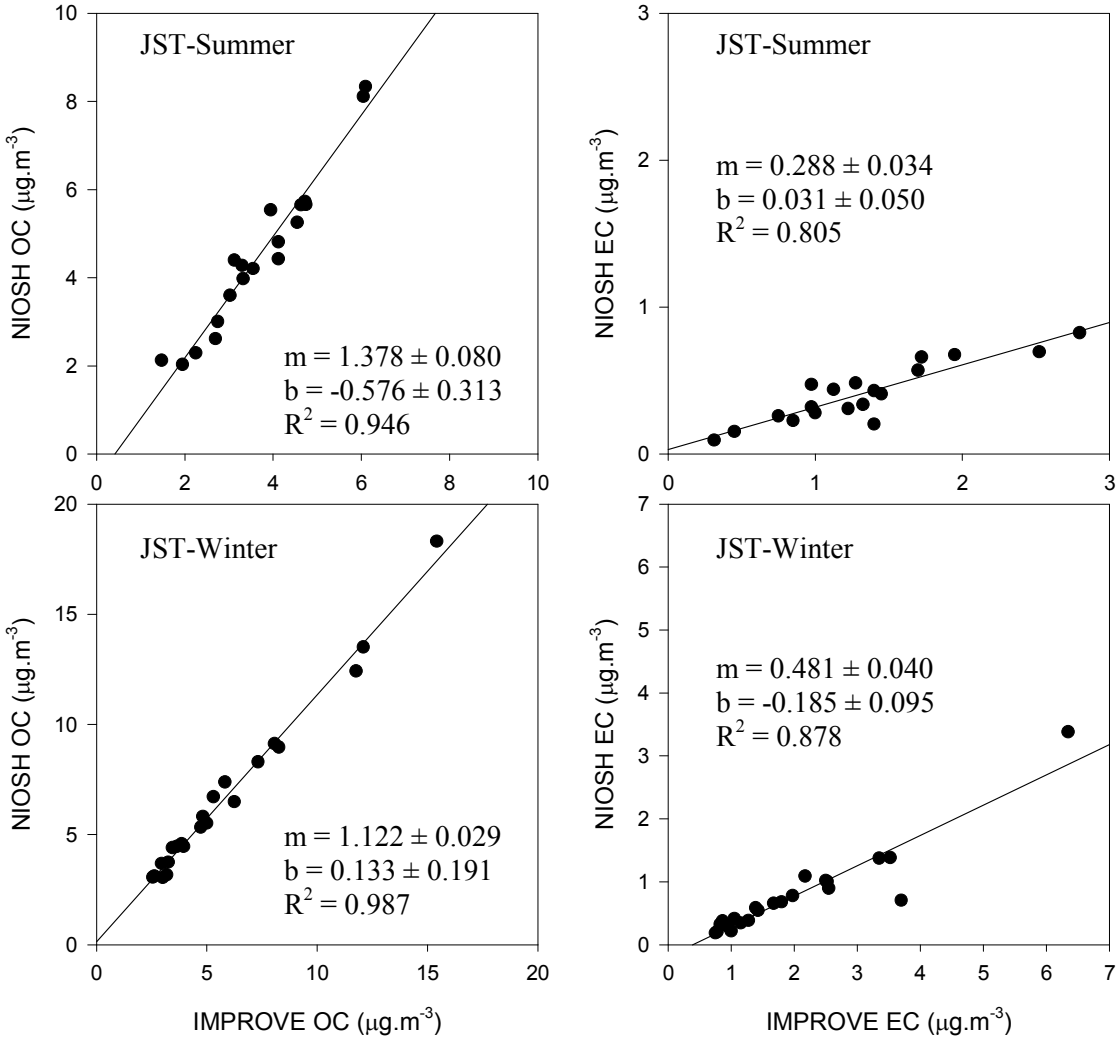

Figure 7.2. Comparison of NIOSH and IMPROVE carbon concentrations for 19 and 22 fine particle daily samples from the summer and the winter at JST site, respectively.

Secondary sulfate, secondary nitrate and secondary ammonium can be estimated in both approaches. Comparisons between the results from the two approaches and possible reasons for the discrepancies are shown and discussed below.

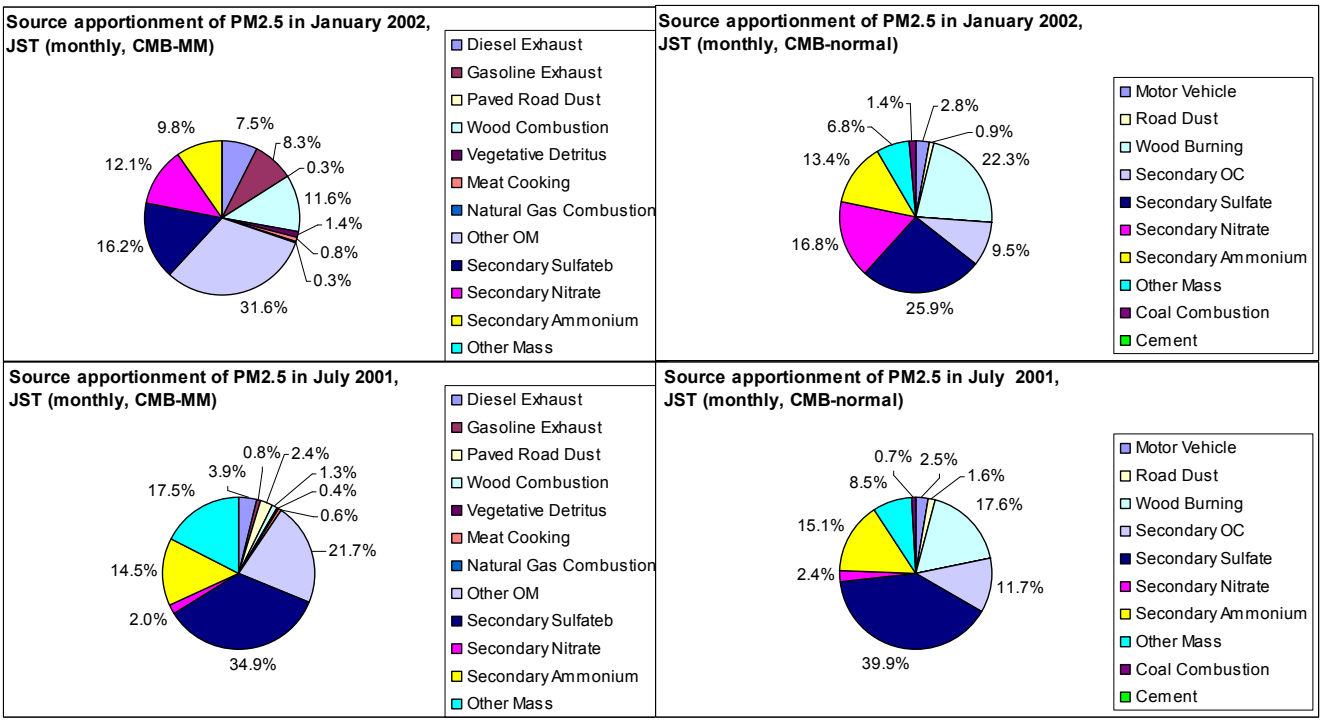

Figure 7.3. Comparison of source apportionments to PM2.5 estimated by CMB-MM and CMB-Regular for Jefferson Street, Atlanta (JST) summer and winter samples (monthly).

7.3.3 Motor Vehicle Exhaust

Relatively comparable source contributions were estimated for motor vehicle exhaust by both CMB-MM and CMB-Regular. As a major primary source of $PM_{2.5}$ in the Southeast, motor vehicle exhaust on average accounts for about 4-10% (summer-winter) and 4-9% (summer-winter) of the $PM_{2.5}$ mass found using CMB-MM and CMB-Regular, respectively. Both methods lead to very similar daily variations in JST site. During the summer, the average discrepancies are less than 10% while CMB-MM results are consistently higher than those from CMB-Regular (41% on average) during the winter (Figures 7.4 and 7.5).

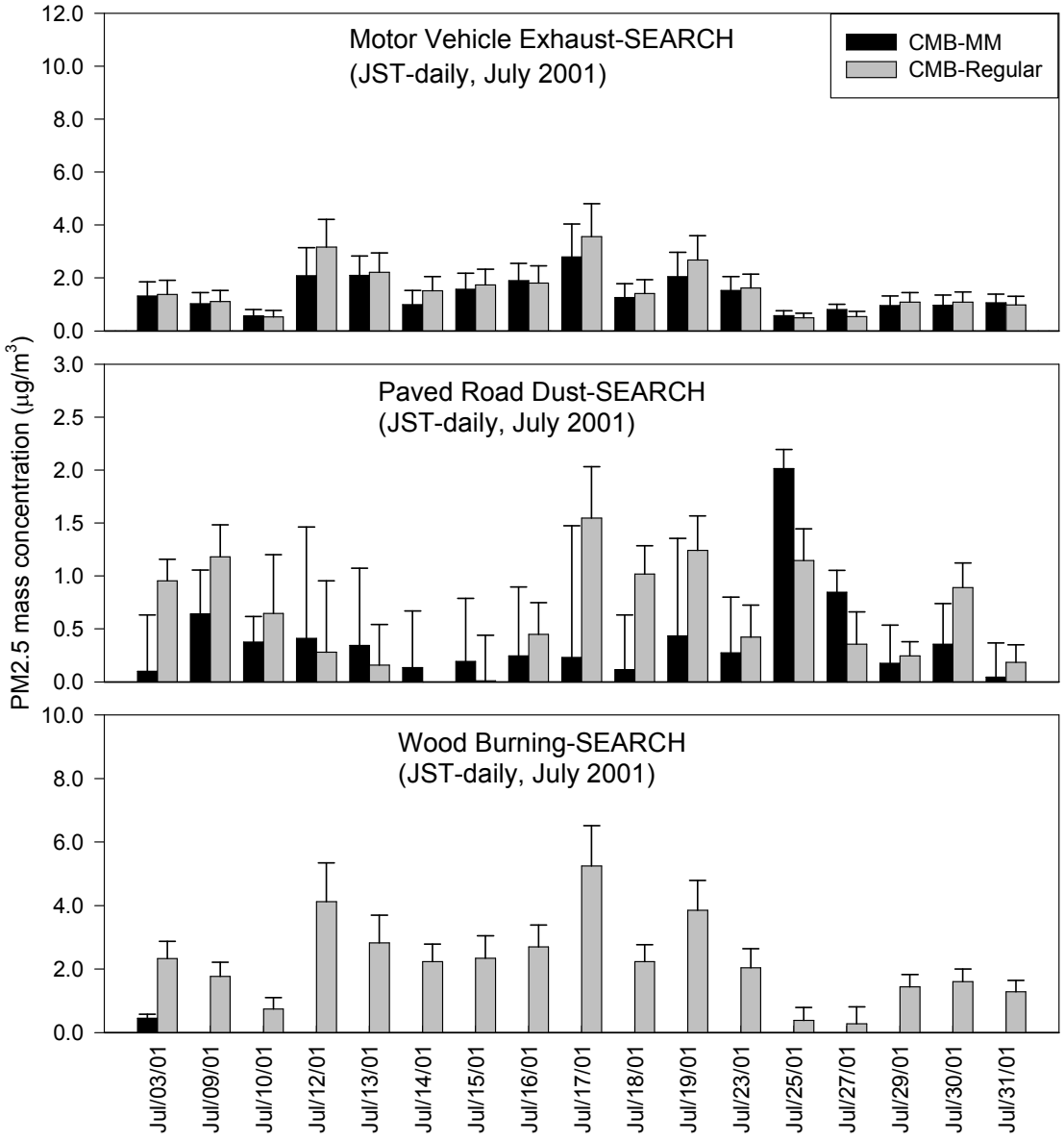

Figure 7.4. Comparison of motor vehicle exhausts, paved road dust and biomass burning contributing to $PM_{2.5}$ estimated by CMB-MM and CMB-Regular for JST summer samples.

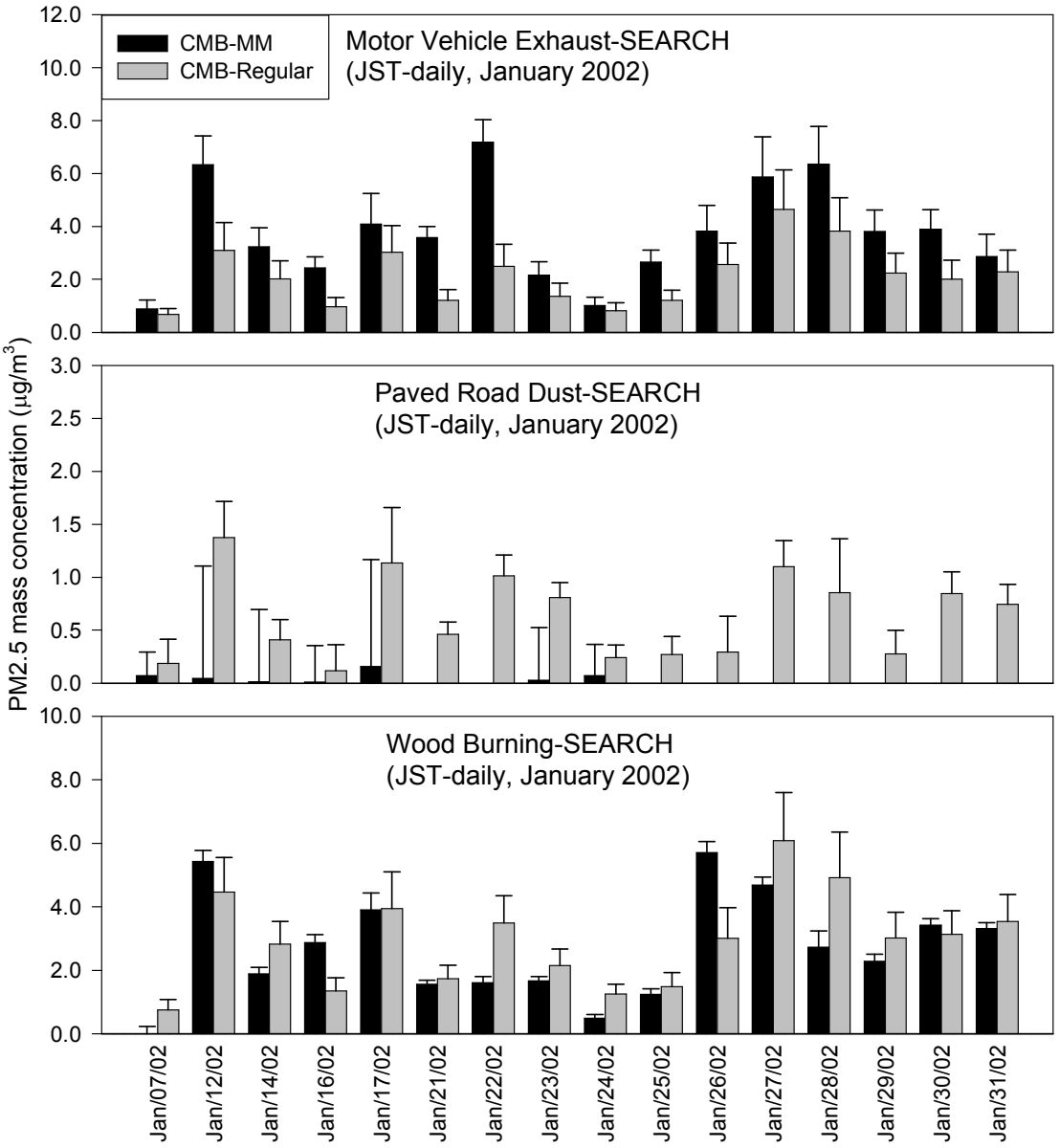

Figure 7.5. Comparison of motor vehicle exhausts, paved road dust and biomass burning contributing to $PM_{2.5}$ estimated by CMB-MM and CMB-Regular for JST winter samples.

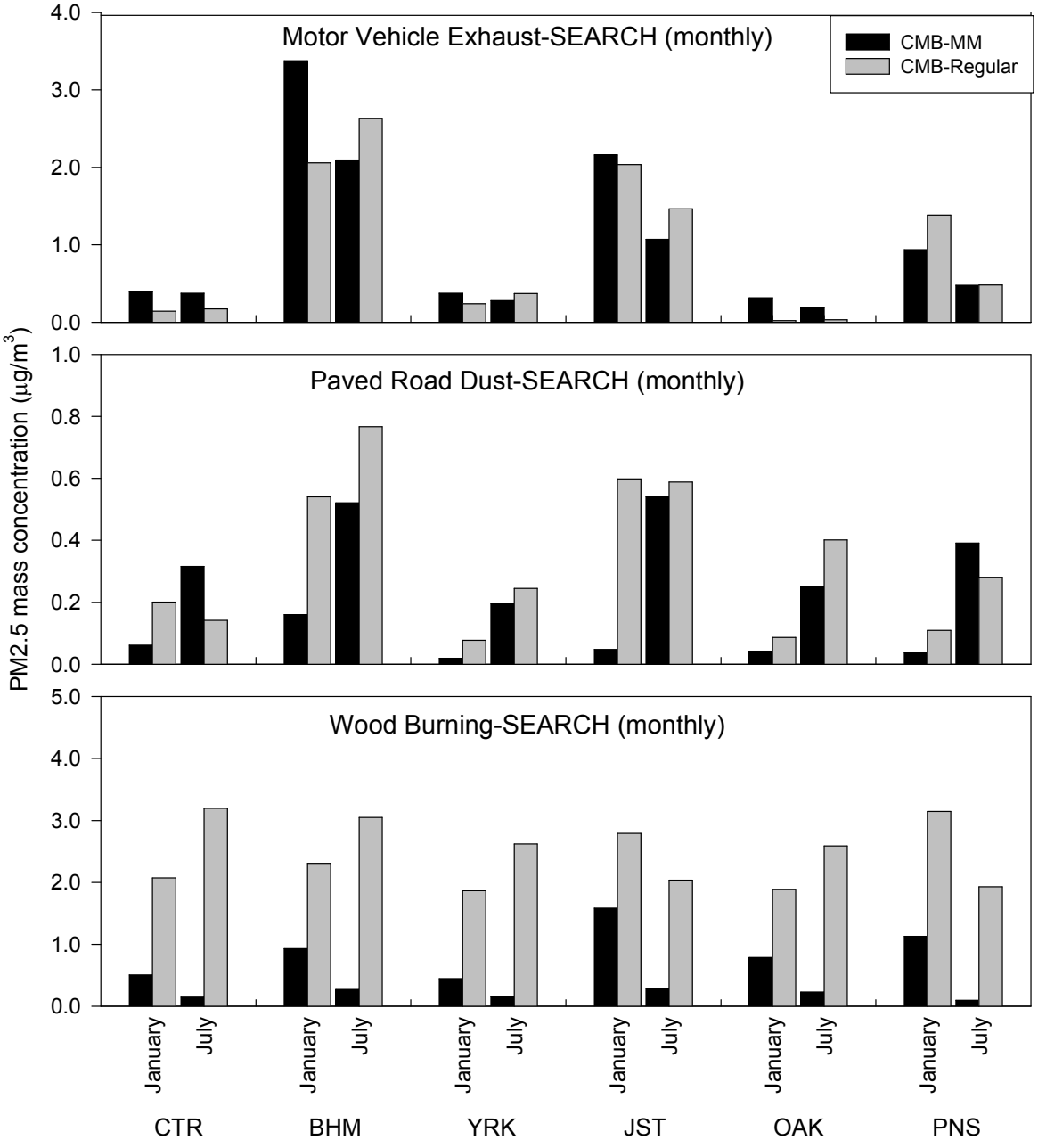

Figure 7.6. Comparison of motor vehicle exhausts, paved road dust and biomass burning contributing to $PM_{2.5}$ estimated by CMB-MM and CMB-Regular for SEARCH monthly (July, 2001; January, 2002) samples.

Table 7.1. Source Contributions to $PM_{2.5}$ Estimated by CMB-MM and CMB-Regular

SEARCH samples (monthly)	Motor vehicle exhausts (μg/m^3)			Paved road dust (μg/m^3)			Biomass burning (μg/m^3)		
	CMB-MM	CMB-Regular	Difference (%)	CMB-MM	CMB-Regular	Difference (%)	CMB-MM	CMB-Regular	Difference (%)
CTR-January	0.39	0.14	-64	0.06	0.20	233	0.51	2.07	306
CTR-July	0.38	0.17	-55	0.32	0.14	-56	0.15	3.19	2027
BHM-January	3.38	2.06	-39	0.16	0.54	238	0.93	2.31	148
BHM-July	2.09	2.63	26	0.52	0.77	48	0.27	3.05	1030
YRK-January	0.37	0.24	-35	0.02	0.08	300	0.45	1.86	313
YRK-July	0.28	0.37	32	0.20	0.24	20	0.15	2.62	1647
JST-January	2.16	2.03	-6	0.05	0.60	1100	1.58	2.79	77
JST-July	1.07	1.46	36	0.54	0.59	9	0.29	2.04	603
OAK-January	0.31	0.02	-94	0.04	0.09	125	0.79	1.89	139
OAK-July	0.19	0.03	-84	0.25	0.40	60	0.23	2.59	1026
PNS-January	0.94	1.38	47	0.04	0.11	175	1.13	3.14	178
PNS-July	0.48	0.48	0	0.39	0.28	-28	0.10	1.93	1830
Average- Jan.	1.26	0.98	-22	0.06	0.27	350	0.90	2.34	160
Average-July	0.75	0.86	15	0.37	0.40	8	0.20	2.57	1185

Notes: the difference (%) = 100* ((CMB-Regular) - (CMB-MM)) / (CMB-MM)

Similar spatial and temporal impacts were also found for monthly samples. Higher source contributions appeared in urban areas, and the maximum at N. Birmingham. Smaller seasonal variations were discovered in rural sites. Motor vehicle exhaust impacts in the summer are generally lower than those in the winter (Figure 7.6). The seasonal variation is expected since the effect of cold start conditions on motor vehicles in winter [*Manchester-Neesvig et al.*, 2003]. Significantly higher PM2.5 emissions are produced from gasoline-powered vehicles in winter compared with in summer [*Cadle et al.*, 1999].

However, results from the different methods are not always comparable to each other for motor vehicle exhaust. The source apportionment differences on monthly samples vary from -93% to 48% with the sites and seasons (Table 7.1; Figure 7.6).

7.3.4 Paved road dust

Comparable source contributions, 0.37 and 0.40 $\mu g.m^{-3}$, were calculated for paved road dust in the summer by both CMB-MM and CMB-Regular, respectively. This source contributed to about 2.1% of $PM_{2.5}$ mass. In the winter, paved road dust contributions are generally much lower than those in summer (Table 7.1; Figures 7.4-7.6). This seasonal variation is further supported by the higher ambient Al and Si concentrations, two elemental tracers and major components of road dust, in the summer when the average ambient concentrations of Al and Si are 3.9 and 2.4 times those in the winter. Warm weather and dry condition in summer might be a reason, which are conducive to road dust reentrainment by passing vehicles [*Fraser et al.*, 2003b]. Higher summer concentrations of Al and Si are also likely caused by long-range transport of African dusts, which are thought to be carried to the southeastern U.S. by the summer trade winds [*Prospero et al.*, 2001].

However, source contributions of paved road dust in CMB-MM show obvious differences with CMB-Regular results in the winter. The average contributions from CMB-Regular are 350% higher than those from CMB-MM (Table 7.1). Moreover, contributions of paved road dust in most winter samples from JST (daily) are not significant based on the results of CMB-MM modeling (Figure 7.5). Aluminum and silicon concentrations are so small that insignificant or negative contributions of paved road dust are calculated, as these two elements are also important species in other source such as vegetative detritus.

7.3.5 Biomass burning

Source contribution results did not agree on biomass burning at all SEARCH sites between CMB-MM and CMB-Regular approaches. The contributions range from 1.0% to 9% (summer and winter) in CMB-MM and from 14% to 23% (summer and winter) in CMB-Regular. In the summer, insignificant or much lower contributions of biomass burning were found with CMB-MM since levoglucosan, a unique organic tracer of biomass burning, is not detected or observed only with very low concentrations. Average levels of biomass burning identified by CMB-MM and CMB-Regular are 0.2 and 2.6 $\mu g.m^{-3}$, respectively, in the summer.

Moreover, CMB-MM results show noticeably higher contributions of biomass burning in the winter (Figures 7.4-7.6). However, slightly higher contributions or even opposite trends were observed at SEARCH sites from the calculated results using CMB-Regular. Those CMB-Regular apportionments are suspect since the levoglucosan concentrations observed in the winter were about 2-15 times higher than in the summer. This trend was also contrary to the local emission inventory where residential biomass burning and prescribed fire events in this region decrease from winter to summer [*Tian*, 2005].

7.3.6 Other Primary Source

Up to 3 additional primary sources were identified in CMB-MM besides those discussed above including meat cooking, natural gas combustion and vegetative detritus. They were found to be minor sources in this areas using CMB-MM.

Impacts from two industrial sources, coal combustion and cement kilns, were quantified using CMB-Regular with average contributions of about 2% (coal combustion) and 0.5% (cement kilns) to the $PM_{2.5}$ mass.

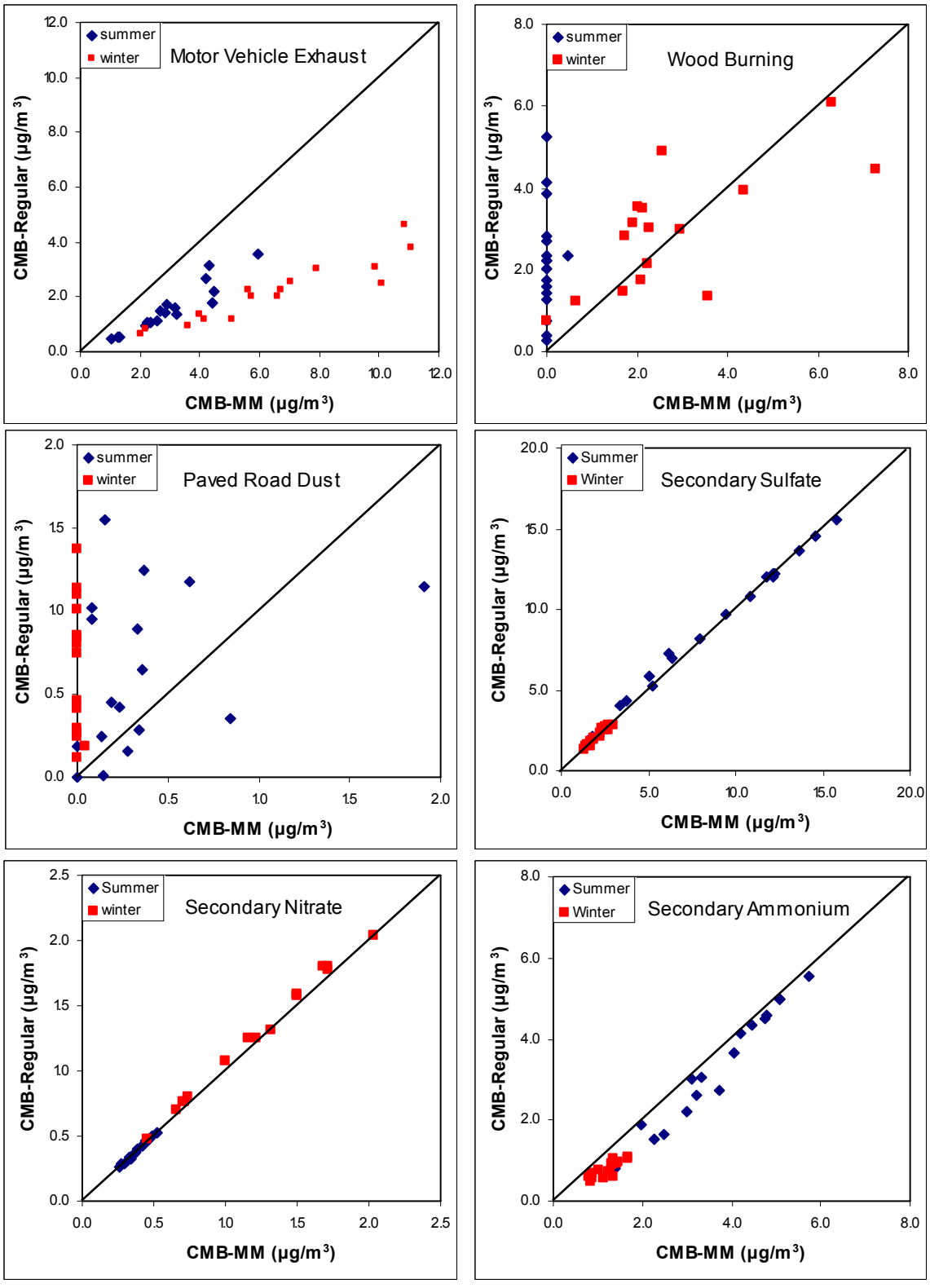

Figure 7.7. Correlations of source contributions to $PM_{2.5}$ estimated by CMB-MM and CMB-Regular for JST winter and summer samples (daily).

7.3.7 Secondary Sources

Both approaches indicated that secondary sulfate, secondary nitrate and secondary ammonium, accounted for the majority of measured $PM_{2.5}$ mass at the Southeast, especially in the summer. Those components make up 51% (summer) and 44% (winter), and 51% (summer) and 42% (winter) of the $PM_{2.5}$ mass as calculated using CMB-MM and CMB-Regular, respectively. Secondary sulfate is the largest component of $PM_{2.5}$ mass (36%, summer; 22%, winter) followed by secondary ammonium (13%, summer; 11%, winter), and secondary nitrate (2%, summer; 11%, winter). Only slight differences are found between the two approaches (Figure 7.7). The perfect agreement is expected since those components were estimated directly based on ambient observations of ions (SO_4^{2-}, NO_3^-, and NH_4^+) and molecular composition ($(NH_4)_2SO_4$, NH_4HSO_4, NH_4NO_3) either in CMB-MM or in CMB-Regular.

In addition to secondary inorganic ions, secondary organic aerosols (SOA) also contribute significantly to the $PM_{2.5}$ mass in this region. The "Other OC" in CMB-MM represents the difference between the measured OC and the sum of calculated primary OC, and would include SOA formed by atmospheric chemical reactions and other factors [*Zheng et al.*, 2002]. Secondary OC in CMB-Regular is calculated by subtracting primary OC (product of primary OC/EC ratio and EC) from the measured OC [*Turpin and Huntzicker*, 1995]. CMB-Regular and CMB-MM indicate that secondary OC might contribute up to 37-44% (winter-summer) and 39-73% (winter-summer) of the measured OC, respectively. This is consistent with the expected seasonal variation in the southeast. Higher temperatures, increased biogenic emissions and more intense solar radiation during the summer provide favorable conditions for photochemical activity and

secondary OC production [*Brown et al.*, 2002]. Secondary OC would account for about 11-9% (winter-summer) and 10-14% (winter-summer) in $PM_{2.5}$ mass calculated using CMB-Regular and CMB-MM, respectively.

7.3.8 Driving Forces of Source Apportionments

Discrepancies between the results from the two CMB approaches are caused by use of different fitting species in the models. To analyze the specific driving forces of source apportionments in the two methods, impacts of fitting species on source contributions were evaluated by correlation coefficients between species concentration and source contributions in numerous data sets. Species with higher correlation coefficients would be more powerful to drive the source apportionment in models (Tables 7.2 and 7.3).

Therefore, in CMB-Regular, motor vehicle exhaust contributions mainly depend on EC and OC, followed by Zn, K, and Fe. Paved road dust contributions are firstly correlated with K and Fe. Biomass burning contributions are also most impacted by EC, OC, K, and Zn. Other influential species in CMB-Regular include Mn (coal combustion), Si (cement kilns).

In CMB-MM, diesel vehicle and gasoline vehicle exhaust contributions are based on EC, OC, hopanes and steranes, followed by *n*-alkanes, and PAHs. Meat cooking contributions are mainly driven by cholesterol and oleic acid (F18:1). Biomass burning contributions are mostly correlated with levoglucosan. Other influential species include *n*-alkanes with high odd carbon numbers (vegetative detritus), and Al, Si (paved road dust). Unique tracers usually have higher correlation coefficients in CMB-MM. Many species influenced natural gas combustion impacts, though PAHs are dominated.

Table 7.2. Correlation Coefficients of Source Contributions and Species Concentrations in CMB-Regular for JST Daily Samples (n=39)

Species	NH_4HSO_4	$(NH_4)_2SO_4$	NH_4NO_3	Motor vehicle	Biomass burning	Coal combustion	Road dust	Cement	Secondary OC
SO_4^{-2}	0.50	**0.96**	-0.51	0.11	0.15	0.02	0.03	-0.15	-0.01
NO_3^-	-0.29	-0.51	**1.00**	0.41	0.39	0.07	0.15	0.06	0.28
NH_4^+	0.30	**0.99**	-0.51	0.13	0.16	0.07	0.05	-0.18	-0.03
EC	-0.19	0.18	0.40	**1.00**	**0.99**	0.23	0.48	-0.26	0.53
OC	-0.19	0.18	0.40	**1.00**	**0.99**	0.23	0.48	-0.26	0.53
As	0.46	-0.12	0.14	0.27	0.24	0.10	0.16	0.24	0.38
Ba	0.08	0.19	-0.24	-0.07	-0.03	-0.13	0.32	-0.04	-0.18
Br	-0.23	0.07	0.44	0.54	0.58	0.04	0.43	0.02	0.40
Cu	0.49	0.11	-0.15	-0.07	-0.09	0.10	-0.09	0.21	0.35
Mn	0.08	0.31	0.08	0.32	0.27	0.58	0.31	0.32	0.22
Pb	0.50	0.07	-0.09	0.00	-0.02	0.13	-0.05	0.23	0.40
Se	0.58	0.27	-0.21	0.08	0.06	0.18	0.18	0.30	0.29
Ti	0.16	0.17	-0.25	0.09	0.05	0.43	0.43	0.43	0.01
Zn	-0.32	-0.20	0.52	**0.65**	**0.62**	0.39	0.21	0.04	0.58
Al	0.08	0.20	-0.36	-0.13	-0.16	0.31	0.35	0.48	-0.05
Si	0.17	0.16	-0.31	-0.09	-0.13	0.31	0.45	0.54	-0.09
K	-0.10	-0.10	0.41	**0.64**	**0.66**	0.19	**0.64**	0.35	**0.60**
Ca	0.35	0.52	-0.25	0.21	0.18	0.42	0.31	0.32	0.17
Fe	0.08	0.18	0.15	**0.62**	0.57	0.53	0.59	0.36	0.45

Note: Significant figures (R>0.6) are shown in bold type.

Table 7.3. Correlation Coefficients of Source Contributions and Species Concentrations in CMB-MM for JST Daily Samples (n=56)

Species	Diesel Exhaust	Gasoline Exhaust	Meat Cooking	Biomass Burning	Road Dust	Natural Gas Combustion	Vegetative Detritus
OC	**0.84**	0.50	0.32	0.57	-0.28	0.53	0.68
EC	**0.96**	0.42	0.31	0.56	-0.27	0.47	0.60
Al	-0.17	-0.24	-0.21	-0.23	**0.97**	-0.15	-0.14
Si	-0.13	-0.17	-0.16	-0.19	**0.95**	-0.12	-0.08
Pentacosane	0.55	**0.83**	0.42	0.40	-0.18	0.64	**0.75**
Hexacosane	0.56	**0.81**	0.43	0.38	-0.22	0.64	**0.77**
Heptacosane	0.64	**0.87**	0.44	0.62	-0.25	**0.72**	**0.82**
Octacosane	0.61	**0.84**	0.43	0.53	-0.25	0.69	**0.81**
Nonacosane	0.69	0.68	0.37	0.49	-0.25	0.52	**0.97**
Triacontane	0.61	**0.84**	0.41	0.49	-0.26	**0.73**	**0.85**
Hentriacontane	0.67	0.58	0.36	0.35	-0.22	0.47	**0.99**
Dotriacontane	0.67	**0.79**	0.45	0.47	-0.26	**0.71**	**0.87**
Tritriacontane	0.69	**0.74**	0.41	0.43	-0.25	0.68	**0.93**
20S,R-5α(H),14β(H),17β(H)-Cholestanes	0.53	**0.98**	0.43	0.58	-0.25	**0.73**	0.62
20R-5α(H),14α(H),17α(H)-Cholestane	0.56	**0.97**	0.45	0.57	-0.24	**0.74**	0.64
20S,R-5α(H),14β(H),17β(H)-Ergostanes	0.51	**0.97**	0.43	0.49	-0.25	0.69	0.60
20S,R-5α(H),14β(H),17β(H)-Sitostanes	0.54	**0.99**	0.46	0.54	-0.26	**0.70**	0.65
22,29,30-Trisnorneohopane	0.49	**0.98**	0.44	0.57	-0.26	**0.73**	0.59
17α(H)-21β(H)-29-Norhopane	0.53	**0.99**	0.47	0.56	-0.27	**0.70**	0.64
17α(H)-21β(H)-Hopane	0.54	**0.98**	0.50	0.54	-0.28	0.69	0.65
9-Hexadecenoic acid	0.03	-0.16	0.25	0.14	-0.02	0.05	0.10

9-Octadecenoic acid	0.39	0.40	**0.70**	0.34	-0.16	0.62	0.51
Nonanal	0.21	-0.16	0.07	-0.04	-0.08	0.05	0.25
8,15-Pimaredienoic acid	0.39	0.41	0.60	0.18	-0.16	0.64	0.25
Pimaric acid	0.36	0.59	0.60	0.46	-0.20	**0.79**	0.34
Isopimaric acid	0.32	0.43	0.61	0.29	-0.15	**0.71**	0.27
Sandaracopimaric acid	0.34	0.54	0.59	0.45	-0.20	**0.74**	0.32
Abietic acid	0.17	0.27	0.67	0.34	-0.10	0.62	0.19
Levoglucosan	0.51	**0.72**	0.40	0.78	-0.28	0.60	0.64
Benzo(k)fluoranthene	0.55	**0.75**	0.55	0.52	-0.19	**0.98**	0.55
Benzo(b)fluoranthene	0.54	**0.80**	0.49	0.60	-0.20	**0.96**	0.59
Benzo(e)pyrene	0.62	**0.81**	0.51	0.56	-0.22	**0.92**	0.63
Indeno(1,2,3-cd)fluoranthene	0.41	0.43	0.52	0.53	-0.08	0.66	0.50
Indeno(1,2,3-cd)pyrene	0.56	0.65	0.60	0.54	-0.17	**0.82**	0.63
Benzo(ghi)perylene	0.67	**0.83**	0.49	0.54	-0.23	**0.81**	**0.72**
Cholesterol	0.38	0.63	**0.79**	0.44	-0.26	0.61	0.51

Note: Significant figures (R>0.7) are shown in bold type.

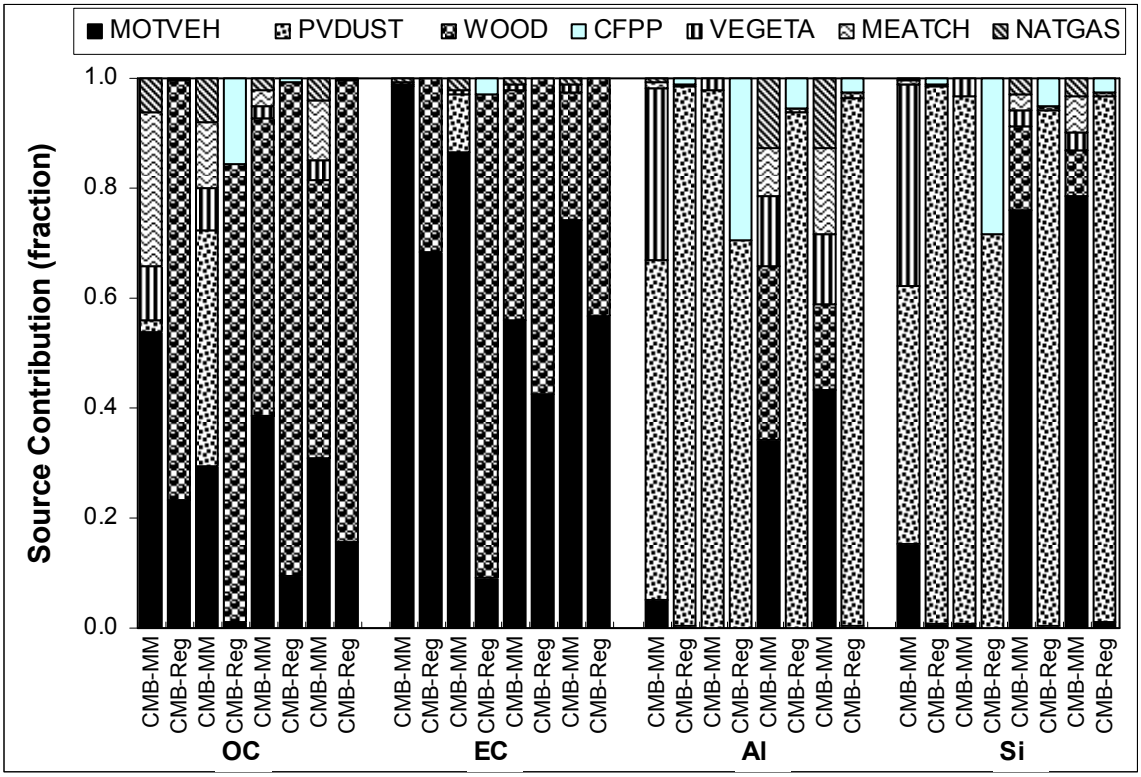

Figure 7.8. Comparison of source contributions to chemical species applied in CMB-MM and CMB-Regular (four JST samples are used: 07/17/01, 07/25/01, 01/12/02, and 01/27/02, in turn from left to right; OC indicates Primary OC; the fraction of source contribution was normalized to identified primary OC).

Comparison of influential species would explain some similarities and differences between CMB-Regular and CMB-MM estimations discussed previously. Most agreements of source contributions were found on motor vehicle exhaust since OC and EC are primary driving species in both models. Therefore, it is expected that fairly comparable contributions were estimated using the two methods. However, a few secondarily influential species are also impacting this source contribution in CMB-Regular (Zn, K, and Fe) and in CMB-MM (hopanes, steranes, *n*-alkanes, and PAHs). Discrepancies of source contributions, therefore, happened between the two approaches under comprehensive driving of those influential factors. Unlike motor vehicle exhaust, paved road dust did not own any common driving species in CMB-Regular (K and Fe) and in CMB-MM (Al and Si) even though both methods used elements as influential factors for this source. As major components of crustal material, Al and Si might provide better support for road dust estimations. Likewise, biomass burning contributions depended on the unique tracer, levoglucosan, in CMB-MM while OC, EC, K and Zn are more influential in CMB-Regular. As a result, it is not surprising that there are large differences existing between the models.

7.3.9 Source Contributions to Fitting Species

To explain these differences of source apportionments, further analysis are stated below. Figure 7.8 illustrates source contributions to specific species in CMB-MM and CMB-Regular. Four samples from Jefferson Street, Atlanta were randomly chosen as examples, including two summer samples (07/17/01 and 07/25/07) and two winter samples (01/12/02 and 01/27/02). About 42% (summer) and 35% (winter) of the primary OC are contributed by motor vehicle exhaust in CMB-MM. Biomass burning is not a

significant source in the summer while it contributes high percentage for primary OC, 53%, as motor vehicle exhaust does in the winter. In contrast, motor vehicle exhaust in CMB-Regular only contributed 12% (summer) and 13% (winter) of the primary OC, and too much primary OC, about 84%, is contributed by biomass burning even in the summer. In CMB-Regular, both EC and OC play more major roles in the quantification of biomass burning than K, which also is an influential species of other sources such as cement kilns and soil dust. Sharing the same influential fitting species, EC and OC, source contributions of motor vehicle exhaust and biomass burning was not distinguished well using CMB-Regular model. Here, as a result, biomass burning contributions are inclined to be overestimated by CMB-Regular while motor vehicle exhaust contributions are probability underestimated. Unlike source apportionments using CMB-Regular, meat cooking was not neglected and definitely a significant source of primary OC (20% in the summer and 7% in the winter) in CMB-MM. The ambient data of unique fitting species, levoglucosan and cholesterol/nonanal, could provide, to some extent, supports for their apportionment. The estimated-measured radios of levoglucosan and nonanal in CMB-MM are around 0.7 and 1.0 for the samples discussed above, respectively.

Most EC, up to 90%, was from motor vehicle exhaust in CMB-MM while the contribution of the same source to EC was less than 50% in CMB-Regular, with the remains mostly contributed by biomass burning. This dissimilar explanation is also corresponding to source contributions to primary OC we stated above. Some source contributions of biomass burning were mixed with ones of motor vehicles in CMB-regular.

Most of the ambient Al and Si come from paved road dust in CMB-Regular without obvious seasonal changes. However, a few sources other than paved road dust contributed significantly to Al and Si in CMB-MM, especially in winter when almost all Al and Si are from other sources instead of paved road dust (Figure 7.8). Underestimation of paved road dust might be caused by incorrect reconstruction of ambient Al and Si in CMB-MM in the presence of other sources such as vegetative detritus and motor vehicle exhaust. Without relative unique tracers, paved road dust contributions possibly mix up with ones from other sources where Al and Si are also account for significant abundances.

7.4 Conclusions

Major emission sources have been apportioned by two CMB-based approaches, one using traditional elemental species, and the other using organic molecular markers. Similar spatial and temporal impacts on source contributions are usually found in both approaches. However, comparisons between the two approaches also indicate a few significant discrepancies.

More sources of OC in $PM_{2.5}$ were distinguished by CMB-MM including diesel vehicle exhaust, gasoline vehicle exhaust, meat cooking, vegetative detritus and natural gas combustion. However, a few more industrial emission sources were quantified using CMB-Regular (coal combustion and cement kilns) with available inorganic species-based source profiles. The main disadvantage of the CMB-regular approach is that it lacks ability to distinguish source impacts of OC where there is little difference in their elemental fingerprints. Motor vehicle exhaust contributions are inclined to mix up with

biomass burning contributions. The main disadvantage of the CMB-MM approach is lack of molecular marker-based source profiles and decay of organic tracers in atmosphere.

The intercomparison of the two approaches also indicates that source apportionment results calculated by the CMB model are sensitive to source profiles and fitting species applied in the models. To effectively decrease bias or uncertainties of source contributions, real-world and representative source profiles should be developed and applied for local emissions, especially for those major sources, such as mobile emissions, biomass burning, and meat cooking. It is also important to select and use appropriate or significant fitting species in the model. Further study is expected in these fields to improve CMB-MM performance.

Acknowledgements

This work was funded in part by the U.S. Environmental Protection Agency STAR grants (R832159, R828976 and R831076). We would like to thank Georgia Power (Southern Company) for their support of work in Laboratory for Atmospheric Modeling, Diagnostics, and Analysis (LAMDA) at Georgia Institute of Technology in this study area. The EC, OC, $PM_{2.5}$ mass, elemental and ionic data are kindly provided by the SEARCH study and STN network.

CHAPTER 8

CONCLUSIONS AND FUTURE RESEARCH

8.1 Conclusions

Airborne particulate matter (PM), especially fine particulate matter ($PM_{2.5}$, particles with an aerodynamic diameter equal to or less than 2.5 μm), has been linked to human health effect, reduced visibility, climate change, and other air quality concerns. Typically, the major contributors of airborne $PM_{2.5}$ include mobile source emissions, biomass burning, and secondary sources with anthropogenic and biogenic nature in origin. The metropolitan Atlanta, GA area, located in the southeastern U.S. and populated by over 5.4 million residents, is of particular interest due to high emissions of mobile sources, biomass burning, coal-fired power plants, and biogenic volatile organic compounds (VOCs), with vigorous photochemical processes occurring as well.

Effective control strategies for air pollutants require an investigation of chemical composition of airborne $PM_{2.5}$ in this area as well as identification and quantification of specific source impacts on ambient air quality. In this research, various $PM_{2.5}$ samples were collected and analyzed, which are impacted or dominated by on-road mobile and other typical urban emissions, regional transport sources, prescribed burning plumes, wildfire plumes, as well as secondary sources with anthropogenic and biogenic nature in origin. Detailed composition of $PM_{2.5}$ and fine organic matter was investigated, including organic carbon (OC), elemental carbon (EC), water-soluble OC (WSOC), ionic species, tens of trace metals, and over one hundred of solvent-extractable organic compounds.

Day-night, seasonal and spatial variations of $PM_{2.5}$ composition were studied as well. Impacts or source contributions of major sources were identified and quantified through receptor-based source apportionment models. The modeling results were assessed by multiple approaches (roadway-related OC, OC/EC ratios, adjusted WSOC, and SOA tracers) to provide information as comprehensive as possible for $PM_{2.5}$ control strategies. Moreover, season- and location-specific source profiles were developed to reflect more real-world and representative emission characterizations of on-road mobile sources in Atlanta, aged prescribed burning plumes, and wildfire plumes. Secondary organic aerosol (SOA), a major component of $PM_{2.5}$, was also explored for tracers, sources and contributions.

Roadside, urban and rural comparison of primary and secondary organic molecular markers in ambient PM2.5

Approximately 110 solvent-extractable particulate organic compounds were identified and quantified by gas chromatography/mass spectrometry (GC/MS). Results indicate that primary organic compounds usually exhibit different attributes of day vs. night, whereas secondary organic tracers varied little. Much higher concentrations of automotive-related primary organic compounds were observed at the roadside site, including *n*-alkanes, hopanes, steranes, and polycyclic aromatic hydrocarbons (PAHs). It is interesting to note that no significant seasonal difference in hopanes and steranes was observed at all sites. Levoglucosan and resin acids, organic tracers of biomass burning, show little spatial variation, especially in the winter when biomass burning is so important that a regionwide background level was measured at all sites. However, significant seasonal variations were found for these biomass burning tracers with much

higher levels in the winter. Cholesterol levels were similar at the two urban sites and significantly lower at Yorkville. Higher concentrations of cholesterol were found in the winter.

Season-specific on-road mobile source profiles for primary OC were developed in Atlanta by using differences in organic species concentrations between the roadside site and the nearby campus site. The calculated on-road source profiles differ from those mobile source profiles measured in the laboratories elsewhere, suggesting that atmospheric decay and/or gas-particle partitioning may play a role in the seasonal variations of mobile source profiles. Therefore, seasonal impacts should be considered in receptor-based source apportionment studies.

Significant concentrations were measured in both seasons for *cis*-pinonic acid and pinic acid, organic tracers of monoterpene-originated SOA. However, 2-methyltetrols, organic tracers of isoprene-originated SOA, were observed to be significant only in the summer. Little correlation is found between 2-methyltetrols with *cis*-pinonic or pinic acid, though *cis*-pinonic and pinic acids are strongly correlated. Aromatic and aliphatic diacids also show strong correlation, implying that atmospheric processes are equally important for both anthropogenic and biogenic VOC.

Characterization of airborne $PM_{2.5}$ at roadside, urban and rural sites in the summer and the winter

Ambient $PM_{2.5}$ concentrations were observed to be about two times higher at all sites in the summer. Organic matter (OM), ammonium, and sulfate are major components of $PM_{2.5}$ in both summer and winter. The sum of these three constituents accounts for 70/66% of the $PM_{2.5}$ mass in the summer/winter, respectively, at the roadside site, 83/78%

at the campus site, and 92/78% at the Yorkville site. Sulfate dominated $PM_{2.5}$ in the summer, particularly on haze days. Nitrate is a major component of $PM_{2.5}$ in the winter, but contributed little in the summer. EC and fine soil dust are significant constituents of the urban $PM_{2.5}$.

Particulate OM was estimated through mass balance analysis of gravimetric $PM_{2.5}$, and the OM/OC ratio was found to depend on season and location. There were significant seasonal variations in OM/OC ratios at the campus and the Yorkville sites, whereas the OM/OC ratio varied little in both seasons at the roadside site. Significantly higher concentrations of automotive-related species were detected at the roadside, including OC, EC, iron, and copper. Season-specific on-road mobile source profiles for primary $PM_{2.5}$ were developed in Atlanta by using differences in individual species concentrations between the roadside site and the nearby campus site. The calculated source profiles differ from in-use mobile source profiles developed elsewhere from the laboratory tests.

The summer concentrations of WSOC are roughly two times the winter, suggesting enhanced formation of SOA in the atmosphere. This is supported by strong correlations between WSOC and OC as well as secondarily formed species such as sulfate, ammonium, and SOA tracers (e.g., dicarboxylic acids, 2-methyltetrols, *cis*-pinonic acid, and pinic acid). Homogeneous distributions of WSOC on a regional scale reflected predominant impacts from SOA in the summer and from biomass burning emissions in the winter. It was estimated that biomass burning contributed less than 8% of WSOC in the summer and over 60% of WSOC in the winter. In addition, on-road mobile source is likely a minor contributor of ambient WSOC, especially in the winter.

Source apportionment of $PM_{2.5}$ organic carbon and SOA impact: spatial and temporal variations

Up to eight primary sources of fine OC were identified and quantified by the molecular marker-based chemical mass balance (CMB-MM) model, including diesel vehicle exhaust, gasoline vehicle exhaust, meat cooking, biomass burning, road dust, natural gas combustion, cigarette smoke, and vegetative detritus. On-road vehicle emissions (or diesel vehicle and gasoline vehicle exhausts) play an important role on composition of ambient OC, especially at the roadside and the nearby sites. Meat cooking, biomass burning, road dust, and cigarette smoke are also significant primary sources of OC at the urban sites. Although the fleet was dominated by gasoline-powered vehicles, diesel vehicle emissions contributed 46% and 24% of the identified OC at the roadside and the campus sites in the summer, respectively, and gasoline vehicle emissions contributed 26% and 23%. Emission control of diesel vehicle exhausts is probably more important for air quality improvement. In the winter, biomass burning source was so important, contributing 46%, 56%, and 53% of the total identified primary OC alone at the roadside, the campus, and rural sites, respectively. This suggests that active biomass burning activities for residential heating greatly increase biomass burning emissions in a cold season.

'Other OC', unidentified OC mass by the CMB-MM model, was large in the summer, taking over 70% of the measured OC, whereas the total measured OC in the winter was well explained by the primary sources. Abundant 'Other OC' in the summer instead of in the winter implies that secondary OC would be the predominant component of the 'Other OC'. This is further supported by strong or significant correlations between

"Other OC" and secondary sulfate, secondary ammonium, WSOC_adj (WSOC subtracting biomass burning effects), and the EC tracer-estimated SOC. In particular, fraction boundaries of the SOC estimate were inferred by using the WSOC_adj value as the lower limit and the CMB-MM-calculated 'Other OC' as the upper limit. Results indicate that 38–59%, 51–74%, and 74–87% of OC were SOC in the summer at the roadside, the campus, and the Yorkville sites, respectively, whereas 13–17%, 18–27%, and about 12% of OC were contributed by SOA in the winter. The average SOC fractions estimated by the EC tracer method are comparable to the WSOC_adj (SOC) values in both seasons.

Organic composition of carbonaceous aerosols in an aged prescribed fire plume

Large increases in $PM_{2.5}$ and OC were captured at the metropolitan Atlanta area, which were caused by an aged prescribed fire plume through direct biomass burning emissions and enhanced formation of biogenic SOA in the atmosphere. A detailed chemical speciation of carbonaceous aerosols was conducted by GC/MS analysis.

Ambient concentrations of many organic species (levoglucosan, resin acids, retene, *n*-alkanes and *n*-alkanoic acids) associated with biomass burning emissions were significantly elevated on the event day. Levoglucosan increased by a factor of 10, while hopanes, steranes, cholesterol and major PAHs did not show obvious increases. The presence of abundant resin acids and retene indicated predominant softwood (conifers) burning. Increases in resin acids were accompanied by high levels of dehydroabietic acids and 7-oxodehydroabietic acids, mainly formed by atmospheric processes during transport. Carbon-number predominance for *n*-alkanes (odd over even) and *n*-alkanoic acids (even over odd) suggested that emissions from heat-exposed vegetation are

important as one of major sources for increasing OC, especially secondary OC. Results indicate that large quantities of biogenic VOC and semivolatile organic compounds (SVOCs) were released both as products of combustion and unburned vegetation heated by the fire. Higher leaf temperature can stimulate biogenic VOC and SVOC emissions, which enhanced formation of SOA in the atmosphere even in the winter. This is supported by elevated ambient concentrations of secondary organic tracers (dicarboxylic acids, 2-methyltetrols, *cis*-pinonic acid and pinic acid).

An approximate source profile was developed for the aged prescribed fire plume to help better understand the evolution of biomass burning emissions and for use in source impact assessment.

Detailed chemical characterization and aging of wildfire aerosols in the southeastern U.S

The metropolitan Atlanta and nearby areas were heavily impacted for hours and even days by massive wildfire smoke plumes from April through June 2007. The highest increases in hourly and 24-hr $PM_{2.5}$ were observed to reach over 340 and 100 μg m^{-3}, respectively. Results indicate that wildfire-derived $PM_{2.5}$ was dominated by OM, making up 60-85% of the $PM_{2.5}$ mass. On the smoke days, large increases were observed for biomass burning tracers (levoglucosan, resin acids, retene, etc.). In particular, levoglucosan increased by 46, 161, and 13 times, respectively, at the downwind Atlanta, Bibb and Coffee sites, and contributed 6%, 11%, and 5% of the total OC. The wildfire emissions also caused large increases of *n*-alkanes and *n*-alkanoic acids. *n*-Alkanes exhibited distinct odd carbon number predominance, and *n*-alkanoic acids had a strong even-to-odd carbon number predominance on the smoke days, suggesting a dominant

contribution from waxes on plant leaves. It is interesting to note that ambient hopanes increased significantly during wildfire smoke events, implying that hopanes, which are thought as unique tracers of mobile source, can also be produced by thermal alteration of biogenic hopanoid precursors in the atmosphere.

Significant increases were also seen in some inorganic species, such as water-soluble potassium (K^+), ammonium (NH_4^+), nitrate (NO_3^-), sulfate (SO_4^{2-}), and EC. The ratios of levoglucosan vs. inorganic indicators of biomass burning (K^+ and EC) did not show significant decreases from the wildfire origin to the monitors 400 km downwind, implying that there is no significant atmospheric decay during half-day transport even in a warm season. However, resin acids are subject to alteration in the atmosphere, leading to their ratios to levoglucosan being variable over time.

Secondary organic tracers, 2-methyltetrols and pinic acid, were observed with significantly higher concentrations at the downwind sites, providing further support for enhanced formation of biogenic SOA. However, *cis*-pinonic acid, another photo-oxidation product of monoterpenes, did not show significant increases, implying that its mechanism of formation and atmospheric fate in aged wildfire plumes is probably different from pinic acid. In addition, elevated aromatic and aliphatic diacids were observed at all downwind sites on the smoke days, suggesting that they are not only secondarily created from anthropogenic emissions but also formed from or enhanced by wildfire-derived biogenic emissions in the atmosphere.

The source profiles for aged wildfire fire plumes were developed as well, which can be used for improving source apportionment of biomass burning by CMB modeling.

Analysis of source apportionment applications for $PM_{2.5}$ in the Southeast: intercomparison between two approaches

Major emission sources have been apportioned by two CMB-based approaches, one using traditional elemental species (CMB-Regular) and the other using organic molecular markers (CMB-MM). Similar spatial and temporal impacts on source contributions are usually found in both approaches. Secondary sources including secondary sulfate, ammonium, and nitrate contribute the majority of the $PM_{2.5}$ mass in the southeastern U.S. in both summer (>50%) and winter (>40%). Motor vehicle exhaust, paved road dust, and biomass burning sources were calculated both using CMB-Regular and CMB-MM. Motor vehicle exhausts and biomass burning are the major primary sources of $PM_{2.5}$ in this area. However, comparisons between the two approaches also identify a few significant discrepancies.

More sources of OC in $PM_{2.5}$ were distinguished by CMB-MM including diesel vehicle exhaust, gasoline vehicle exhaust, meat cooking, vegetative detritus, and natural gas combustion. However, a few more industrial emission sources were quantified using CMB-Regular (coal combustion and cement kilns) with available inorganic species-based source profiles. The main disadvantage of the CMB-regular approach is that it lacks ability to distinguish major sources of OC, especially those without elemental fingerprints. For example, it was not rare to see that motor vehicle exhaust mixed up with biomass burning source. The main disadvantage of the CMB-MM approach is lack of local molecular marker-based source profiles and stability of organic tracers in the atmosphere. Further research is expected as to how to integrate two approaches for better source apportionment of $PM_{2.5}$.

8.2 Future Research

Rethinking Tracers of PM2.5 Sources: Implication of Cross-Correlation Analysis on Inorganic and Organic Components

Various airborne $PM_{2.5}$ samples have been collected and analyzed in this research, which are directly impacted or dominated by on-road mobile and other typical urban emissions, regional transport sources, prescribed burning plumes, wildfire plumes, as well as secondary sources with anthropogenic and biogenic nature in origin. Detailed $PM_{2.5}$ characterization has also been investigated seasonally and spatially, including over one hundred of organic compounds, ionic species, and tens of trace metals, some of which were proposed or proved as relatively unique tracers for specific sources. These measurements provide a great opportunity to screen out those potential tracers of $PM_{2.5}$ sources and to further evaluate the tracers currently applied in source apportionment models. Statistical cross-correlation analysis of $PM_{2.5}$ components will be performed in various intensive emissions to better link measured constituents to specific sources. Spatial and seasonal variations of their correlations not only provide information to select appropriate fitting species or refine the selection in receptor-based models but also help better understand contributions to $PM_{2.5}$ and OC from primary and secondary sources. Preliminary results indicate that water-soluble potassium (K+) and zinc are likely not suitable as tracers of biomass burning and gasoline vehicle emissions in receptor-based models, respectively, recognizing that they can also come from unknown or unidentified sources. SOA tracers will also be assessed for potential sources. For example, aromatic and aliphatic diacids may be formed in the atmosphere both from anthropogenic and biogenic precursors.

Source Apportionment of PM2.5 and OC Using the Molecular Marker-Based CMB-LGO Method

Through introducing some gaseous measurements, together with boundary constraints of fitting species, the chemical mass balance-Lipschitz Global Optimizer (CMB-LGO) method provides a possibility to optimize the current source apportionment models, e.g., the CMB-MM air quality model. In particular, application of gaseous tracers of mobile sources, CO and NO_x, may be helpful in splitting $PM_{2.5}$ source contributions between diesel vehicle emissions and gasoline vehicle emissions. In the future study, the CMB-LGO model will be used for source apportionment of $PM_{2.5}$ impacted by intensive emissions, such as on-road emissions, prescribed burning plume, wildfire plumes, and secondary sources, with focus on application of organic molecular markers. Constraints in individual species could be determined through overall literature review of ambient levels and local emission inventories. Calculated source contribution results will be assessed by $PM_{2.5}$ and OC measurements in a few special case studies, e.g., measurement between the roadside site and the nearby campus site, as well as observation in prescribed burning and wildfire plumes. Furthermore, molecular marker-based source profiles will be approximated for major primary sources in this area by application of CMB-LGO.

Comparative Analysis of Source Contributions Apportioned by the CMB Model Using New Developed Source Profiles

Season-specific on-road mobile source profiles for primary OC and primary $PM_{2.5}$ were newly developed in Atlanta, as shown in Chapters 2 and 3. Source

composition profiles were also built for aged prescribed burning plumes and aged wildfire plumes in this research, as shown in Chapters 5 and 6. How could these real-world and representative source profiles improve or change source apportionment performance of the CMB model, which is applied to the metropolitan Atlanta area and the southeastern U.S.? To address this question, these newly developed source profiles, together with other available mobile source and biomass burning profiles tested in the laboratories elsewhere, will be applied in source apportionment using the CMB model. The sensitivities of CMB modeling results will be investigated for these different source profiles. Moreover, the ambient $PM_{2.5}$ data from the roadside and the nearby campus sites will be used to evaluate performance of various mobile source profiles in the CMB model, whereas the ambient data from the prescribed burning plume and wildfire plumes for assessing these biomass burning profiles. Finally, these assessments are vital in providing the best estimates of $PM_{2.5}$ and OC source apportionment using CMB.

APPENDIX A

Table A.1. Detection Limits (MDL) of Organic Compounds Quantified with The GC/MS Method (unit: ng m^{-3}).

Resin Acids	**MDL**	**Hopane and Sterane**	**MDL**
Isopimaric acid	0.038	17α(H)-21β(H)-Hopane	0.010
Dehydroabietic acid	0.028	22,29,30-Trisnorhopane	0.010
Abietic acid	0.032	20S,R-5α(H),14β(H),17β(H)-Cholestanes	0.008
1,2-Benzenedicarboxylic acid	0.008	20R-5α(H),14α(H),17α(H)-Cholestane	0.006
1,4-Benzenedicarboxylic acid	0.005	20S,R-5α(H),14β(H),17β(H)-Ergostanes	0.008
1,3-Benzenedicarboxylic acid	0.008	20S,R-5α(H),14β(H),17β(H)-Sitostanes	0.019
Fatty Acids		**PAHs**	
Tetradecanoic acid	0.010	Fluoranthene	0.012
Hexadecanoic acid	0.014	Pyrene	0.005
Octadecanoic acid	0.007	Benz(a)anthracene	0.005
Eicosanoic acid	0.022	Chrysene/Triphenylene	0.006
Docosanoic acid	0.022	Benzo(b)fluoranthene	0.029
Tetracosanoic acid	0.030	Benzo(k)fluoranthene	0.018
Octacosanoic acid	0.086	Benzo(a)pyrene	0.010
Triacontanoic acid	0.049	Indeno(cd)pyrene	0.007
9-Hexadecenoic acid	0.032	Benzo(ghi)perylene	0.011
9,12-Octadecanedienoic acid	0.031	Coronene	0.007
9-Octadecenoic acid	0.024		
Alkanedioic Acids		***n*-Alkanes**	
Propanedioic acid	0.025	Heptadecane	0.008
Butanedioic acid	0.006	Octadecane	0.012
Pentanedioic acid	0.039	Eicosane	0.016
Hexanedioic acid	0.014	Tetracosane	0.031
Heptanedioic acid	0.014	Octacosane	0.024
Octanedioic acid	0.014	Triacontane	0.046
Nonanedioic acid	0.013	Dotriacontane	0.035
Others			
2-Methyltetrols	0.090		
cis-Pinonic acid	0.040		
Pinic acid	0.070		

APPENDIX B

Table B.1. Source Apportionment of Fine Organic Carbon at The Three Sampling Sites in Summer 2005 (unit: μg m^{-3})

Sampling Date	Diesel Exhaust	Gasoline Exhaust	Meat Cooking	Wood Combustion	Road Dust	Cigarette Smoke	Natural Gas Combustion	Vegetative Detritus	Identified OC	Measured OC	Other OC	OC Mass Identified (%)
FQ0615A1	0.641	0.308	0.000	0.135	0.140	0.012	0.004	0.106	1.346	5.545	4.199	24.3
FQ0615A2	0.783	0.793	0.580	0.478	0.132	0.059	0.000	0.053	2.878	6.343	3.465	45.4
FQ0616A1	0.185	0.254	0.316	0.268	0.146	0.026	0.000	0.043	1.236	4.312	3.076	28.7
FQ0616A2	0.203	0.253	0.168	0.407	0.077	0.027	0.000	0.031	1.166	4.914	3.748	23.7
FQ0617A1	0.019	0.293	0.020	0.143	0.008	0.007	0.003	0.051	0.543	4.624	4.080	11.8
FQ0617A2	0.762	0.350	0.079	0.725	0.129	0.118	0.000	0.083	2.247	7.008	4.761	32.1
FQ0618A1	0.218	0.313	0.081	0.296	0.016	0.000	0.000	0.077	1.001	5.979	4.977	16.7
FQ0615B1	2.177	0.809	0.409	0.126	0.169	0.030	0.000	0.121	3.841	8.659	4.818	44.4
FQ0615B2	1.879	0.840	0.562	0.780	0.209	0.082	0.003	0.157	4.512	8.869	4.357	50.9
FQ0616B1	1.823	1.309	0.104	0.414	0.169	0.149	0.000	0.337	4.305	7.167	2.862	60.1
FQ0616B2	0.841	0.383	0.044	0.506	0.084	0.049	0.001	0.098	2.005	7.237	5.232	27.7
FQ0617B1	1.565	0.770	0.134	0.108	0.088	0.184	0.011	0.098	2.958	6.545	3.586	45.2
FQ0617B2	1.527	0.629	0.142	0.561	0.000	0.087	0.000	0.023	2.969	9.241	6.272	32.1
FQ0618B1	0.815	1.129	0.011	0.266	0.085	0.090	0.000	0.065	2.460	9.407	6.947	26.2
FQ0708A	0.374	0.402	0.593	0.522	0.147	0.024	0.000	0.033	2.095	5.855	3.760	35.8
FQ0709A	0.058	0.069	0.072	0.136	0.364	0.017	0.000	0.006	0.723	2.829	2.106	25.6
FQ0718A	0.215	0.421	0.037	0.154	0.199	0.087	0.001	0.011	1.126	4.758	3.632	23.7
FQ0719A	0.774	0.287	0.689	0.388	0.033	0.115	0.008	0.057	2.350	5.622	3.272	41.8
FQ0723A	0.338	0.443	0.703	0.652	0.000	0.170	0.000	0.078	2.384	7.113	4.729	33.5
FQ0724A	0.442	0.584	0.020	0.392	0.110	0.022	0.000	0.048	1.618	10.664	9.046	15.2
FQ0725A	0.523	0.603	0.319	0.666	0.166	0.109	0.003	0.062	2.450	10.589	8.139	23.1
FQ0726A	0.333	0.299	0.253	0.432	0.306	0.057	0.000	0.012	1.691	11.274	9.583	15.0
FQ0708B	0.298	0.085	0.057	0.149	0.078	0.000	0.000	0.014	0.680	4.531	3.851	15.0
FQ0709B	0.225	0.066	0.029	0.078	0.220	0.000	0.001	0.019	0.638	2.763	2.125	23.1
FQ0718B	0.177	0.025	0.343	0.123	0.026	0.000	0.002	0.017	0.713	3.435	2.722	20.7
FQ0719B	0.208	0.151	0.023	0.081	0.016	0.000	0.003	0.010	0.492	3.367	2.875	14.6
FQ0723B	0.156	0.028	0.000	0.220	0.012	0.000	0.001	0.015	0.432	4.978	4.546	8.7
FQ0724B	0.000	0.050	0.112	0.188	0.025	0.000	0.000	0.007	0.381	5.626	5.245	6.8
FQ0725B	0.051	0.028	0.000	0.223	0.098	0.000	0.000	0.009	0.409	7.220	6.811	5.7
FQ0726B	0.076	0.013	0.050	0.309	0.136	0.000	0.000	0.010	0.593	7.735	7.141	7.7

Average	0.590	0.400	0.198	0.331	0.113	0.051	0.001	0.058	1.741	6.474	4.732	26.2

Note: 'A1', 'A2', 'B1' and 'B2' indicate the daytime campus, nighttime campus, daytime highway and nighttime highway 12-hr samples, respectively. 'A' and 'B' denote the campus and the Yorkville 24-hr samples.

Table B.2. Source Apportionment of Fine Organic Carbon at The Three Sampling Sites in Winter 2006 (unit: $\mu g\ m^{-3}$)

Sampling Date	Diesel Exhaust	Gasoline Exhaust	Meat Cooking	Wood Combustion	Road Dust	Cigarette Smoke	Natural Gas Combustion	Vegetative Detritus	Identified OC	Measured OC	Other OC	OC Mass Identified (%)
FQ0119B1	1.350	0.988	0.958	1.778	0.010	0.258	0.103	0.183	5.627	4.038	-	139.3
FQ0119B2	1.724	1.065	1.080	4.877	0.056	0.138	0.000	0.100	9.039	10.454	1.415	86.5
FQ0120B1	1.788	0.529	0.521	2.977	0.082	0.084	0.000	0.051	6.032	9.154	3.122	65.9
FQ0120B2	0.693	0.479	0.125	2.914	0.033	0.042	0.000	0.055	4.342	7.879	3.536	55.1
FQ0121B1	0.836	0.267	0.571	1.654	0.004	0.047	0.004	0.034	3.417	4.653	1.236	73.4
FQ0121B2	0.504	1.324	1.926	6.429	0.000	0.371	0.087	0.302	10.943	7.270	-	150.5
FQ0122B1	0.262	1.694	1.660	4.697	0.000	0.349	0.100	0.138	8.901	3.764	-	236.5
FQ0122B2	0.755	1.028	0.417	1.223	0.002	0.389	0.056	0.000	3.869	2.084	-	185.7
FQ0123B1	2.752	0.729	0.737	0.852	0.000	0.403	0.173	0.039	5.684	6.327	0.643	89.8
FQ0123B2	0.478	0.763	0.146	1.838	0.003	0.032	0.004	0.009	3.272	2.446	-	133.8
FQ0124B1	0.950	0.669	0.154	0.685	0.048	0.066	0.029	0.018	2.619	3.197	0.578	81.9
FQ0124B2	0.824	0.514	0.061	0.783	0.019	0.039	0.021	0.040	2.301	2.936	0.635	78.4
FQ0125B1	0.751	0.859	0.233	0.741	0.037	0.049	0.016	0.027	2.713	3.274	0.562	82.8
FQ0125B2	0.475	0.412	0.014	0.950	0.048	0.042	0.012	0.025	1.978	2.972	0.994	66.6
FQ0126B1	1.200	0.501	0.113	1.184	0.056	0.056	0.020	0.033	3.163	4.967	1.804	63.7
FQ0126B2	1.311	0.578	0.184	2.670	0.028	0.071	0.000	0.067	4.909	5.876	0.968	83.5
FQ0119A1	0.478	0.697	0.758	1.467	0.112	0.076	0.001	0.111	3.700	3.151	-	117.4
FQ0119A2	0.955	1.166	1.240	7.331	0.056	0.229	0.018	0.319	11.314	11.408	0.094	99.2
FQ0120A1	0.554	0.363	0.423	2.329	0.050	0.041	0.000	0.092	3.851	6.443	2.592	59.8
FQ0120A2	0.729	0.120	0.144	2.305	0.000	0.019	0.000	0.050	3.366	6.841	3.474	49.2
FQ0121A1	0.350	0.120	0.526	0.909	0.000	0.014	0.000	0.020	1.940	3.129	1.190	62.0
FQ0121A2	0.263	0.143	0.092	2.230	0.047	0.055	0.000	0.072	2.903	5.318	2.415	54.6
FQ0122A1	0.298	0.008	0.088	0.599	0.000	0.009	0.000	0.013	1.014	2.442	1.428	41.5
FQ0122A2	0.236	0.044	0.043	0.294	0.036	0.006	0.000	0.006	0.666	1.005	0.339	66.2
FQ0123A1	0.832	0.470	0.546	0.943	0.011	0.060	0.003	0.007	2.871	4.150	1.279	69.2

FQ0123A2	0.301	0.118	0.047	0.455	0.026	0.009	0.000	0.004	0.961	1.592	0.632	60.3
FQ0124A1	0.232	0.102	0.038	0.250	0.023	0.058	0.030	0.099	0.833	1.646	0.813	50.6
FQ0124A2	0.339	0.066	0.014	0.404	0.029	0.015	0.002	0.031	0.900	1.757	0.856	51.3
FQ0125A1	0.118	0.291	0.488	0.342	0.028	0.007	0.000	0.019	1.292	0.654	-	197.6
FQ0125A2	0.255	0.252	0.541	0.708	0.026	0.010	0.000	0.015	1.807	1.567	-	115.3
FQ0126A1	0.321	0.774	0.755	1.972	0.116	0.060	0.005	0.076	4.078	2.807	-	145.3
FQ0126A2	0.173	0.340	0.700	3.408	0.035	0.000	0.009	0.083	4.747	3.625	-	131.0
FQ0119C	0.012	0.186	0.147	2.392	0.011	0.000	0.000	0.101	2.848	3.140	0.292	90.7
FQ0120C	0.132	0.352	0.231	4.415	0.007	0.000	0.000	0.061	5.198	4.832	-	107.6
FQ0122C	0.029	0.145	0.084	1.387	0.078	0.000	0.000	0.067	1.790	1.350	-	132.6
FQ0123C	0.074	0.136	0.089	0.659	0.004	0.000	0.010	0.027	0.998	0.397	-	251.7
FQ0124C	0.057	0.022	0.011	0.497	0.028	0.000	0.000	0.024	0.638	1.430	0.793	44.6
FQ0125C	0.159	0.021	0.018	0.519	0.016	0.000	0.000	0.024	0.755	0.796	0.041	94.9
FQ0126C	0.078	0.088	0.192	1.604	0.015	0.000	0.000	0.031	2.008	2.304	0.296	87.2
Average	0.606	0.472	0.413	1.889	0.030	0.080	0.018	0.063	3.572	3.925	1.232	98.8

Note: ‘A1’, ‘A2’, ‘B1’ and ‘B2’ indicate the daytime campus, nighttime campus, daytime highway and nighttime highway 12-hr samples, respectively. ‘C’ denotes the Yorkville 24-hr samples. ‘-’ means negative value.

Table B.3. Source Apportionment of $PM_{2.5}$ at The Three Sampling Sites in Summer 2005 (unit: $\mu g\ m^{-3}$)

Sampling Date	Diesel Exhaust	Gasoline Exhaust	Meat Cooking	Wood Combustion	Road Dust	Cigarette Smoke	Natural Gas Combustion	Vegetative Detritus	Other OM	Secondary Sulfate	Secondary Nitrate	Secondary Ammonium	Identified Mass	$PM_{2.5}$ Mass	Others	% Mass Explained
FQ0615A1	3.254	0.572	0.000	0.180	1.072	0.026	0.004	0.328	6.864	2.889	0.321	1.198	16.708	16.38	-	102.0
FQ0615A2	3.977	1.474	1.716	0.639	1.007	0.129	0.000	0.163	2.609	2.401	3.823	0.965	18.902	15.55	-	121.6
FQ0616A1	0.937	0.471	0.934	0.357	1.115	0.057	0.000	0.132	6.850	5.128	0.057	1.905	17.942	18.55	0.61	96.7
FQ0616A2	1.029	0.470	0.497	0.544	0.592	0.059	0.000	0.095	4.819	3.671	0.078	1.525	13.378	13.81	0.44	96.8
FQ0617A1	0.096	0.545	0.059	0.190	0.058	0.015	0.004	0.158	5.500	5.650	0.632	1.869	14.776	15.66	0.88	94.4
FQ0617A2	3.868	0.650	0.234	0.968	0.989	0.257	0.000	0.256	3.128	4.107	3.343	1.711	19.512	16.99	-	114.8
FQ0618A1	1.107	0.582	0.239	0.396	0.122	0.000	0.000	0.237	6.123	6.415	0.160	2.444	17.824	17.58	-	101.4
FQ0615B1	11.052	1.503	1.210	0.168	1.292	0.065	0.000	0.374	2.970	2.796	0.090	1.185	22.706	17.92	-	126.7
FQ0615B2	9.536	1.561	1.664	1.041	1.604	0.179	0.003	0.483	7.124	2.785	0.000	1.105	27.085	27.00	-	100.3
FQ0616B1	9.254	2.433	0.308	0.552	1.297	0.324	0.000	1.040	3.098	5.353	0.099	2.168	25.926	23.47	-	110.4

FQ0616B2	4.268	0.712	0.129	0.676	0.640	0.107	0.001	0.302	7.707	3.551	0.000	1.521	19.613	20.97	1.36	93.5
FQ0617B1	7.943	1.432	0.398	0.144	0.672	0.399	0.013	0.303	3.213	5.620	0.484	2.205	22.826	20.21	-	113.0
FQ0617B2	7.752	1.169	0.419	0.749	0.000	0.189	0.000	0.071	8.352	3.903	0.043	1.646	24.293	22.95	-	105.9
FQ0618B1	4.135	2.099	0.033	0.355	0.651	0.195	0.000	0.199	7.973	7.127	0.449	2.925	26.141	26.24	0.10	99.6
FQ0708A	1.898	0.747	1.754	0.697	1.127	0.053	0.000	0.102	5.771	5.152	2.382	1.919	21.602	20.56	-	105.1
FQ0709A	0.296	0.129	0.214	0.182	2.786	0.038	0.000	0.017	4.239	3.113	0.244	1.159	12.418	12.85	0.43	96.7
FQ0718A	1.093	0.783	0.109	0.205	1.527	0.189	0.002	0.035	5.833	3.395	0.047	1.246	14.464	14.65	0.19	98.7
FQ0719A	3.929	0.534	2.037	0.517	0.249	0.249	0.009	0.177	5.832	7.462	0.034	2.709	23.741	22.73	-	104.4
FQ0723A	1.717	0.823	2.081	0.871	0.000	0.369	0.000	0.242	6.034	6.934	2.159	2.682	23.910	22.15	-	107.9
FQ0724A	2.244	1.086	0.058	0.523	0.843	0.048	0.000	0.148	14.874	18.839	0.049	6.922	45.634	45.88	0.25	99.5
FQ0725A	2.653	1.121	0.944	0.890	1.267	0.237	0.003	0.190	13.860	17.433	0.037	6.248	44.883	44.82	-	100.1
FQ0726A	1.690	0.555	0.747	0.577	2.344	0.123	0.000	0.038	13.642	19.245	1.417	6.679	47.055	46.98	-	100.2
FQ0708B	1.512	0.157	0.169	0.198	0.595	0.000	0.001	0.042	6.460	7.136	0.141	2.769	19.180	18.75	-	102.3
FQ0709B	1.143	0.123	0.085	0.104	1.688	0.000	0.001	0.058	4.701	4.252	0.052	1.610	13.816	13.61	-	101.5
FQ0718B	0.900	0.046	1.014	0.164	0.198	0.000	0.003	0.052	4.999	3.405	0.020	1.347	12.148	11.59	-	104.8
FQ0719B	1.057	0.280	0.069	0.109	0.123	0.000	0.003	0.030	5.692	4.899	0.153	1.809	14.225	14.06	-	101.2
FQ0723B	0.793	0.052	0.000	0.294	0.093	0.000	0.001	0.046	9.699	9.517	0.074	3.636	24.205	24.49	0.29	98.8
FQ0724B	0.000	0.093	0.333	0.250	0.188	0.000	0.000	0.021	12.511	14.398	0.029	5.405	33.227	33.79	0.56	98.3
FQ0725B	0.261	0.052	0.000	0.298	0.747	0.000	0.000	0.027	14.408	16.149	0.066	5.441	37.450	38.01	0.56	98.5
FQ0726B	0.388	0.024	0.147	0.412	1.043	0.000	0.000	0.030	15.801	18.273	0.126	5.331	41.574	42.09	0.51	98.8
Average	2.993	0.743	0.587	0.442	0.864	0.110	0.002	0.180	7.356	7.367	0.554	2.709	23.905	23.343	-	103.1

Note: 'A1', 'A2', 'B1' and 'B2' indicate the daytime campus, nighttime campus, daytime highway and nighttime highway 12-hr samples, respectively. 'A' and 'B' denote the campus and the Yorkville 24-hr samples. '-' represents negative value.

Table B.4. Source Apportionment of $PM_{2.5}$ at The Three Sampling Sites in Winter 2006 (unit: $\mu g\ m^{-3}$)

Sampling Date	Diesel Exhaust	Gasoline Exhaust	Meat Cooking	Wood Combustion	Road Dust	Cigarette Smoke	Natural Gas Combustion	Vegetative Detritus	Other OM	Secondary Sulfate	Secondary Nitrate	Secondary Ammonium	Identified Mass	PM2.5 Mass	Others	% Mass Explained
FQ0119B1	6.855	1.836	2.833	2.374	0.073	0.560	0.121	0.566	0.000	0.942	4.361	0.320	20.842	12.92	-	161.3
FQ0119B2	8.752	1.980	3.196	6.511	0.427	0.299	0.000	0.307	1.774	0.927	1.040	0.418	25.632	22.23	-	115.3
FQ0120B1	9.077	0.984	1.542	3.975	0.628	0.183	0.000	0.156	3.567	2.947	0.453	1.419	24.931	23.40	-	106.5
FQ0120B2	3.518	0.890	0.370	3.891	0.253	0.092	0.000	0.171	6.106	2.326	0.180	1.000	18.799	20.22	1.42	93.0

FQ0121B1	4.242	0.496	1.689	2.209	0.031	0.102	0.004	0.104	1.477	2.767	0.795	1.316	15.233	14.67	-	103.9
FQ0121B2	2.559	2.461	5.699	8.583	0.000	0.807	0.103	0.931	0.000	3.027	3.135	2.391	29.696	21.14	-	140.4
FQ0122B1	1.332	3.149	4.913	6.271	0.000	0.760	0.118	0.425	0.000	4.222	1.038	1.860	24.086	15.42	-	156.2
FQ0122B2	3.832	1.910	1.234	1.633	0.013	0.845	0.066	0.000	0.000	1.606	0.074	0.598	11.811	7.21	-	163.8
FQ0123B1	13.967	1.356	2.179	1.137	0.000	0.876	0.204	0.120	0.794	1.346	0.297	0.455	22.730	17.65	-	128.8
FQ0123B2	2.425	1.417	0.432	2.454	0.022	0.070	0.005	0.029	0.000	2.629	8.704	1.434	19.621	11.03	-	177.9
FQ0124B1	4.822	1.243	0.455	0.914	0.368	0.145	0.034	0.055	0.765	2.163	0.000	0.949	11.914	11.20	-	106.3
FQ0124B2	4.184	0.956	0.182	1.046	0.142	0.085	0.025	0.123	0.488	1.076	0.000	0.469	8.774	7.13	-	123.0
FQ0125B1	3.813	1.597	0.688	0.989	0.286	0.107	0.018	0.082	0.604	0.346	0.000	0.080	8.611	8.42	-	102.2
FQ0125B2	2.413	0.766	0.042	1.268	0.369	0.091	0.014	0.078	1.294	1.315	1.694	1.070	10.413	11.11	0.70	93.7
FQ0126B1	6.091	0.931	0.335	1.581	0.430	0.122	0.023	0.102	2.292	1.386	1.368	1.026	15.687	15.94	0.26	98.4
FQ0126B2	6.656	1.074	0.544	3.565	0.213	0.154	0.000	0.206	1.177	1.749	2.198	0.773	18.309	16.40	-	111.6
FQ0119A1	2.425	1.295	2.242	1.959	0.857	0.166	0.001	0.344	0.000	0.737	0.000	0.272	10.298	10.80	0.50	95.3
FQ0119A2	4.849	2.168	3.669	9.788	0.426	0.497	0.022	0.984	0.133	0.899	1.100	0.399	24.933	23.50	-	106.1
FQ0120A1	2.812	0.674	1.251	3.109	0.384	0.089	0.000	0.284	3.980	2.501	0.709	1.102	16.895	16.73	-	101.0
FQ0120A2	3.699	0.223	0.425	3.078	0.000	0.042	0.000	0.154	5.114	1.810	1.331	0.859	16.733	15.93	-	105.0
FQ0121A1	1.777	0.223	1.558	1.214	0.000	0.030	0.000	0.062	2.377	2.403	0.525	1.108	11.275	11.04	-	102.2
FQ0121A2	1.336	0.266	0.273	2.977	0.361	0.119	0.000	0.224	3.289	2.462	5.786	2.006	19.098	19.34	0.24	98.8
FQ0122A1	1.511	0.015	0.261	0.800	0.000	0.019	0.000	0.039	2.643	2.719	2.163	1.644	11.814	11.72	-	100.8
FQ0122A2	1.200	0.083	0.126	0.392	0.274	0.013	0.000	0.020	0.861	0.458	0.069	0.504	4.000	4.80	0.80	83.4
FQ0123A1	4.221	0.873	1.616	1.258	0.082	0.131	0.003	0.023	1.924	0.366	0.848	0.449	11.793	11.30	-	104.4
FQ0123A2	1.527	0.220	0.139	0.608	0.202	0.020	0.000	0.012	1.770	1.726	0.381	1.060	7.664	8.40	0.73	91.3
FQ0124A1	1.179	0.190	0.112	0.334	0.178	0.127	0.035	0.306	1.555	1.307	0.976	0.787	7.086	7.40	0.32	95.7
FQ0124A2	1.722	0.122	0.043	0.540	0.224	0.032	0.002	0.095	2.137	0.000	0.000	0.402	5.319	5.85	0.53	90.9
FQ0125A1	0.597	0.541	1.443	0.457	0.211	0.015	0.000	0.060	0.000	0.000	0.393	0.072	3.789	3.99	0.20	95.0
FQ0125A2	1.295	0.468	1.600	0.945	0.199	0.023	0.000	0.045	0.000	0.755	2.175	0.966	8.471	7.86	-	107.8
FQ0126A1	1.628	1.438	2.232	2.633	0.889	0.131	0.006	0.234	0.000	0.828	1.229	0.564	11.811	10.55	-	112.0
FQ0126A2	0.878	0.631	2.071	4.550	0.264	0.000	0.011	0.257	0.000	0.741	13.147	0.602	23.152	12.20	-	189.8
FQ0119C	0.061	0.346	0.434	3.194	0.085	0.000	0.000	0.310	0.242	0.841	3.659	0.392	9.564	8.27	-	115.6
FQ0120C	0.672	0.654	0.684	5.895	0.055	0.000	0.000	0.188	0.000	2.440	0.565	0.984	12.137	13.15	1.01	92.3
FQ0122C	0.149	0.269	0.248	1.852	0.595	0.000	0.000	0.207	0.000	2.557	7.363	1.308	14.548	7.74	-	187.9
FQ0123C	0.374	0.252	0.263	0.879	0.027	0.000	0.012	0.084	0.000	0.760	0.306	0.418	3.377	3.92	0.54	86.2
FQ0124C	0.289	0.040	0.031	0.663	0.215	0.000	0.000	0.073	1.159	1.176	0.067	0.522	4.236	4.38	0.14	96.8
FQ0125C	0.807	0.038	0.053	0.692	0.120	0.000	0.000	0.073	0.055	0.609	1.035	0.347	3.830	4.37	0.54	87.6
FQ0126C	0.396	0.163	0.568	2.142	0.114	0.000	0.000	0.097	0.465	1.109	2.833	0.642	8.529	9.07	0.54	94.1
Average	3.075	0.878	1.222	2.522	0.231	0.173	0.021	0.196	1.232	1.538	1.846	0.846	13.781	12.010	-	113.4

Note: ‘A1’, ‘A2’, ‘B1’ and ‘B2’ indicate the daytime campus, nighttime campus, daytime highway and nighttime highway 12-hr samples, respectively. ‘C’ denotes the Yorkville 24-hr samples. ‘-’ represents negative value.

APPENDIX C

Table C.1. Ambient Concentrations of Organic Compounds in Prescribed Burning Impacted $PM_{2.5}$ Quantified with GC/MS (unit: ng m^{-3})

Compound	Before_Fire	Event	After_Fire	Compound	Before_Fire	Event	After_Fire
Heptadecane	0.660	0.487	0.695	Heptacosane	0.689	4.812	0.668
Octadecane	0.631	0.000	0.952	Octacosane	0.601	1.725	0.230
Nonadecane	0.711	0.669	0.778	Nonacosane	1.054	8.485	0.819
Eicosane	0.998	0.854	0.654	Triacontane	0.000	1.077	0.000
Heneicosane	1.153	1.525	0.579	Hentriacontane	0.949	7.060	0.655
Docosane	1.205	1.744	0.537	Dotriacontane	0.000	0.697	0.000
Tricosane	1.398	2.877	0.615	Tritriacontane	0.268	1.526	0.258
Tetracosane	1.169	2.065	0.549	Tetratriacontane	0.000	0.000	0.000
Pentacosane	1.273	2.959	0.650	Pentatriacontane	0.000	0.000	0.000
Hexacosane	1.014	1.553	0.355	Hexatriacontane	0.000	0.000	0.000
Sum of alkanes	13.775	40.113	8.991				
iso-Nonacosane	0.000	0.000	0.000	iso-Hentriacontane	0.000	0.000	0.000
anteiso-Triacontane	0.000	0.000	0.000				
Sum of Branch-alkanes	0.000	0.000	0.000				
17α(H)-21β(H)-29-Norhopane	0.403	0.455	0.237	22R,17α(H),21β(H)-Homohopane	0.160	0.204	0.072
17α(H)-21β(H)-Hopane	0.383	0.422	0.227	22S,17α(H),21β(H)-Bishomohopane	0.099	0.121	0.059
22,29,30-Trisnorneohopane	0.145	0.197	0.035	22R,17α(H),21β(H)-Bishomohopane	0.068	0.045	0.035
22,29,30-Trisnorhopane	0.098	0.000	0.035	22S,17α(H),21β(H)-Trishomohopane	0.000	0.000	0.025
22S,17α(H),21β(H)-Homohopane	0.198	0.265	0.116	22R,17α(H),21β(H)-Trishomohopane	0.028	0.000	0.000
Sum of hopanes	1.581	1.710	0.840				
20S,R-5α(H),14β(H),17β(H)-Cholestanes	0.000	0.000	0.000	20S,R-5α(H),14β(H),17β(H)-Ergostanes	0.000	0.000	0.000
20R-5α(H),14α(H),17α(H)-Cholestane	0.000	0.000	0.121	20S,R-5α(H),14β(H),17β(H)-Sitostanes	0.140	0.000	0.058
Sum of steranes	0.140	0.000	0.179				

Fluoranthene	0.212	0.195	0.146	Benzo(b)fluoranthene	0.178	0.282	0.082
Acephenanthrylene	0.019	0.041	0.005	Benzo(k)fluoranthene	0.124	0.192	0.058
Pyrene	0.172	0.159	0.078	Benzo(j)fluoranthene	0.016	0.027	0.000
Retene	0.059	0.738	0.112	Benzo(e)pyrene	0.147	0.242	0.068
Methyl substituted MW 202 PAH	0.209	0.239	0.090	Benzo(a)pyrene	0.134	0.148	0.044
Benzo(ghi)fluoranthene	0.130	0.176	0.000	Perylene	0.029	0.026	0.000
Cyclopenta(cd)pyrene	0.046	0.045	0.012	Indeno(1,2,3-cd)fluoranthene	0.055	0.113	0.029
Benz(a)anthracene	0.140	0.154	0.033	Indeno(1,2,3-cd)pyrene	0.176	0.244	0.069
Chrysene/Triphenylene	0.237	0.409	0.099	Picene	nd	nd	nd
Methyl substituted MW 228 PAH	0.131	0.291	0.088	Benzo(ghi)perylene	0.318	0.382	0.098
Methyl substituted MW 226 PAH	nd	nd	nd	Coronene	0.261	0.356	0.085
Sum of PAHs	2.792	4.459	1.197				
8,15-Pimaredienoic acid	nd	nd	nd	Abietic acid	0.168	0.437	0.301
Pimaric acid	0.105	0.549	0.313	Abieta-6,8,11,13,15-pentae-18-oic acid	0.040	0.251	0.070
Sandaracopimaric acid	0.328	1.661	1.566	Abieta-8,11,13,15-tetraen-18-oic acid	0.059	0.687	0.216
Isopimaric acid	nd	nd	nd	7-Oxodehydroabietic acid	0.790	18.516	6.105
Dehydroabietic acid	4.647	41.519	35.977				
Sum of Resin acids	6.136	63.619	44.547				
1,2-Benzenedicarboxylic acid	0.702	3.530	0.543	1,3-Benzenedicarboxylic acid	0.447	1.130	0.198
1,4-Benzenedicarboxylic acid	1.036	2.078	1.076				
Sum of Aromatic acids	2.186	6.738	1.818				
Tetradecanoic acid	0.707	2.477	0.788	Pentacosanoic acid	0.102	1.266	0.171
Pentadecanoic acid	0.510	1.368	0.459	Hexacosanoic acid	0.454	7.639	0.903
Hexadecanoic acid	6.580	13.224	4.324	Heptacosanoic acid	0.021	0.433	0.067
Heptadecanoic acid	0.285	0.780	0.191	Octacosanoic acid	0.143	2.603	0.241
Octadecanoic acid	3.226	6.432	1.655	Nonacosanoic acid	0.000	0.516	0.036
Nonadecanoic acid	0.106	0.732	0.100	Triacontanoic acid	0.136	2.808	0.233
Eicosanoic acid	0.447	4.648	0.551	9-Hexadecenoic acid	nd	nd	nd
Heneicosanoic acid	0.157	1.923	0.225	9,12-Octadecanedienoic acid	0.360	0.341	0.103
Docosanoic acid	0.711	9.762	1.050	9-Octadecenoic acid	1.034	0.346	0.384
Tricosanoic acid	0.237	3.697	0.389	Pinonic acid	2.909	4.991	4.362
Tetracosanoic acid	1.087	14.297	1.797	Pinic acid	1.163	3.108	2.733
sum of Fatty acids	20.374	83.390	20.759				
Propanedioic acid	nd	nd	nd	Hexanedioic acid	0.481	2.587	0.408

Methylpropanedioic acid	nd	nd	nd	Heptanedioic acid	nd	nd	nd
Butanedioic acid	2.705	21.812	3.445	Octanedioic acid	0.350	3.898	0.409
Methylbutanedioic acid	0.377	4.472	0.613	Nonanedioic acid	0.877	8.002	0.957
Pentanedioic acid	0.512	3.371	0.749				
Sum of dicarboxylic diacids	5.301	44.143	6.583				
Nonanal	0.559	0.859	0.282	3,5-Dimethoxy-4-hydroxyacetophenone	0.000	0.657	0.000
Sinapyl aldehyde	nd	nd	nd	Levoglucosan	114.4	1209.7	144.9
Acetonylsyringol	0.413	1.799	0.202	Cholesterol	0.582	0.429	0.421
Coniferyl aldehyde	nd	nd	nd	2-Methylthreitol	0.000	0.243	0.000
Propionylsyringol	nd	nd	nd	2-Methylerythritol	0.000	0.510	0.000
Benz(de)anthracen-7-one	0.146	0.233	0.081				
Sum of Other compounds	116.148	1214.414	145.865				
Organic Carbon (ug/m3)	3.52	17.69	3.11	Element Carbon (ug/m3)	1.70	2.25	0.74
EC/OC	0.483	0.127	0.238				

Note: [a] 'nd', not detected.

Table C.2. Source Composition Profiles from The Aged Plume on The Event and The Previous Prescribed Burning Emissions (unit: ng/µg OC)

Compound	Aged Plume [a]	POC_{fc} [b]	Lee's [c]	Compound	Aged Plume [a]	POC_{fc} [b]	Lee's [c]
	Fraction [d] ± std [e]	Fraction ± std	Fraction ± std		Fraction ± std	Fraction ± std	Fraction ± std
***n*-alkanes**							
Tetracosane	0.0632 ± 0.0338	0.1128 ± 0.0609	0.1388 ± 0.0705	Triacontane	0.0759 ± 0.0161	0.1357 ± 0.0305	0.1939 ± 0.0937
Pentacosane	0.1189 ± 0.0463	0.2124 ± 0.0840	0.2500 ± 0.1276	Hentriacontane	0.4313 ± 0.1054	0.7703 ± 0.1962	0.2883 ± 0.1375
Hexacosane	0.0380 ± 0.0263	0.0679 ± 0.0472	0.2281 ± 0.1250	Dotriacontane	0.0492 ± 0.0104	0.0879 ± 0.0197	0.0000 ± 0.0001
Heptacosane	0.2910 ± 0.0719	0.5196 ± 0.1336	0.2498 ± 0.1639	Tritriacontane	0.0887 ± 0.0228	0.1584 ± 0.0423	0.0900 ± 0.0723
Octacosane	0.0792 ± 0.0264	0.1415 ± 0.0482	0.1155 ± 0.0538	Tetratriacontane	0.0000 ± 0.0001	0.0000 ± 0.0001	0.0000 ± 0.0001
Nonacosane	0.5245 ± 0.1267	0.9367 ± 0.2360	0.8067 ± 0.3847				

Branch-alkanes							
iso-Nonacosane	0.0000 ± 0.0001	0.0000 ± 0.0001	0.0000 ± 0.0001	iso-Hentriacontane	0.0000 ± 0.0001	0.0000 ± 0.0001	0.0000 ± 0.0001
anteiso-Triacontane	0.0000 ± 0.0001	0.0000 ± 0.0001	0.0000 ± 0.0001				
Hopanes							
17α(H)-21β(H)-29-Norhopane	0.0037 ± 0.0085	0.0066 ± 0.0153	0.0000 ± 0.0001	22R,17α(H),21β(H)-Homohopane	0.0031 ± 0.0036	0.0055 ± 0.0065	0.0000 ± 0.0001
17α(H)-21β(H)-Hopane	0.0027 ± 0.0080	0.0048 ± 0.0143	0.0000 ± 0.0001	22S,17α(H),21β(H)-Bishomohopane	0.0015 ± 0.0022	0.0028 ± 0.0039	0.0000 ± 0.0001
22,29,30-Trisnorneohopane	0.0037 ± 0.0034	0.0066 ± 0.0062	0.0000 ± 0.0001	22R,17α(H),21β(H)-Bishomohopane	0.0000 ± 0.0001	0.0000 ± 0.0001	0.0000 ± 0.0001
22,29,30-Trisnorhopane	0.0000 ± 0.0001	0.0000 ± 0.0001	0.0000 ± 0.0001	22S,17α(H),21β(H)-Trishomohopane	0.0000 ± 0.0001	0.0000 ± 0.0001	0.0000 ± 0.0001
22S,17α(H),21β(H)-Homohopane	0.0047 ± 0.0046	0.0084 ± 0.0083	0.0000 ± 0.0001	22R,17α(H),21β(H)-Trishomohopane	0.0000 ± 0.0001	0.0000 ± 0.0001	0.0000 ± 0.0001
Steranes							
20S,R-5α(H),14β(H),17β(H)-Cholestanes	0.0000 ± 0.0001	0.0000 ± 0.0001	0.0000 ± 0.0001	20S,R-5α(H),14β(H),17β(H)-Ergostanes	0.0000 ± 0.0001	0.0000 ± 0.0001	0.0000 ± 0.0001
20R-5α(H),14α(H),17α(H)-Cholestane	0.0000 ± 0.0001	0.0000 ± 0.0001	0.0000 ± 0.0001	20S,R-5α(H),14β(H),17β(H)-Sitostanes	0.0000 ± 0.0001	0.0000 ± 0.0001	0.0000 ± 0.0001
PAHs							
Fluoranthene	0.0000 ± 0.0001	0.0000 ± 0.0001	0.0895 ± 0.0390	Benzo(j)fluoranthene	0.0007 ± 0.0004	0.0013 ± 0.0008	0.0128 ± 0.0067
Acephenanthrylene	0.0015 ± 0.0006	0.0028 ± 0.0011	0.0280 ± 0.0140	Benzo(e)pyrene	0.0066 ± 0.0040	0.0119 ± 0.0072	0.0499 ± 0.0208
Pyrene	0.0000 ± 0.0001	0.0000 ± 0.0001	0.1068 ± 0.0450	Benzo(a)pyrene	0.0010 ± 0.0028	0.0018 ± 0.0050	0.0298 ± 0.0124
Retene	0.0479 ± 0.0110	0.0856 ± 0.0206	0.3490 ± 0.1645	Perylene	0.0000 ± 0.0001	0.0000 ± 0.0001	0.0039 ± 0.0022
Benzo(ghi)fluoranthene	0.0031 ± 0.0030	0.0057 ± 0.0055	0.0972 ± 0.0778	Indeno(1,2,3-cd)fluoranthene	0.0041 ± 0.0018	0.0073 ± 0.0032	0.0000 ± 0.0001
Cyclopenta(cd)pyrene	0.0000 ± 0.0001	0.0000 ± 0.0001	0.2888 ± 0.1381	Indeno(1,2,3-cd)pyrene	0.0048 ± 0.0042	0.0085 ± 0.0076	0.0737 ± 0.0342
Benz(a)anthracene	0.0010 ± 0.0029	0.0018 ± 0.0052	0.0800 ± 0.0329	Picene	0.0000 ± 0.0001	0.0000 ± 0.0001	0.0000 ± 0.0001
Chrysene/Triphenylene	0.0121 ± 0.0067	0.0216 ± 0.0121	0.0978 ± 0.0411	Benzo(ghi)perylene	0.0045 ± 0.0070	0.0080 ± 0.0125	0.0358 ± 0.0149
Benzo(b)fluoranthene	0.0073 ± 0.0047	0.0131 ± 0.0085	0.0505 ± 0.0210	Coronene	0.0066 ± 0.0062	0.0119 ± 0.0111	0.0074 ± 0.0044
Benzo(k)fluoranthene	0.0048 ± 0.0032	0.0086 ± 0.0058	0.0407 ± 0.0167				
Resin Acids							
8,15-Pimaredienoic acid	0.0000 ± 0.0001	0.0000 ± 0.0001	0.0000 ± 0.0001	Abietic acid	0.0189 ± 0.0067	0.0339 ± 0.0123	0.0000 ± 0.0001
Pimaric acid	0.0312 ± 0.0082	0.0558 ± 0.0152	2.4658 ± 1.0099	Abieta-6,8,11,13,15-pentae-18-oic acid	0.0149 ± 0.0037	0.0266 ± 0.0069	0.0000 ± 0.0001
Sandaracopimaric acid	0.0941 ± 0.0248	0.1680 ± 0.0460	0.0000 ± 0.0001	Abieta-8,11,13,15-tetraen-18-oic acid	0.0443 ± 0.0102	0.0791 ± 0.0191	0.0000 ± 0.0001
Isopimaric acid	0.0000 ± 0.0001	0.0000 ± 0.0001	2.9594 ± 1.2311	7-Oxodehydroabietic acid	1.2512 ± 0.2774	2.2343 ± 0.5204	0.0000 ± 0.0001
Dehydroabietic acid	2.6027 ± 0.6202	4.6477 ± 1.1562	33.316 ± 14.302				
Aromatic Acids							

1,2-Benzenedicarboxylic acid	0.1995 ± 0.0528	0.3563 ± 0.0978	0.0147 ± 0.0088	1,3-Benzenedicarboxylic acid	0.0482 ± 0.0175	0.0861 ± 0.0318	0.0000 ± 0.0001
1,4-Benzenedicarboxylic acid	0.0735 ± 0.0332	0.1312 ± 0.0600	0.0090 ± 0.0071				
Alkanoic Acids							
Tetradecanoic acid	0.1249 ± 0.0375	0.2230 ± 0.0688	2.0065 ± 0.9764	Tricosanoic acid	0.2442 ± 0.0553	0.4361 ± 0.1035	0.6541 ± 0.2863
Pentadecanoic acid	0.0605 ± 0.0210	0.1081 ± 0.0384	0.6371 ± 0.3281	Tetracosanoic acid	0.9325 ± 0.2137	1.6651 ± 0.3998	4.9519 ± 2.2088
Hexadecanoic acid	0.4689 ± 0.2113	0.8374 ± 0.3821	6.7301 ± 2.9428	Pentacosanoic acid	0.0822 ± 0.0189	0.1468 ± 0.0353	0.3831 ± 0.1679
Heptadecanoic acid	0.0349 ± 0.0119	0.0623 ± 0.0218	0.2481 ± 0.1184	Hexacosanoic acid	0.5071 ± 0.1143	0.9056 ± 0.2141	3.6714 ± 1.6200
Octadecanoic acid	0.2262 ± 0.1029	0.4040 ± 0.1860	2.2421 ± 1.0502	Heptacosanoic acid	0.0290 ± 0.0064	0.0518 ± 0.0121	0.1410 ± 0.0652
Nonadecanoic acid	0.0442 ± 0.0109	0.0789 ± 0.0203	0.4882 ± 0.2505	Octacosanoic acid	0.1736 ± 0.0389	0.3100 ± 0.0730	0.9881 ± 0.4472
Eicosanoic acid	0.2965 ± 0.0694	0.5295 ± 0.1296	1.1947 ± 0.5701	Nonacosanoic acid	0.0364 ± 0.0077	0.0650 ± 0.0146	0.1684 ± 0.0868
Heneicosanoic acid	0.1247 ± 0.0287	0.2226 ± 0.0537	0.2886 ± 0.1278	Triacontanoic acid	0.1885 ± 0.0420	0.3367 ± 0.0788	0.8029 ± 0.4244
Docosanoic acid	0.6388 ± 0.1459	1.1408 ± 0.2731	1.7855 ± 0.8199				
Alkenoic Acids							
9-Hexadecenoic acid	0.0000 ± 0.0001	0.0000 ± 0.0001	0.5076 ± 0.3254	9-Octadecenoic acid	0.0000 ± 0.0001	0.0000 ± 0.0001	2.4381 ± 1.1394
9,12-Octadecanedienoic acid	0.0000 ± 0.0001	0.0000 ± 0.0001	2.2530 ± 1.2726				
Alkanedioic Acids							
Propanedioic acid	0.0000 ± 0.0001	0.0000 ± 0.0001	0.0000 ± 0.0001	Hexanedioic acid	0.1486 ± 0.0387	0.2655 ± 0.0717	0.0265 ± 0.0196
Methylpropanedioic acid	0.0000 ± 0.0001	0.0000 ± 0.0001	0.0000 ± 0.0001	Heptanedioic acid	0.0000 ± 0.0001	0.0000 ± 0.0001	0.0300 ± 0.0240
Butanedioic acid	1.3487 ± 0.3258	2.4084 ± 0.6067	0.3964 ± 0.2064	Octanedioic acid	0.2504 ± 0.0582	0.4473 ± 0.1088	0.0595 ± 0.0409
Methylbutanedioic acid	0.2890 ± 0.0668	0.5162 ± 0.1249	0.0000 ± 0.0001	Nonanedioic acid	0.5029 ± 0.1195	0.8981 ± 0.2229	0.2586 ± 0.1358
Pentanedioic acid	0.2018 ± 0.0503	0.3604 ± 0.0935	0.0813 ± 0.0429				
Others							
Nonanal	0.0211 ± 0.0145	0.0378 ± 0.0261	0.0000 ± 0.0001	Benz(de)anthracen-7-one	0.0061 ± 0.0039	0.0109 ± 0.0070	0.0000 ± 0.0001
Sinapyl aldehyde	0.0000 ± 0.0001	0.0000 ± 0.0001	0.0000 ± 0.0001	3,5-Dimethoxy-4-hydroxyacetophenone	0.0463 ± 0.0098	0.0827 ± 0.0186	0.0000 ± 0.0001
Acetonylsyringol	0.0978 ± 0.0270	0.1747 ± 0.0498	0.0000 ± 0.0001	Levoglucosan	77.311 ± 18.076	138.05 ± 33.752	94.750 ± 40.256
Coniferyl aldehyde	0.0000 ± 0.0001	0.0000 ± 0.0001	0.0000 ± 0.0001	Cholesterol	0.0000 ± 0.0001	0.0000 ± 0.0001	0.0000 ± 0.0001
Propionylsyringol	0.0000 ± 0.0001	0.0000 ± 0.0001	0.0000 ± 0.0001				

Note: [a] source composition profiles where individual organic compounds are normalized to the fire-caused total OC mass on the event day; [b] source composition profiles where individual organic compounds are normalized to the fire-caused primary OC mass estimated on the event day; [c] source composition profiles from the prescribed burning emission in Georgia [*Lee et al.*, 2005a]; [d] fraction of organic compound in the associated OC mass (ng/μg OC); [e] standard deviation.

APPENDIX D

Table D.1. Ambient Concentrations of Organic Compounds in $PM_{2.5}$ Quantified with GC/MS (unit: ng m^{-3})

Compound	NonSmoke-1	Smoke-1	NonSmoke-2	Smoke-2	NonSmoke-3	Smoke-3	NonSmoke-4	NoSmoke-Coffee	Smoke_Coffee	NoSmoke-Bibb	Smoke_Bibb
Heptadecane	0.000	0.000	0.000	0.377	0.000	0.000	0.000	0.000	0.000	0.000	0.000
Octadecane	0.000	0.000	0.000	0.000	0.000	0.000	0.000	0.000	0.000	0.000	0.000
Nonadecane	0.000	0.000	0.000	0.000	0.000	0.000	0.000	0.000	0.000	0.000	0.000
Eicosane	0.000	0.000	0.000	0.400	0.000	0.000	0.000	0.000	0.000	0.000	0.000
Heneicosane	0.326	0.237	0.435	1.165	0.284	0.466	0.208	0.068	0.225	0.422	3.017
Docosane	0.418	0.335	0.338	1.848	0.223	1.627	0.286	0.000	0.235	0.000	2.551
Tricosane	1.210	1.187	0.772	6.911	0.767	7.236	0.914	0.000	1.345	0.413	11.292
Tetracosane	0.665	1.803	0.367	7.945	0.520	10.807	0.566	0.000	3.897	0.227	18.328
Pentacosane	0.803	3.767	0.390	14.854	0.560	18.265	0.692	0.580	7.805	1.032	42.216
Hexacosane	0.397	2.834	0.165	12.470	0.205	14.600	0.333	0.381	5.935	0.591	33.382
Heptacosane	0.632	5.244	0.591	18.695	0.421	26.671	0.501	0.371	8.654	0.935	60.810
Octacosane	0.160	2.321	0.149	11.548	0.000	14.938	0.124	0.108	4.734	0.165	31.441
Nonacosane	0.697	10.350	0.491	37.785	0.000	50.620	0.400	0.398	9.413	0.764	107.846
Triacontane	0.065	1.211	0.000	6.554	0.000	8.120	0.074	0.000	1.405	0.000	19.119
Hentriacontane	0.183	3.187	0.163	12.424	0.129	13.539	0.161	0.000	2.066	0.000	31.637
Dotriacontane	0.000	0.234	0.000	2.373	0.000	2.338	0.000	0.000	0.127	0.000	3.196
Tritriacontane	0.000	0.567	0.000	2.425	0.000	1.702	0.000	0.000	0.194	0.000	4.628
Tetratriacontane	0.000	0.000	0.000	0.000	0.000	0.000	0.000	0.000	0.000	0.000	0.000
Pentatriacontane	0.000	0.000	0.000	0.000	0.000	0.000	0.000	0.000	0.000	0.000	0.000
Hexatriacontane	0.000	0.000	0.000	0.000	0.000	0.000	0.000	0.000	0.000	0.000	0.000
Sum of alkanes	5.558	33.277	3.862	137.775	3.108	170.929	4.260	1.906	46.034	4.549	369.463
Iso-Nonacosane	0.000	0.000	0.000	0.000	0.000	0.000	0.000	0.000	0.000	0.000	0.000
anteiso-Triacontane	0.000	0.000	0.000	0.000	0.000	0.000	0.000	0.000	0.000	0.000	0.000
Iso-Hentriacontane	0.000	0.000	0.000	0.000	0.000	0.000	0.000	0.000	0.000	0.000	0.000
Sum of Branch-alkanes	0.000	0.000	0.000	0.000	0.000	0.000	0.000	0.000	0.000	0.000	0.000
17α(H)-21β(H)-29-Norhopane	0.092	0.166	0.097	0.432	0.081	0.510	0.068	0.068	0.066	0.101	0.915
17α(H)-21β(H)-Hopane	0.114	0.141	0.105	0.199	0.067	0.370	0.057	0.000	0.085	0.106	0.730
22,29,30-Trisnorneohopane	0.017	0.000	0.030	0.000	0.000	0.000	0.000	0.000	0.000	0.000	0.000

22,29,30-Trisnorhopane	0.010	0.000	0.026	0.182	0.000	0.402	0.000	0.000	0.074	0.000	1.053
22S,17α(H),21β(H)-Homohopane	0.053	0.068	0.042	0.090	0.074	0.133	0.057	0.000	0.000	0.098	0.358
22R,17α(H),21β(H)-Homohopane	0.055	0.150	0.044	0.322	0.037	0.786	0.067	0.000	0.342	0.076	1.403
22S,17α(H),21β(H)-Bishomohopane	0.057	0.091	0.031	0.054	0.049	0.000	0.036	0.000	0.000	0.073	0.556
22R,17α(H),21β(H)-Bishomohopane	0.033	0.236	0.037	0.266	0.034	0.322	0.028	0.000	0.152	0.054	1.146
22S,17α(H),21β(H)-Trishomohopane	0.018	0.104	0.029	0.492	0.000	0.666	0.017	0.000	0.122	0.000	2.073
22R,17α(H),21β(H)-Trishomohopane	0.031	0.000	0.017	0.000	0.000	0.000	0.000	0.000	0.000	0.000	0.000
Sum of hopanes	0.479	0.956	0.459	2.036	0.342	3.188	0.330	0.068	0.842	0.507	8.233
20S,R-5α(H),14β(H),17β(H)-Cholestanes	0.000	0.000	0.000	0.000	0.000	0.000	0.000	0.000	0.000	0.000	0.000
20R-5α(H),14α(H),17α(H)-Cholestane	0.000	0.000	0.000	0.000	0.000	0.000	0.000	0.000	0.000	0.000	0.000
20S,R-5α(H),14β(H),17β(H)-Ergostanes	0.000	0.000	0.000	0.000	0.000	0.000	0.000	0.000	0.000	0.000	0.000
20S,R-5α(H),14β(H),17β(H)-Sitostanes	0.000	0.000	0.000	0.000	0.000	0.000	0.000	0.000	0.000	0.000	0.000
Sum of steranes	0.000	0.000	0.000	0.000	0.000	0.000	0.000	0.000	0.000	0.000	0.000
Fluoranthene	0.048	0.071	0.051	0.134	0.042	0.059	0.041	0.022	0.023	0.034	0.113
Acephenanthrylene	0.003	0.024	0.000	0.040	0.000	0.040	0.000	0.000	0.000	0.000	0.087
Pyrene	0.025	0.049	0.028	0.111	0.027	0.084	0.022	0.011	0.029	0.027	0.117
Retene	0.003	0.037	0.008	0.085	0.008	0.193	0.005	0.020	0.056	0.021	0.142
Methyl substituted MW 202 PAH	0.000	0.118	0.000	0.254	0.000	0.170	0.000	0.000	0.000	0.000	0.000
Benzo(ghi)fluoranthene	0.020	0.028	0.021	0.058	0.013	0.010	0.013	0.000	0.000	0.000	0.000
Cyclopenta(cd)pyrene	0.007	0.012	0.008	0.070	0.007	0.022	0.008	0.000	0.000	0.000	0.000
Benz(a)anthracene	0.031	0.048	0.019	0.070	0.026	0.088	0.017	0.050	0.055	0.055	0.226
Chrysene/Triphenylene	0.054	0.101	0.049	0.214	0.049	0.120	0.043	0.015	0.032	0.052	0.217
Methyl substituted MW 228 PAH	0.000	0.119	0.000	0.293	0.000	0.356	0.000	0.000	0.000	0.000	0.000
Methyl substituted MW 226 PAH	0.000	0.000	0.000	0.000	0.000	0.000	0.000	0.000	0.000	0.000	0.000
Benzo(b)fluoranthene	0.032	0.056	0.023	0.168	0.041	0.127	0.036	0.000	0.031	0.041	0.110
Benzo(k)fluoranthene	0.027	0.076	0.022	0.153	0.049	0.122	0.027	0.000	0.025	0.056	0.075
Benzo(j)fluoranthene	0.000	0.000	0.000	0.000	0.000	0.000	0.000	0.000	0.000	0.000	0.000
Benzo(e)pyrene	0.008	0.074	0.008	0.193	0.007	0.157	0.006	0.005	0.000	0.037	0.278
Benzo(a)pyrene	0.015	0.038	0.014	0.067	0.020	0.032	0.026	0.007	0.000	0.032	0.040
Perylene	0.000	0.000	0.000	0.029	0.000	0.044	0.000	0.000	0.000	0.000	0.117
Indeno(1,2,3-cd)fluoranthene	0.018	0.000	0.000	0.015	0.000	0.021	0.000	0.000	0.000	0.000	0.000
Indeno(1,2,3-cd)pyrene	0.047	0.104	0.023	0.125	0.048	0.128	0.035	0.000	0.025	0.057	0.358
Picene	0.000	0.000	0.000	0.000	0.000	0.000	0.000	0.000	0.000	0.000	0.000
Benzo(ghi)perylene	0.068	0.132	0.056	0.187	0.076	0.104	0.051	0.000	0.000	0.033	0.128
Coronene	0.044	0.144	0.059	0.148	0.044	0.095	0.034	0.000	0.000	0.021	0.120
Sum of PAHs	0.450	1.233	0.388	2.413	0.456	1.971	0.364	0.129	0.276	0.465	2.126
8,15-Pimaredienoic acid	0.000	0.000	0.000	0.000	0.000	0.000	0.000	0.000	0.000	0.000	0.000

Pimaric acid	0.009	0.237	0.000	0.808	0.000	0.966	0.011	0.090	0.218	0.016	0.424
Sandaracopimaric acid	0.034	0.453	0.005	1.542	0.081	2.171	0.023	0.250	0.445	0.075	0.217
Isopimaric acid	0.000	0.000	0.000	0.000	0.000	0.000	0.000	0.000	0.000	0.000	0.000
Dehydroabietic acid	0.656	13.377	0.149	26.611	0.726	57.180	0.527	24.212	25.845	2.202	37.912
Abietic acid	0.000	0.000	0.000	0.115	0.000	0.079	0.000	0.000	0.000	0.000	0.000
Abieta-6,8,11,13,15-pentae-18-oic acid	0.010	0.056	0.008	0.142	0.008	0.216	0.000	0.000	0.102	0.000	0.346
Abieta-8,11,13,15-tetraen-18-oic acid	0.015	0.172	0.010	0.295	0.013	0.589	0.010	0.167	0.257	0.058	0.745
7-Oxodehydroabietic acid	0.720	4.006	0.260	5.538	0.523	10.606	0.458	4.629	6.321	1.899	19.648
Sum of Resin acids	1.444	18.301	0.432	35.053	1.351	71.809	1.030	29.349	33.188	4.251	59.292
1,2-Benzenedicarboxylic acid	0.777	1.013	0.530	4.043	0.171	3.236	0.321	0.000	0.000	0.000	3.125
1,4-Benzenedicarboxylic acid	0.317	0.628	0.278	0.818	0.208	0.726	0.254	0.010	0.031	0.265	2.114
1,3-Benzenedicarboxylic acid	0.132	0.357	0.090	0.808	0.069	0.660	0.084	0.000	0.000	0.000	1.632
Sum of Aromatic acids	1.226	1.998	0.898	5.669	0.448	4.622	0.659	0.010	0.031	0.265	6.871
Tetradecanoic acid	1.764	3.546	1.468	4.533	2.855	6.771	1.727	0.971	1.023	0.000	20.304
Pentadecanoic acid	1.024	2.399	1.066	3.760	1.792	5.204	1.080	0.000	0.000	0.000	12.684
Hexadecanoic acid	9.326	22.138	8.491	42.898	10.425	51.856	10.260	0.000	0.000	0.000	114.147
Heptadecanoic acid	0.348	1.317	0.437	3.449	0.375	4.738	0.468	0.000	0.000	0.000	9.204
Octadecanoic acid	2.565	7.401	2.467	18.703	2.256	25.562	3.337	0.000	0.000	0.000	48.732
Nonadecanoic acid	0.140	1.509	0.134	5.214	0.110	7.138	0.189	0.425	2.258	0.271	19.580
Eicosanoic acid	0.565	6.574	0.381	20.079	0.371	26.324	0.618	0.632	5.705	0.422	66.980
Heneicosanoic acid	0.171	3.109	0.117	10.330	0.082	12.532	0.202	0.273	3.261	0.372	34.621
Docosanoic acid	0.796	13.178	0.487	41.184	0.520	48.798	0.765	1.255	9.556	0.904	123.827
Tricosanoic acid	0.251	4.258	0.152	13.854	0.104	15.527	0.252	0.400	3.190	0.320	40.079
Tetracosanoic acid	0.847	16.518	0.604	52.830	0.503	72.198	0.892	1.025	12.967	1.013	157.697
Pentacosanoic acid	0.137	3.174	0.096	12.364	0.047	13.204	0.120	0.000	2.473	0.114	30.233
Hexacosanoic acid	0.464	14.841	0.264	52.666	0.146	70.863	0.518	0.402	11.937	0.636	141.746
Heptacosanoic acid	0.029	1.748	0.018	8.071	0.000	9.347	0.053	0.000	1.083	0.000	18.859
Octacosanoic acid	0.234	9.793	0.121	38.450	0.042	52.337	0.270	0.130	6.166	0.258	94.773
Nonacosanoic acid	0.000	1.580	0.000	6.986	0.000	7.312	0.016	0.000	0.321	0.000	14.517
Triacontanoic acid	0.080	5.907	0.035	25.116	0.000	26.333	0.076	0.000	1.739	0.099	59.368
9-Hexadecenoic acid	0.000	0.000	0.000	0.000	0.000	0.000	0.000	0.000	0.000	0.000	0.000
9,12-Octadecanedienoic acid	0.000	0.000	0.000	0.000	0.000	0.000	0.000	0.000	0.000	0.000	0.000
9-Octadecenoic acid	0.214	0.000	0.275	0.000	0.414	0.637	0.200	0.000	0.000	0.000	0.000
Pinonic acid	10.207	7.973	4.152	5.744	3.427	3.254	4.181	40.116	41.308	81.314	26.521
Pinic acid	4.257	8.408	1.282	10.416	2.709	8.312	3.797	1.563	3.639	14.493	99.455
sum of Fatty acids	33.420	135.369	22.047	376.647	26.179	468.247	29.022	47.191	106.624	100.214	1133.327
Propanedioic acid	0.000	0.000	0.000	0.000	0.000	0.000	0.000	0.000	0.000	0.000	0.000

Methylpropanedioic acid	0.000	0.000	0.000	0.000	0.000	0.000	0.000	0.000	0.000	0.000	0.000
Butanedioic acid	3.512	5.619	1.578	13.153	0.778	10.248	1.843	0.000	0.250	0.219	20.587
Methylbutanedioic acid	0.282	0.919	0.136	2.894	0.066	2.928	0.338	0.000	0.000	0.000	5.958
Pentanedioic acid	0.875	1.462	0.467	3.292	0.330	3.030	0.543	0.000	0.000	0.000	10.776
Hexanedioic acid	0.728	1.092	0.904	2.348	0.207	2.163	0.388	0.000	0.000	0.000	7.908
Heptanedioic acid	0.348	1.048	0.129	2.950	0.138	3.000	0.212	0.000	0.000	0.000	12.634
Octanedioic acid	0.547	1.618	0.321	5.209	0.195	5.088	0.366	0.000	0.000	0.000	17.469
Nonanedioic acid	1.030	4.884	0.618	14.445	0.601	13.896	0.978	0.000	0.000	0.133	49.874
Sum of dicarboxylic diacids	7.321	16.643	4.153	44.292	2.315	40.354	4.667	0.000	0.250	0.352	125.207
Nonanal	0.286	0.488	0.482	1.787	0.283	1.896	0.566	0.189	0.309	0.235	1.949
sinapyl aldehyde	0.000	0.000	0.000	0.000	0.000	0.000	0.000	0.000	0.000	0.000	0.000
acetonylsyringol	0.000	1.012	0.000	3.945	0.000	3.446	0.000	0.000	0.176	0.000	4.421
coniferyl aldehyde	0.000	0.000	0.000	0.000	0.000	0.000	0.000	0.000	0.000	0.000	0.000
propionylsyringol	0.000	0.000	0.000	0.000	0.000	0.000	0.000	0.000	0.000	0.000	0.000
benz(de)anthracen-7-one	0.000	0.000	0.000	0.166	0.000	0.000	0.000	0.000	0.000	0.000	0.000
3,5-dimethoxy-4-hydroxyacetophenone	0.000	0.310	0.000	0.926	0.000	1.034	0.000	0.000	0.000	0.000	2.613
Levoglucosan	31.842	604.289	19.410	1736.307	25.609	1402.624	28.726	21.850	308.902	41.144	6663.574
Cholesterol	0.304	0.429	0.316	0.028	0.324	0.419	0.103	0.000	0.089	0.000	0.000
2-Methylthreitol	9.873	14.524	1.559	14.836	3.548	12.006	0.000	0.000	0.959	0.000	26.714
2-Methylerythritol	20.087	29.891	2.884	33.650	7.801	25.737	0.000	0.000	2.154	0.000	56.883
Sum of Other compounds	62.391	650.944	24.652	1791.644	37.566	1447.163	29.395	22.040	312.590	41.379	6756.153
Organic Carbon (ug/m3)	4.09	10.29	2.56	25.32	3.22	22.67	3.41	3.27	7.75	5.13	62.84
Element Carbon (ug/m3)	0.74	1.25	0.62	2.10	0.75	1.68	0.65	0.23	0.58	0.51	1.22
EC/OC	0.180	0.121	0.244	0.083	0.234	0.074	0.192	0.071	0.074	0.099	0.019

Table D.2. Source Apportionment of Organic Carbons Measured in The Non-Smoke and Smoke Days Using CMB-MM and Different Biomass Burning Source Profiles (unit: μg m^{-3})

Samples	Diesel Exhaust [a]	Gasoline Exhaust [b]	Vegetative Detritus [c]	Meat Cooking [d]	Road Dust [e]	Combined Wood burning [f]	Prescribed Wood Burning [g]	Aged Prescribed Wood Burning [h]	Others	Measured OC	R^2	χ^2	% Mass
NonSmoke-1	0.291	0.023	0.006	0.242	0.024	0.295			3.21	4.10	0.92	1.5	22
NonSmoke-1	0.293	0.012	0.002	0.234	0.024	0.033	0.478		3.02	4.10	0.90	1.5	26
NonSmoke-1	0.289	0.013	0.001	0.232	0.024		0.520		3.02	4.10	0.90	1.3	26
NonSmoke-1	0.250	0.043	0.002	0.264	0.027	0.165		0.249	3.09	4.10	0.84	3.2	24
NonSmoke-1	0.192	0.071	0.000	0.257	0.027			0.360	3.19	4.10	0.82	3.0	22
Smoke-1	0.346	0.050	0.064	0.375	0.019	4.828			4.61	10.3	0.93	1.9	55
Smoke-1	0.452	0.028	0.052	0.403	0.020		6.101		3.24	10.3	0.85	1.8	69
Smoke-1	0.432	0.053	0.000	0.409	0.028			5.590	3.78	10.3	0.81	2.2	63
NonSmoke-2	0.246	0.021	0.007	0.281	0.020	0.170			1.81	2.56	0.86	2.5	29
NonSmoke-2	0.226	0.021	0.004	0.241	0.021	0.055	0.192		1.80	2.56	0.87	2.2	30
NonSmoke-2	0.217	0.023	0.003	0.232	0.021		0.267		1.80	2.56	0.88	1.9	30
NonSmoke-2	0.213	0.032	0.004	0.272	0.021	0.095		0.088	1.83	2.56	0.86	2.8	28
NonSmoke-2	0.200	0.034	0.002	0.254	0.022			0.189	1.86	2.56	0.87	2.6	27
Smoke-2	0.283	0.235	0.236	0.024	0.056	13.744			10.8	25.3	0.93	2.2	58
Smoke-2	0.513	0.157	0.271	0.025	0.048		15.918		8.39	25.3	0.77	3.6	67
Smoke-2	0.541	0.039	0.012	0.024	0.088			16.219	8.40	25.3	0.89	1.0	67
NonSmoke-3	0.287	0.001	0.004	0.298	0.021	0.323			2.29	3.22	0.87	2.5	29
NonSmoke-3	0.266	0.000	0.001	0.282	0.022		0.310		2.34	3.22	0.89	2.0	27
NonSmoke-3	0.196	0.031	0.000	0.285	0.024			0.246	2.44	3.22	0.79	3.9	24
Smoke-3	0.211	0.415	0.171	0.367	0.020	11.190			10.3	22.7	0.90	3.7	55
Smoke-3	0.255	0.401	0.108	0.367	0.030		17.580		3.93	22.7	0.93	0.9	83
Smoke-3	0.433	0.245	0.007	0.367	0.043			11.579	10.0	22.7	0.95	0.7	56
Smoke-3	0.470	0.216	0.011	0.367	0.041			11.253	10.3	22.7	0.96	0.4	55
NonSmoke-4	0.270	0.002	0.007	0.096	0.030	0.284			2.73	3.41	0.84	3.1	20
NonSmoke-4	0.202	0.001	0.001	0.084	0.031		0.428		2.67	3.41	0.94	0.7	22
NonSmoke-4	0.170	0.029	0.000	0.089	0.034			0.260	2.83	3.41	0.86	2.5	17
NoSmok-Bibb	0.204	0.078	0.042	0.000	0.132	0.397			2.77	3.62	0.87	2.5	24
NoSmok-Bibb	0.169	0.062	0.009	0.000	0.130		0.595		2.66	3.62	0.97	0.4	27
NoSmok-Bibb	0.129	0.111	0.021	0.000	0.134			0.352	2.87	3.62	0.90	2.5	21
Smoke_Bibb		0.923	0.467	0.000	0.000	11.932			39.9	53.2	0.74	5.2	25

Smoke_Bibb		0.925	0.276	0.000	0.031		40.101		11.9	53.2	0.84	2.0	78
Smoke_Bibb		0.587	0.000	0.000	0.074			33.234	19.3	53.2	0.93	0.6	64
NoSmok-Coffe	0.111	0.087	0.020	0.000	0.088	0.176			1.54	2.02	0.89	3.0	24
NoSmok-Coffe	0.084	0.076	0.005	0.000	0.089		0.360		1.41	2.02	0.90	1.9	30
NoSmok-Coffe	0.093	0.085	0.010	0.000	0.089			0.177	1.57	2.02	0.91	2.5	22
Smoke_Coffee	0.102	0.050	0.015	0.078	0.203	2.467			2.95	5.87	0.92	1.8	50
Smoke_Coffee	0.158	0.028	0.013	0.078	0.194		2.704		2.69	5.87	0.81	2.6	54
Smoke_Coffee	0.155	0.026	0.000	0.078	0.189			1.732	3.69	5.87	0.94	0.6	37

Note: [a] source profile of medium duty diesel truck exhaust [*Schauer et al.*, 1999b]; [b] combined gasoline vehicle exhaust of catalyst-equipped and noncatalyst-equipped gasoline-powered vehicles [*Schauer et al.*, 2002b]; [c] vegetative detritus [*Hildemann et al.*, 1991; *Rogge et al.*, 1993a]; [d] meat cooking [*Schauer et al.*, 1999a]; [e] Alabama paved road dust [*Schauer*, 1998; *U.S.EPA*, 2002; *Zheng et al.*, 2002]; [f] combined wood combustion in the Southeastern states [*Fine et al.*, 2002]; [g] prescribed burning in Georgia [*Lee et al.*, 2005a]; [h] aged prescribed burning in Georgia [*Yan et al.*, 2008a].

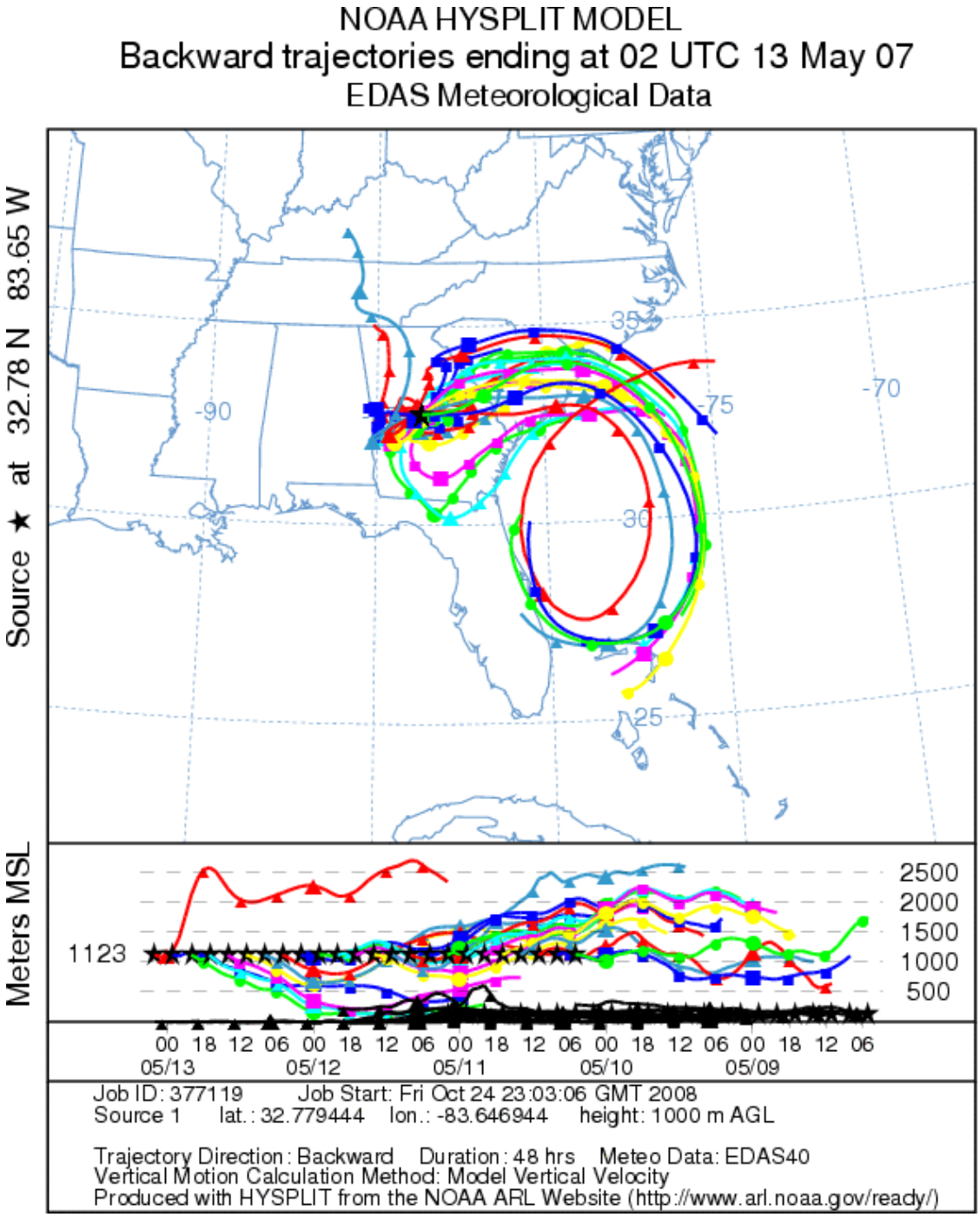

Figure D.1. 48-hr back trajectories for the ambient air monitors in metro Atlanta, Bibb, Coffee and Okefenokee sites impacted by the wildfire smoke plumes occurred in May 2007.

REFERENCES

Alessio, G. A., et al. (2004), Direct and indirect impacts of fire on isoprenoid emissions from Mediterranean vegetation, *Functional Ecology*, *18*(3), 357-364.

Allan, J. D., et al. (2003), Quantitative sampling using an Aerodyne aerosol mass spectrometer: 1. Techniques of data interpretation and error analysis (vol 108, art no 4090, 2003), *Journal of Geophysical Research-Atmospheres*, *108*(D9).

Baumann, K., et al. (2003), Discrete measurements of reactive gases and fine particle mass and composition during the 1999 Atlanta Supersite experiment, *Journal of Geophysical Research-Atmospheres*, *108*(D7), Artn 8416, doi: 8410.1029/2001jd001210.

Bhave, P. V., et al. (2007), Diagnostic model evaluation for carbonaceous PM2.5 using organic markers measured in the southeastern US, *Environ. Sci. Technol.*, *41*(5), 1577-1583.

Bond, T. C., et al. (2004), A technology-based global inventory of black and organic carbon emissions from combustion, *J. Geophys. Res.-Atmos.*, *109*(D14), 43.

Brewer, P. F., and J. P. Adlhoch (2005), Trends in speciated fine particulate matter and visibility across monitoring networks in the southeastern United States, Air & Waste Management Assoc.

Britt, H. I., and R. H. Luecke (1973), Estimation of parameters in nonlinear, implicit models, *Technometrics*, *15*(2), 233-247.

Brown, S. G., et al. (2002), Characterization of organic aerosol in Big Bend National Park, Texas, *Atmos. Environ.*, *36*(38), 5807-5818.

Buseck, P. R., and M. Posfai (1999), Airborne minerals and related aerosol particles: Effects on climate and the environment, Natl Acad Sciences.

Butler, A. J., et al. (2003), Daily sampling of PM2.5 in Atlanta: results of the first year of the assessment of spatial aerosol composition in Atlanta study, *Journal of Geophysical Research-Atmospheres*, *108*(D1), Artn 8415, doi: 8410.1029/2002jd002234.

Cabada, J. C., et al. (2004), Estimating the secondary organic aerosol contribution to PM2.5 using the EC tracer method, *Aerosol Science and Technology*, *38*, 140-155.

Cadle, S. H., et al. (1999), Composition of light-duty motor vehicle exhaust particulate matter in the Denver, Colorado area, *Environ. Sci. Technol.*, *33*(14), 2328-2339.

Canagaratna, M. R., et al. (2007), Chemical and microphysical characterization of ambient aerosols with the aerodyne aerosol mass spectrometer, *Mass Spectrometry Reviews*, *26*(2), 185-222.

Cass, G. R., and G. J. Mcrae (1983), Source receptor reconciliation of routine air monitoring data for trace-metals - an emission inventory assisted approach, *Environ. Sci. Technol.*, *17*(3), 129-139.

Cass, G. R. (1998), Organic molecular tracers for particulate air pollution sources, *Trac-Trends in Analytical Chemistry*, *17*(6), 356-366.

Chan, Y. C., et al. (1999), Source apportionment of PM2.5 and PM10 aerosols in Brisbane (Australia) by receptor modelling, *Atmos. Environ.*, *33*(19), 3251-3268.

Charlson, R. J., et al. (1992), Climate forcing by anthropogenic aerosols, *Science*, *255*(5043), 423-430.

Chen, K. S., et al. (2001), Determination of source contributions to ambient PM2.5 in Kaohsiung, Taiwan, using a receptor model, *J. Air Waste Manage. Assoc.*, *51*(4), 489-498.

Chow, J., et al. (2001), Comparison of IMPROVE and NIOSH carbon measurements, *AEROSOL SCI TECH*, *34*(1), 23-34.

Chow, J. C., et al. (1992), PM10 source apportionment in California San-Joaquin valley, *Atmospheric Environment Part a-General Topics*, *26*(18), 3335-3354.

Chow, J. C., et al. (1995), Source apportionment of wintertime PM(10) at San-Jose, Calif, *Journal of Environmental Engineering-Asce*, *121*(5), 378-387.

Chow, J. C., and J. G. Watson (2002), Review of PM2.5 and PM10 apportionment for fossil fuel combustion and other sources by the chemical mass balance receptor model, *Energy & Fuels*, *16*(2), 222-260.

Chow, J. C., et al. (2004a), Equivalence of elemental carbon by thermal/optical reflectance and transmittance with different temperature protocols, *Environ. Sci. Technol.*, *38*(16), 4414-4422.

Chow, J. C., et al. (2004b), Source profiles for industrial, mobile, and area sources in the Big Bend Regional Aerosol Visibility and Observational study, *Chemosphere*, *54*(2), 185-208.

Chow, J. C., et al. (2005), Refining temperature measures in thermal/optical carbon analysis, *Atmospheric Chemistry and Physics*, *5*, 2961-2972.

Chu, S. H., et al. (2004), PM data analysis - a comparison of two urban areas: Fresno and Atlanta, *Atmos. Environ.*, *38*(20), 3155-3164.

Chu, S. H. (2005), Stable estimate of primary OC/EC ratios in the EC tracer method, *Atmos. Environ.*, *39*(8), 1383-1392.

Claeys, M., et al. (2004a), Formation of secondary organic aerosols through photooxidation of isoprene, *Science*, *303*(5661), 1173-1176.

Claeys, M., et al. (2004b), Formation of secondary organic aerosols from isoprene and its gas-phase oxidation products through reaction with hydrogen peroxide, *Atmos. Environ.*, *38*(25), 4093-4098.

Cooper, J. A., and J. G. Watson (1980), Receptor oriented methods of air particulate source apportionment, *Journal of the Air Pollution Control Association*, *30*(10), 1116-1125.

Cooper, J. A., et al. (1987), PM10 source composition library for the south coast air basin, Volume I and II. , Prepared for the South Coast Air Quality Management District, El Monte, CA.

Cottrell, L. D., et al. (2008), Submicron particles at Thompson Farm during ICARTT measured using aerosol mass spectrometry, *Journal of Geophysical Research-Atmospheres*, *113*(D8).

DeCarlo, P. F., et al. (2008), Fast airborne aerosol size and chemistry measurements above Mexico City and Central Mexico during the MILAGRO campaign, *Atmospheric Chemistry and Physics*, *8*(14), 4027-4048.

Demerjian, K. L. (2000), A review of national monitoring networks in North America, *Atmos. Environ.*, *34*(12-14), 1861-1884.

Ding, X., et al. (2008), Spatial and seasonal trends in biogenic secondary organic aerosol tracers and water-soluble organic carbon in the southeastern United States, *Environ. Sci. Technol.*, *42*(14), 5171-5176.

Docherty, K. S., et al. (2008), Apportionment of primary and secondary organic aerosols in southern California during the 2005 Study of Organic Aerosols in Riverside (SOAR-1), *Environ. Sci. Technol.*, *42*(20), 7655-7662.

Dockery, D. W., et al. (1993), An association between air-pollution and mortality in 6 United-States cities, *N. Engl. J. Med.*, *329*(24), 1753-1759.

Donahue, N. M., et al. (2006), Coupled partitioning, dilution, and chemical aging of semivolatile organics, *Environ. Sci. Technol.*, *40*(8), 2635-2643.

Edgerton, E. S., et al. (2005), The southeastern aerosol research and characterization study: Part II. Filter-based measurements of fine and coarse particulate matter mass and composition, *Journal of the Air & Waste Management Association*, *55*(10), 1527-1542.

Edgerton, E. S., et al. (2006), The Southeastern Aerosol Research and Characterization Study, part 3: Continuous measurements of fine particulate matter mass and composition, *J. Air Waste Manage. Assoc.*, *56*(9), 1325-1341.

Edney, E. O., et al. (2005), Formation of 2-methyl tetrols and 2-methylglyceric acid in secondary organic aerosol from laboratory irradiated isoprene/NOX/SO2/air mixtures and their detection in ambient PM2.5 samples collected in the eastern United States, *Atmos. Environ.*, *39*(29), 5281-5289.

El-Zanan, H. S., et al. (2009), Analytical determination of the aerosol organic mass-to-organic carbon ratio, *J. Air Waste Manage. Assoc.*, *59*(1), 58-69.

Eldred, R. A., et al. (1997), Composition of PM(2.5) and PM(10) aerosols in the IMPROVE network, Air & Waste Management Assoc.

Engelbrecht, J. P. (2003), Cairo Air Improvement Project (CAIP): positive matrix factorization (PMF) receptor modeling; preliminary report prepared for Chemonics International Inc., Washington, DC.

Engling, G., et al. (2006), Determination of levoglucosan in biomass combustion aerosol by high-performance anion-exchange chromatography with pulsed amperometric detection.

EPA, U. S. (2000), National Air Pollutant Emission Trends 1900-1998, EPA 454/R-400–002, Office: Washington, DC.

Escamilla-Nunez, M. C., et al. (2008), Traffic-related air pollution and respiratory symptoms among asthmatic children, resident in Mexico City: the EVA cohort study, *Respir. Res.*, *9*, 10.

Fine, P. M., et al. (2001), Chemical characterization of fine particle emissions from fireplace combustion of woods grown in the northeastern United States, *Environ. Sci. Technol.*, *35*(13), 2665-2675.

Fine, P. M., et al. (2002), Chemical characterization of fine particle emissions from the fireplace combustion of woods grown in the southern United States, *Environ. Sci. Technol.*, *36*(7), 1442-1451.

Fine, P. M., et al. (2004a), Chemical characterization of fine particle emissions from the wood stove combustion of prevalent United States tree species, *Environmental Engineering Science*, *21*(6), 705-721.

Fine, P. M., et al. (2004b), Diurnal variations of individual organic compound constituents of ultrafine and accumulation mode particulate matter in the Los Angeles basin, *Environ. Sci. Technol.*, *38*(5), 1296-1304.

Flannigan, M. D., et al. (1998), Future wildfire in circumboreal forests in relation to global warming, Opulus Press Uppsala Ab.

Fraser, M. P., and K. Lakshmanan (2000), Using levoglucosan as a molecular marker for the long-range transport of biomass combustion aerosols, *Environ. Sci. Technol.*, *34*(21), 4560-4564.

Fraser, M. P., et al. (2003a), Air quality model evaluation data for organics. 6. C-3-C-24 organic acids, *Environ. Sci. Technol.*, *37*(3), 446-453.

Fraser, M. P., et al. (2003b), Source apportionment of fine particulate matter in Houston, TX, using organic molecular markers, *Atmos. Environ.*, *37*(15), 2117-2123.

Friedlander, S. K. (1973), Chemical element balances and identification of air-pollution sources, *Environmental Science & Technology*, *7*(3), 235-240.

Gartrell, G., and S. K. Friedlander (1975), Relating particulate pollution to sources - 1972 California Aerosol Characterization Study, *Atmos. Environ.*, *9*(3), 279-299.

Georgia Department of Transportation. (2006), The annual daily average traffic report of 2006, http://www.dot.ga.gov/statistics/Documents/cov2006.xls record 8492.

Georgia DOT (2006), The annunal daily average traffic count at I-75/85, edited, http://www.dot.ga.gov/statistics/Documents/cov2006.xls, record 8492.

Georgia EPD (2007), Exceedances of federal air quality standards in Georgia (2007) edited, http://www.air.dnr.state.ga.us/tmp/exceedances/index.php?yr=2007.

Geron, C., et al. (2000), A review and synthesis of monoterpene speciation from forests in the United States, *Atmos. Environ.*, *34*(11), 1761-1781.

Gordon, G. E. (1980), Receptor models, *Environ. Sci. Technol.*, *14*(7), 792-800.

Hansen, D. A., et al. (2003), The Southeastern Aerosol Research and Characterization Study (SEARCH): 1. Overview, *Journal of Air & Waste Management Association*, *53*, 1460-1471.

Hawthorne, S. B., et al. (1988), Identification of methoxylated phenols as candidate tracers for atmospheric wood smoke pollution, *Environ. Sci. Technol.*, *22*(10), 1191-1196.

Hawthorne, S. B., et al. (1989), Collection and quantitation of methoxylated phenol tracers for atmospheric-pollution from residential wood stoves, *Environ. Sci. Technol.*, *23*(4), 470-475.

Hays, M. D., et al. (2002), Speciation of gas-phase and fine particle emissions from burning of foliar fuels, *Environ. Sci. Technol.*, *36*(11), 2281-2295.

Hays, M. D., et al. (2003), Polycyclic aromatic hydrocarbon size distributions in aerosols from appliances of residential wood combustion as determined by direct thermal desorption-GC/MS, *Journal of Aerosol Science*, *34*, 1061-1084.

Haywood, J., and O. Boucher (2000), Estimates of the direct and indirect radiative forcing due to tropospheric aerosols: A review, *Rev. Geophys.*, *38*(4), 513-543.

Hidy, G. M., and C. Venkataraman (1996), The chemical mass balance method for estimating atmospheric particle sources in southern California, *Chemical Engineering Communications*, *151*, 187-209.

Hildemann, L. M., et al. (1991), Chemical composition of emissions from urban sources of fine organic aerosol, *Environ. Sci. Technol.*, *25*(4), 744-759.

Hildemann, L. M., et al. (1993), Mathematical-modeling of urban organic aerosol - properties measured by high-resolution gas-chromatography, *Environ. Sci. Technol.*, *27*(10), 2045-2055.

Hildemann, L. M., G.R. Markowski, G.R. Cass (1991), Chemical composition of emissions from urban sources of the organic aerosol, *Environmental Science and Technology*, *25*, 744-759.

Hobbs, P. V., et al. (1997), Direct radiative forcing by smoke from biomass burning, *Science*, *275*(5307), 1776-1778.

Hopke, P. K. (2003), Recent developments in receptor modeling, *Journal of Chemometrics*, *17*(5), 255-265.

Horvath, H. (1993), Atmospheric light-absorption - A review, *Atmospheric Environment Part a-General Topics*, *27*(3), 293-317.

Hu, Y. T., et al. (2008), Simulation of air quality impacts from prescribed fires on an urban area, *Environmental Science & Technology*, *42*(10), 3676-3682.

IPCC (2007), Climate change 2007: synthesis report - IPCC fourth assessment report, 184 pp, IPCC: Geneva, Switzerland.

Jimenez, J. L., et al. (2003), Ambient aerosol sampling using the Aerodyne Aerosol Mass Spectrometer, *Journal of Geophysical Research-Atmospheres*, *108*(D7).

Kall, D., and R. Guensler (2007), 2007 Study of peak-period highway users on I-85 in metropolitan Atlanta, Georgia Department of Transportation.

Kavouras, I. G., et al. (1998), Formation of atmospheric particles from organic acids produced by forests, *Nature*, *395*(6703), 683-686.

Kim, E., et al. (2003), Source identification of Atlanta aerosol by positive matrix factorization, *J. Air Waste Manage. Assoc.*, *53*(6), 731-739.

Kleindienst, T. E., et al. (2007a), Estimates of the contributions of biogenic and anthropogenic hydrocarbons to secondary organic aerosol at a southeastern US location, *Atmos. Environ.*, *41*(37), 8288-8300.

Kleindienst, T. E., et al. (2007b), Ozone-isoprene reaction: Re-examination of the formation of secondary organic aerosol, *Geophysical Research Letters*, *34*(1), Artn L01805, doi 01810.01029/02006gl027485.

Kondo, Y., et al. (2007), Oxygenated and water-soluble organic aerosols in Tokyo, *Journal of Geophysical Research-Atmospheres*, *112*(D1), 11.

Kowalczyk, G. S., et al. (1978), Chemical element balances and identification of air-pollution sources in Washington, DC, *Atmos. Environ.*, *12*(5), 1143-1153.

Lamb, B., et al. (1987), A national inventory of biogenic hydrocarbon emissions, *Atmos. Environ.*, *21*(8), 1695-1705.

Lee, S., et al. (2005a), Gaseous and particulate emissions from prescribed burning in Georgia, *Environ. Sci. Technol.*, *39*(23), 9049-9056.

Lee, S., et al. (2005b), Source apportionment of PM2.5 in the southeastern United States, paper presented at AAAR international specialty conference: particulate matter supersites program and related studies. Oral presentation 8B-5, February 7-11, Atlanta, GA.

Lee, S., et al. (2007), Source apportionment of fine particulate matter in the southeastern united states, *J. Air Waste Manage. Assoc.*, *57*(9), 1123-1135.

Lee, S., et al. (2008), Diagnosis of aged prescribed burning plumes impacting an urban area, *Environmental Science & Technology*, *42*(5), 1438-1444.

Lewandowski, M., et al. (2008), Primary and secondary contributions to ambient PM in the midwestern United States, *Environ. Sci. Technol.*, *42*(9), 3303-3309.

Liao, H., et al. (2007), Biogenic secondary organic aerosol over the United States: Comparison of climatological simulations with observations, *Journal of Geophysical Research-Atmospheres*, *112*(D6), Artn D06201, doi 06210.01029/02006jd007813.

Lighty, J. S., et al. (2000), Combustion aerosols: Factors governing their size and composition and implications to human health, *J. Air Waste Manage. Assoc.*, *50*(9), 1565-1618.

Lim, H. J., and B. J. Turpin (2002), Origins of primary and secondary organic aerosol in Atlanta: Results of time-resolved measurements during the Atlanta Supersite experiment, *Environmental Science and Technology*, *36*, 4489-4496.

Lipsky, E. M., and A. L. Robinson (2006), Effects of dilution on fine particle mass and partitioning of semivolatile organics in diesel exhaust and wood smoke, *Environ. Sci. Technol.*, *40*(1), 155-162.

Liu, W., et al. (2005), Atmospheric aerosol over two urban-rural pairs in the southeastern United States: Chemical composition and possible sources, *Atmos. Environ.*, *39*(25), 4453-4470.

Lough, G. C., et al. (2005a), Summer and winter nonmethane hydrocarbon emissions from on-road motor vehicles in the Midwestern United States, *J. Air Waste Manage. Assoc.*, *55*(5), 629-646.

Lough, G. C., et al. (2005b), Emissions of metals associated with motor vehicle roadways, *Environ. Sci. Technol.*, *39*(3), 826-836.

Lough, G. C., et al. (2007), Development of molecular marker source profiles for emissions from on-road gasoline and diesel vehicle fleets, *J. Air Waste Manage. Assoc.*, *57*(10), 1190-1199.

Lough, G. C., and J. J. Schauer (2007), Sensitivity of source apportionment of urban particulate matter to uncertainty in motor vehicle emissions profiles, *J. Air Waste Manage. Assoc.*, *57*(10), 1200-1213.

Malm, W. C., et al. (1994), Spatial and seasonal trends in particle concentration and optical extinction in the United-States, *Journal of Geophysical Research-Atmospheres*, *99*(D1), 1347-1370.

Manchester-Neesvig, J. B., et al. (2003), The distribution of particle-phase organic compounds in the atmosphere and their use for source apportionment during the southern California children's health study, *Journal of Air & Waste Management Association*, *53*, 1065-1079.

Marmur, A., et al. (2005), Optimization-based source apportionment of PM2.5 incorporating gas-to-particle ratios, *Environ. Sci. Technol.*, *39*(9), 3245-3254.

Mazurek, M. A., and B. R. T. Simoneit (1984), Characterization of biogenic and petroleum derived organic matter in aerosols over remote, rural and urban areas. In: Keith, L.H. (Ed.), Identification and Analysis of Organic Pollutants in Air, edited, pp. 353-370, Ann Arbor Science/Butterworth Publisher, Boston, MA.

Miller, M. S., et al. (1972), Chemical element balance for Pasadena aerosol, *Journal of Colloid and Interface Science 39*(1), 165-176.

Miyazaki, Y., et al. (2006), Time-resolved measurements of water-soluble organic carbon in Tokyo, *Journal of Geophysical Research-Atmospheres*, *111*(D23), Artn D23206, doi 23210.21029/22006jd007125.

NIFC (2007), National Interagency Fire Center: fire information - wildland fire statistics edited.

NIFC (2008), National Interagency Fire Center: fire information - wildland fire statistics, available at: http://www.nifc.gov/fire_info/prescribed_fires.htm, access: November, 2008.

Ning, Z., et al. (2008), Emission factors of PM species based on freeway measurements and comparison with tunnel and dynamometer studies, *Atmospheric Environment*, *42*(13), 3099-3114.

Nolte, C. G., et al. (2002), Trimethylsilyl derivatives of organic compounds in source samples and in atmospheric fine particulate matter, *Environ. Sci. Technol.*, *36*(20), 4273-4281.

Nopmongcol, U., et al. (2007), Estimates of heterogeneous formation of secondary organic aerosol during a wood smoke episode in Houston, Texas, *Atmos. Environ.*, *41*(14), 3057-3070.

Odum, J. R., et al. (1996), Gas/particle partitioning and secondary organic aerosol yields, *Environ. Sci. Technol.*, *30*(8), 2580-2585.

Offenberg, J. H., et al. (2007), Contributions of toluene and alpha-pinene to SOA formed in an irradiated toluene/alpha-pinene/NOx/air mixture: Comparison of results using C-14 content and SOA organic tracer methods, *Environ. Sci. Technol.*, *41*(11), 3972-3976.

Oros, D. R., and B. R. T. Simoneit (2000), Identification and emission rates of molecular tracers in coal smoke particulate matter, *Fuel*, *79*(5), 515-536.

Oros, D. R., and B. R. T. Simoneit (2001), Identification and emission factors of molecular tracers in organic aerosols from biomass burning Part 1. Temperate climate conifers, *Applied Geochemistry*, *16*(13), 1513-1544.

Oros, D. R., et al. (2006), Identification and emission factors of molecular tracers in organic aerosols from biomass burning: Part 3. Grasses, *Applied Geochemistry*, *21*(6), 919-940.

Pankow, J. F. (1987), Review and comparative-analysis of the theories on partitioning between the gas and aerosol particulate phases in the atmosphere, *Atmos. Environ.*, *21*(11), 2275-2283.

Penner, J. E., et al. (1992), Effects of aerosol from biomass burning on the global radiation budget, *Science*, *256*(5062), 1432-1434.

Pope, C. A., et al. (1995), Review of epidemiological evidence of health-effects of particulate air-pollution, Taylor & Francis.

Pope, C. A., et al. (2002), Lung cancer, cardiopulmonary mortality, and long-term exposure to fine particulate air pollution, *Jama-Journal of the American Medical Association*, *287*(9), 1132-1141.

Pope, C. A. (2007), Mortality effects of longer term exposures to fine particulate air pollution: Review of recent epidemiological evidence, *Inhalation Toxicology*, *19*, 33-38.

Pope, C. A., et al. (2009), Fine-particulate air pollution and life expectancy in the United States, *N. Engl. J. Med.*, *360*(4), 376-386.

Prospero, J. M., et al. (2001), Al and Fe in PM 2.5 and PM 10 suspended particles in south-central Florida: The impact of the long range transport of African mineral dust, *Water Air Soil Pollut.*, *125*(1-4), 291-317.

Ramdahl, T. (1983), Retene - a molecular marker of wood combustion in ambient air, *Nature*, *306*(5943), 580-583.

Reid, J. S., et al. (2005), A review of biomass burning emissions part II: intensive physical properties of biomass burning particles, *Atmos. Chem. Phys.*, *5*, 799-825.

Robinson, A. L., et al. (2006a), Photochemical oxidation and changes in molecular composition of organic aerosol in the regional context, *Journal of Geophysical Research-Atmospheres*, *111*(D3).

Robinson, A. L., et al. (2006b), Source apportionment of molecular markers and organic aerosol. 2. Biomass smoke, *Environ. Sci. Technol.*, *40*(24), 7811-7819.

Robinson, A. L., et al. (2006c), Source apportionment of molecular markers and organic aerosol. 3. Food cooking emissions, *Environ. Sci. Technol.*, *40*(24), 7820-7827.

Robinson, A. L., et al. (2007), Rethinking organic aerosols: Semivolatile emissions and photochemical aging, *Science*, *315*(5816), 1259-1262.

Robinson, M. S., et al. (2004), Chemical speciation of PM2.5 fires of the coconino national collected during prescribed forest near Flagstaff, Arizona, *J. Air Waste Manage. Assoc.*, *54*(9), 1112-1123.

Rogge, W. F., et al. (1991), Sources of fine organic aerosol .1. Charbroilers and meat cooking operations, *Environ. Sci. Technol.*, *25*(6), 1112-1125.

Rogge, W. F., et al. (1993a), Sources of fine organic aerosol .4. Particulate abrasion products from leaf surfaces of urban plants, *Environ. Sci. Technol.*, *27*(13), 2700-2711.

Rogge, W. F., et al. (1993b), Sources of fine organic aerosol .5. Natural-gas home appliances, *Environ. Sci. Technol.*, *27*(13), 2736-2744.

Rogge, W. F., et al. (1993c), Sources of fine organic aerosol .3. Road dust, tire debris, and organometallic brake lining dust - roads as sources and sinks, *Environ. Sci. Technol.*, *27*(9), 1892-1904.

Rogge, W. F., et al. (1993d), Sources of fine organic aerosol .2. Noncatalyst and catalyst-equipped automobiles and heavy-duty diesel trucks, *Environ. Sci. Technol.*, *27*(4), 636-651.

Rogge, W. F., et al. (1993e), Quantification of urban organic aerosols at a molecular-level - identification, abundance and seasonal-variation, *Atmospheric Environment Part a-General Topics*, *27*(8), 1309-1330.

Rogge, W. F., et al. (1998), Sources of fine organic aerosol. 9. Pine, oak and synthetic log combustion in residential fireplaces, *Environ. Sci. Technol.*, *32*(1), 13-22.

Rogge, W. F., L.M. Hildemann, M.A. Mazurek, G.R. Cass, B.R.T. Simoneit (1994), Sources of fine organic aerosol. 6. Cigarette smoke in the urban atmosphere, *Environmental Science and Technology*, *28*, 1375-1388.

Sarnat, J. A., et al. (2008), Fine particle sources and cardiorespiratory morbidity: An application of chemical mass balance and factor analytical source-apportionment methods, *Environmental Health Perspectives*, *116*(4), 459-466.

Saylor, R. D., et al. (2006), Linear regression techniques for use in the EC tracer method of secondary organic aerosol estimation, *Atmos. Environ.*, *40*(39), 7546-7556.

Schauer, J. J., et al. (1996), Source apportionment of airborne particulate matter using organic compounds as tracers, *Atmos. Environ.*, *30*(22), 3837-3855.

Schauer, J. J. (1998), Source contributions to atmospheric organic compound concentrations: Emissions measurement and model predictions, Ph.D. thesis, California Institute of Technology, Pasadena.

Schauer, J. J., et al. (1999a), Measurement of emissions from air pollution sources. 1. C-1 through C-29 organic compounds from meat charbroiling, *Environ. Sci. Technol.*, *33*(10), 1566-1577.

Schauer, J. J., et al. (1999b), Measurement of emissions from air pollution sources. 2. C-1 through C-30 organic compounds from medium duty diesel trucks, *Environ. Sci. Technol.*, *33*(10), 1578-1587.

Schauer, J. J., and G. R. Cass (2000), Source apportionment of wintertime gas-phase and particle-phase air pollutants using organic compounds as tracers, *Environ. Sci. Technol.*, *34*(9), 1821-1832.

Schauer, J. J., et al. (2001), Measurement of emissions from air pollution sources. 3. C-1-C-29 organic compounds from fireplace combustion of wood, *Environ. Sci. Technol.*, *35*(9), 1716-1728.

Schauer, J. J., et al. (2002a), Source reconciliation of atmospheric gas-phase and particle-phase pollutants during a severe photochemical smog episode, *Environ. Sci. Technol.*, *36*(17), 3806-3814.

Schauer, J. J., et al. (2002b), Measurement of emissions from air pollution sources. 5. C-1-C-32 organic compounds from gasoline-powered motor vehicles, *Environ. Sci. Technol.*, *36*(6), 1169-1180.

Schauer, J. J. (2003), Evaluation of elemental carbon as a marker for diesel particulate matter, *Journal of Exposure Analysis and Environmental Epidemiology*, *13*(6), 443-453.

Schauer, J. J., Lough, G.C., Shafer, M.M., Christensen, W.F., Arndt, M.F., DeMinter, J.T., Park, J.S. (2006), Characterization of metals emitted from motor vehicles, Health Effects Institute.

Sheehan, P. E., and F. M. Bowman (2001), Estimated effects of temperature on secondary organic aerosol concentrations, *Environ. Sci. Technol.*, *35*(11), 2129-2135.

Sheesley, R. J., et al. (2004), Trends in secondary organic aerosol at a remote site in Michigan's upper peninsula, *Environ. Sci. Technol.*, *38*(24), 6491-6500.

Sheesley, R. J., et al. (2007), Sensitivity of molecular marker-based CMB models to biomass burning source profiles, *Atmos. Environ.*, *41*(39), 9050-9063.

Shrivastava, M. K., et al. (2006), Modeling semivolatile organic aerosol mass emissions from combustion systems, *Environ. Sci. Technol.*, *40*(8), 2671-2677.

Simoneit, B. R. T., and M. A. Mazurek (1982), Organic-matter of the troposphere .2. Natural background of biogenic lipid matter in aerosols over the rural western United-States, *Atmos. Environ.*, *16*(9), 2139-2159.

Simoneit, B. R. T. (1985), Application of molecular marker analysis to vehicular exhaust for source reconciliations, *International Journal of Environmental Analytical Chemistry*, *22*(3-4), 203-233.

Simoneit, B. R. T., et al. (1993), Lignin pyrolysis products, lignans, and resin acids as specific tracers of plant classes in emissions from biomass combustion, *Environ. Sci. Technol.*, *27*(12), 2533-2541.

Simoneit, B. R. T., et al. (1999), Levoglucosan, a tracer for cellulose in biomass burning and atmospheric particles, *Atmos. Environ.*, *33*(2), 173-182.

Simoneit, B. R. T. (2002), Biomass burning - A review of organic tracers for smoke from incomplete combustion, *Applied Geochemistry*, *17*(3), 129-162.

Sloane, C. S., et al. (1991), Size-segregated fine particle measurements by chemical-species and their impact on visibility impairment in Denver, *Atmospheric Environment Part a-General Topics*, *25*(5-6), 1013-1024.

Standley, L. J., and B. R. T. Simoneit (1987), Characterization of extractable plant wax, resin, and thermally matured components in smoke particles from prescribed burns *Environ. Sci. Technol.*, *21*(2), 163-169.

Standley, L. J., and B. R. T. Simoneit (1994), Resin diterpenoids as tracers for biomass combustion aerosols, *J. Atmos. Chem.*, *18*(1), 1-15.

Subramanian, R., et al. (2006), Contribution of motor vehicle emissions to organic carbon and fine particle mass in Pittsburgh, Pennsylvania: Effects of varying source profiles and seasonal trends in ambient marker concentrations, *Atmos. Environ.*, *40*(40), 8002-8019.

Subramanian, R., et al. (2007), Insights into the primary-secondary and regional-local contributions to organic aerosol and PM2.5 mass in Pittsburgh, Pennsylvania, *Atmos. Environ.*, *41*(35), 7414-7433.

Sullivan, A. P., et al. (2004), A method for on-line measurement of water-soluble organic carbon in ambient aerosol particles: Results from an urban site, *Geophysical Research Letters*, *31*(13).

Sullivan, A. P., et al. (2006), Airborne measurements of carbonaceous aerosol soluble in water over northeastern United States: Method development and an investigation into water-soluble organic carbon sources, *Journal of Geophysical Research-Atmospheres*, *111*(D23), Artn D23s46, doi 10.1029/2006jd007072.

Sullivan, A. P., and R. J. Weber (2006), Chemical characterization of the ambient organic aerosol soluble in water: 2. Isolation of acid, neutral, and basic fractions by modified size-exclusion chromatography, *Journal of Geophysical Research-Atmospheres*, *111*(D5), Artn D05315, doi 05310.01029/02005jd006486.

Tian, D., Russell, A.G. (2005), Uncertainty and variability of emissions from Silvicuture burn in Georgia, *in preparation*.

Turpin, B. J., and J. J. Huntzicker (1995), Identification of secondary organic aerosol episodes and quantitation of primary and secondary organic aerosol concentrations during scaqs, *Atmos. Environ.*, *29*(23), 3527-3544.

Turpin, B. J., et al. (2000), Measuring and simulating particulate organics in the atmosphere: problems and prospects, *Atmos. Environ.*, *34*(18), 2983-3013.

Turpin, B. J., and H. J. Lim (2001), Species contributions to PM2.5 mass concentrations: Revisiting common assumptions for estimating organic mass, *Aerosol Science and Technology*, *35*(1), 602-610.

U.S DOT (2001), Department of Transportation, Federal Highway Administration, Highway Statistics 2001, Publication No. FHWA-PL-02-020. Washington, D.C.

U.S. EPA (2000), National air pollutant emission trends 1900-1998, EPA 454/R-400–002, Office: Washington, DC.

U.S. EPA (2004), EPA 2001 modeling platform emission inventory, http://www.epa.gov/ttn/chief/emch/invent/.

U.S. Forest Service (2004), Forest iventory & analysis factsheet: Georgia 2004, edited, http://srsfia2.fs.fed.us/states/ga/GA%20Factsheet.pdf.

U.S.EPA (2001), CMB user's manual (Version 8.0), U.S. Environmental Protection Agency, Research Triangle Park, NC.

U.S.EPA (2002), Speciate 3.2, edited, U.S. Environmental Protection Agency, Research Triangle Park, NC.

U.S.EPA (2004), EPA-CMB8.2 User's Manual, edited by U. S. E. P. A. Office of Air Quality & Standards, Research Triangle Park, NC., Publication No. EPA-452/R-04-011.

Ward, T. J., and G. C. Smith (2005), The 2000/2001 Missoula Valley PM2.5 chemical mass balance study, including the 2000 wildfire season - seasonal source apportionment, *Atmos. Environ.*, *39*(4), 709-717.

Ward, T. J., et al. (2006), Characterization and evaluation of smoke tracers in PM: Results from the 2003 Montana wildfire season, *Atmos. Environ.*, *40*(36), 7005-7017.

Watson, J. G. (1979), Chemical element balance receptor model methodology for assessing the sources of fine and total particulate matter.

Watson, J. G., et al. (1984), The effective variance weighting for least-squares calculations applied to the mass balance receptor model, *Atmos. Environ.*, *18*(7), 1347-1355.

Watson, J. G., et al. (1990), The USAEPA/DRI chemical mass balance receptor model, CMB 7.0, *Environmental Software*, *5*, 38-49.

Watson, J. G., et al. (1994), Chemical mass balance source apportionment of PM(10) during the Southern California Air-Quality Study, *Aerosol Science and Technology*, *21*(1), 1-36.

Watson, J. G., et al. (1998), Northern Front Range Air Quality Study. Final report., Prepared for Colorado State University, Fort Collins, CO, by Desert Research Institute, Reno, NV. http://charon.cira.colostate.edu/DRIFinal/ZipFiles.

Watson, J. G., et al. (2002), Receptor modeling application framework for particle source apportionment, *Chemosphere*, *49*(9), 1093-1136.

Weber, R. J., et al. (2007), A study of secondary organic aerosol formation in the anthropogenic-influenced southeastern United States, *Journal of Geophysical Research-Atmospheres*, *112*(D13), Artn D13302, doi 13310.11029/12007jd008408.

Westerling, A. L., et al. (2006), Warming and earlier spring increase western US forest wildfire activity, *Science*, *313*(5789), 940-943.

White, W. H., and P. T. Roberts (1977), Nature and origins of visibility-reducing aerosols in Los-Angeles air basin, *Atmos. Environ.*, *11*(9), 803-812.

Xia, X., and P. K. Hopke (2006), Seasonal variation of 2-methyltetrols in ambient air samples, *Environ. Sci. Technol.*, *40*(22), 6934-6937.

Yan, B., et al. (2008a), Organic composition of carbonaceous aerosols in an aged prescribed fire plume, *Atmospheric Chemistry and Physics*, *8*(21), 6381-6394.

Yan, B., et al. (2008b), Organic composition of carbonaceous aerosols in an aged prescribed fire plume, *Atmos. Chem. Phys.*, *8*, 6381-6394.

Yan, B., et al. (2009a), Detailed chemical characterization and aging of wildfire aerosols in the southeastern U.S, *in preparation*.

Yan, B., et al. (2009b), Detailed chemical characterization and aging of wildfire aerosols in the southeastern U.S, *in preparation*.

Yan, B., et al. (2009c), Roadside, urban, and rural comparison of primary and secondary organic molecular markers in ambient PM2.5, *Environ. Sci. Technol.*, *43*(12), 4287-4293.

Yan, B., et al. (2009d), Characterization of airborne PM2.5 at roadside, urban and rural sites in the summer and the winter *in preparation*.

Yu, J. Z., et al. (1999a), Gas-phase ozone oxidation of monoterpenes: Gaseous and particulate products, *J. Atmos. Chem.*, *34*(2), 207-258.

Yu, J. Z., et al. (1999b), Observation of gaseous and particulate products of monoterpene oxidation in forest atmospheres, *Geophysical Research Letters*, *26*(8), 1145-1148.

Yu, S., et al. (2007), Seasonal and regional variations of primary and secondary organic aerosols over the Continental United States: Semi-empirical estimates and model evaluation, *Environ. Sci. Technol.*, *41*(13), 4690-4697.

Zhang, Q., et al. (2005), Deconvolution and quantification of hydrocarbon-like and oxygenated organic aerosols based on aerosol mass spectrometry, *Environmental Science & Technology*, *39*(13), 4938-4952.

Zheng, M., et al. (2002), Source apportionment of PM2.5 in the southeastern United States using solvent-extractable organic compounds as tracers, *Environ. Sci. Technol.*, *36*(11), 2361-2371.

Zheng, M., et al. (2005), Seasonal trends in PM2.5 source contributions in Beijing, China, *Atmos. Environ.*, *39*(22), 3967-3976.

Zheng, M., et al. (2006a), Composition and sources of carbonaceous aerosols at three contrasting sites in Hong Kong, *Journal of Geophysical Research-Atmospheres*, *111*(D20).

Zheng, M., et al. (2006b), Spatial distribution of carbonaceous aerosol in the southeastern United States using molecular markers and carbon isotope data, *Journal of Geophysical Research-Atmospheres*, *111*(D10), doi: 10.1029/2005JD006777

Zheng, M., et al. (2007), Source apportionment of daily fine particulate matter at Jefferson street, Atlanta, GA, during summer and winter, *J. Air Waste Manage. Assoc.*, *57*(2), 228-242.

Zielinska, B., et al. (1998), Motor vehicle and wood burning from Northern Front Range Air Quality Study, Volume B: Source measurements.

Zielinska, B., et al. (2004), Emission rates and comparative chemical composition from selected in-use diesel and gasoline-fueled vehicles, *J. Air Waste Manage. Assoc.*, *54*(9), 1138-1150.